



**Calhoun: The NPS Institutional Archive**  
**DSpace Repository**

---

Theses and Dissertations

1. Thesis and Dissertation Collection, all items

---

1993

Experimental evaluation of an instrumented  
synthesis method for the real-time estimation  
of reactivity.

Selby, Lorin C.

---

<http://hdl.handle.net/10945/24163>

---

*Downloaded from NPS Archive: Calhoun*



Calhoun is the Naval Postgraduate School's public access digital repository for research materials and institutional publications created by the NPS community. Calhoun is named for Professor of Mathematics Guy K. Calhoun, NPS's first appointed -- and published -- scholarly author.

**Dudley Knox Library / Naval Postgraduate School**  
**411 Dyer Road / 1 University Circle**  
**Monterey, California USA 93943**

<http://www.nps.edu/library>















# EXPERIMENTAL EVALUATION OF AN INSTRUMENTED SYNTHESIS METHOD FOR THE REAL-TIME ESTIMATION OF REACTIVITY

by

LORIN C. SELBY

Submitted to the Department of Nuclear Engineering on  
7 May 1993 in partial fulfillment of the requirements for  
the Degree of Nuclear Engineer and the Degree of Master of Science  
in Nuclear Engineering.

## ABSTRACT

This research is part of an investigation into the feasibility of using reactor-generated signals in an instrumented synthesis method for the real-time estimation of reactivity. The method utilizes in-core neutron detectors to evaluate local core power distributions for eventual use in an on-line controller. Although numerical evaluation of the synthesis method has proven successful, this experimental work was conducted to determine if the signals provided by actual in-core sensors in an operating reactor could be used with this technique. For this study, an instrumentation system was designed and built to obtain neutron flux data from three fission chamber neutron detectors. This instrumentation system was installed in the 5 Mw(thermal) research reactor at the Massachusetts Institute of Technology (MITR-II). The flux data resulting from the experiments was used to determine the optimal locations for additional detectors to be used in future experiments and to show the limitations and difficulties of this method. Recommendations are presented for correcting these short-comings in the research and for future areas of study.

This research was supported in part by the U.S. Department of Energy under contract number DE-FG02-92ER75710

Thesis Supervisor: John A. Bernard  
Title: Director of Reactor Operations, MIT Nuclear Reactor Laboratory

Thesis Supervisor: David D. Lanning  
Title: Professor of Nuclear Engineering





# EXPERIMENTAL EVALUATION OF AN INSTRUMENTED SYNTHESIS METHOD FOR THE REAL-TIME ESTIMATION OF REACTIVITY

by

LORIN C. SELBY

B.S., Nuclear Engineering  
University of Virginia  
(December, 1986)

Submitted to the Department of Nuclear Engineering  
in Partial Fulfillment of the Requirements for the Degree of

NUCLEAR ENGINEER

and the Degree of

MASTER OF SCIENCE IN NUCLEAR ENGINEERING

at the

MASSACHUSETTS INSTITUTE OF TECHNOLOGY

June 1993

© Lorin Cave Selby, 1993. All rights reserved.

The author hereby grants to MIT and the U.S. Government permission to reproduce and  
distribute copies of this thesis in whole or in part.



# EXPERIMENTAL EVALUATION OF AN INSTRUMENTED SYNTHESIS METHOD FOR THE REAL-TIME ESTIMATION OF REACTIVITY

by

LORIN C. SELBY

Submitted to the Department of Nuclear Engineering on  
7 May 1993 in partial fulfillment of the requirements for  
the Degree of Nuclear Engineer and the Degree of Master of Science  
in Nuclear Engineering.

## ABSTRACT

This research is part of an investigation into the feasibility of using reactor-generated signals in an instrumented synthesis method for the real-time estimation of reactivity. The method utilizes in-core neutron detectors to evaluate local core power distributions for eventual use in an on-line controller. Although numerical evaluation of the synthesis method has proven successful, this experimental work was conducted to determine if the signals provided by actual in-core sensors in an operating reactor could be used with this technique. For this study, an instrumentation system was designed and built to obtain neutron flux data from three fission chamber neutron detectors. This instrumentation system was installed in the 5 Mw(thermal) research reactor at the Massachusetts Institute of Technology (MITR-II). The flux data resulting from the experiments was used to determine the optimal locations for additional detectors to be used in future experiments and to show the limitations and difficulties of this method. Recommendations are presented for correcting these short-comings in the research and for future areas of study.

This research was supported in part by the U.S. Department of Energy under contract number DE-FG02-92ER75710

Thesis Supervisor: John A. Bernard  
Title: Director of Reactor Operations, MIT Nuclear Reactor Laboratory

Thesis Supervisor: David D. Lanning  
Title: Professor of Nuclear Engineering





## ACKNOWLEDGMENTS

I would like to express my sincere appreciation and thanks to my thesis supervisors, Professor David D. Lanning and Dr. John A. Bernard for their guidance and support throughout the course of this work. They provided me with a great deal of advice and encouragement which was always welcome and enlightening. In addition, a special thanks goes to Mr. Edward S. H. Lau for his help in setting up and conducting the experiments with the MIT reactor. I am also indebted to all of the individuals on the Reactor Operations and Reactor Plant Protection Office Staffs who assisted me in completing all testing.

I must also thank my fellow students in the Nuclear Engineering Department for making my stay here at MIT an enjoyable one. This is especially true of the "gang" on the third floor of NW 12 where my office was located. To my office mates, thanks for all of those rousing political discussions that we got into. I would also like to thank Tim Lawrence for being such a good friend during both our ups and downs here in academia...good luck at the Academy. I will see what I can do about getting you a life subscription to the *Thistle*.

I would also like to thank the U.S. Navy for allowing me this incredible opportunity to pursue my education while on active duty. I am now more "psyched" than ever to get back to sea on a submarine as a Department Head.

To my family, thanks for all of those words of encouragement and support on the telephone over the past few years. Not bad for your son, eh?!

Finally, I would like to thank Vicky Rowley for providing me with a great deal of love and support throughout the course of my stay here at MIT. You gave me the incentive I needed to get my work done so that we could play on the weekends. I wish things could have worked out differently. Thanks for trying and for being you.

This research was supported in part by the U.S. Department of Energy under contract number DE-FG02-92ER75710. This support is gratefully acknowledged.





# TABLE OF CONTENTS

<b>ABSTRACT .....</b>	<b>2</b>
<b>ACKNOWLEDGMENTS .....</b>	<b>3</b>
<b>LIST OF FIGURES .....</b>	<b>8</b>
<b>LIST OF TABLES .....</b>	<b>11</b>
 <b>CHAPTER ONE: INTRODUCTION .....</b>	 <b>14</b>
1.1 RESEARCH OBJECTIVES .....	14
1.2 BACKGROUND .....	15
1.3 INTEGRATION OF RESEARCH WITH MIT CONTROL STUDIES .....	17
1.4 EXPERIMENTAL FACILITIES .....	19
1.5 ORGANIZATION OF REPORT .....	25
 <b>CHAPTER TWO: DESCRIPTION OF INSTRUMENTED SYNTHESIS METHOD .....</b>	 <b>27</b>
2.1 INTRODUCTION .....	27
2.2 THE INSTRUMENTED SYNTHESIS METHOD .....	29
2.2.1 BASIS .....	29
2.2.2 INSTRUMENT INPUT .....	30
2.3 POTENTIAL PROBLEMS WITH METHOD .....	32
 <b>CHAPTER THREE: PRELIMINARY PLANNING FOR THE EXPERIMENTAL EVALUATION .....</b>	 <b>34</b>
3.1 INTRODUCTION .....	34
3.2 DETECTOR PLACEMENT FOR EXPERIMENT .....	35
3.2.1 DETERMINATION OF THE LIMITING DIMENSIONS .....	39
3.2.2 IN-CORE DIMENSIONAL MEASUREMENT .....	40
3.3 CONSEQUENCES OF WATER VENT HOLE BLOCKAGE .....	41
3.4 DETERMINATION OF NEUTRON DETECTOR REQUIREMENTS .....	45
3.4.1 REQUIRED DETECTOR SENSITIVITY .....	46



<b>3.5 DETECTOR SUPPORT WITHIN THE CORE</b>	<b>54</b>
3.5.1 SUPPORT RIG REQUIREMENTS	54
3.5.2 SUPPORT RIG DESIGN	56
3.5.3 IMPLEMENTATION OF THE SUPPORT RIG	59
<b>3.6 OTHER DESIGN PLANNING</b>	<b>59</b>

<b>CHAPTER FOUR: DESIGN, CONFIGURATION, AND TESTING OF ELECTRICAL EQUIPMENT</b>	<b>60</b>
4.1 INTRODUCTION	60
4.2 ACQUISITION OF THE FISSION CHAMBER DETECTORS	61
4.3 FISSION CHAMBER ADAPTER BOXES	64
4.4 POWER SUPPLY	64
4.5 DATA ACQUISITION EQUIPMENT	66
4.5.1 AMMETER	66
4.5.2 ANALOG-TO-DIGITAL CONVERTER	69
4.5.3 A/D BOARD SOFTWARE	72
4.6 INSTRUMENTATION SYSTEM CONFIGURATION	72
4.6.1 DESCRIPTION OF INSTRUMENTATION SYSTEM	74
4.7 TESTING OF ELECTRONIC EQUIPMENT	75
4.7.1 FISSION CHAMBER DETECTORS	75
4.7.2 TESTING OF A/D BOARD AND ASSOCIATED SOFTWARE	79
4.7.3 TESTING OF FULL INSTRUMENTATION SYSTEM	79
<b>CHAPTER FIVE: THE EXPERIMENT</b>	<b>81</b>
5.1 INTRODUCTION	81
5.2 REQUIREMENTS FOR TESTING	82
5.2.1 PREREQUISITES FOR EXPERIMENT	83
5.3 PHASE I OF EXPERIMENT	85
5.3.1 SETUP FOR THE EXPERIMENT	86
5.3.2 INITIAL SHUTDOWN BACKGROUND READINGS	89
5.3.3 STEADY-STATE ANALYSIS	89
5.3.4 FLUX TILTING	90
5.3.5 TRANSIENT ANALYSIS	92





5.3.6 FINAL SHUTDOWN BACKGROUND READINGS	93
5.3.7 RESTOWING EQUIPMENT	93
5.3.8 REPAIR OF THE A/D BOARD	94
5.4 PHASE II OF EXPERIMENT	95
5.4.1 SETUP FOR THE EXPERIMENT	95
5.4.2 SHUTDOWN BACKGROUND READINGS	97
5.4.3 FLUX TILTING	97
5.4.5 SECURING FROM EXPERIMENT	98
5.5 LESSONS LEARNED	99
 CHAPTER SIX: ANALYSIS OF DATA	 102
6.1 INTRODUCTION	102
6.2 PHASE I OF EXPERIMENT	103
6.2.1 SHUTDOWN BACKGROUND MEASUREMENTS	103
6.2.2 STEADY-STATE MEASUREMENTS AT 500 WATTS	109
6.2.3 STEADY-STATE MEASUREMENTS AT 5 kW	112
6.2.4 FLUX TILTING AT 1 kW	114
6.2.5 FLUX TILTING AT 10 kW	125
6.2.6 FLUX TILTING AT 50 kW	134
6.2.7 FINAL SHUTDOWN BACKGROUND READINGS	143
6.3 PHASE II OF EXPERIMENT	146
6.3.1 SHUTDOWN BACKGROUND MEASUREMENTS	146
6.3.2 FLUX TILTING AT 1 kW	148
6.3.3 FLUX TILTING AT 10 kW	160
6.3.4 FLUX TILTING AT 50 kW	171
6.3.7 FINAL SHUTDOWN BACKGROUND READINGS	182
6.4 RESULTS FROM RADIATION SURVEYS	184
6.5 DETECTOR AND GUIDE TUBE MATERIAL COMPOSITION	187
6.6 SUMMARY	189
 CHAPTER SEVEN: CONCLUSIONS AND RECOMMENDATIONS FOR FURTHER EXPERIMENTS	   190



7.1 SUMMARY OF EXPERIMENTAL RESULTS .....	190
7.2 CONCLUSIONS .....	192
7.3 RECOMMENDATIONS FOR FURTHER EXPERIMENTS .....	193
 <b>APPENDIX A: INITIAL TESTING .....</b>	 <b>195</b>
A.1: PROCEDURE FOR DIMENSIONAL MEASUREMENT AND SHIM BLADE DROP TIME TESTING OF WATER VENT HOLES .....	196
 <b>APPENDIX B: RAW DATA .....</b>	 <b>204</b>
B.1: EXPERIMENT PHASE I DATA .....	205
B.2: EXPERIMENT PHASE II DATA .....	211
 <b>APPENDIX C: EXPERIMENTAL PROCEDURES .....</b>	 <b>218</b>
C.1: EXPERIMENT PHASE I PROCEDURE .....	219
C.2: EXPERIMENT PHASE II PROCEDURE .....	230
 <b>REFERENCES .....</b>	 <b>244</b>





## LIST OF FIGURES

Figure 1.4-1: View Of MITR-II Research Reactor	20
Figure 1.4-2: Vertical Cross-Section of MITR-II	22
Figure 1.4-3: MITR-II Coolant Flow Path	23
Figure 1.4-4: MITR-II Core Section	24
Figure 3.2-1: Top View of MITR-II Core	37
Figure 3.2-2: Vertical-Cross Section of MITR-II Core Showing a Water Vent Hole	38
Figure 3.4.1-1: Azimuthal Mesh Used in CITATION Code	47
Figure 3.4.1-2: Thermal Flux in Water Vent Hole #1 @ 50 kW	52
Figure 3.4.1-3: Thermal Flux in Water Vent Hole #3 @ 50 kW	52
Figure 3.4.1-4: Thermal Flux in Water Vent Hole #5 @ 50 kW	53
Figure 3.5.2-1: Typical Instrument Guide Tube	58
Figure 3.5.2-2: Detector Axial Position Keeping Scheme	58
Figure 4.2-1: Specifications for NY-10336 Fission Chamber Detector	63
Figure 4.4-1: Typical Operating Curve for WL-23798 Fission Chamber	65
Figure 4.6-1: Block Diagram of Instrumentation System	73
Figure 4.7.1-1: Operating Curve for Fission Chamber Detector #1	76
Figure 4.7.1-2: Operating Curve for Fission Chamber Detector #2	76
Figure 4.7.1-3: Operating Curve for Fission Chamber Detector #3	77
Figure 6.2.1-1: Top View of MITR-II Reactor Core	106
Figure 6.2.1-2: Reference Axial Position	107
Figure 6.2.1-3: Initial Shutdown Background Readings	108



Figure 6.2.2-1: Neutron Flux at 500 Watts	111
Figure 6.2.3-1: Neutron Flux at 5 kW	113
Figure 6.2.4-1: Neutron Flux at 1 kW with No Tilt	116
Figure 6.2.4-2: Neutron Flux at 1 kW with Tilt	119
Figure 6.2.4-3: Normalized Tilt and No-Tilt Fluxes in Vent Hole #1 at 1 kW	121
Figure 6.2.4-4: Normalized Tilt and No-Tilt Fluxes in Vent Hole #3 at 1 kW	122
Figure 6.2.4-5: Normalized Tilt and No-Tilt Fluxes in Vent Hole #5 at 1 kW	123
Figure 6.2.5-1: Neutron Flux at 10 kW with No Tilt	128
Figure 6.2.5-2: Neutron Flux at 10 kW with Tilt	129
Figure 6.2.5-3: Normalized Tilt and No-Tilt Fluxes in Vent Hole #1 at 10 kW	131
Figure 6.2.5-4: Normalized Tilt and No-Tilt Fluxes in Vent Hole #3 at 10 kW	132
Figure 6.2.5-5: Normalized Tilt and No-Tilt Fluxes in Vent Hole #5 at 10 kW	133
Figure 6.2.6-1: Neutron Flux at 50 kW with No Tilt	137
Figure 6.2.6-2: Neutron Flux at 50 kW with Tilt	138
Figure 6.2.6-3: Normalized Tilt and No-Tilt Fluxes in Vent Hole #1 at 50 kW	140
Figure 6.2.6-4: Normalized Tilt and No-Tilt Fluxes in Vent Hole #3 at 50 kW	141
Figure 6.2.6-5: Normalized Tilt and No-Tilt Fluxes in Vent Hole #5 at 50 kW	142
Figure 6.2.7-1: Final Shutdown Background Readings	145
Figure 6.3.1-1: Initial Shutdown Background Readings - Phase II	147
Figure 6.3.2-1: Neutron Flux at 1 kW with No Tilt - Phase II	151
Figure 6.3.2-2: Neutron Flux at 1 kW with Tilt One	153
Figure 6.3.2-3: Neutron Flux at 1 kW with Tilt Two	155





Figure 6.3.2-4: Normalized Tilt and No-Tilt Fluxes in Vent Hole #1 at 1 kW	157
Figure 6.3.2-5: Normalized Tilt and No-Tilt Fluxes in Vent Hole #3 at 1 kW	158
Figure 6.3.2-6: Normalized Tilt and No-Tilt Fluxes in Vent Hole #5 at 1 kW	159
Figure 6.3.3-1: Neutron Flux at 10 kW with No Tilt - Phase II	162
Figure 6.3.3-2: Neutron Flux at 10 kW with Tilt One	164
Figure 6.3.3-3: Neutron Flux at 10 kW with Tilt Two	166
Figure 6.3.3-4: Normalized Tilt and No-Tilt Fluxes in Vent Hole #1 at 10 kW	168
Figure 6.3.3-5: Normalized Tilt and No-Tilt Fluxes in Vent Hole #3 at 10 kW	169
Figure 6.3.3-6: Normalized Tilt and No-Tilt Fluxes in Vent Hole #5 at 10 kW	170
Figure 6.3.4-1: Neutron Flux at 50 kW with No Tilt - Phase II	173
Figure 6.3.4-2: Neutron Flux at 50 kW with Tilt One	175
Figure 6.3.4-3: Neutron Flux at 50 kW with Tilt Two	177
Figure 6.3.4-4: Normalized Tilt and No-Tilt Fluxes in Vent Hole #1 at 50 kW	179
Figure 6.3.4-5: Normalized Tilt and No-Tilt Fluxes in Vent Hole #3 at 50 kW	180
Figure 6.3.4-6: Normalized Tilt and No-Tilt Fluxes in Vent Hole #5 at 50 kW	181
Figure 6.3.7-1: Final Shutdown Background Readings - Phase II	183
Figure 6.5-1: Detector and Instrument Guide Tube Material Compositions	188



## LIST OF TABLES

Table 3.3-1: Shim Blade Drop Times .....	44
Table 3.3-2: Blade Drop Times with Water Vent Holes 1, 3, and 5 Blocked .....	44
Table 3.4.1-1: Radial Mesh Used by CITATION Code .....	48
Table 3.4.1-2: Thermal Flux in Water Vent Hole #1 from CITATION .....	49
Table 3.4.1-3: Thermal Flux in Water Vent Hole #3 from CITATION .....	50
Table 3.4.1-4: Thermal Flux in Water Vent Hole #5 from CITATION .....	51
Table 4.5.2-1: Features of DT-2801 A/D Board .....	71
Table 6.2.2-1: Net Flux at 500 Watts .....	109
Table 6.2.3-1: Net Flux at 5 kW .....	112
Table 6.2.4-1: Net Flux at 1 kW with No Tilt .....	115
Table 6.2.4-2: Shim Blade and Regulating Rod Heights for Tilt @ 1kW .....	118
Table 6.2.4-3: Net Flux at 1 kW with Tilt .....	118
Table 6.2.4-4: Normalized Flux Readings @ 1 kW .....	120
Table 6.2.5-1: Net Flux at 10 kW with No Tilt .....	126
Table 6.2.5-2: Shim Blade and Regulating Rod Heights for Tilt @ 10 kW .....	126
Table 6.2.5-3: Net Flux at 10 kW with Tilt .....	127
Table 6.2.5-4: Normalized Flux Readings @ 10 kW .....	130
Table 6.2.6-1: Net Flux at 50 kW with No Tilt .....	135
Table 6.2.6-2: Shim Blade and Regulating Rod Heights for Tilt @ 50 kW .....	136
Table 6.2.6-3: Net Flux at 50 kW with Tilt .....	136
Table 6.2.6-4: Normalized Flux Readings @ 50 kW .....	139
Table 6.3.2-1: Net Flux at 1 kW with No Tilt - Phase II .....	150



Table 6.3.2-2: Shim Blade and Regulating Rod Heights for Tilt One @ 1kW	152
Table 6.3.2-3: Net Flux at 1 kW with Tilt One	152
Table 6.3.2-4: Shim Blade and Regulating Rod Heights for Tilt Two @ 1kW	154
Table 6.3.2-5: Net Flux at 1 kW with Tilt Two	154
Table 6.3.2-6: Normalized Flux Readings @ 1 kW	156
Table 6.3.3-1: Net Flux at 10 kW with No Tilt - Phase II	161
Table 6.3.3-2: Shim Blade and Regulating Rod Heights for Tilt One @ 10kW	163
Table 6.3.3-3: Net Flux at 10 kW with Tilt One	163
Table 6.3.3-4: Shim Blade and Regulating Rod Heights for Tilt Two @ 10 kW	165
Table 6.3.3-5: Net Flux at 10 kW with Tilt Two	165
Table 6.3.3-6: Normalized Flux Readings @ 10 kW	167
Table 6.3.4-1: Net Flux at 50 kW with No Tilt - Phase II	172
Table 6.3.4-2: Shim Blade and Regulating Rod Heights for Tilt One @ 50 kW	174
Table 6.3.4-3: Net Flux at 50 kW with Tilt One	174
Table 6.3.4-4: Shim Blade and Regulating Rod Heights for Tilt Two @ 50 kW	176
Table 6.3.4-5: Net Flux at 50 kW with Tilt Two	176
Table 6.3.4-6: Normalized Flux Readings @ 50 kW	178
Table 6.4-1: Radiation Surveys for Phase I of Experiment	185
Table 6.4-2: On-Contact Readings from Detectors and Aluminum Tubes	185
Table 6.4-3: Radiation Surveys for Phase II of Experiment	186
Table 6.4-4: On-Contact Readings from Detectors and Aluminum Tubes	186
Table B.1-1: Initial Shutdown Background Readings	205
Table B.1-2: Steady State Readings at 500 Watts	206
Table B.1-3: Steady State Readings at 5 kW	206





Table B.1-4: Baseline Readings at 1 kW	207
Table B.1-5: Readings at 1 kW with Flux Tilt	207
Table B.1-6: Baseline Readings at 10 kW	208
Table B.1-7: Readings at 10 kW with Flux Tilt	208
Table B.1-8: Baseline Readings at 50 kW	209
Table B.1-9: Readings at 50 kW with Flux Tilt	209
Table B.1-10: Final Shutdown Background Readings	210
Table B.2-1: Initial Shutdown Background Readings	211
Table B.2-2: Baseline Readings at 1 kW	212
Table B.2-3: Readings at 1 kW with First Flux Tilt	212
Table B.2-4: Readings at 1 kW with Second Flux Tilt	213
Table B.2-5: Baseline Readings at 10 kW	213
Table B.2-6: Readings at 10 kW with First Flux Tilt	214
Table B.2-7: Readings at 10 kW with Second Flux Tilt	214
Table B.2-8: Baseline Readings at 50 kW	215
Table B.2-9: Readings at 50 kW with First Flux Tilt	215
Table B.2-10: Readings at 50 kW with Second Flux Tilt	216
Table B.2-11: Final Shutdown Background Readings	216



# CHAPTER ONE: INTRODUCTION

## 1.1 RESEARCH OBJECTIVES

The primary objective of the thesis research as outlined in this report is to evaluate the feasibility of using reactor-generated signals with an on-line synthesis analysis for the real-time **estimation** of reactivity. This method utilizes in-core neutron detectors to evaluate **local power** distributions and to derive global reactivity values for eventual use in an on-line controller. Although numerical evaluation of the synthesis method has proven successful, this experimental work is intended to determine if the signals provided by actual in-core sensors in an operating reactor can be used with this method.





For this study an instrumentation system was designed and built to obtain neutron flux data from three fission chamber neutron detectors. This instrumentation system was installed in the 5 Mw(thermal) research reactor at the Massachusetts Institute of Technology (MITR-II). The signals provided by these detectors were used to provide the base-line data necessary to benchmark the synthesis method. While this project did not involve actual calculations using the synthesis method, evaluations were made to determine the suitability of the data for future use. In addition, detector material composition information was determined for use in obtaining cross section data.

## 1.2 BACKGROUND

In order to operate a modern nuclear reactor safely it is necessary to monitor certain parameters continuously. Examples of some of the most important parameters are reactivity, total power, axial and radial neutron flux distributions, local neutron flux density, heat generation rate, and fuel and coolant temperatures. It is theoretically possible to obtain this information by solving a set of time-dependent, multidimensional, coupled neutronic-thermal-hydraulic equations. However, to do so requires significant computing power, especially if real-time calculations are needed [1]. In addition, if these parameters are to be used as inputs to a control system, any errors between the computer model and the real reactor must be identified. An alternative to estimating these parameters with a computer simulation is to measure as many of the parameters as possible directly. Although this provides sufficient information for safe operation, it is not



possible to measure all of the parameters of interest, and thus true global automatic control is impossible

A compromise between the two approaches described above is to devise a computer model which approximates the instantaneous, local neutron flux and then compares it with actual flux data obtained from in-core sensors. The calculation of the local neutron flux is done with a linear combination of a set of precomputed, three-dimensional, static expansion-functions that bracket the expected reactor transient conditions. Because the actual flux is measured, the time-dependent coefficients of the combination are found by forcing the calculated flux to match the actual flux. This technique is called the instrumented synthesis method because of its reliance on neutron flux "instruments" in the calculations [2,3].

Although the neutron flux density is not of major concern to the reactor operator, most important reactor control parameters are directly or indirectly related to it. It is unfortunate then that the solution to the neutron flux as a function of position,  $r$ , relative energy,  $E$ , and time,  $t$ , requires the solution of the time-dependent, three-dimensional, group diffusion equations, a very computer-intensive task. In order to avoid this problem, most techniques currently in use for real-time controllers rely on a point-kinetics model [4]. Unfortunately, this model does not allow the automatic and optimal control of spatially-dependent cores.

By using an instrumented synthesis method, the modeling of the time-dependent neutron flux is eliminated. As a result the bulk of the computing is now centered on the solution of the thermodynamic, hydraulic and other parameters inferred from the neutron



flux. Numerical evaluation of this method has proven successful, and the results obtained have been extremely good [5]. By using sufficient numbers of neutron counters and strategically placing them in the core, so that no local flux shape-variation goes undetected, the synthesis method is expected to give good results. This thesis research is intended to show the feasibility of the method by measuring neutron flux directly under a number of steady-state and transient conditions. Because actual detectors may experience excessive noise, experimental testing is needed to ascertain the effects on the method. The flux data resulting from the experiments will be analyzed to determine the optimal location of additional detectors and to show any limitations or difficulties with the method. Recommendations will be made for correcting any of the short-comings of the research and future areas of study will be proposed.

### **1.3 INTEGRATION OF RESEARCH WITH MIT CONTROL STUDIES**

The Department of Nuclear Engineering and the Nuclear Reactor Laboratory at the Massachusetts Institute of Technology have been involved in automatic control studies for nuclear reactors since the late 1970's. The initial work concentrated on developing real-time models of various plant components such as the pressurizer, steam generator and condenser. In 1980 the Charles Stark Draper Laboratory (CSDL) initiated experimental testing using the MITR-II to demonstrate signal validation and instrument fault detection. This testing, in conjunction with the development of real-time models, led to the design of a closed-loop digital controller [6]. The initial controllers were intended to maintain steady-state conditions and their use was limited to the facility's regulating rod which was





of low reactivity worth. The introduction of a supervisory algorithm by Dr. John Bernard in 1983 led to a full fledged controller capable of conducting actual power transients. The supervisory algorithm precluded challenges to the reactor's safety system and thus allowed an associated controller to increase power without risk of exceeding specified limits. The controller, designated the 'MIT-CSDL Non-Linear Digital Controller', utilized the reactivity constraint approach to determine the time during which reactor power could be allowed to rise before negative reactivity would have to be inserted using the designated control device to level power at the desired point without overshoot [7-10]. In April 1985 the Nuclear Regulatory Commission licensed this reactivity constraint approach and on line testing at the MITR-II began with the facility's shim blades being used as the control device. In July 1986 MIT, in conjunction with Sandia National Laboratories (SNL), started work to develop control strategies for space nuclear reactors. These efforts led to the 'MIT-SNL Period-Generated Minimum Time Control Laws' which allowed for rapid power increases without overshoot. This control strategy was successfully tested at both the MITR-II and Sandia's Annular Core Research Reactor. Additional information on the reactivity constraint approach and period-generated control, as well as the results of the MIT program, has recently been compiled [11].

The present research is intended to evaluate the feasibility of the instrumented synthesis method in an actual reactor environment. If this work shows that the method is feasible, then additional work will be needed to join the detection system with the running synthesis program. Eventually a controller will be designed that uses the output from this method to maintain in-core parameters within specified boundaries.



Use of the instrumented synthesis method to determine reactivity will greatly enhance the capabilities of an automated controller. In an automated controller designed to control reactor power, it is extremely important that the reactivity be known at all times and that the value calculated be extremely accurate over the entire range of automated operations. Because reactivity is directly inferred from the neutron flux within the operating core, errors associated with a reactivity balance approach will be eliminated. In addition changes in reactivity will be seen very rapidly. This is not necessarily the case for the reactivity balance approach since there are time delays associated with the instrumentation (thermocouples for instance are relatively slow to respond to temperature changes).

Use of the instrumented synthesis method to determine in-core parameters may enhance the output of a reactor core. Because this method allows one to obtain on-line three-dimensional evaluation of core parameters, instead of inferring them from ex-core sensors, it may allow the core power output to be increased with no decrease in thermal margins. This will result in achieving higher burnups from existing cores and more economical use of our available fuel resources.

## **1.4 EXPERIMENTAL FACILITIES**

All experiments for this report were conducted using the 5 MW(thermal) Research Reactor at the Massachusetts Institute of Technology (MITR-II). The Massachusetts Institute of Technology has been operating a research reactor since its first reactor, MITR-I, achieved initial criticality on 21 July 1958. The current reactor, MITR-II (See



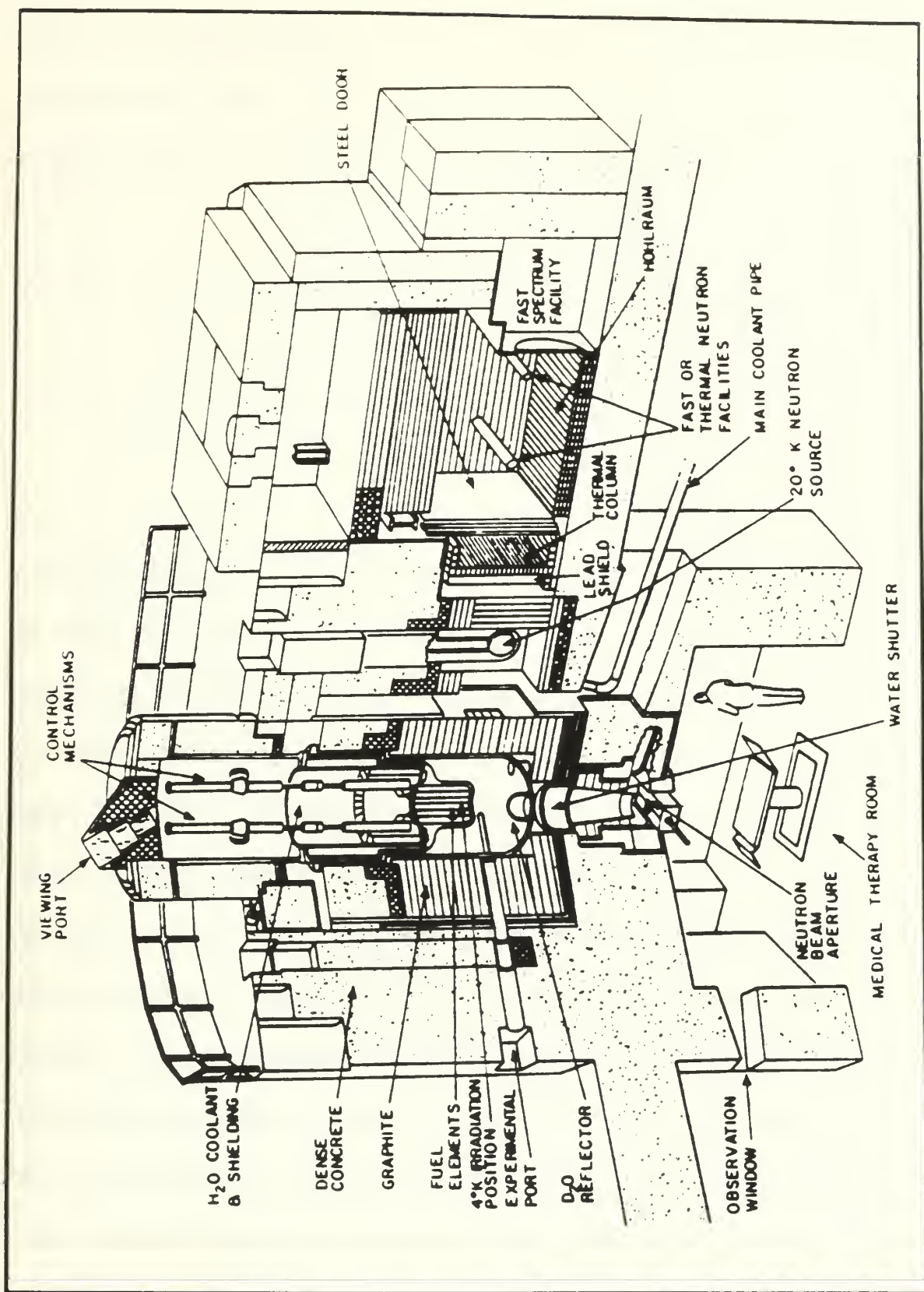


Figure 1 4-1 View Of MITR-II Research Reactor





Figure 1.4-1), started operation in July 1976. MITR-II is a light-water cooled and moderated reactor with a heavy-water reflector. It utilizes a plate fuel design with highly enriched uranium fuel (93% U-235) clad with aluminum. The heat generated in the core is removed by forced circulation of a light-water coolant. Because the primary system is not pressurized, the maximum allowable coolant temperature is limited to 55 °C. The reactor is used primarily for educational and research purposes. In addition it serves as a source of radioisotopes for medical work in the Boston area.

The reactor core is contained and supported by two concentric tanks and a core shroud (See Figure 1.4-2). The innermost of these tanks contains the light-water coolant/moderator. This tank is called the H<sub>2</sub>O core tank. The light water coolant enters the reactor via an inlet plenum where it is directed downward between the core shroud and the H<sub>2</sub>O core tank (See Figure 1.4-3). The coolant is then channeled down past the core through six flow slots formed by the hexagonal core support housing assembly (See Figure 1.4-4) before it is redirected up through the fueled region of the core. Upon exiting the core, the coolant mixes in the upper regions of the H<sub>2</sub>O tank before being directed to the outlet plenum. The outermost of the concentric tanks contains the D<sub>2</sub>O reflector and is thus referred to as the D<sub>2</sub>O reflector tank. This tank is four feet in diameter. The D<sub>2</sub>O contained in this tank is circulated through a heat exchanger to remove the heat generated in the reflector. The D<sub>2</sub>O system has been designed so that the heavy-water reflector can be dumped in an emergency. The loss of the heavy-water reflector around the core will insert negative reactivity which serves as a backup shutdown mechanism in the very unlikely event that the control blades do not work properly [12].





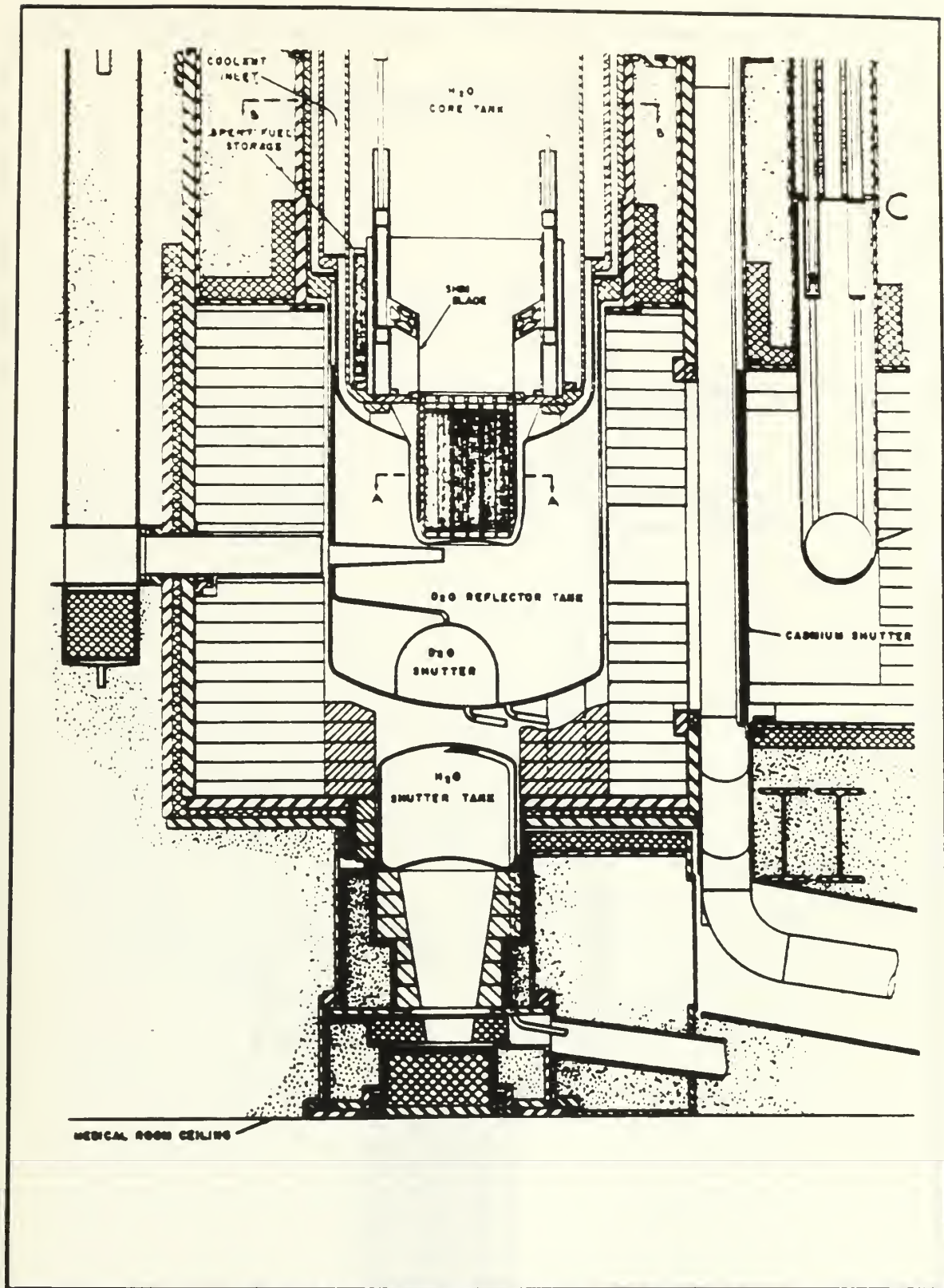


Figure 1.4-2: Vertical Cross-Section of MITR-II



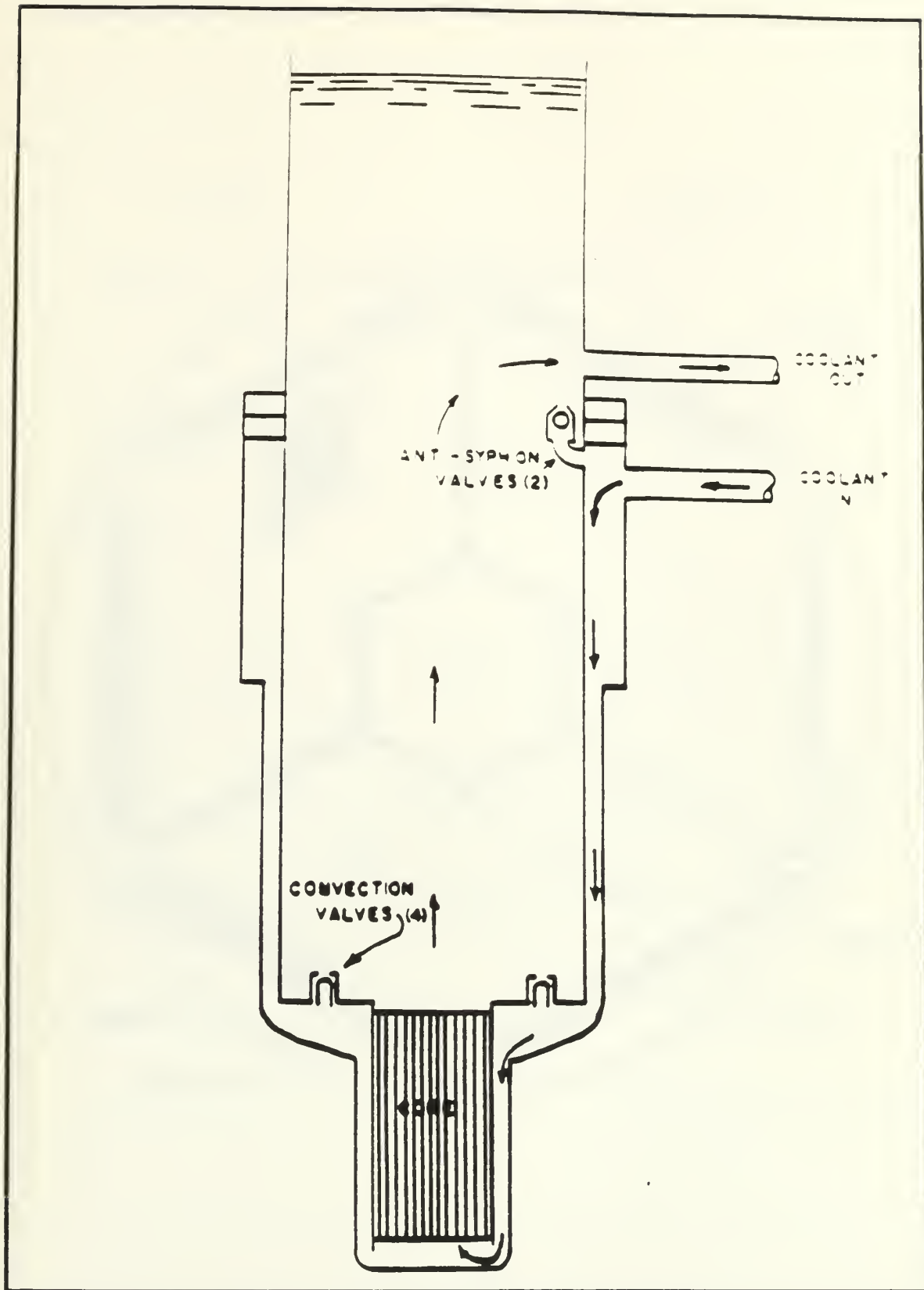


Figure 1.4-3: MITR-II Coolant Flow Path



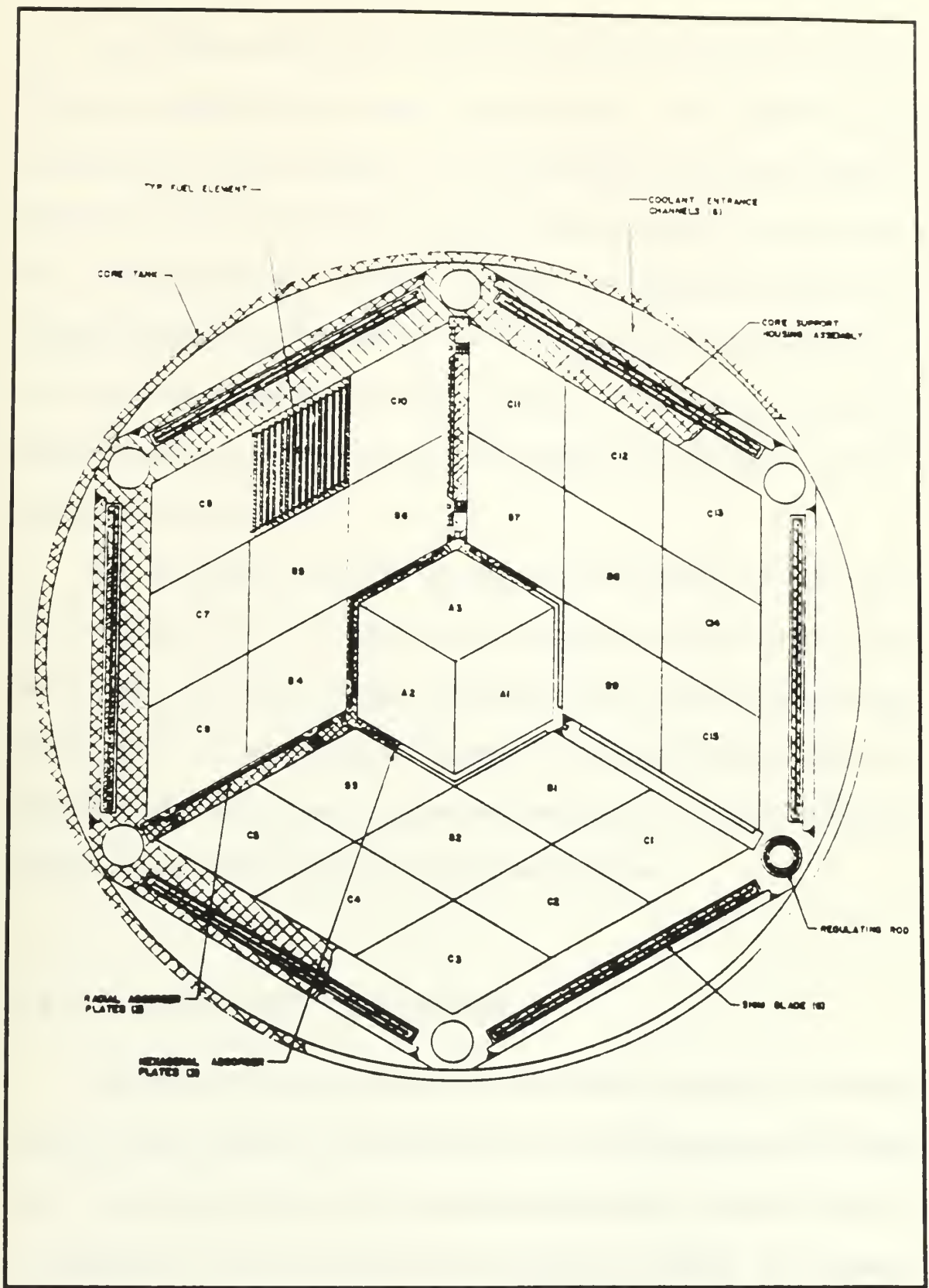


Figure 1.4-4: MITR-II Core Section





The MITR-II utilizes six boron-stainless steel shim/safety blades and one cadmium fine-motion regulating rod for control and flux-shaping. The locations of these components can be seen in Figure 1.4-4. The shim blades provide coarse control of reactor power and can be lowered as a bank or individually raised or lowered one at a time. Each blade normally moves at a fixed speed of 4.25 inches per minute with a maximum range of travel of twenty-one inches. The regulating rod also normally moves at 4.25 inches per minute, but the reactivity associated with its motion is much less than the shim blades and as a result is the preferred method of controlling the neutron flux while operating at power.

For this research both the control blades and the regulating rod were used to initiate transients and to tilt the neutron flux. During this work the operators had to remain within the allowable minimum period limits of fifty seconds steady and thirty seconds dynamic. In addition the shim blades must all remain within two inches of the bank height when reactor power is greater than one kilowatt. At powers less than one kilowatt, however, there is no limit on control blade orientation.

## **1.5 ORGANIZATION OF REPORT**

**This report has been organized in the order in which the research was performed.** This first chapter provides a brief explanation of the work performed and the facilities used. In subsequent chapters the instrumented synthesis method is described followed by an explanation of how the reactor-generated signals are obtained. This includes a discussion of the problems encountered in building the electronic detection system and the



preliminary testing done to ensure that the design would fit into the core with no impact on reactor operations. The development of the test plan is explained and the results are outlined. In the final section of this report recommendations are presented for further testing and integration of the data signals with a real time controller.

It should be noted that the primary focus of this report is on the preliminary steps of the experiment and the results of the experiment itself. The theoretical discussion of the instrumented synthesis method in Chapter Two is provided as background material for the reader. This author takes no credit for that work and so directs the reader to the referenced publications for further information.



## **CHAPTER TWO: DESCRIPTION OF INSTRUMENTED SYNTHESIS METHOD**

### **2.1 INTRODUCTION**

In order to gain the optimum performance from a modern nuclear reactor, it is necessary to know the status of the neutron flux and power distribution within the core at all times. There are currently two ways that this information can be obtained.

In the first method a set of time-dependent, three-dimensional, coupled neutronic and thermal-hydraulic equations are solved computationally. In order to determine the solution to this problem, the initial and boundary conditions must be provided and the external perturbations must be known. This method has been termed the model-based



approach because of its reliance on a complex computer model. While this method is theoretically rational, it requires much computing power and takes up a large portion of a computer's memory when running. Another drawback to this method is that a great deal of information must be supplied and updated frequently to maintain a current "picture" of the core's conditions. In addition, the effects of modeling uncertainties must be considered.

The alternative approach is to determine the neutron flux distribution in a semi-experimental manner without the use of a computer model. Instead, reliance is placed on reactor-generated signals from plant sensors. Because the number of these sensors is limited, there must be a means of inferring or estimating readings for locations within the core which are not monitored. The greatest advantage to this method is that it is relatively simple and inexpensive. Some of the disadvantages include the possibility that some or all of the detectors might fail during operation and the introduction of inaccuracies from the output signals of the different sensors. While periodic trip point and calibration checks can be performed to keep the accuracy within certain limits, failures cannot be totally eliminated. As a result of these uncertainties, the operational margins associated with these signals are often very conservative. This leads to less than optimal performance for the core and restricts the flexibility of operations.

The instrumented synthesis method is designed to incorporate each of the above methods to generate a detailed real-time power distribution for the core by using distributed in-core sensors to augment a simplified model. This synthesis method will be briefly described in this chapter. As was previously mentioned, this description is provided





as background material for the reader. For a more detailed description of the method, Robert Jacqmin's 1991 doctoral thesis should be consulted. The title of this work is *A Semi-Experimental Nodal Synthesis Method for the On-Line Reconstruction of Three-Dimensional Neutron Flux-Shapes and Reactivity* [13].

## 2.2 THE INSTRUMENTED SYNTHESIS METHOD

### 2.2.1 BASIS

The basis for the instrumented synthesis method is a collapsed-group point-synthesis approximation [3,14-15] where the NG-element vector  $\phi(t)$  of instantaneous fluxes  $\phi_{gn}(t)$  with energy groups  $g = 1,2,3, \dots, G$  in regions  $n = 1,2,3, \dots, N$  and is written as a linear combination of  $K$  precomputed expansion functions  $\Psi^{(k)}$ :

$$\phi(t) \approx \hat{\phi}(t) \equiv \sum_{k=1}^K \Psi^{(k)} T^{(k)}(t) \quad (1)$$

These expansion functions are in the fundamental  $\lambda$  modes [15-16]. These functions are generated by conducting a set of criticality calculations for different reactor conditions which bracket the expected transient states. The variable  $T^{(k)}(t)$  is called the mixing coefficient and is only dependent on time. The  $K$  expansion vectors  $\Psi^{(k)}$  contain all of the spatial and spectral effects. Because of this, the number of unknowns is greatly reduced from  $G \times N$  to  $K$ . This drops the total number of unknowns from several thousand to approximately ten.



The mixing coefficients,  $T^{(k)}(t)$ , are found by substituting equation (1) into the time-dependent neutron diffusion equation for  $\phi(t)$  and requiring the resulting formula to be correct in a weighted integral sense. The solution of this results in a set of  $K$  first-order, nonlinear, ordinary differential equations for the  $T^{(k)}$  values. If all initial conditions are known, the solution of these equations is relatively straight forward. The difficulty arises in the determination of the coefficients found in the integral equations.

In the instrumented synthesis method the idea is to avoid this difficulty by determining the  $T^{(k)}$  values in a semi-experimental way. Instead of relying on a purely theoretical global method as described above, local flux measurements are obtained experimentally and used to determine the unknown coefficients. In order for this method to be effective the neutron detectors must have a relatively fast response to changes in the neutron flux density within the core.

## 2.2.2 INSTRUMENT INPUT

Under a neutron flux  $\phi(t)$ , the  $j$ -th detector's output,  $C^{(j)}(t)$  is:

$$C^{(j)}(t) = \sum_{g=1}^G \sum_{n=1}^N V_n \Sigma_{gn}^{(j)} \phi_{gn}(t); \quad j = 1, 2, 3, \dots, J \quad (2)$$

Or equivalently with an inner-product notation:

$$C^{(j)}(t) = \Sigma^{(j)r} \phi(t); \quad j = 1, 2, 3, \dots, J \quad (3)$$



Homogenization calculations are performed to determine the cross sections in equation (2). The summations in this equation cover all neutron energies and extend across the entire core volume. The cross sections are, however, zero outside of the homogenization region. Because these cross sections only vary extremely slowly with time, they are considered time-independent. In equation (3) the node volume,  $V_n$ , is combined into each element of the row vector  $\Sigma^{(j)T}$ .

Equation (3) represents the output from the  $j$  different neutron detectors. For simplicity equation (3) can be put in matrix format. In addition an error vector,  $\delta\phi(t)$ , is implemented as follows:

$$\phi(t) = \hat{\phi}(t) - \delta\phi(t) = \Psi T(t) - \delta\phi(t) \quad (4)$$

and the matrix form of (3) is

$$\Sigma^T \phi(t) = C(t). \quad (5)$$

If equation (4) is substituted into equation (5) the result is:

$$\Sigma^T \Psi T(t) - \Sigma^T \delta\phi(t) = C(t) \quad (6)$$

which can be simplified to:

$$A T(t) + E(t) = C(t) \quad (7)$$

where

$$A = \Sigma^T \Psi \quad (8)$$

This is a **J-by-K** matrix, and

$$E(t) = -\Sigma^T \delta\phi(t) \quad (9)$$





is a column vector of length  $J$  of systematic errors. If the assumption is made that the unknown error vector,  $\delta\phi(t)$ , is small, then  $E(t)$  will also be small with respect to  $AT(t)$  in equation (7). Under this assumption, equation (7) can be rewritten as follows:

$$AT(t) \approx C(t). \quad (10)$$

Upon inverting  $A$  in equation (10),  $T(t)$  can be solved every time that signals are received from the detectors. Unfortunately  $J \neq K$  in most cases and as a result this matrix is not square and cannot be simply inverted. Regardless, a minimum-norm least-squares solution,  $T_{LS}(t)$ , can always be found. Once  $T(t)$  is found, the reconstructed flux-vector can be calculated.

## 2.3 POTENTIAL PROBLEMS WITH METHOD

One of the first problems which may be encountered with the flux synthesis method is that there is no theoretical way to quantify the systematic error term,  $\delta\phi(t)$ . Part of this problem results because there is no set method for generating the expansion functions,  $\Psi^{(k)}$ . In addition, there is no restriction on the selection of the reactor configuration for which the basis functions should be computed.

Other possible sources of error result from uncertainties in calculating the  $\Sigma^{(j)}$  terms. This can lead to systematic errors in both  $A$  and  $C(t)$ . There can also be errors with the vector  $C(t)$  from noise in the detector output. A final source of error can occur



from numerical problems in determining the expansion functions. Some of these functions can be linear combinations of other expansion functions causing the matrix  $\mathbf{A} = \Sigma^T \Psi$  to be very ill-conditioned. In many cases this ill-conditioning can lead to least squares solutions which are completely meaningless because of round-off error amplification. Fortunately, this problem has been solved by Robert Jacqmin and is explained in detail in his 1991 doctoral thesis.



## **CHAPTER THREE: PRELIMINARY PLANNING FOR THE EXPERIMENTAL EVALUATION**

### **3.1 INTRODUCTION**

In the days and months leading up to the in-core experiments, a great deal of planning and testing was conducted in preparation for the actual tests. This chapter provides a chronological accounting of the steps undertaken and the problems that were overcome to make the project a success. This section will go into some detail so that the reader can fully understand the scope of the thesis. Some of the issues which were dealt with include the selection of the location for the detectors and the verification that the detectors would fit into the core and that their placement would have no detrimental affect on core performance. In particular it was necessary to verify that the presence of the



detectors would not cause control blade drop times to exceed the specified limit. In addition, there was some concern that the detectors might block cooling flow to the point of overheating the control blades. Some of the other items discussed were the problems encountered in devising a method of holding the detectors within the core and keeping track of their position within the core.

### 3.2 DETECTOR PLACEMENT FOR EXPERIMENT

The first problem which had to be solved in conducting this research was to find a location in the MITR-II core where neutron detectors could be housed for the experiment. Given the limited space and the tight core configuration (See Figure 3.2-1), the only reasonable choice was to utilize the water vent holes located at the outer periphery of the core tank. The function of these water vent holes is to allow for the movement of water displaced by the motion of the shim blades. Whenever a control blade moves in its slot (Again see Figure 3.2-1) in the core support housing assembly, there must be a means for water to enter or leave the slot. The required passage is provided by six small through-holes located along the side of each slot that allow water to flow into the water vent holes at the corners of the core support housing. Of the six water vent holes, one is occupied by the reactor's regulating rod and is unavailable for use. The remaining five are unoccupied and available to receive the neutron detectors for this research. Figure 3.2-2 is a vertical cross-section of the reactor core showing a typical water vent hole. Note that the hole does not penetrate along the full length of the core. In fact, the bottom of the water vent hole is 5.69 inches above the bottom plane of the fueled core region. While it





would be preferred to have a means of moving the detectors all the way to the bottom of the core, there is unfortunately no alternative.

For budgetary considerations, it was decided that only three neutron detectors would be used for this initial research. In order to best monitor the neutron flux profile in the reactor and to detect any perturbations in its shape, the detectors were to be arranged in a symmetric pattern around the core. Because water vent hole number six was occupied with the regulating rod, the best locations for the detectors were determined to be water vent holes 1, 3, and 5. This pattern was chosen to promote symmetry.



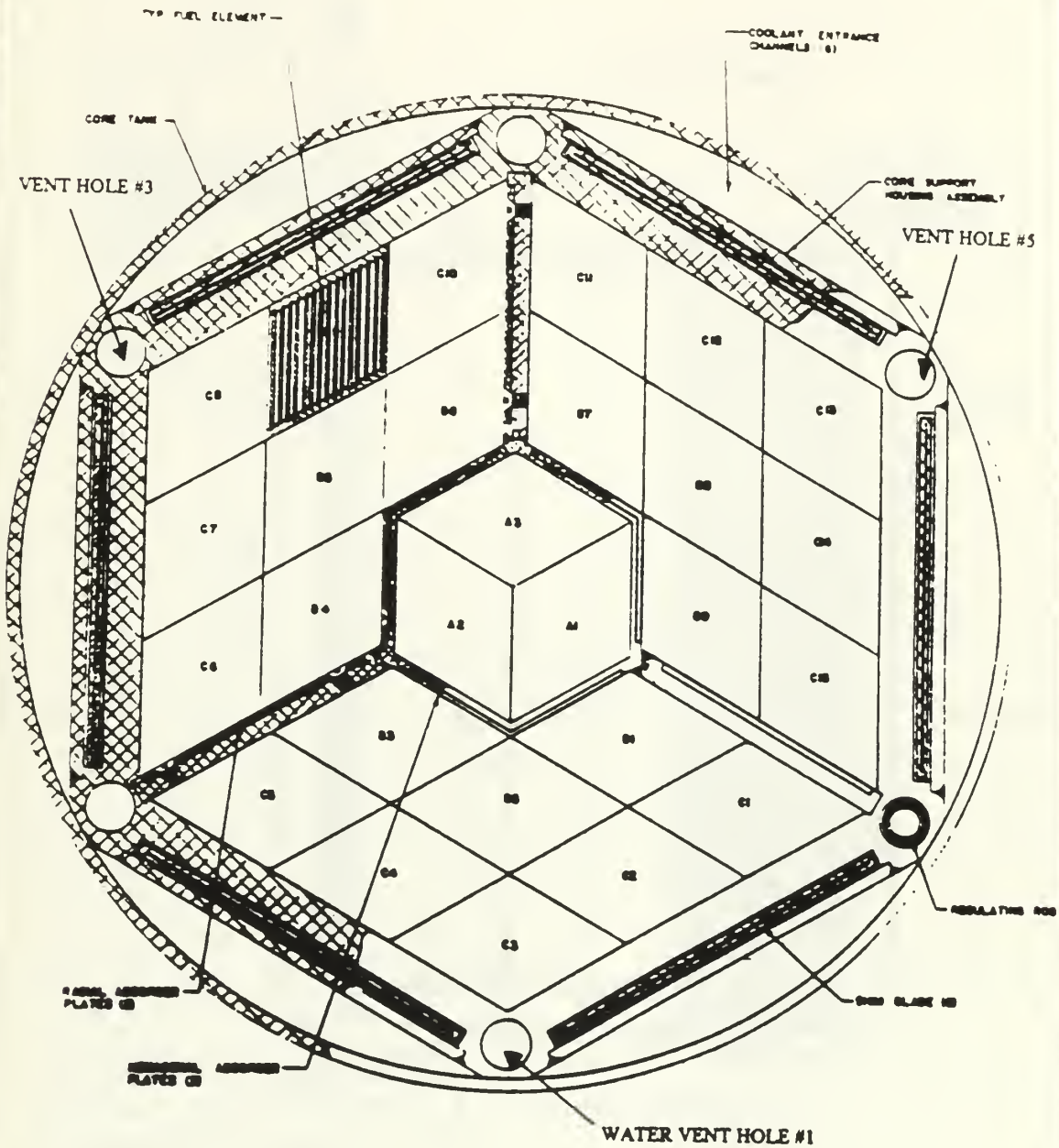


Figure 3.2-1: Top View of MITR-II Core



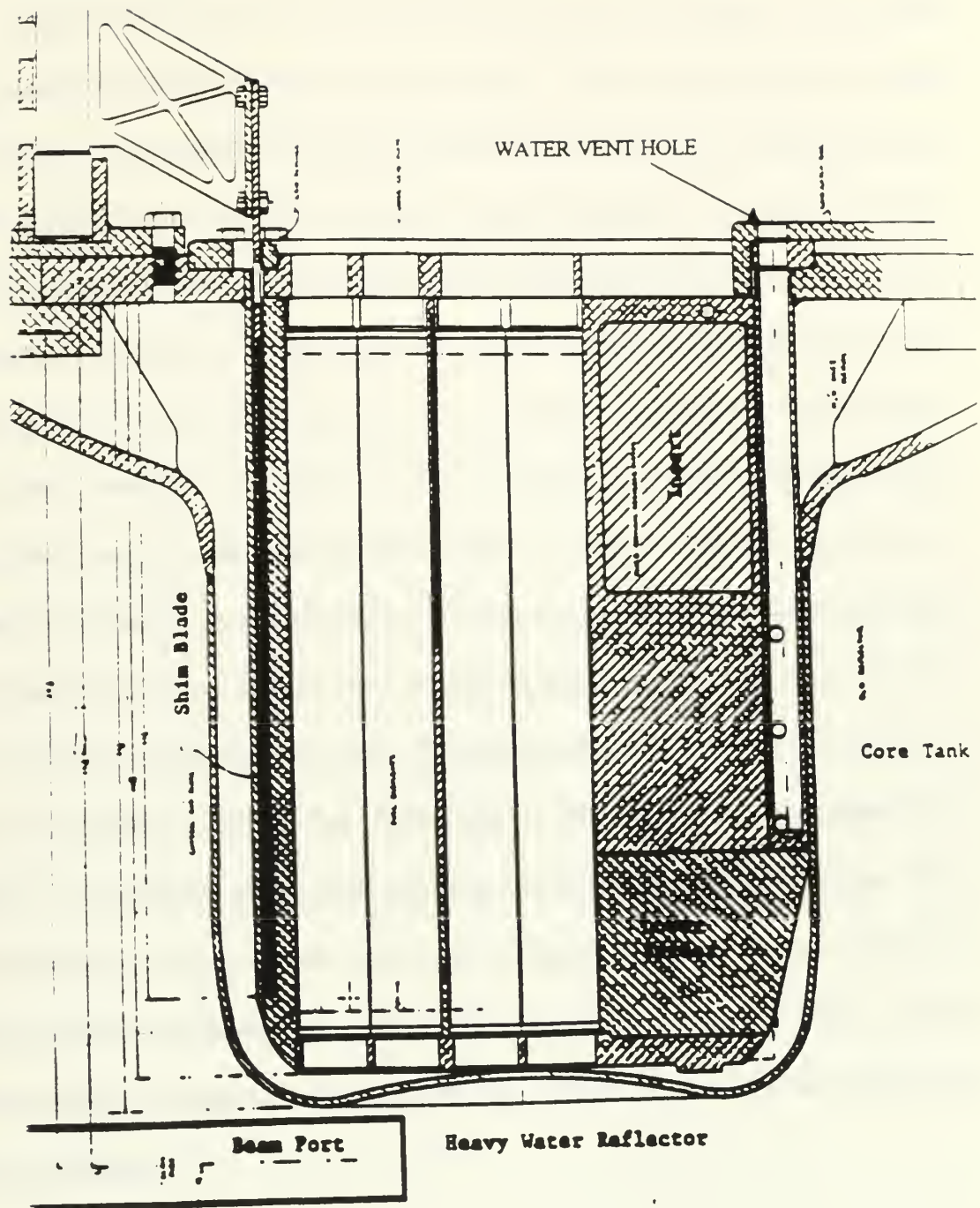


Figure 3.2-2: Vertical-Cross Section of MITR-II Core Showing a Water Vent Hole





### 3.2.1 DETERMINATION OF THE LIMITING DIMENSIONS

With the decision to place the neutron detectors in water vent holes 1, 3 and 5, the maximum allowable dimensions could then be found. This was accomplished by using MITR-II prints obtained from the MIT Nuclear Reactor Laboratory. In order to get a neutron detector down into the water vent holes, the detector must first pass down through a hole in the corner of the flow shroud. The flow shroud sits on top of the upper grid assembly of the core. It's purpose is to channel the flow leaving the core into the upper regions of the core tank without creating turbulence in the region where the shim blade control assemblies are located. After the initial startup of the MITR-II it was noticed that reactor power oscillated slightly even with no apparent shim blade or regulating rod motion. It was determined that this was caused by vibrations of the shim blades caused by the flow of light water leaving the fueled region of the core. The flow shroud was then added to prevent this. The inside diameter of the holes located in the corner of this shroud is 1.031 inches. Unfortunately, this is not the limiting dimension for a detector. The diameter of the water vent holes was determined to be 0.75 inches. With this information in hand the next step was to begin contacting detector vendors to determine what was available with a maximum outside diameter of 0.75 inches. Before we were willing to commit to buying any detectors however, an actual in-core dimensional test was conducted.



### 3.2.2 IN-CORE DIMENSIONAL MEASUREMENT

In order to verify that the information obtained from the prints was correct and to ensure that no unforeseen obstacles were present, an actual in-core dimensional measurement was conducted. In the first part of the test a one inch outside diameter three foot aluminum blank was inserted into the holes in the corners of the flow shroud to determine if the detectors that were eventually to be purchased would fit into all of these holes. This portion of the test was conducted to determine if a tube with a one inch outside diameter could be used in this location to house a support assembly from which the detectors could be lowered into the water vent holes below. This test was conducted on 9 June 1992 in accordance with the test procedure in Appendix A. With the reactor shut down and the reactor top lid removed, the aluminum blank was lowered into the core tank at the end of a long extension arm. Unfortunately, the aluminum blank didn't fit into any of the holes at the top of the flow shroud. While it appeared that the rod was very close to fitting into each of these holes, the tolerance of the measurements on the blueprints could put the dimensions slightly less than one inch. After these attempts failed, a hand-held spotlight was used to conduct a visual inspection of each water vent hole. By using the light and a pair of binoculars it was possible to look down into each hole. This inspection revealed yet another difficulty which had not been anticipated. At the base of the flow shroud, on top of the reactor core, it was noted that the diameter of the holes drilled through the upper grid plate appeared smaller than the diameter of the water vent holes. From this observation it was apparent that the limiting size for the detector was even smaller than the 3/4 inch diameter of the water vent holes.



Armed with this new information, the MITR-II prints were once again consulted. Unfortunately, it was very difficult to determine the exact dimensions of the holes in the grid plate assembly. After consulting with different members of the MIT Nuclear Reactor Laboratory Staff, it was decided that two additional aluminum blanks would be machined; one 3/4 inch outside diameter and the other 1/2 inch outside diameter. On 10 July 1992 the dimensional test was repeated. In the first attempt, the 3/4 inch rod was lowered into the core. While this rod did fit into the holes in the flow shroud it wouldn't quite fit through the grid plate. When the 1/2 inch rod was tried in water vent hole #1 it went all the way to the bottom of the vent hole. In order to ensure that all of the holes were uniform, this aluminum blank was lowered into vent holes two through five as well. The 1/2 inch aluminum blank fit into all of the vent holes except #2. It was later determined that the grid plate latching mechanism was blocking the aluminum blank in this hole. Since we had already decided to use water vent holes 1, 3 and 5 for symmetry reasons, this was not a concern. From this test it was decided that the detectors used would have to be limited to a maximum outside diameter of one-half inch. One more test needed to be performed, however, before any detectors could be purchased.

### **3.3 CONSEQUENCES OF WATER VENT HOLE BLOCKAGE**

With the maximum allowable size dictated by the limiting dimensions determined as above, it was next necessary to examine the possible consequences of blocking three water vent holes with an object of this size. Two possible consequences were postulated; first the blockage might reduce the control blade drop time because the vent passage was





now partially blocked, and second the blockage might cause a reduction in the control blade cooling flow resulting in their overheating

In order to accomplish this test, three separate half-inch aluminum blanks were machined. This procedure was conducted in conjunction with the in-core dimensional measurement described above on 10 July 1992. The full procedure is contained in Appendix A. To conduct this test, the half-inch outside diameter aluminum blank was sequentially placed into water vent holes 1, 3, 4, and 5 and the two adjacent shim blades were then raised and dropped one at a time. The drop time of each blade was measured to ensure it was within the allowable one second specification (MITR Technical Specification No. 3.9). The results of this test are recorded in Table 3.3-1. As can be seen from this table, all drop times are well within the required specification. Because the drop time on shim blade #1 was the longest of the six blades it was decided that the test should be repeated (and hence the two values for drop time). It is believed that the longer drop time associated with this blade is due to the presence of the regulating rod in water vent hole #6. In the final portion of this test, a half-inch aluminum rod was placed in water vent holes 1, 3, and 5 simultaneously. With the three rods in this configuration, the shim blade drop time test was performed on each rod. This portion of the test was intended to assure that the drop times would still be within the required specification with three water vent holes blocked, just as they would be during the experiment. The results of this test are shown in Table 3.3-2. As before, all times are well within the required specification. These tests confirmed that a detector with a half-inch outside diameter could be used in the water vent holes with no adverse affect on the control blade drop times.





To answer the question concerning the affect of blocking the water vent holes on the cooling of the shim blades, the MITR-II prints were once again consulted. From Figure 3.2-2 it is apparent that by blocking the water vent holes, the water flow to the control blade is actually increased, and not decreased. This would result in an increase in the cooling of the shim blades. Additionally because the detector will not completely block the water vent holes, there is still adequate room for the minimal cooling flow required by the shim blades. As a consequence of the above steps, the maximum outside diameter for a neutron detector was set at half-inch.



Table 3.3-1 Shim Blade Drop Times

Blocked Water Vent Hole	Shim Blade Tested	Drop Time (ms)
#1	Blade #1	602/589
#1	Blade #2	519
#3	Blade #3	481
#3	Blade #4	469
#4	Blade #4	468
#4	Blade #5	486
#5	Blade #5	479
#5	Blade #6	504

Table 3.3-2: Blade Drop Times with Water Vent Holes 1, 3, and 5 Blocked

Shim Blade Tested	Drop Time (ms)
Blade #1	568
Blade #2	554
Blade #3	480
Blade #4	474
Blade #5	494
Blade #6	503



### 3.4 DETERMINATION OF NEUTRON DETECTOR REQUIREMENTS

Once the maximum allowable size for the detector was determined, it was possible to begin contacting neutron detector vendors to get price estimates for three detectors. Because of the small size requirement, it quickly became apparent that there was really only one type of detector which would suit the needs of this research: the fission chamber neutron detector. While a self-powered neutron detector was small enough to work, the available sensitivities were considerably lower than those of fission chamber detectors. In addition, the response of the Rhodium wire type detectors was much too slow to be of use for transient measurements. This slow response results because of the relatively long half-life of the Rhodium-104 beta decay ( $T_{1/2} = 42.3$  seconds). Gas-type detectors such as He-3 and BF<sub>3</sub> were not considered because they are not typically designed for use in an in-core application. In addition, it was decided that the detectors used for this research should operate in a current mode, and as such they must have sufficient sensitivity to provide a detectable output. Current mode was selected over the pulse mode because this greatly simplifies the instrumentation system. Specifically, because the current is proportional to the neutron flux, the only piece of equipment needed to analyze the signals is a picoammeter. For a pulse mode detector, additional equipment is needed to integrate the output pulses and to count them. In order to satisfy these requirements for a current mode detector with adequate sensitivity, the fission chamber detector was selected [17].





### 3.4.1 REQUIRED DETECTOR SENSITIVITY

After consulting with a number of vendors of electronic equipment and also with staff members at the Nuclear Reactor Laboratory, it became evident that the detector current output should be in the range between 0.1 and 100  $\mu$ amps to simplify the electronic design. If the current was much below this range, then amplification equipment would have to be used to boost the signal to a useful value. This would add unnecessary cost and complexity to the instrumentation.

In order to determine the detector sensitivity needed to provide the desired current, it was necessary to estimate the thermal neutron flux in the reactor in the region of the water vent holes. This was accomplished by acquiring the most recent flux map from the CITATION data run for the reactor core. CITATION is a finite difference diffusion theory code developed by Oak Ridge National Laboratory [12]. The data provided was calculated for full power operations (5 MWth). The thermal flux values were therefore scaled to 50 kW. The results are shown in Tables 3.4.1-2 through 3.4.1-4. The axial position refers to the height above the bottom plane of the fueled region of the core. Figure 3.4.1-1 shows the azimuthal mesh used in the CITATION code. Water vent holes 1, 3 and 5 are located in azimuthal zones 6, 16 and 26 respectively. Table 3.4.1-1 shows the mesh interval that contains the water vent holes to be between radial zones 12 and 13. In order to get an estimate of the flux within the water vent holes, the readings for these two regions were averaged. Figures 3.4.1-2 through 3.4.1-4 are the graphical representations of the resulting flux profiles in water vent holes 1, 3 and 5.



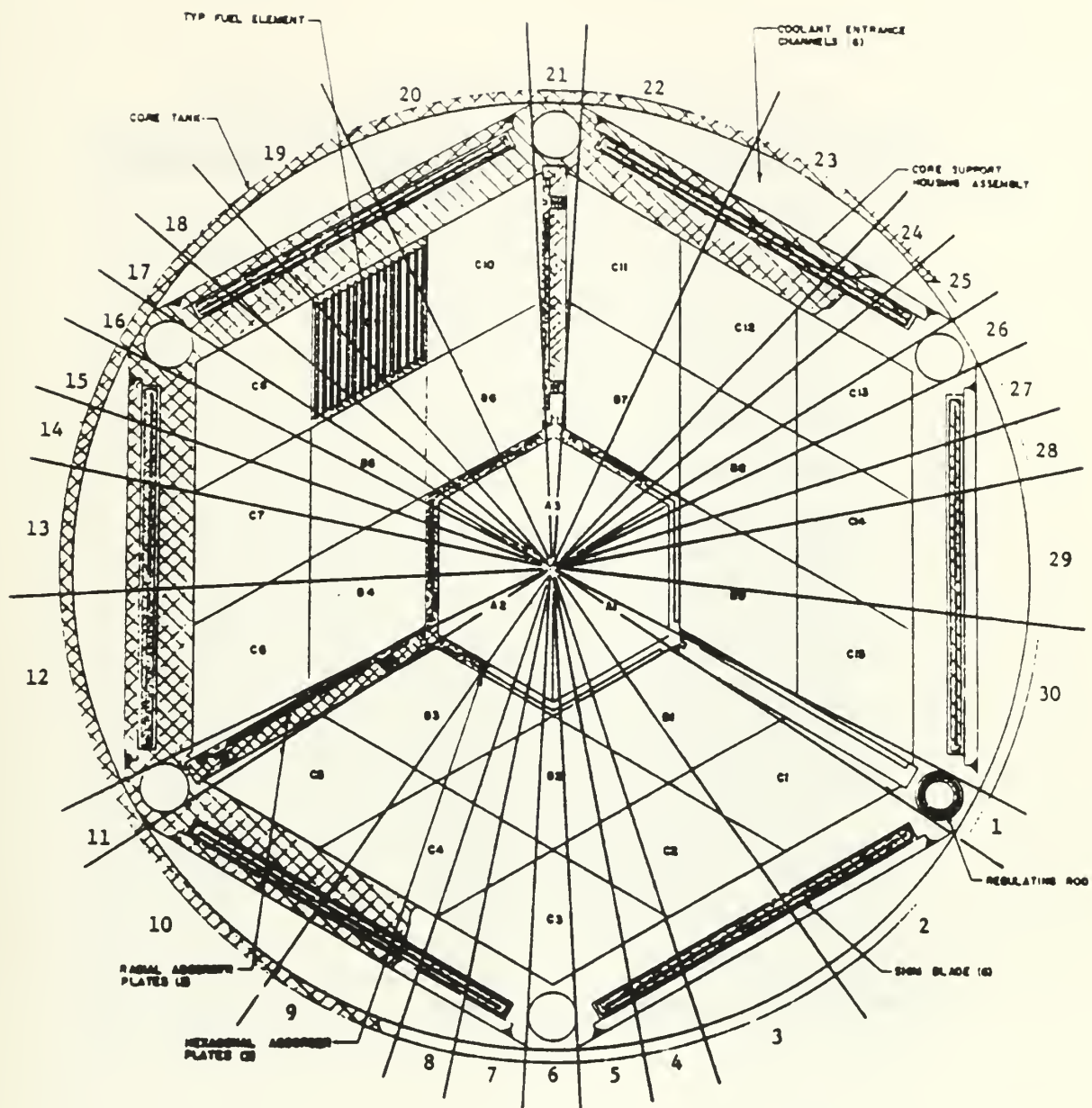


Figure 3.4.1-1: Azimuthal Mesh Used in CITATION Code



Table 3.4.1-1 Radial Mesh Used by CITATION Code

Radial Zone	Mesh Interval (cm)	Location
1	3.55	Inner A-Ring
2	0.9	Middle A-Ring
3	1.89	Outer A-Ring
4	0.63	Hexagonal Spider
5	1	Inner B-Ring
6	5.2	Middle B-Ring
7	1	Outer B-Ring
8	1	Inner C-Ring
9	3.28	Middle C-Ring
10	1	Outer C-Ring
11	0.95	Core Housing
12	1.08	Regulating Rod
13	0.64	Control Blades
14	0.95	Core Structure/Coolant
15	0.68	Core Tank
16	1.72	Heavy Water Reflector
17	15.44	Heavy Water Reflector
18	15.44	Heavy Water Reflector
19	68.03	Reflector Tank/Graphite



Table 3.4.1-2: Thermal Flux in Water Vent Hole #1 from CITATION

Axial Position	Radius=12	Radius=13	Avg Flux	Flux @ 50Kw
0.5	5.92E+13	6.84E+13	6.38E+13	6.3795E+11
1.5	5.88E+13	7.12E+13	6.498E+13	6.498E+11
3	6.07E+13	7.51E+13	6.789E+13	6.789E+11
5	6.48E+13	7.99E+13	7.235E+13	7.235E+11
7	6.77E+13	8.28E+13	7.524E+13	7.5235E+11
9	6.82E+13	8.29E+13	7.555E+13	7.5545E+11
11	6.58E+13	7.98E+13	7.28E+13	7.2795E+11
13	6.01E+13	7.30E+13	6.656E+13	6.656E+11
15	4.92E+13	6.14E+13	5.528E+13	5.528E+11
17	3.02E+13	4.18E+13	3.602E+13	3.6015E+11
19	2.22E+13	3.22E+13	2.724E+13	2.7235E+11
21	1.74E+13	2.57E+13	2.154E+13	2.154E+11
22.5	1.48E+13	2.22E+13	1.851E+13	1.8505E+11
23.5	1.34E+13	2.03E+13	1.687E+13	1.6865E+11





Table 3.4.1-3: Thermal Flux in Water Vent Hole #3 from CITATION

Axial Position	Radius=12	Radius=13	Avg Flux	Flux @ 50Kw
0.5	5.69E+13	6.59E+13	6.142E+13	6.142E+11
1.5	5.67E+13	6.88E+13	6.276E+13	6.276E+11
3	5.86E+13	7.29E+13	6.579E+13	6.5785E+11
5	6.26E+13	7.78E+13	7.022E+13	7.0215E+11
7	6.54E+13	8.07E+13	7.305E+13	7.305E+11
9	6.58E+13	8.09E+13	7.337E+13	7.337E+11
11	6.35E+13	7.79E+13	7.073E+13	7.073E+11
13	5.81E+13	7.14E+13	6.471E+13	6.4705E+11
15	4.75E+13	6.00E+13	5.379E+13	5.3785E+11
17	2.90E+13	4.09E+13	3.496E+13	3.4955E+11
19	2.14E+13	3.16E+13	2.652E+13	2.6515E+11
21	1.68E+13	2.53E+13	2.105E+13	2.1045E+11
22.5	1.43E+13	2.19E+13	1.812E+13	1.8115E+11
23.5	1.30E+13	2.01E+13	1.652E+13	1.652E+11



Table 3.4.1-4: Thermal Flux in Water Vent Hole #5 from CITATION

Axial Position	Radius=12	Radius=13	Avg Flux	Flux @ 50Kw
0.5	6.28E+13	7.31E+13	6.793E+13	6.7925E+11
1.5	6.21E+13	7.57E+13	6.892E+13	6.8915E+11
3	6.39E+13	7.96E+13	7.172E+13	7.1715E+11
5	6.80E+13	8.44E+13	7.621E+13	7.621E+11
7	7.10E+13	8.73E+13	7.915E+13	7.915E+11
9	7.15E+13	8.74E+13	7.942E+13	7.942E+11
11	6.89E+13	8.40E+13	7.648E+13	7.6475E+11
13	6.29E+13	7.68E+13	6.985E+13	6.985E+11
15	5.15E+13	6.45E+13	5.8E+13	5.7995E+11
17	3.17E+13	4.40E+13	3.783E+13	3.7825E+11
19	2.33E+13	3.39E+13	2.86E+13	2.86E+11
21	1.82E+13	2.70E+13	2.26E+13	2.26E+11
22.5	1.55E+13	2.33E+13	1.941E+13	1.9405E+11
23.5	1.40E+13	2.13E+13	1.769E+13	1.7685E+11



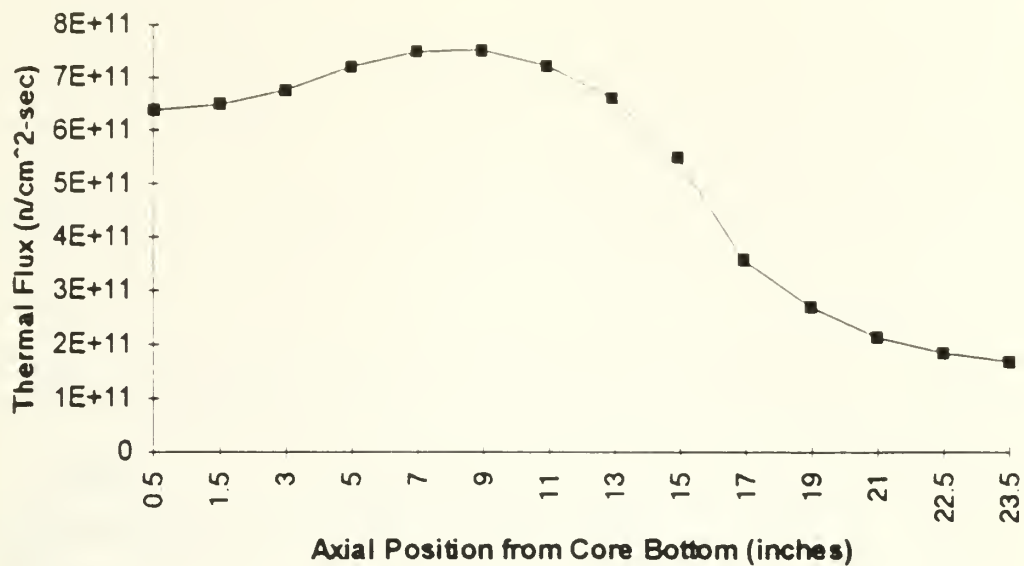


Figure 3.4.1-2: Thermal Flux in Water Vent Hole #1 @ 50 kW

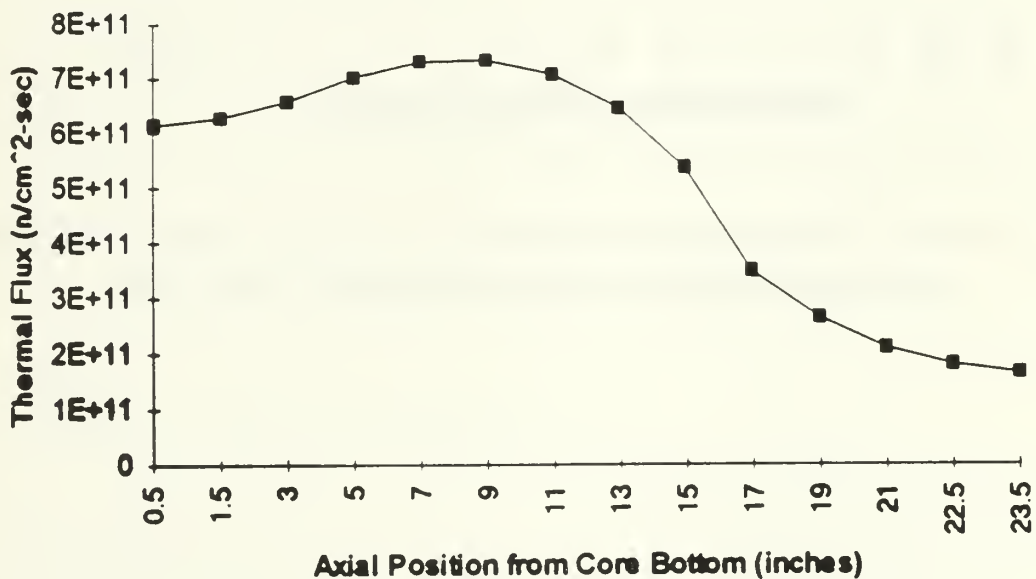


Figure 3.4.1-3: Thermal Flux in Water Vent Hole #3 @ 50 kW





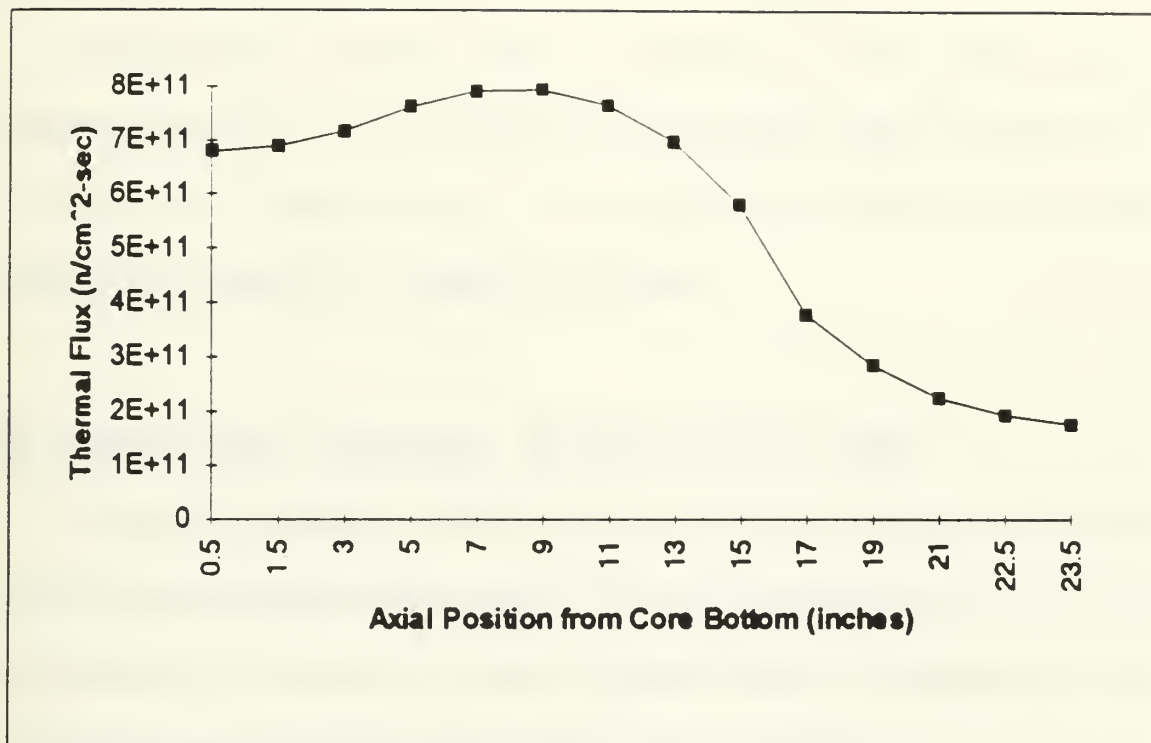


Figure 3.4.1-4: Thermal Flux in Water Vent Hole #5 @ 50 kW



From these figures and tables, one can note that the thermal neutron flux at 50 kW is in the range between  $1 \times 10^{11}$  and  $8 \times 10^{11}$  neutrons/cm<sup>2</sup>-s. While the shim bank and regulating rod heights will be different at 50 kW than at 5 MW because of the differences in equilibrium Xenon, the magnitude of the thermal flux will still scale reasonably well. This will not, however, be the case for determining the location of the peak flux or analyzing the shape of the neutron flux profile at powers other than 5 MW.

In order to get a detector current in the range of 0.1 to 100  $\mu$ Amps with an average thermal flux of  $1.5 \times 10^{11}$  neutrons/cm<sup>2</sup>-s, the sensitivity must be between  $6.67 \times 10^{-16}$  and  $6.67 \times 10^{-19}$  Amps/nv(thermal). For this application it would be preferred to have a detector with a sensitivity at the higher end of this scale.

### **3.5 DETECTOR SUPPORT WITHIN THE CORE**

During the experiment it will be necessary to position the detectors within the water vent holes at different axial positions. In order to accomplish this and to know the exact position of the detectors at all times, a support rig had to be designed and built. This section explains the thought process used to develop this design.

#### **3.5.1 SUPPORT RIG REQUIREMENTS**

The support rig should be capable of positioning the detectors within each of the water vent holes and allowing for their movement up and down these channels during critical operation. This requirement is greatly simplified because the reactor top shield lid



will be removed during the experiment. In addition to knowing the precise axial position of the detectors, they must be centered precisely within the three water vent holes.

Because of the last requirement for centering the detectors within the water vent holes, it did not appear feasible to lower the detectors into these holes from the core top without some sort of guide tube. As was discussed earlier, the limiting dimension for placing any object into the water vent holes was set at a half-inch. If a tube was used to guide and position the detectors within the vent holes, then the detectors would now be limited by the inside diameter of the tube used for this purpose. After consulting with the fission chamber detector vendors, this problem was negated because they had detectors with outside diameters down to the 0.20 inch range.

Because the fission chamber detectors being considered for this research were designed for use within commercial pressurized water reactor cores, there would be no problem with allowing them to be exposed to the primary coolant. However this would result in their becoming contaminated because of contact with the light water coolant within the core. In order to prevent this contamination problem, it was decided that the detectors and all associated cabling should be kept dry during the in-core phase of the experiment. An added benefit of keeping the detectors encased within a tube was that the detectors would not be affected by any flow in the water vent holes.

The final requirement for the support rig was that it be easily transported and be designed for temporary installation only. Because this experiment is only an evaluation of the feasibility of a concept and not a full scale implementation, the rig was to be designed



to be placed in the reactor fairly quickly and easily for testing purposes, and then be completely removed once that testing was completed.

### 3.5.2 SUPPORT RIG DESIGN

In order to satisfy all of the above requirements it was determined that a half-inch outside diameter tube would be purchased for each of the three water vent holes to be used in the experiment. Because the tubes were to keep the detectors dry, they needed to be long enough to pass from the bottom of the water vent hole to a height above the core tank water level. It was decided that the tops of the tubes should extend approximately three feet above the top of the reactor shield lid seating surface to facilitate the movement of the detectors during the experiment. By consulting with the blue prints for the MITR-II, the tube length was set at fifteen feet.

For compatibility reasons, the material selected for the tubes was 6061 aluminum. The tube selected for this research was a half-inch outside diameter tube with a 0.065 inch wall thickness (0.370 inch inside diameter). Unfortunately the longest length tube available was twelve feet. After consulting with the machine shop at the Nuclear Reactor Laboratory, it was determined that four of these tubes should be purchased and the fourth tube cut up into three foot segments to be welded to the longer lengths. Because the tubes were open ended, the machine shop was contracted to machine aluminum caps and weld them to the bottom end of the tubes.

Because these tubes were to remain dry during critical operations, a minimum of two bends had to be placed in them to prevent streaming of radiation via the tops of the





tubes. The first of these bends was placed in a section of the tube approximately two feet above the top plane of the core. Figure 3.5 2-1 is an illustration of one of the instrument guide tubes. In order to track the axial location of the fission chambers, the cabling running to the each detectors was marked. Once the detectors were purchased this was accomplished by pushing each of the detectors to the bottom of its respective guide tube. Because the detector cabling was relatively rigid, this was easily done. With the detectors at the bottom of the tubes, the cabling was marked. This bottom position corresponds to the zero inch position. The detectors were then withdrawn one inch at a time and the cable marked again. This was done up to the twenty-four inch position. At each of the marked positions a half-inch wide strip of heavy masking tape was attached (folded over the wire and back on top of itself so it held firmly). The tape was then cut to form a notch which would rest on the top lip of the instrument tube when it was positioned vertically, just as it would be when in the core. The tape was then marked with the zero through twenty-four inch positions. Figure 3.5.2-2 shows how this scheme was implemented.



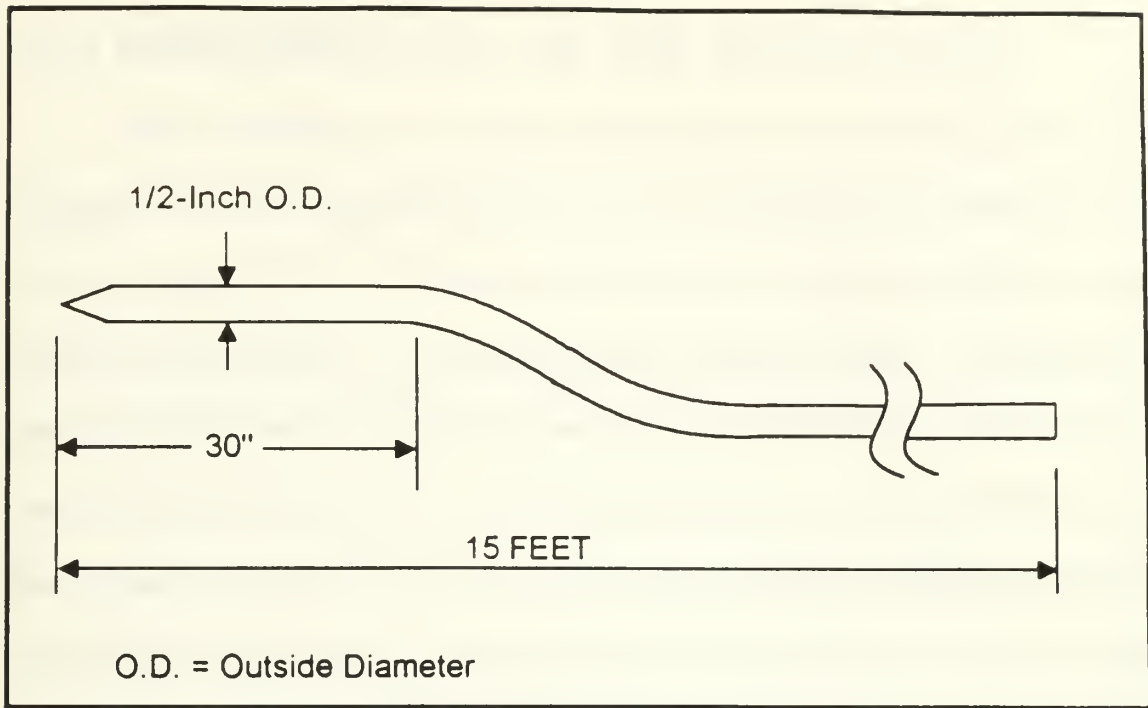


Figure 3.5.2-1: Typical Instrument Guide Tube

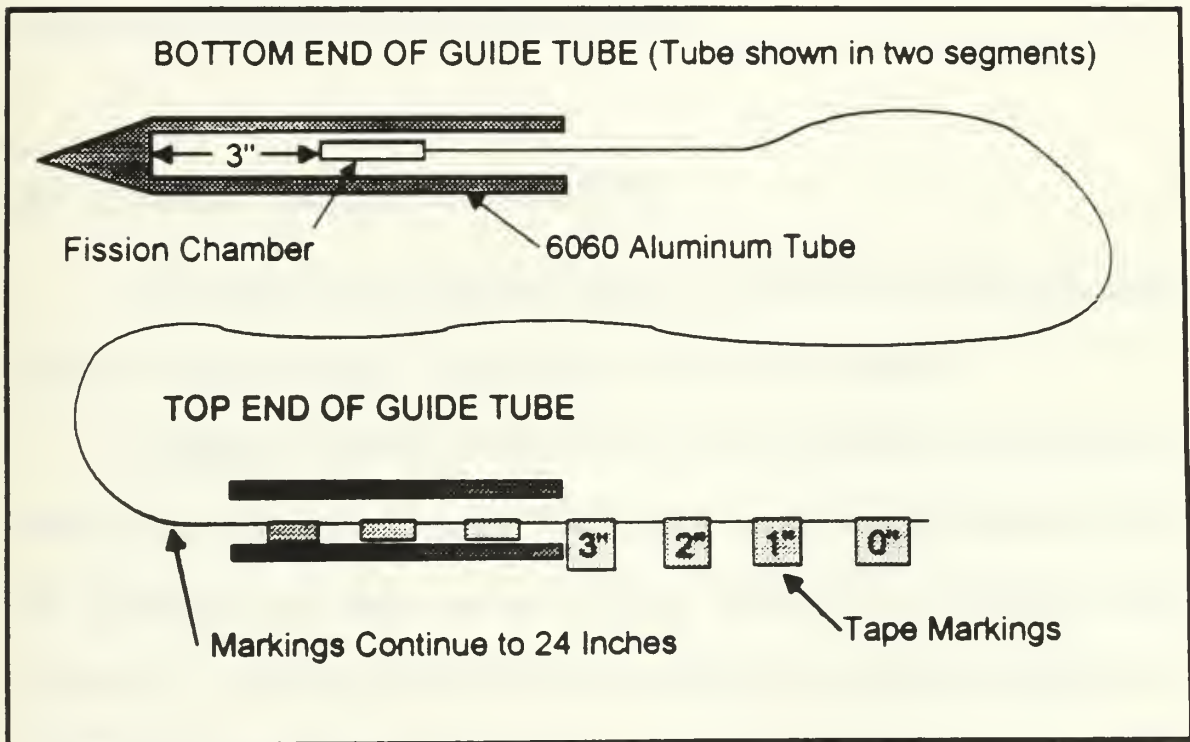


Figure 3.5.2-2: Detector Axial Position Keeping Scheme



### 3.5.3 IMPLEMENTATION OF THE SUPPORT RIG

Prior to conducting the experiment, with the reactor shut down and the top shield lid removed, the three instrument guide tubes are to be lowered into the reactor core. The two bends placed in each of the tubes will allow the tops of them to be pulled up snug to the sides of the core tank. They will then be firmly attached with tape. This accomplishes two things; first it secures the tubes so they will not be affected by any flow within the core, and second it positions the tubes at the edge of the core so the experimenters do not have to reach over the top of the core tank while the reactor is operating. During the experiment the axial position of each detector can be varied by moving the detector cabling in or out of the guide tube and resting the taped notch on the top of the tube at the desired height. Once the experiment is completed, the tubes and detectors can be removed and stored until the next test is conducted.

### 3.6 OTHER DESIGN PLANNING

The remainder of the preliminary planning conducted for this experiment was in the area of electronic design. This area is discussed in the next chapter.

In addition to equipment design, the other area of preliminary work done for this research was administrative in nature. This involved scheduling experiment times, writing test procedures and filling out the necessary paperwork for conducting in-core experiments. All of the procedures for this research can be found in the appendices and are discussed in more detail in Chapter Five.





## **CHAPTER FOUR: DESIGN, CONFIGURATION, AND TESTING OF ELECTRICAL EQUIPMENT**

### **4.1 INTRODUCTION**

In this chapter the methods used to analyze the output current from each of the three fission chamber detectors are described. This includes a description of the required analysis and the hardware used to interpret and record the data. Some explanation of the steps taken in actually acquiring the hardware is included so future researchers can gain an understanding of the process. Finally, the design and configuration of the data collection system is described in some detail and the initial testing of the system is explained.



## 4.2 ACQUISITION OF THE FISSION CHAMBER DETECTORS

The first step in acquiring the fission chamber detectors was to determine which companies were actually manufacturing these types of detectors. It turns out that there are currently only four vendors in the United States that sell fission chambers. These are Imaging and Sensing Technology, TGM, Reuter-Stokes, and LND. Of these only three had detectors small enough for this research and only two of them had a detector specifically designed to operate in the current mode. These two companies were Imaging and Sensing Technology (IST) and Reuter-Stokes. After receiving price quotations from each of these companies, the clear winner was IST. Their detectors were priced at least 70% less than the comparable models at Reuter-Stokes. The actual model purchased from IST was the WL-23798. It has a minimum neutron sensitivity of  $1 \times 10^{-17}$  Amps/nv (thermal) and can operate in a thermal flux up to  $8.7 \times 10^{13}$  nv. A specification sheet from the company is included as Figure 4.2-1. The detector described on this sheet is the NY-10336. This detector is identical to the WL-23798 with the exception that the NY-10336 has a drive cable and reel which is used in pressurized water reactor applications.

For this research three WL-23798 fission chamber detectors were purchased. The detector order was placed on 11 September 1992 and the three detectors were received at the Nuclear Reactor Laboratory on 30 December 1992. The decision to purchase only three detectors was based on financial constraints. While the project will eventually use a total of nine detectors (three per hole), it was decided that for the first year it would be prudent to evaluate the detectors and electronics prior to committing large resources to an



as yet unproved experimental method. The results from this experiment will be used to evaluate the feasibility of the method and the purchase of the six additional detectors will be contingent upon these results.





IMAGING & SENSING TECHNOLOGY  
Westinghouse Circle  
Horseneheads, NY 14845

## Sensor and Control

### In-Core Radiation Detector

Up to  $8.7 \times 10^{13}$  [nv]  
650°F (340°C) Operation  
 $1.0 \times 10^{-17}$  [A/nv] Sensitivity

Type Number: NY-10336

#### Application

The NY-10336 is a miniature fission chamber designed for in-core operation in thermal neutron flux levels up to  $8.7 \times 10^{13}$  neutrons/(cm<sup>2</sup> second). The chamber is constructed of stainless steel with high purity aluminum oxide insulation and will operate in any position at ambient temperatures up to 650°F in a wet or dry environment. The detector is provided with an integral coaxial cable which has a stainless steel jacket and aluminum oxide insulation. The coaxial cable length is specified by customer at time of order and can vary from 10 feet to 180 feet. The NY-10336 has a minimum neutron sensitivity of  $1.0 \times 10^{-17}$  amperes/nv and a maximum gamma sensitivity of  $3.0 \times 10^{-14}$  amperes/roentgen/hour.

#### Mechanical

Chamber Diameter (max./min.)	(0.188/0.183) / (4.78/4.65) [inch / mm]
Cable Diameter (max./min.)	(0.041/0.038) / (1.04/0.98) [inch / mm]
Length:	
Chamber (Maximum)	2.3 / 58.4 [inch / mm]
Sensitive Length	1.0 / 25.4 [inch / mm]
Connector	Subminax Plug Amphenol 27-7 or Standard Male BNC
Net Weight	2 / 0.9 [lbs / kgs]
Shipping Weight	14 / 6.4 [lbs / kgs]

#### Materials

Cable Sheath	321 Stainless Steel
Detector Outer Case	304 Stainless Steel
Inner Electrode	304 Stainless Steel
Detector Insulation	Al <sub>2</sub> O <sub>3</sub>
Cable Insulation	Al <sub>2</sub> O <sub>3</sub>
Neutron Sensitive Material	U <sub>3</sub> O <sub>8</sub> enriched to more than 90% U <sub>235</sub>
Gas Fill	Argon

#### Impedance

Resistance to 100°F (min.)	$5 \times 10^6$ [Ω]
Resistance with first 25 (7.6 m) feet of cable at 650°F and remainder at 120°F (min.)	$5 \times 10^7$ [Ω]
Resistance with first 25 (7.6 m) feet of cable at 120°F and remainder at 120°F (min.)	$7 \times 10^6$ [Ω]
Capacitance, Detector plus Cable	73 [pF/ft]

#### Ratings

Maximum Voltage Between Electrodes	250 [Vdc]
Temperature, excluding internal heating (max.)	340°C / 650°F
Pressure (max.)	50 / 3.5 [psig / kg/cm <sup>2</sup> ]
Thermal Neutron Flux (max.)	$8.7 \times 10^{13}$ [nv]
Gamma Flux (max.)	$1.7 \times 10^6$ [R/Hr]
Total Integrated Neutron Flux at 650°F for 10% Loss in Sensitivity (min.)	$3.0 \times 10^{20}$ [nvt]

#### Typical Operation

Operating Voltage (Note 1)	30 to 150 [Vdc]
Thermal Neutron Flux Range	$1 \times 10^6$ - $8.7 \times 10^{13}$ [nv]
Minimum Thermal Neutron Sensitivity	$1.0 \times 10^{-17}$ [A/nv]
Maximum Gamma Sensitivity	$3.0 \times 10^{-14}$ [A/R/Hr]

#### Notes

1. Saturation voltage varies with neutron flux level.

Form 1000 / IST/IN-CORE/FORMS/NY-10336 TES / Rev. 2 (10/6/93)

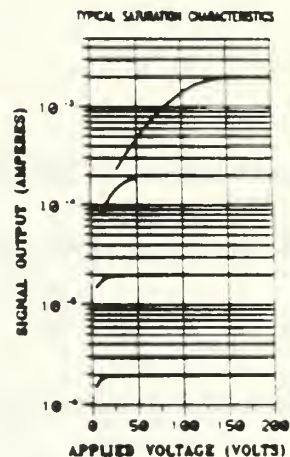
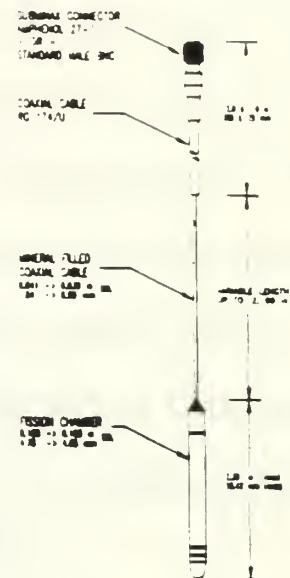


Figure 4.2-1: Specifications for NY-10336 Fission Chamber Detector





### 4.3 FISSION CHAMBER ADAPTER BOXES

In order to interface the fission chamber detectors with an ammeter it was necessary to purchase a special adapter box which isolates the bias signal from the detector output signal. The designation of these adapter boxes, manufactured by IST, is E-2709A. One of these boxes is required for each detector. The adapter box has one input for the DC power supply and one input for the fission chamber detector signal. The adapter box sets up the proper current path for the signal returning from the fission chambers and routes it to the output which is fed to an ammeter. The two inputs have female BNC connectors and the one output for the ammeter has a tri-axial connector. It turns out that this is unfortunate because the ammeter purchased has only a BNC input. This was corrected by purchasing a tri-axial to BNC adapter. In the future, however, these adapter boxes should be requested with a BNC output fitting.

### 4.4 POWER SUPPLY

The manufacturer's recommended operating voltage range for the fission chamber detectors is 30 to 150 volts. The technicians at IST noted that the operating sensitivity of the detectors is more constant at the upper end of this scale. Figure 4.4-1 is a typical operating curve for the type of fission chamber detectors that were purchased. In order to take advantage of the flat plateau region of this curve, a potential of approximately 140 volts was desired.

Because the currents involved in this research were on the order of microamps, a floating DC power supply was selected to minimize the noise in the signal output. While



these units are available commercially, they are expensive. In order to minimize the expense of the power supply the author built his own from batteries supplied by the MIT Nuclear Reactor Laboratory. The power supply consisted of two 67.5 volt Ever-Ready dry cell batteries hooked together in series. One power supply was built for each of the three fission chamber detectors. In order to hook these power supplies up to the E-2709A adapter boxes, a coaxial cable was soldered to each unit and a male BNC connector was attached to the end of each cable.

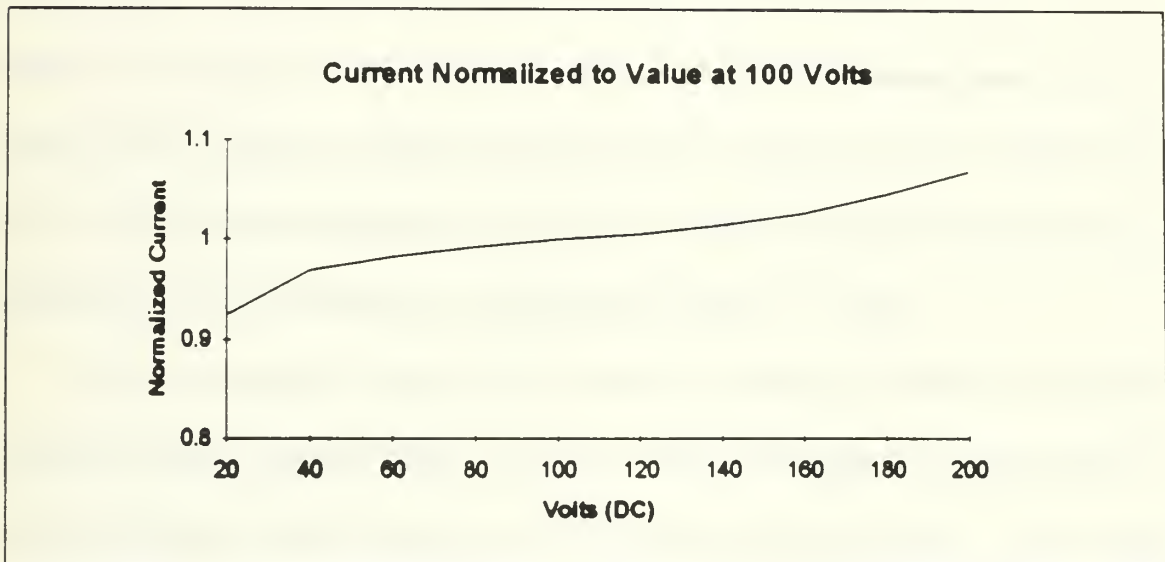


**Figure 4.4-1: Typical Operating Curve for WL-23798 Fission Chamber**



## 4.5 DATA ACQUISITION EQUIPMENT

### 4.5.1 AMMETER

In order to measure the output current from the fission chamber detectors, a very sensitive ammeter was required. The device selected was the Keithley Instruments Model 485 Autoranging Picoammeter. This model was selected because it was competitively priced, had sufficient sensitivity to operate in the current range of interest, and because it has an analog output which can be used as an input for analog-to-digital conversion.

The Model 485 is basically a 4 1/2 digit autoranging picoammeter with seven DC current ranges from zero to two milliamps all the way down to zero to two nanoamps. The heart of the Model 485 is a current-to-voltage converter followed by an analog-to-digital converter that translates the conditioned analog input signals into a form usable by the microcomputer. The current measurements are based on a comparison of an unknown signal with an internal -2 volt reference voltage. During each measurement cycle the microprocessor samples the unknown signal and uses it along with a zero measurement and the -2 volt signal measurement to compute the unknown voltage. The manufacturer's specifications for this instrument are summarized in Table 4.5.1-1 [18].

Another important output from the current-to-voltage converter is an analog output signal which is proportional to the input current. This signal is monitored using the analog output banana jacks located on the rear panel of the picoammeter. The voltage output from these jacks is between zero and 2 volts for all scales except the 2 nA range. In this range, the output is between zero and 200 millivolts.

In addition to the picoammeters hooked up directly to the three fission chamber detectors, there is also a Keithley Model 485 in the MITR-II control room which is used



to read the output signal from channel seven, one of the ex-core fission chambers used for reactor operations and control. This detector is physically located below the core and provides the most stable indication of neutronic power at varying shim blade heights. The analog output from this detector will be used in this research to provide a baseline power signal.





Table 4 5.1-1. Specifications of Keithley Model 485 Picoammeter

Range	Resolution	Accuracy (1 year) 18 - 28 °C $\pm(\% \text{ rdg} + \text{counts})^\dagger$	Analog Rise Time (10 - 90 %)	Normal Mode Rejection Ratio (50 or 60 Hz)	Maximum Continuous Input *
2 nA	0.1 pA	0.4 + 4	60 ms	70 dB	350 VDC
20 nA	1 pA	0.4 + 1	60 ms	70 dB	350 VDC
200 nA	10 pA	0.2 + 1	6 ms	65 dB	350 VDC
2 $\mu$ A	100 pA	0.15 + 1	3 ms	65 dB	350 VDC
20 $\mu$ A	1 nA	0.1 + 1	3 ms	65 dB	50 VDC
200 $\mu$ A	10 nA	0.1 + 1	1 ms	65 dB	50 VDC
2 mA	100 nA	0.1 + 1	1 ms	55 dB	50 VDC

$^\dagger$  When properly zeroed.

\* With no limiting resistance: 1000 VDC with external 100 k $\Omega$  series resistance.

INPUT VOLTAGE BURDEN: Less than 200  $\mu$ V.

RANGING: Manual or Autoranging.

AUTORANGING TIME: Average 250 ms per range.

SETTLING TIME AT DISPLAY: Less than 1 second to within 2 counts on fixed range.

CONVERSION PERIOD: 300 ms.

TEMPERATURE COEFFICIENT(0°-18°C & 28°-50°C): $\pm(0.1 \times \text{applicable accuracy spec})$ per °C.

MAXIMUM COMMON MODE VOLTAGE: 30V rms, DC to 60 Hz sine wave.

ANALOG OUTPUT:

Output Voltage: +1V = -10000 counts, except +100 mV = -10000 counts on 2nA range.

Output Resistance: 1000 $\Omega$

REL: Pushbutton allows zeroing of on range readings. Allows relative readings to be made with respect to baseline value. Front panel annunciator indicates REL mode.

DATA STORE and MIN/MAX: 100 reading storage capacity; records data at one of six selectable rates from 3 readings/second to 1 reading/hour, or by manual triggering. Also detects and stores maximum and minimum readings continuously while in the data store mode.

LOG: Displays logarithm (base 10) of the absolute value of the measured current (examples: -3.000 =  $\pm 1$ mA; -6.301 =  $\pm 0.5$  $\mu$ A).

DISPLAY: 4 1/2 digit LCD, 0.5" height; polarity, range and status indication.

OVERRANGE INDICATION: "OL" displayed.

CONNECTORS:

Input: BNC.

Analog Output: Banana Jacks.

OPERATING ENVIRONMENT: 0-50°C, less than 70% R.H. up to 35 °C; linearly derate 3% R.H./°C up to 50°C.

STORAGE ENVIRONMENT: -25°C to +60°C.

POWER: 105-125V or 210-250V (switch selected), 90-110V available, 50-60Hz, 12 VA.

DIMENSIONS, WEIGHT: 85 mm high x 235 mm wide x 275 mm deep. (3 1/2"x9 1/4"x10 3/4")

Net Weight: 1.8 kg (4 lbs.)



## 4.5.2 ANALOG-TO-DIGITAL CONVERTER

In order to record the data received from the fission chamber detectors an analog-to-digital (A/D) converter was purchased. An A/D board receives an analog input and converts it to a digital signal which can be stored in computer memory for later analysis. This information can then be transferred to floppy disks for transfer to different machines.

In deciding which type of A/D board to buy, five vendors were consulted. These were: Data Translation, Digital Distributors, Keithley Metrabyte, National Instruments, and Omega Technologies. Each company offered several A/D boards which would fit the needs of the research and all were comparably priced, but Data Translation was finally selected over the other four companies because their sales personnel were the most helpful and they are a local company.

Because the rate of change of neutronic power is relatively slow, it was decided that money could be saved by purchasing a board with a "slower" throughput. The model finally settled on was the DT2801 designed for use with IBM-compatible computers. This A/D board has a maximum throughput of 13.7 kHz. It accommodates either eight differential inputs or 16 single-ended inputs. For this research the board will be used in the single-ended configuration. Even if all 16 inputs were utilized, the maximum sampling rate for each channel would still be 856.25 Hz. That is to say that a signal could be read and recorded at the rate of 856.25 times per second. That is much faster than any transient that would ever be encountered for this work. The manufacturer's specifications for this board are listed in Table 4.5.2-1.



The input voltage signals to the A/D board are read and converted with 12 bit resolution into binary code. The 12 bit resolution means that the converter can assume  $2^{12}$  different states and thus divides the input voltage range into 4096 pieces or segments. Thus, for a unipolar input range of zero to ten volts, the resolution would be 2.44 mV; and for a zero to 2.5 volt input range, the resolution would be 0.61 mV. The A/D board takes this input voltage and converts it to a binary word which represents the input voltage for the channel being read. This binary code is then transferred by the computer's operating system to the A/D board software program. It is then stored on the computer's hard disk drive for future analysis [19].



Table 4.5.2-1: Features of DT-2801 A/D Board

- IBM PC/XT/AT-compatible analog and digital I/O board with 13.7 kHz throughput A/D, 16 Single-Ended or 8 Differential Inputs and an onboard microprocessor that controls critical timing and error checking operations.
- A/D features:
  - 13.7 kHz throughput
  - 12 bit resolution
  - Input voltage ranges: 0-1.25, 2.5, 5, 10; or  $\pm 1.25$ , 2.5, 5, 10
  - Up to 16 single-ended or 8 differential input channels
- Onboard programmable clock which initiates A/D operations





### 4.5.3 A/D BOARD SOFTWARE

In order to configure the DT2801 A/D board and to analyze the stored data, the Global Lab Data Acquisition software package was purchased from Data Translation. Global Lab is an MS-DOS compatible menu-driven software package specifically designed for data acquisition, display, and analysis. The data acquisition module supports key hardware architectural features, including dual-DMA continuous performance data transfers, onboard and external clocks, channel-gain list, and counter/timer circuits. Extended and expanded memory are also supported to accommodate large data sets.

The Global Lab software provides continuous real-time display of data as it is acquired. It also provides post-acquisition data display for more detailed examination and analysis. This package also performs statistical analysis of acquired data values, and can calculate minimum and maximum data values, maximum delta, arithmetic mean, and the standard deviation. In addition, the STATPACK signal processing module performs much more involved statistical analysis.

## 4.6 INSTRUMENTATION SYSTEM CONFIGURATION

Figure 4.6-1 shows the assembly of the various components used to form the instrumentation system. Because this system will be used on a temporary basis only, it must be easily transportable. For this reason the equipment is not hardwired together and the components remain separated. If this system were ever to be used on a more permanent basis it would be wise to mount the components into one solid chassis and hardwire them all together.



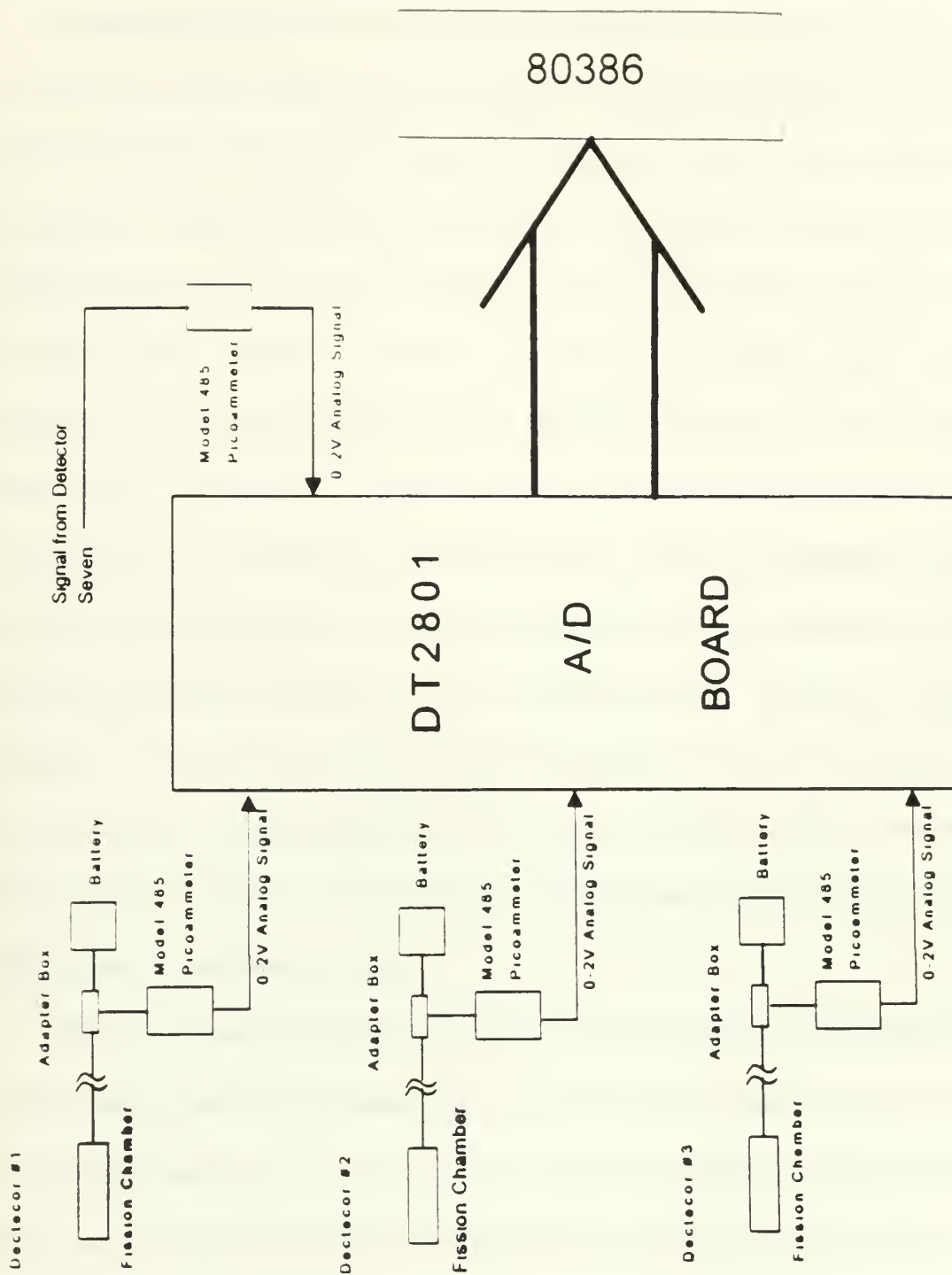


Figure 4.6-1. Block Diagram of Instrumentation System



#### 4.6.1 DESCRIPTION OF INSTRUMENTATION SYSTEM

Figure 4.6-1 shows how each of the three fission chamber detectors connects to its respective E-2709A adapter box. As was mentioned previously this junction is made with BNC connectors. Each detector also has its own battery power supply connected to this adapter box. Again the connection is made with a BNC fitting. The signal from each adapter box is routed to its respective Keithley Model 485 Picoammeter. During testing, the current output from each detector can be read on the digital display on each picoammeter. The analog output from each Keithley, including the one in the MITR-II control room for channel seven, is routed to the DT 2801 A/D board. For this research the A/D board will be configured for single-ended inputs. This is accomplished by routing the positive analog output signal to the selected channel on the A/D board's screw terminal panel and connecting the negative leads to a common ground. In order to minimize interference, the unused channels are shorted to ground on the screw terminal panel. After conversion to a digital signal the data is stored on the hard drive of the 80386 IBM-compatible computer. This data can then be transferred to a 3 1/2" floppy disk for transfer to another machine for analysis.

While the amount of equipment involved makes the system fairly cumbersome, it is easily hooked up and can be placed almost anywhere near the reactor top for testing provided that at least four 110 volt outlets are accessible. In addition the fission chamber detector leads are only 50 feet long so the equipment must be located close enough to the reactor top for these to reach the electronics. This could easily be changed by adding an extension cable to each of the fission chambers.



## 4.7 TESTING OF ELECTRONIC EQUIPMENT

### 4.7.1 FISSION CHAMBER DETECTORS

Each of the three fission chamber detectors were tested by the manufacturer prior to being shipped to MIT and the detector sensitivities were calculated. The paperwork from IST showing these test results is included in Appendix A. In addition, the normalized detector current to voltage curves are shown below for each detector.

The thermal neutron fluxes used for the above calibration testing were  $4.03 \times 10^{11}$ ,  $4.15 \times 10^{11}$ , and  $3.85 \times 10^{11}$  neutrons/cm<sup>2</sup>-s for detectors 1, 2 and 3 respectively. With these fluxes the sensitivity of the detectors at 140 volts was found to be :

Detector #1:  $1.419 \times 10^{-17}$  Amps/nv thermal

Detector #2:  $1.733 \times 10^{-17}$  Amps/nv thermal

Detector #3:  $2.390 \times 10^{-17}$  Amps/nv thermal

In addition to the detector sensitivity, the leakage current for each detector was determined. This is the current which will flow through the detector when it is hooked up to the power supply with no neutron source. The leakage currents were measured with a 200 volt DC bias and found to be:

Leakage Current #1:  $2.2 \times 10^{-11}$  Amps

Leakage Current #2:  $2.0 \times 10^{-11}$  Amps

Leakage Current #3:  $1.9 \times 10^{-11}$  Amps





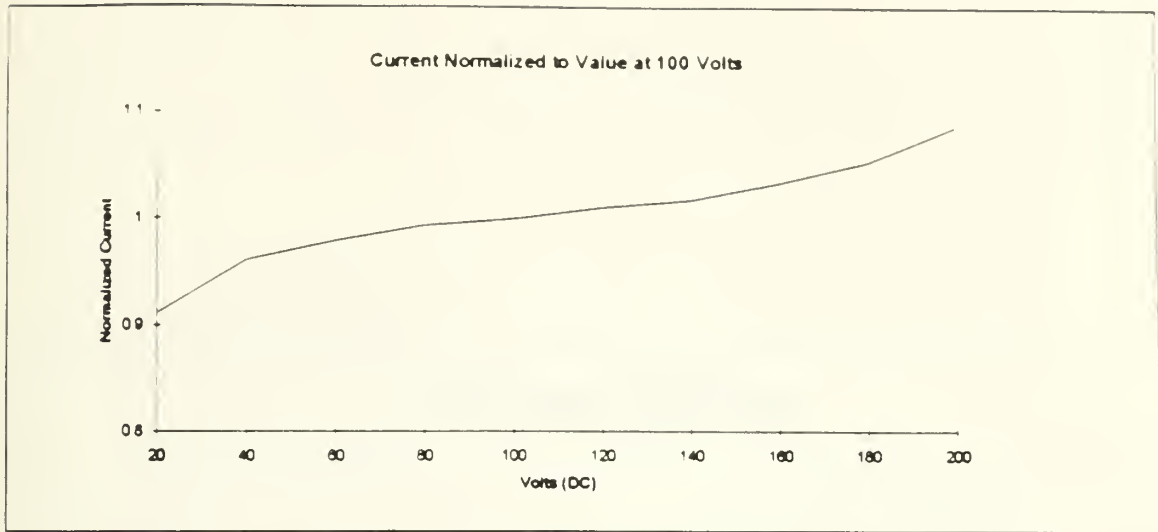


Figure 4.7.1-1: Operating Curve for Fission Chamber Detector #1

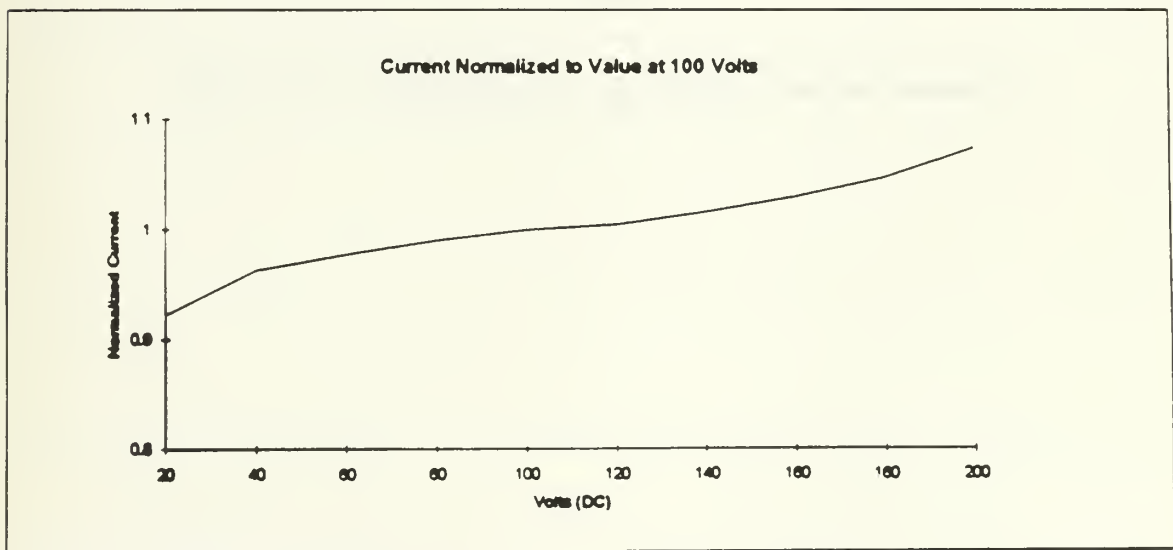


Figure 4.7.1-2: Operating Curve for Fission Chamber Detector #2



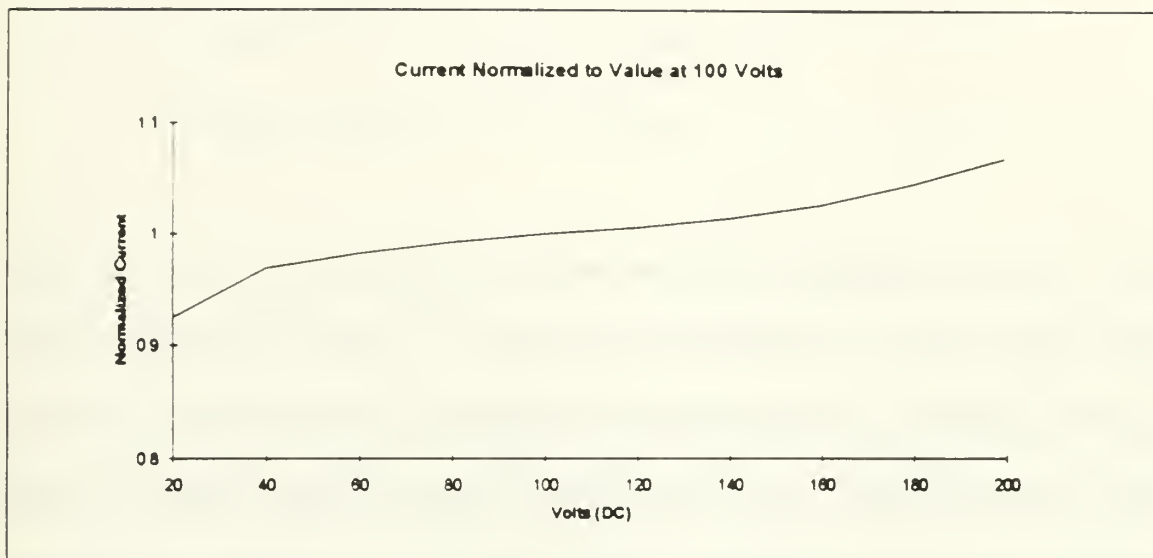


Figure 4.7.1-3: Operating Curve for Fission Chamber Detector #3



Once the detectors were received at the Nuclear Reactor Laboratory the leakage current test was repeated with a 140 volt DC power source. The results of this test showed that the leakage current was slightly less than the values measured at 200 volts DC. This is as one would expect. At 140 volts, they were:

Leakage Current #1:  $8.5 \times 10^{-12}$  Amps

Leakage Current #2:  $8.6 \times 10^{-12}$  Amps

Leakage Current #3:  $8.9 \times 10^{-12}$  Amps

During this test the author decided to experiment with changing the polarity to the detector to determine the effect. According to the manufacturer it doesn't matter which lead is the positive and which is the negative. When the leads were switched the leakage current was slightly lower and slowly increased over time. Because this was totally unexpected the manufacturer was consulted. The explanation given was that the mineral insulated cabling running to the detector sets up a space charge effect from the initial polarization. When the polarity was reversed the alignment of the atoms was reversed and thus the lower current with the rising trend. The technician claimed that it would take approximately two hours for the polarity to completely reverse. The lesson to be learned here is that one polarity should be chosen from the start and made the convention for the entire experiment.

While it would have been preferred to conduct some testing with the fission chamber detectors with a neutron flux prior to the actual experiment in the MITR-II core,



it turned out to be impractical. Aside from the reactor itself, the strongest neutron flux available was from a 111 mCi Cf-252 source. The maximum thermal flux from this source is approximately  $1 \times 10^6$  neutrons/cm<sup>2</sup>-sec. Using an approximate detector sensitivity of  $1 \times 10^{-17}$  Amps/nv thermal, this would yield a detector current of  $1 \times 10^{-11}$  Amps. As was shown above this signal would be barely perceptible above the leakage current.

#### **4.7.2 TESTING OF A/D BOARD AND ASSOCIATED SOFTWARE**

Once the A/D board and associated Global Lab software was installed in the 80386 computer it was tested to verify proper operation. This task turned out to be relatively simple because the use of a tutorial program provided with the Global Lab Package. This program explains the use of all of the major features of the package. It also explains how the A/D board is configured for operation. Once the explanation is completed, the tutorial actually sets up to perform an analog-to-digital conversion. For simplicity a 1.5 volt battery was used to provide the voltage signal. This voltage was dropped across a variable resistor so a time-varying signal could be observed. Once this testing was completed satisfactorily, the entire system was hooked up and connected to the A/D board.

#### **4.7.3 TESTING OF FULL INSTRUMENTATION SYSTEM**

In this test, all of the associated electronic hardware and software was configured as if an actual experiment was going to be performed. Because a sufficiently strong thermal neutron flux source was not available, the detectors were replaced by a 100 M $\Omega$





resistor. This provided a 1.4  $\mu$ Amp signal for an output to the picoammeter. Also the voltage signal from reactor channel seven was not available since this test was not performed in the reactor containment building. As a result this signal was neglected for this test. With all of the equipment hooked up, the A/D board was used to confirm that the voltage signal recorded in the computer was indeed proportional to the current reading on the LCD display of the picoammeter. The expected voltage reading is found by knowing that the analog output from the picoammeter covers two volts for the selected range that the detector display is on (except for the 2 nA range). The analog voltage output is then found by determining the fraction of full scale that the current reading takes, and then multiplying that same fraction by the 2 volt output signal. Thus if the ammeter is on the 0-20  $\mu$ A scale, a reading of 20  $\mu$ Amps should yield an analog output voltage of 2 volts. A reading of 15  $\mu$ Amps will give a 1.5 volt output and so on. For the expected 1.4  $\mu$ Amp signal from this test, the 2  $\mu$ A scale was selected. The analog voltage output which should be detected by the A/D board is then:

$$\frac{1.4}{2.0} \bullet 2Volts = 1.4Volts$$

When the A/D board was initialized and readings were taken, the voltage received was exactly as expected. With this test completed the full instrumentation system was deemed ready for the actual experiment.



## CHAPTER FIVE: THE EXPERIMENT

### 5.1 INTRODUCTION

It has been said that 90% of the work for a typical graduate student's thesis is accomplished in 10% of the allotted time. When the thesis is experimental in nature this is especially true. While a great deal of work must be done in the months prior to the experiment in order to prepare all of the necessary equipment, the final results come down to one or two short days when the actual testing is conducted. The outcome of these few days can make or break the success of the entire project. If a complex piece of equipment or machinery is involved, like a nuclear reactor, there is added uncertainty due to possible outages or shutdowns of the facility which are beyond the control of the researcher.



In this chapter the author describes the experiment conducted for this research. In addition the full procedure is outlined with an explanation of why the different steps were taken. The data resulting from this experiment will be presented in the following chapter.

## **5.2 REQUIREMENTS FOR TESTING**

Before the actual experiment could be conducted a formal procedure had to be written and approved by the MIT Nuclear Reactor Laboratory's Operations office. Prior to writing this procedure, a meeting was held with Dr. John Bernard, Professors Lanning and Henry and this author to outline the items to be accomplished by the experiment. In this meeting all of the members present listed the objectives for the test.

In order to get the data required to validate the feasibility of the instrumented synthesis method the following readings were proposed:

- 1) Initial background readings with the reactor shutdown.
- 2) Steady-state readings with the reactor at various power levels.
- 3) Readings with the flux in the reactor skewed by the positioning of the shim blades.
- 4) Transient readings during both up-power and down-power maneuvers.
- 5) Readings during a severe down-power transient resulting from a shim blade being dropped.
- 6) Final shutdown background readings.



During each of these different conditions flux readings would have to be taken with all three fission chambers at varying axial positions in the instrument guide tubes. It was decided that the axial interval would be one inch for the background readings and three or six inches for the transient conditions (interval to depend on the length of time involved with repeating the given transient multiple times). The details of the mechanics of establishing the transient conditions were left for the author to determine with the help of Mr. Edward S. H. Lau, the Superintendent for Reactor Operations at MITR-II. These details will be discussed below.

### **5.2.1 PREREQUISITES FOR EXPERIMENT**

Prior to conducting the actual experiment several important prerequisites should be met. In order to conduct this testing, the reactor top shield lid must be removed. To accomplish this the reactor must be shutdown and the reactor coolant temperature must be less than 25 °C. Because the reactor will be started up once all initial preparations are made, the reactor startup checklist must be completed, or else be nearly complete prior to starting the experiment. This prerequisite is meant to prevent unnecessary delays between the initial shutdown background readings and the reactor startup. There were also several limiting conditions imposed on the experiment. First, the tests would be conducted with the reactor coolant pumps secured. This was done because it is important that the detectors and the instrument guide tubes not move while readings are being taken. Accordingly, it was decided that all flow would be secured for the duration of the test. As a result the coolant temperature may rise during the course of the experiment, and if it





approaches the upper limit of 50 °C, the reactor must be shutdown and flow reestablished to reduce the temperature. However, because the majority of the testing will be conducted at low powers it is not anticipated that this will be a problem. A second limitation was that because of the possibility of inserting cold water into the core when the pumps are restarted, the reactor must be fully shutdown before any pump is restarted. A third limitation involved the reactivity worth of the fission chambers being inserted into the core. Because these detectors contain highly enriched Uranium-235, it is important to calculate the amount of reactivity which they will add to the core to ensure the absence of any unexpected transients. This was done by assuming the reactivity worth of the uranium was 3.55 mβ per gram of U-235. This corresponds to the reactivity worth of the fuel in the reactor's C-ring. Since the detectors will be added in the water vent holes and not in the C-ring, this will result in a conservative estimate of the reactivity. Each of the fission chamber detectors contains 0.0087 μCi of U-235 activity. The reactivity worth of each of the detectors was determined as follows:

$$T_{\frac{1}{2}}(U-235) = 7.04 \times 10^8 \text{ years}$$

$$\lambda^{235} = \frac{\ln 2}{T_{\frac{1}{2}}(U-235)} = \frac{\ln 2}{7.04 \times 10^8 \text{ yrs}} \times \frac{1 \text{ yr}}{365.25 \text{ d}} \times \frac{1 \text{ day}}{86,400 \text{ sec}} = 3.1199586 \times 10^{-17} \text{ secs}^{-1}$$

Activity =  $\lambda x N$ ; where N = # of atoms.

$$N = \frac{A}{\lambda} = \frac{0.0087 \mu\text{Ci}}{3.1199586 \times 10^{-17} \text{ sec}^{-1}} \times \frac{3.7 \times 10^4 \text{ dps}}{1 \mu\text{Ci}} = 1.03174445 \times 10^{19} \text{ U-235 atoms}$$



$$Mass U-235 = 1.03174445 \times 10^{19} \text{ atoms} \times \frac{1 \text{ mole}}{6.022 \times 10^{23}} \times \frac{235 \text{ g}}{\text{mole}} = 4.026 \times 10^{-3} \text{ grams}$$

Total Mass U-235 for all three detectors = 0.0121 grams

$$\text{Total reactivity for all three detectors} = 3.55 \frac{\text{m}\beta}{\text{g U-235}} \times 0.0121 \text{ g} = 4.29 \times 10^{-2} \text{ m}\beta$$

From this it is evident that inserting this minuscule amount of reactivity will not even be noticeable on the reactor's neutron detectors. In addition to adding positive reactivity, there was also a question of the possible neutron absorbing effects of the detector cladding and the wire lead. A quick calculation of the neutron absorption cross section for the detector material showed that this effect would be insignificant. In spite of this, the experiment procedure requires that the neutronic power be monitored closely the first time that the detectors are moved within the core while at power. If, as expected, it is found that there is no noticeable effect, this precaution will be dropped in the future.

### 5.3 PHASE I OF EXPERIMENT

The experiment could not be completed during the first attempt. As a result the procedure was repeated several weeks later in an attempt to get the data which was not obtained earlier. These two days of testing will be called phase I and phase II, respectively. The two procedures used for these tests are included in Appendix C. In the course of the following description these procedures will be described.



### 5.3.1 SETUP FOR THE EXPERIMENT

The initial phase of testing was conducted on Monday, 29 March 1993. Beginning at 0830 that morning, all of the equipment for the test was moved into the reactor containment building. Because several fuel elements were to be replaced in the core that morning before conducting the experiment, the test equipment was initially assembled on the catwalk around the reactor top. Because of delays, the refueling didn't start until 1100 and wasn't completed until 1230. Once the refueling equipment was stowed and the personnel involved had cleared the area, the test equipment was moved to the reactor top. All of the electronic equipment was set up on the front mezzanine. In order to minimize the possibility of contaminating the equipment, brown paper was laid under everything.

Because the refueling had just been conducted, the reactor top shield lid was already removed. Once all required material and equipment were staged in the vicinity of the reactor top, the hand-held spot light was used to inspect the reactor core. This was conducted to ensure that the water vent holes were still accessible for the insertion of the aluminum guide tubes. Because of other experiments being conducted in the core, some additional equipment had been installed in the reactor since the dimensional measurement experiment in July 1992. This inspection showed that the tubes would still fit into the core easily.

Each of the three aluminum guide tubes was cleaned with acetone and inserted into the appropriate water vent holes by a reactor technician. Once all three tubes were fully inserted into their water vent holes, the tops of the tubes were taped to the side of the reactor top's seating surface. At this point, each of the three fission chamber detectors



was inserted into its respective instrument guide tube. This was contrary to the order specified in the procedure. The procedure had called for the detectors to be inserted into the aluminum tubes first and then the entire tube, with the detector in it, be lowered into the core. It was discovered that by doing it this way, the tube would be very awkward to raise up in the air with the detector lead coming out of it. As a result, permission was obtained from the Senior Reactor Operator to modify this step.

To keep the three detector leads out of the way of personnel working around the reactor top, the crane was positioned so the three wires could be raised above people's heads during the testing. All three detector leads were routed to the three model 485 picoammeters on the front mezzanine.

By 1300 all of the electronics were fully hooked up and testing began. When each of the battery power supplies were plugged into the E-2709A adapter boxes the three detectors were found to be operating correctly. The analog outputs from the three picoammeters were then connected to the screw terminal panel for the A/D board.

Unfortunately, when the computer was turned on and the A/D board initialized, no output was received from any of the analog inputs. After some troubleshooting it was determined that no signals were being passed by the A/D board. A 1.5 volt battery was obtained and hooked up as an input to one of the A/D board channels and still no signal was received. Some of the initial areas checked were the screw terminal panel and the cable ribbon from the screw terminal panel to the computer. After these items were checked out satisfactorily, the vendor, Data Translations, was consulted. The first thing that they requested was that the diagnostic program be run. After checking several times







it was discovered that this disk was never received with the A/D board hardware. Without this disk it was impossible to pinpoint the actual problem with the board. The technician from Data Translations was however able to verify that something was definitely wrong with the hardware after a few voltage readings on the board were checked. By this time it was already 1630 and Reactor Operations was trying to determine if we should continue trouble-shooting or abandon the effort and start up the reactor and conduct the steady-state portions of the experiment.

One suggestion offered by Dr. John Bernard was to cannibalize an A/D board from a computer in the reactor's control room which was used in earlier control experiments. This was attempted but unfortunately the board was not configured properly for the equipment used in this research. Because the steady state portions of the experiment could still be conducted by manually reading and recording the current output off of the picoammeters, it was decided that the reactor should be started and the experiment conducted to the extent possible.

During the time that the trouble-shooting was being conducted on the A/D board, personnel from the Radiation Protection Office installed a containment tent over the top of the reactor core. This was accomplished by taping a plastic sheet to the seating surface for the reactor's top shield lid. The three aluminum instrument guide tubes penetrated this sheet but the plastic was taped tightly around each tube. A suction hose was taped to this tent to remove any fission product gasses generated in the core during operations. This containment was devised by the personnel in the Radiation Protection Office to minimize



any possible exposure to the personnel working in the vicinity of the reactor top during critical operations for the experiment.

### 5.3.2 INITIAL SHUTDOWN BACKGROUND READINGS

Before the reactor was started up, the initial shutdown background readings were taken. This was done at approximately 1800 with the reactor core temperature at 32.5 °C. These readings were taken at one inch intervals from the base of the instrument guide tubes to a position 24" above the bottom of the tube. At the time these readings were taken the reactor had been shutdown since 1919 on Friday, 26 March 1993. The shutdown time interval was then 70.68 hours. Once this was completed the reactor control room was notified and the reactor was started up. The reactor startup commenced at 1830. (Note: All of the data associated with the experiment is displayed in Appendix B.1 and is analyzed in Chapter Six.)

### 5.3.3 STEADY-STATE ANALYSIS

Because of concern over the radiation levels from operating with the reactor lid removed, Reactor Operations ordered the power to initially be leveled at 500 watts. It was decided that if the fission chamber current outputs were sufficiently above background at this power level, then all powers called for within the procedure would be scaled down by a factor of ten.

The reactor power was first leveled at 500 watts at 1925. With the power at this point it was decided that flux measurements would be taken with the three fission chamber



detectors at three-inch axial intervals. Because the current measured at this power was relatively low (0.05  $\mu$ amps), it was decided that power should be raised to 5 kW to determine the current level there. Power was leveled there at 1948. The flux mapping was once again conducted at this power in three-inch increments. It is interesting to note that the core temperature didn't rise very much between the 500 watt and 5 kW data runs. At 500 watts, the core temperature was 33.5 °C and at 5 kW this temperature rose to only 33.7 °C. These steady-state flux readings will be used to construct the flux shapes in the core at these different power levels.

At both 500 watts and 5 kW, Reactor Radiation Protection personnel performed radiation surveys around the reactor top. These surveys showed that reactor power could be safely raised to the higher levels without any serious radiological consequences.

### 5.3.4 FLUX TILTING

In this portion of the experiment, the flux profile in the reactor was skewed or tilted by placing the six shim blades at different heights. Because this tilting can shift the power distribution within the core, there are limits placed on the severity of the allowed tilt. These limits are implemented in the form of restrictions on the maximum difference between any shim blade heights. Normally, this limitation is four inches between any two shim blades. For powers less than or equal to 1 kW this limit is not required. As a result, it is possible to initiate some very severe flux tilts at or below this lower power.

Before taking the reactor to higher power levels it was decided to lower it to 1 kW to take advantage of this tilting. Power was leveled at 1 kW at approximately 2010. The





core temperature at this time was 34.8 °C. The shim bank height at this power was 8.60 inches. Before the flux tilt was initiated, a full set of no-tilt flux measurements were taken. As before this consisted of taking readings at three-inch intervals up the water vent hole. These measurements were needed to show the effect of the flux tilt which was initiated next. Once the no-tilt data was taken, it was decided that for the first tilt, the maximum difference between the shim blades would be eight inches. After the reactor operator had all of the shim blades in the requested positions and power was steadied at 1 kW, a full set of flux measurements were taken at three-inch intervals. The results from this data run are shown in Chapter Six.

After data was recorded with the flux tilt at 1 kW, the shim blades were reshimmed to the same bank height and reactor power was then raised to 10 kW. Power reached this level at 2136. By this time the temperature in the core tank was 35.4 °C. Once power was leveled at this new value the flux mapping was repeated as before. For this flux tilt, the maximum difference between the shim blade heights was limited to four inches. After this tilt was implemented, a full set of flux measurements was taken.

The reactor power was next raised to 50 kW. The reactor reached this power at 2216 and the core tank temperature was 37.6 °C. The no-tilt and tilt flux conditions were measured as before with the power steady at 50 kW. This step was completed at 2248 and by this time the core tank temperature had risen to 44 °C. From this it is obvious that it would not be possible to hold power at these higher levels for too long before the core temperature would reach the upper limit of 50 °C.





Because of the increasing temperature and the higher radiation levels experienced at 50 kW, it was decided that reactor power would not be raised above this level for the experiment at this time. Instead of going to a higher power, the control blades were reshimmed to an even bank height and a down-power transient was initiated. With this, the steady-state portions of the experiment were completed.

### 5.3.5 TRANSIENT ANALYSIS

Because the A/D board was not functioning properly, no transients could be recorded for this phase of the experiment. Because reactor power was going to be reduced anyway, it was decided that a down-power transient would be initiated so that the trend could be observed on the three picoammeters. The intent was to allow the experimenter to observe the transient and determine what type of shim would be requested during phase II of this experiment. Before this was conducted, all three fission chamber detectors were placed at the nine-inch position. The author and the Senior Reactor Operator decided that shim blade #5 would be shimmed in for a total of 10 seconds. After observing the down-power transient for 90 seconds, the reactor operator was instructed to level power and reshim. With this, the experiment was completed for the evening. The only step remaining was to conduct a full set of background flux readings once the reactor was shutdown. Because the reactor was to continue to operate for several hours, the experimental equipment was secured and the personnel involved in conducting the test went home for the night.



In order to minimize the neutron flux seen by the three fission chamber detectors, they were all raised to a position above the active core region. They could not be removed from the core because they were activated from their exposure to the high neutron fluxes within the core and needed to decay for several hours

### **5.3.6 FINAL SHUTDOWN BACKGROUND READINGS**

The reactor was shutdown at 0300 on 30 March 1993. At 0750 that same morning the final shutdown background readings were taken. As in the case of the initial background readings, the measurements were taken at one-inch intervals from zero to twenty-four inches. Once this was done, phase I of the experiment was completed.

### **5.3.7 RESTOWING EQUIPMENT**

Once the final background readings were taken, all of the electronic equipment was secured and disconnected. With the assistance of a reactor technician and personnel from the Radiation Protection Office, each of the fission chamber detectors was carefully removed from the reactor and the long detector lead for each fission chamber was wound onto its **respective reel**. As each detector neared the top of the instrument guide tube, radiation **readings were taken** to determine the activity of the detectors. The results of these **surveys are included** in Chapter Six. Because each of the detectors was activated, they were stowed in an area where personnel would not be **unnecessarily exposed**.

The next step was to remove each of the three aluminum instrument guide tubes from the core. Before this could be done, the plastic containment had to be removed from



the reactor top. After these tubes were removed and dried, they were stowed on the back mezzanine of the reactor top on the piping racks. Each of these tubes was slightly activated from the production of Al-28 which gives off  $\gamma$  and  $\beta$  radiation.

The final step in the cleanup was to remove all of the electronic equipment from the front mezzanine and move it back to the lab area outside of the containment building. In order to do this, all equipment had to be surveyed and swiped to ensure that it had not been contaminated while on the reactor top. Once this was completed all of the equipment was stowed in the lab.

### 5.3.8 REPAIR OF THE A/D BOARD

After all of the equipment had been stored, the A/D board was removed from the computer and placed in its shipping box. Because the manufacturer was local, plans were made to take the board directly to the company for repairs. The A/D board was dropped off at Data Translations late in the day on Tuesday, 30 March 1993. The technician discovered the problem in about five minutes. It turned out to be a problem with the multiplexer board. He reported that this was a fairly common problem and was usually caused by a voltage spike from the line powering the computer. Because of administrative requirements, the board could not be returned until the following day. Two days later the board was received via Federal Express. In addition a trouble-shooting disk was included.

Although a surge protector had been used originally, it was decided that a new one would be purchased for added assurance. This surge protector was purchased the day



after the A/D board arrived. With this in hand, the A/D board was reinstalled into the computer and tested. This test showed that the board was working properly.

## 5.4 PHASE II OF EXPERIMENT

With the A/D board repaired the experimenter approached the Reactor Operations Staff and requested that the experiment be placed on the schedule. Because of prior commitments, Phase II of the experiment could not be conducted until Tuesday, 20 April 1993. A new procedure was written for this test incorporating the lessons learned during Phase I of the experiment. This procedure is included in Appendix C. All of the prerequisites for this portion of the experiment are identical to those already discussed in section 5.2.1.

### 5.4.1 SETUP FOR THE EXPERIMENT

All of the equipment for this portion of the experiment was staged on the front mezzanine of the reactor beginning at 0815. All electronics, with the exception of the fission chamber detectors, were hooked up by 0845. Because of an another test being performed ~~that~~ morning on the reactor top, the instrument guide tubes and the fission chambers ~~would not~~ be placed in the reactor until after it was completed. While waiting, the computer was turned on and the A/D board was checked. Unlike before, the board performed perfectly. The signal from the reactor's channel seven was then wired to the A/D board and it was once again checked. As before, it worked fine.







At 1355 Reactor Operations granted permission for the experiment to continue. Each of the three aluminum instrument guide tubes was cleaned and inserted into water vent holes 1, 3 and 5. Once these were in place, a plastic sheet was taped on the reactor top to contain any fission product gasses produced during critical operations. Each of the three fission chamber detectors was then placed into its respective tube. With this completed, the detectors were then connected to the Model 485 picoammeters. With the entire system configured, the A/D board was once again tested. Unfortunately, it was at this stage that a problem was detected. The output being read by the A/D board was 2.5 volts, which was the maximum range for the gain setting of the board. Because this was totally unexpected, a voltmeter was used to read the input voltage across the terminals for the A/D board. The voltmeter read 67 volts DC! The leads to the board were immediately disconnected to save the computer. Luckily the A/D board was not damaged by this voltage. It is now assumed that this is what caused the failure of the board during Phase I of the experiment. As before, trouble-shooting was immediately conducted. It was determined that there was a ground incompatibility between the computer and the Keithley Model 485 analog outputs. This was not detected during the preliminary testing because the detectors were not actually hooked up to the picoammeters. Recall from section 4.7.3 that a 100 M $\Omega$  resistor was used in place of the detectors. Because of the way these were wired, they were floating and not grounded like the fission chambers are when they are connected. As a result, the ground incompatibility was not detected.

With time running out, the decision was once again made to continue the experiment with the intention of performing only the steady-state portions of the



procedure. The trouble-shooting of this problem was terminated for the time being so the reactor could be started up.

### **5.4.2 SHUTDOWN BACKGROUND READINGS**

Prior to conducting the startup, the background readings were taken in the core. These readings were performed at 1608, 71.47 hours after the reactor had been shutdown on the previous Saturday. Once again the core was essentially Xenon free. The temperature in the reactor core tank at this time was 31.2 °C. With this step complete, the reactor startup was commenced at 1635. All data for this phase of the experiment is listed in Appendix B.2 and is displayed graphically in Chapter Six.

### **5.4.3 FLUX TILTING**

In this phase of the experiment, flux tilting was once again conducted to determine if the fission chambers could detect the perturbations in the flux shape. This was conducted at 1 kW, 10 kW, and 50 kW. The flux tilt initiated at 1 kW was even more extreme than the one performed in phase I of the experiment. Additionally, the flux tilt was shifted to the opposite side of the core at each power level to show differences in each detector's response.

After the reactor was started up, power was leveled at 1 kW at 1711. The core tank temperature was 32.0 °C. The shim bank height at this power was 10.30 inches and the regulating rod position was 2.64 inches. The no-tilt flux measurements were then performed in the same manner as before. Once all of these readings were recorded, the



first flux tilt was initiated. While moving the shim blades into the requested positions, a spurious ~~scram~~ occurred. Once the problem was corrected, the reactor was restarted at 1907. Power was once again leveled at 1 kW at 2000. Because the shim bank height was the same as before, the decision was made to go right to the first tilt without repeating the no-tilt measurements. The actual configuration of the shim blades for this tilt will be described in Chapter Six. With the flux tilt in place, and power steady at 1 kW, readings were again recorded. Once complete, the flux tilt was shifted to the opposite side of the core by changing the shim blade configuration. Again the detector current measurements were recorded. By this time the core tank temperature had risen to 39.7 °C.

Reactor power was next raised to 10 kW and the control blades were reshimmed. Power reached this level at 2102 with a core tank temperature of 41.4 °C. Following the same procedures as before, the no-tilt and tilt flux conditions in the core were measured. Also as before, the flux tilt was shifted to the opposite side of the core and a full set of measurements were taken.

The final flux tilt was performed at 50 kW. Power was leveled there at 2218 with a core tank temperature of 46.8 °C. All measurements at this power were performed exactly as above.

#### **5.4.5 SECURING FROM EXPERIMENT**

Once the measurements were completed at 50 kW the reactor was immediately shutdown. The shutdown commenced at 2240. At 2253 the final background measurements were taken. The temperature in the core tank during these measurements





was 48.0 °C. The final step which was to be performed was to take measurements with each fission chamber moved sequentially into each instrument guide tube. The purpose for this was to ensure that all three detector's read the same flux in each water vent hole. Unfortunately, because of equipment in the core, it was not possible to switch all of the tubes without lifting them up above the water level. Because of extremely high radiation levels from the detectors and the aluminum tubes, Radiation Protection Personnel would not allow them to be removed from the core for this portion of the experiment. Instead all three instrument guide tubes were lifted out of the active region of the core and placed in the spent fuel storage ring for approximately one hour to decay. Following this decay period the three fission chamber detectors were removed and placed in the hot box to decay. The three fission chamber detectors were highly radioactive. The highest one yielded 20 R/hr  $\beta$ ,  $\gamma$  on contact. The results of these surveys is included in Chapter Six. Each of the aluminum instrument guide tubes was then removed and dried and placed in the hot cell to decay.

All of the electronic equipment was then removed from the reactor top and moved out of the containment building. After all of the gear was frisked, it was free released for storage in the reactor laboratory.

## **5.5 LESSONS LEARNED**

The conduct of the two phases of the experiment revealed several problems which had not been anticipated prior to conducting the testing. The most troubling problem encountered was the one related to the ground between the A/D board and the





picoammeters. The lesson to be learned from this is that it is not good enough to test equipment in a lab environment with simulated conditions. The equipment must be staged in the actual positions to be used for the experiment with all of the required gear hooked up as if the test was to be performed at that moment. Even if the detectors couldn't be placed into the core, they could have at least been hooked up and routed to a location close to the reactor lid. It is likely that this would have resulted in the problem being detected earlier.

A review of some of the other lessons learned are listed below:

- Fission chamber detectors should be placed into the aluminum tubes after the tubes have been inserted into the core.
- If the instrument guide tubes are to be moved to different water vent holes for normalization data, then this should be done before they become highly activated.
- Prior to starting up the reactor, the temperature in the core should be reduced as low as possible to prevent having to shutdown in the middle of the test to cool down.

Each of these items should be incorporated into any future procedures written for this research. While all of the desired data was not obtained due to the problems with the A/D



board, this research is off to a good start and a lot of valuable information has been gained from the tests conducted.



## CHAPTER SIX: ANALYSIS OF DATA

### 6.1 INTRODUCTION

In this chapter all of the data received in the two phases of the experiment are introduced and analyzed. The actual raw data obtained during the testing is included in Appendix B. Using the tables and graphs of data found in the following pages, the feasibility of using the instrumented synthesis method with the instrumentation system developed for this research will be discussed. In addition, ideas will be introduced for changing the detection scheme to take advantage of the lessons learned during the two phases of this experiment. As in the previous one, this chapter will be broken down into two sections for the two separate phases of the experiment. In addition, another section



will discuss the results of the radiation surveys. A final section is included which shows the calculations for determining the detector and instrument guide tube's material composition. This information is needed to determine the neutron cross sections for use with other research being conducted in support of this project.

## 6.2 PHASE I OF EXPERIMENT

### 6.2.1 SHUTDOWN BACKGROUND MEASUREMENTS

As was discussed in Chapter Five the background measurements were taken after the reactor had been shutdown for 70.68 hours. As a result of this long weekend shutdown, the core was effectively free from Xenon. The core installed in the reactor at the time of this test was core 103. In this core configuration, fuel locations A1, A3, and B4 each contained a dummy fuel element with no fuel. A top view of the reactor core is once again included as Figure 6.2.1-1 to show the locations of these dummy elements in relation to the fission chamber positions.

Another issue which must be discussed prior to reviewing the graph of background data is the location of the fission chamber detectors with respect to the bottom plane of the actively fueled region of the core. It was determined that all axial measurements should be referenced to the bottom of the fuel meat in the fuel elements. Unfortunately, this measurement is not easily found. Figure 6.2.1-2 shows the actual dimensions involved in determining the distance between the bottom of the fuel and the bottom of the instrument guide tube within the water vent hole. From this figure the reader can easily see that the bottom of the water vent hole is 5.688 inches above the bottom of the fuel.





The distance between the bottom of the vent hole and the bottom of the inside of the instrument guide tube is 0.844 inches. It is to the bottom of the instrument guide tube that the detector's positions are referenced on all of the raw data and in the procedures. The actual measurement point for each detector is determined to be the center point of the fission chamber's active volume. At the head of each detector there is a 0.25 inch "bullet nose" which is not included in the active region. Immediately after this the 1.656 inch active region begins. The middle of this active region is then 1.078 inches from the pointed end of the detector ( $0.25 + \frac{1.656}{2} = 1.078$ ). By summing all of these different dimensions it is found that the distance between the bottom of the fuel and the center of the active region of the detector (when it is at the bottom of the instrument guide tube or the zero inch position) is 7.61 inches. Thus all dimensions listed on the graphs will take this correction into consideration.

The graph of the initial background readings is shown as Figure 6.2.1-3. As was previously mentioned this data was taken at 1800 on 29 March 1993. The core tank temperature at the time of the measurement was 32.5 °C. From this data it is evident that the flux was highest in water vent hole #3 (Flux 3 on graph) over the entire axial range analyzed. At the bottom of the instrument guide tube the flux in vent hole #3 was 22.6 % greater than the flux in water vent hole #5. The flux in water vent hole #5 was the lowest reading at the bottom of the vent hole, but at about eleven inches above the fuel, it became greater than the flux in water vent hole #1. These irregularities are probably due to the presence of the dummy fuel elements as well as effects outside of the fueled region of the core. Regardless of the cause, it is important that these initial shapes be known so that they can be subtracted from the remainder of the data taken at different powers.



Because the flux level for the detector in water vent hole #3 was so much higher than the other two, it was decided that during the next phase of the experiment each of the detectors would be cycled through each of the three instrument guide tubes to ensure they were all getting the same neutron flux reading. This would serve as a means of checking the consistency of each detector and ensuring that they are all normalized to the same flux.



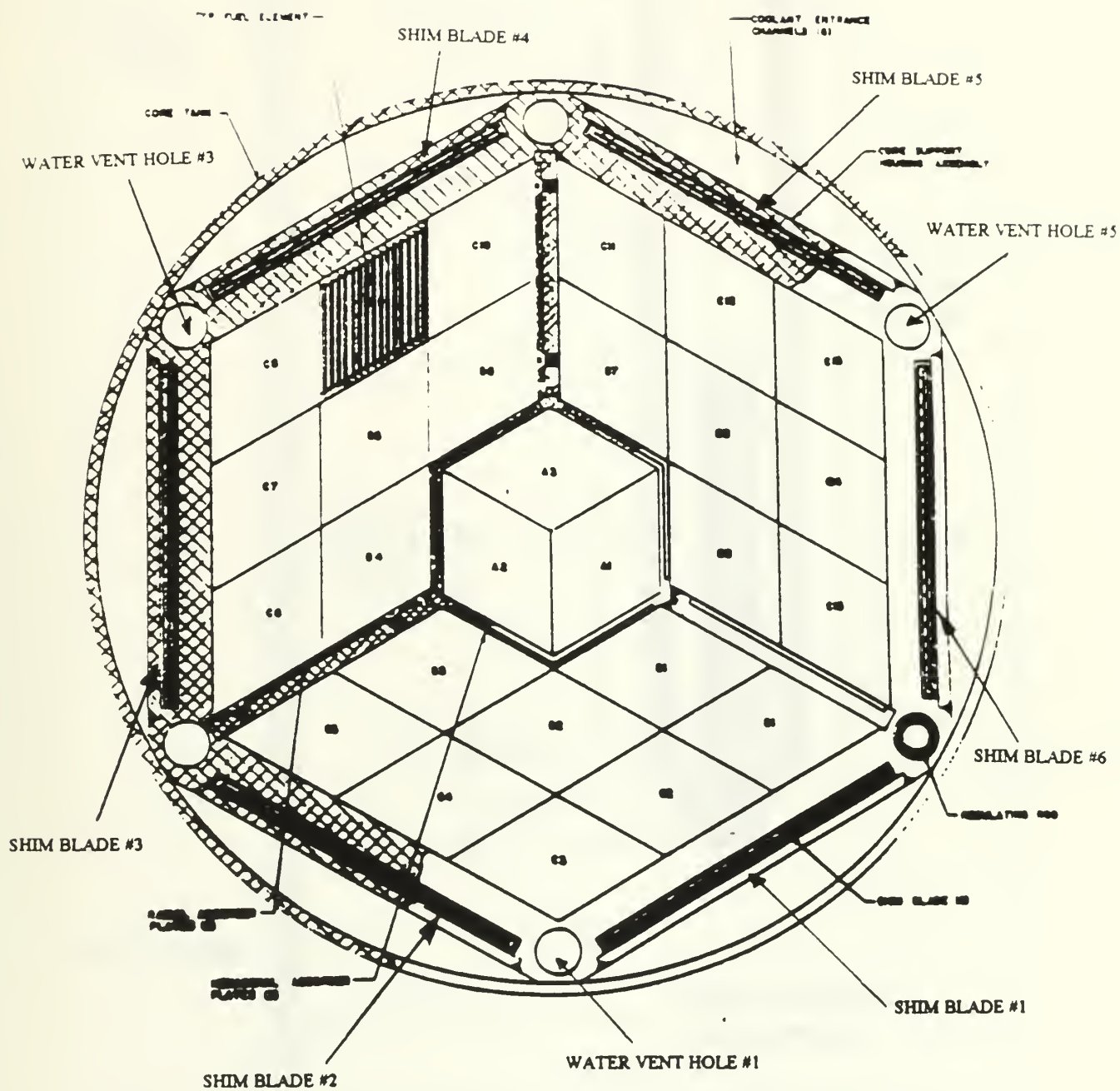


Figure 6.2.1-1: Top View of MTR-II Reactor Core



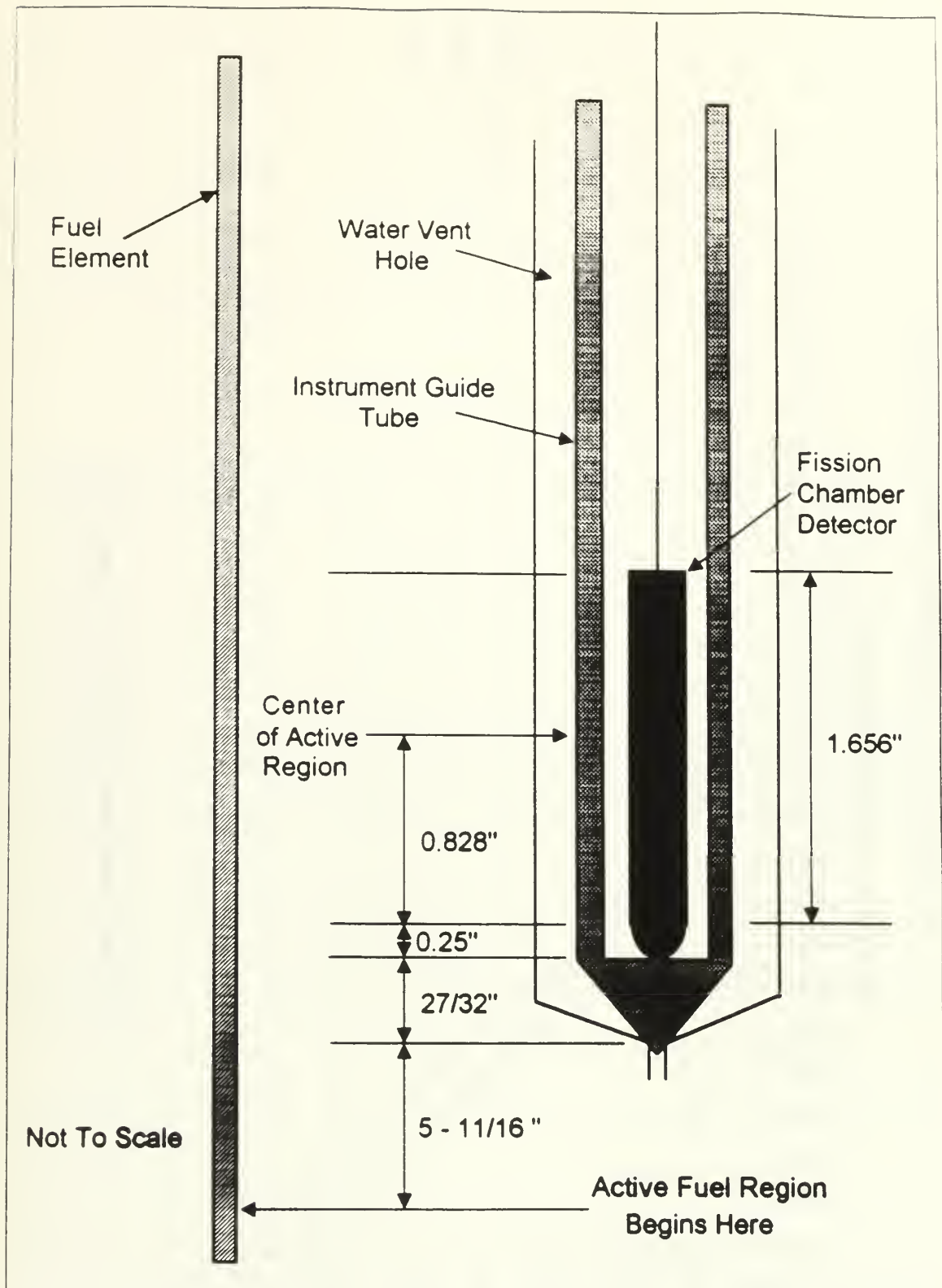


Figure 6.2.1-2: Reference Axial Position





# Initial Shutdown Background Readings

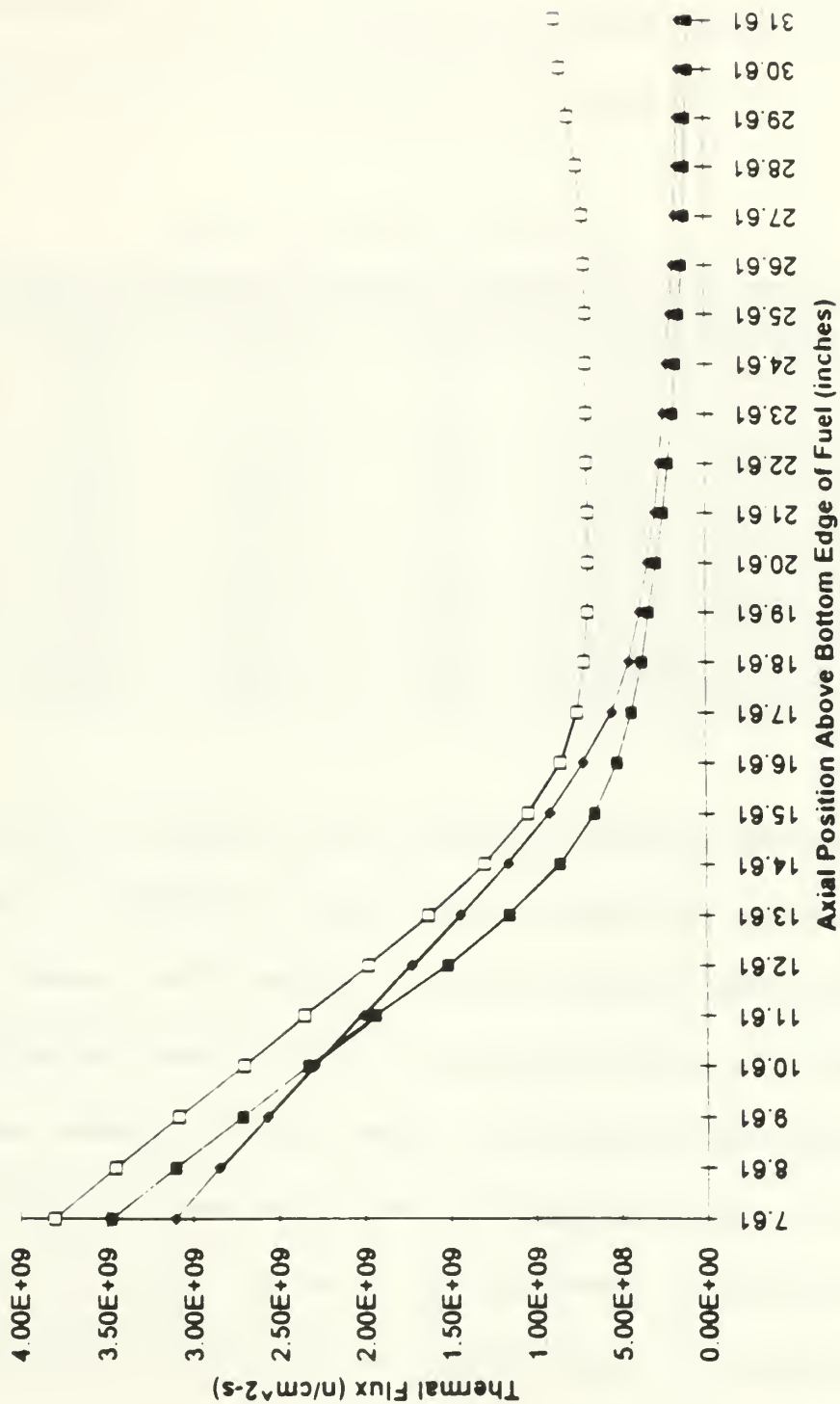


Figure 6 2.1-3 Initial Shutdown Background Readings



## 6.2.2 STEADY-STATE MEASUREMENTS AT 500 WATTS

Once the background readings were taken the reactor was started up and power was raised to 500 watts. The net flux for each axial position was determined by subtracting the shutdown background readings from the readings obtained at power for each axial position. Table 6.2.2-1 shows the results of this correction.

Table 6.2.2-1: Net Flux at 500 Watts

Axial Position	Water Hole #1 ( $\mu$ Amps)	Water Hole #3 ( $\mu$ Amps)	Water Hole #5 ( $\mu$ Amps)	Net Flux 1	Net Flux 3	Net Flux 5
7.61	0.0839	0.1032	0.1303	2.44E+09	2.15E+09	2.35E+09
10.61	0.0545	0.0718	0.0931	1.51E+09	1.44E+09	1.60E+09
13.61	0.027	0.0428	0.0575	7.47E+08	8.42E+08	9.62E+08
16.61	0.0132	0.0229	0.0292	4.09E+08	4.67E+08	5.02E+08
19.61	0.0071	0.0162	0.0171	1.69E+08	2.42E+08	3.26E+08
22.61	0.0034	0.0121	0.0083	2.11E+07	0.00E+00	7.53E+07
25.61	0.002	0.0109	0.0045	0.00E+00	0.00E+00	0.00E+00
28.61	0.0014	0.0121	0.0032	0.00E+00	0.00E+00	0.00E+00
31.61	0.0012	0.0149	0.003	0.00E+00	0.00E+00	0.00E+00

From this table it is evident that the flux readings at 500 watts are barely above the background levels. In addition the current levels are extremely low, especially above 13.61 inches. Because it will be necessary to observe as much of the flux profile as possible so that changes in it can be analyzed, this power level would not yield satisfactory results. For these readings the shim bank height was 8.60 inches and the regulating rod position was 3.00 inches. The core tank temperature during these readings was 33.5 °C.

Figure 6.2.2-1 is a graph of the net flux data at 500 watts. One will note that the flux profile drops off rather quickly in the lower regions of the core. Part of this is due to



the low height of the shim bank. The low bank height forces the neutron flux to be peaked in the lower regions of the core. One of the unfortunate aspects of using the water vent holes can be seen in this figure. Because the fission chamber detectors cannot get below the 7.61 inch position above the fuel, it will not be possible to see the location of the peak flux at the low powers that will be used for this research. As in Figure 6.2.2-1 the flux profile that can be seen by the detectors in the water vent holes will be above the peak and as a result the only part of the profile that will be seen is the upper section which tails off to lower values with increasing axial position. Because it is important to detect changes in the neutron flux shape, it would be preferred to observe the entire flux profile. Barring this, it would be nice to at least be able to observe the flux peak and track its response to power level changes. The only conceivable way to do this with the current arrangement would be to conduct the test at higher power levels and with a more fully depleted core. Possibly this experiment could be conducted with equilibrium Xenon present within the core. If this experiment is to ever be conducted at higher power levels (above 100 kW) then a new support rig would have to be built and arrangements would have to be made for routing the detector cabling through the upper shield lid in such a way that the detectors can be moved remotely while the lid is on.

Another interesting thing to note about the data is the location of the higher fluxes with respect to the regulating rod and the dummy elements. From Figure 6.2.2-1 it is noted that the flux in water vent hole #1 is the highest at the base of all instrument guide tubes. Reviewing Figure 6.2.1-1 shows that this is as would be expected. The next highest flux occurred in water vent hole #5.



# Thermal Flux at 500 Watts

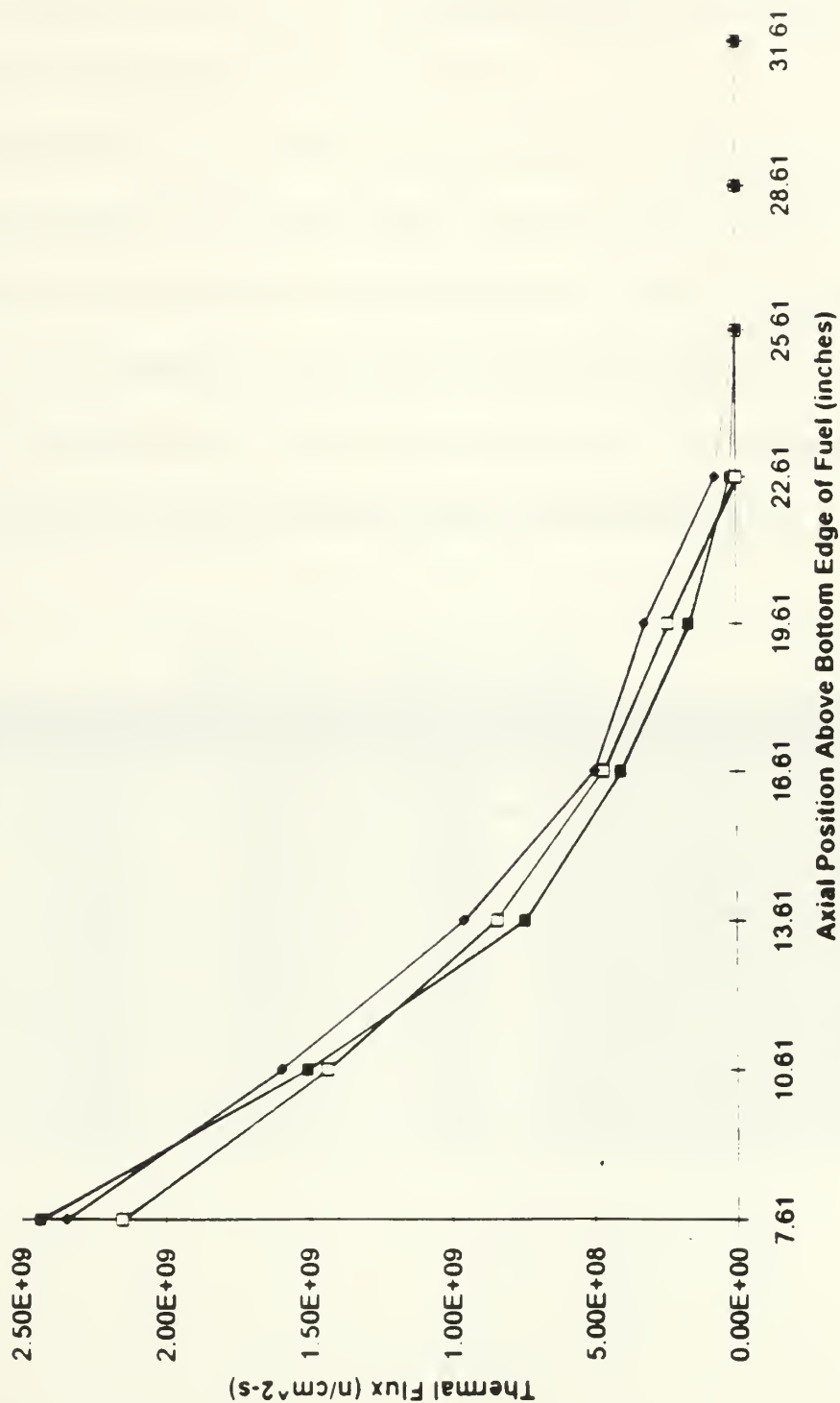


Figure 6.2.2-1: Neutron Flux at 500 Watts





### 6.2.3 STEADY-STATE MEASUREMENTS AT 5 kW

With power raised to 5 kW the flux and current readings were only slightly better than those at 500 watts. These values can be seen in Table 6.2.3-1. For this power level the shim bank height was 8.70 inches and the regulating rod height was 1.50 inches. The core temperature for this portion of the test was 33.7 °C.

The resulting flux profile is included as Figure 6.2.3-1. As in the previous case at 500 watts, the flux tends to drop off rather rapidly in the lower regions of the core. Also as before, the flux in water vent hole #1 was the highest for the bottom axial position of the detectors. It is reassuring to note that the flux levels detected at 5 kW are approximately ten times the values recorded earlier at 500 watts. If for nothing else, this tends to confirm that all three fission chamber detectors were tracking properly.

Table 6.2.3-1: Net Flux at 5 kW

Axial Position	Water Hole #1 ( $\mu$ Amps)	Water Hole #3 ( $\mu$ Amps)	Water Hole #5 ( $\mu$ Amps)	Net Flux 1	Net Flux 3	Net Flux 5
7.61	0.416	0.465	0.6616	2.58E+10	2.30E+10	2.46E+10
10.61	0.2661	0.3126	0.459	1.64E+10	1.53E+10	1.69E+10
13.61	0.1318	0.1856	0.2783	8.13E+09	9.08E+09	1.02E+10
16.61	0.0702	0.1024	0.1486	4.43E+09	5.05E+09	5.50E+09
19.61	0.0336	0.0636	0.0965	2.04E+09	2.98E+09	3.65E+09
22.61	0.01	0.0255	0.0347	4.86E+08	7.73E+08	1.18E+09
25.61	0.0038	0.0143	0.0113	1.20E+08	1.21E+08	2.68E+08
28.61	0.002	0.0131	0.0053	2.82E+07	0.00E+00	5.44E+07
31.61	0.0014	0.0152	0.0038	7.05E+06	0.00E+00	1.26E+07



# Thermal Flux at 5 kWatts

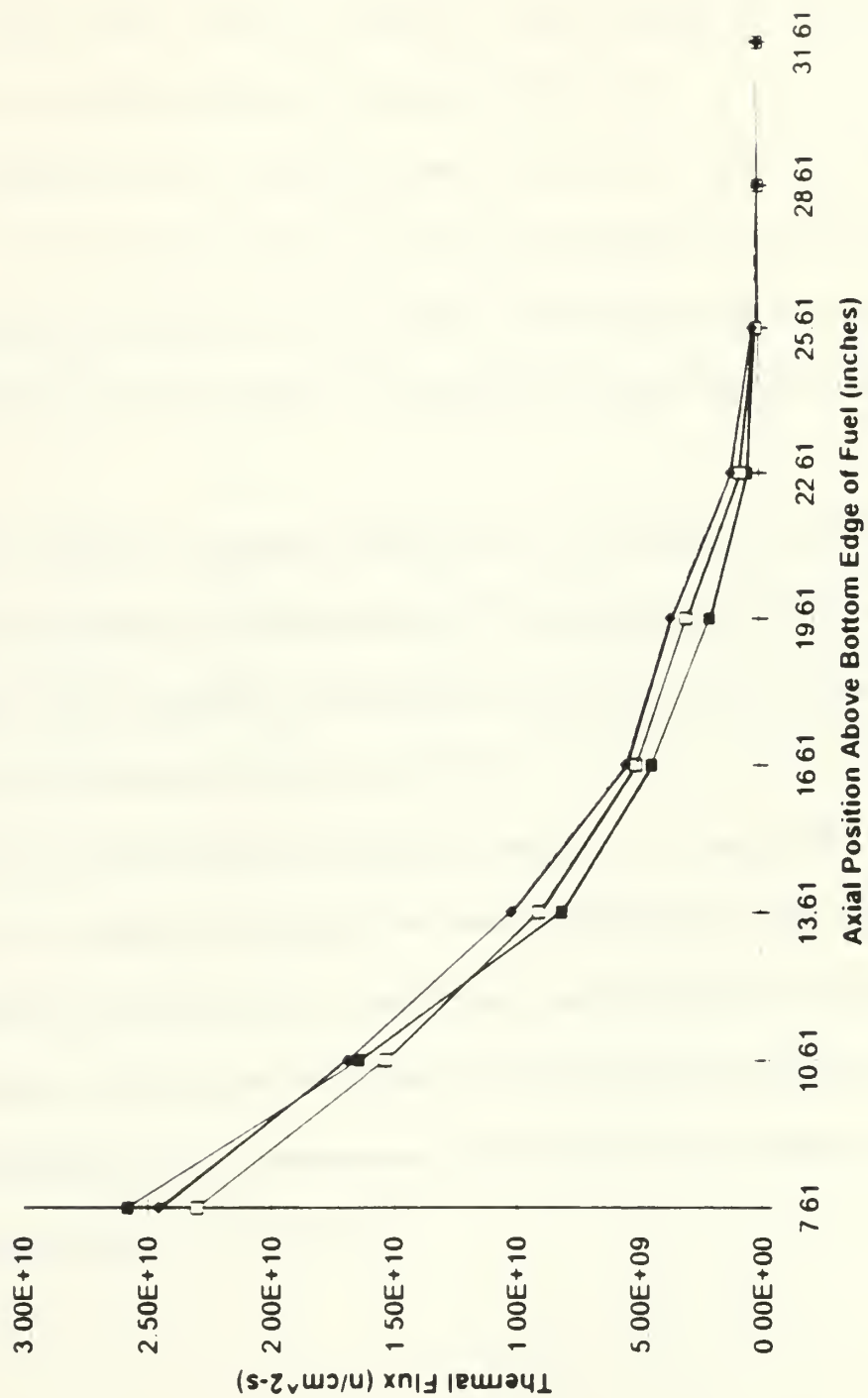


Figure 6 2 3-1: Neutron Flux at 5 kW



## 6.2.4 FLUX TILTING AT 1 kW

After receiving the steady-state readings at 5 kW, it was decided that the power should be dropped to 1 kW in order to allow for some extreme flux tilting. By doing the tilting at this lower power, it would be possible to take advantage of the relaxed requirements on the shim blade positions as discussed in section 5.3.4.

Before doing the flux tilt it was first necessary to determine the no-tilt flux profile within the core. As in each of the previous cases this was accomplished by taking readings at three-inch axial intervals within the water vent holes. The background levels were then subtracted off to give the net flux condition. The results from this data set are included in Table 6.2.4-1.

The data in this table is plotted in Figure 6.2.4-1. This figure is provided for comparison to the tilt condition to be described next. The shim bank height for this power was 8.60 inches and the regulating rod position was 3.63 inches. The core tank temperature at the time this data was taken was 34.8 °C.

The flux tilt was next initiated as described in section 5.3.4. The positions of the shim blades and the regulating rod for this tilt are shown in Table 6.2.4-2. Figure 6.2.1-1 should be consulted to see the location of these different control elements with respect to the different detectors. The core tank temperature for this portion of the testing was 35.1 °C. The data resulting from the measurements with this flux tilt are provided in Table 6.2.4-3. This data is plotted in Figure 6.2.4-2.



Table 6.2.4-1: Net Flux at 1 kW with No Tilt

Axial Position	Water Hole #1 ( $\mu$ Amps)	Water Hole #3 ( $\mu$ Amps)	Water Hole #5 ( $\mu$ Amps)	Net Flux 1	Net Flux 3	Net Flux 5
7.61	0.1192	0.1406	0.1859	4.93E+09	4.31E+09	4.67E+09
10.61	0.0777	0.0967	0.131	3.14E+09	2.87E+09	3.18E+09
13.61	0.0378	0.0577	0.0801	1.51E+09	1.70E+09	1.91E+09
16.61	0.0193	0.0313	0.042	8.39E+08	9.52E+08	1.04E+09
19.61	0.01	0.0211	0.0255	3.74E+08	5.25E+08	6.78E+08
22.61	0.0042	0.0133	0.0111	7.75E+07	6.92E+07	1.92E+08
25.61	0.0021	0.0111	0.0052	0.00E+00	0.00E+00	1.26E+07
28.61	0.0015	0.012	0.0034	0.00E+00	0.00E+00	0.00E+00
31.61	0.0012	0.0146	0.003	0.00E+00	0.00E+00	0.00E+00





# Baseline Readings at 1 kW

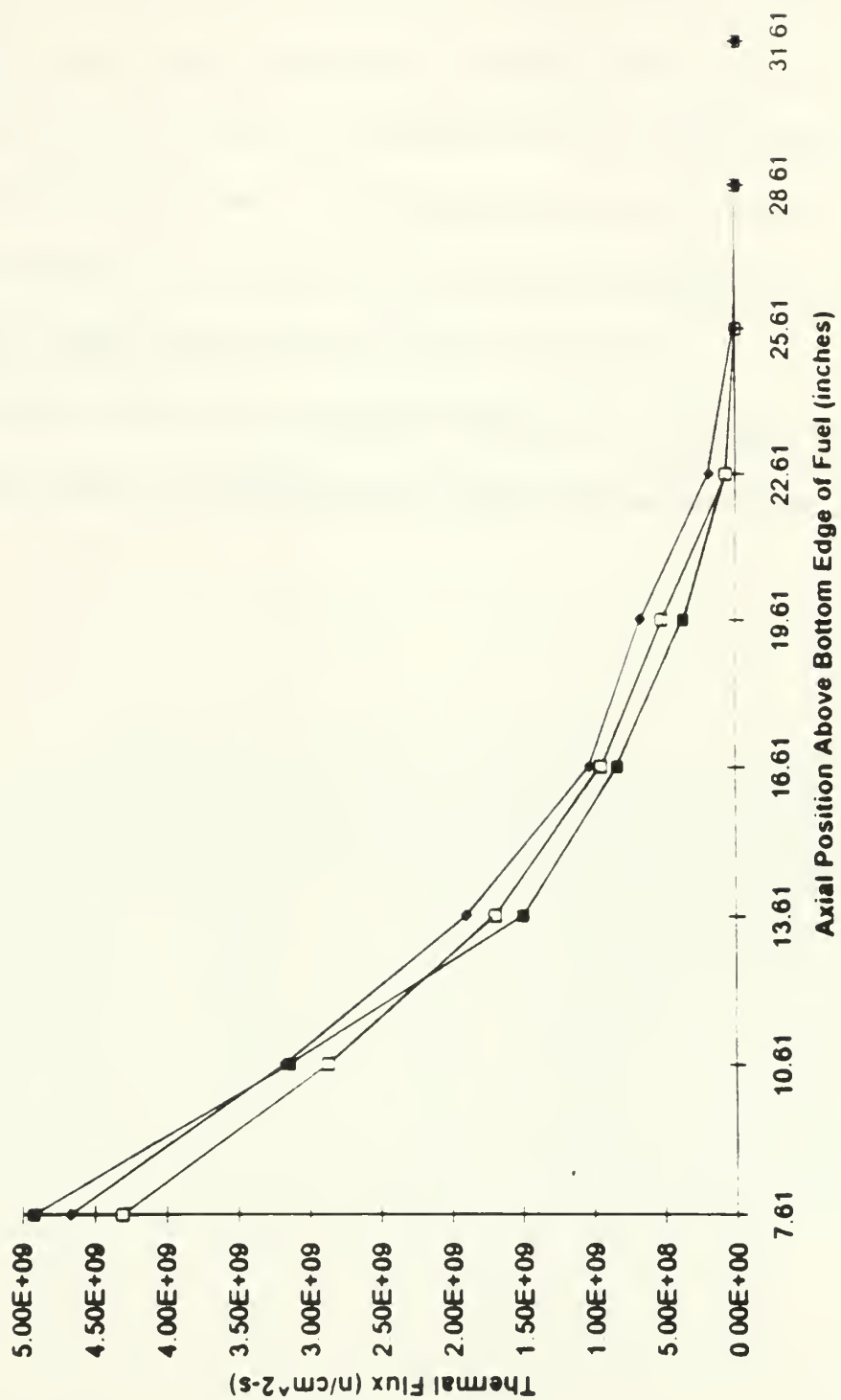


Figure 6.2.4-1: Neutron Flux at 1 kW with No Tilt



From Figure 6.2.4-2 it is evident that the flux tilt was present. This was especially true for detector #1. In order to really show the differences that each detector saw, the curves will be re-plotted with the tilt and no-tilt condition for each detector placed on one graph. In addition the curves will be normalized to the maximum detector reading for the no-tilt condition in each water vent hole. For the readings in water vent hole #1, for instance, all of the fluxes were divided by the measured flux for the no-tilt condition at the bottom of the instrument guide tube. This was repeated for each water vent hole. In this way the relative magnitude of the changes will be easily noted and the shape of the curves will be preserved. These normalized values are shown in Table 6.2.4-4.

All of the data in Table 6.2.4-4 is graphed in Figures 6.2.4-3 through 6.2.4-5. In each graph the tilt and no-tilt normalized fluxes for each individual water vent hole are plotted.



Table 6.2.4-2: Shim Blade and Regulating Rod Heights for Tilt @ 1kW

Control Component	Height with respect to Bank	Actual Height
Shim Blade #1	SBH + 4"	12.60"
Shim Blade #2	SBH + 2"	10.60"
Shim Blade #3	SBH + 0"	8.60"
Shim Blade #4	SBH - 2"	6.60"
Shim Blade #5	SBH - 4"	4.60"
Shim Blade #6	SBH + 1"	9.60"
Regulating Rod	N/A	3.58"

Note: SBH = Shim Bank Height

Table 6.2.4-3: Net Flux at 1 kW with Tilt

Axial Position	Water Hole #1 ( $\mu$ Amps)	Water Hole #3 ( $\mu$ Amps)	Water Hole #5 ( $\mu$ Amps)	Net Flux 1	Net Flux 3	Net Flux 5
7.61	0.1313	0.14	0.1862	5.78E+09	4.28E+09	4.69E+09
10.61	0.0827	0.0972	0.1332	3.50E+09	2.90E+09	3.28E+09
13.61	0.041	0.0587	0.0828	1.73E+09	1.76E+09	2.02E+09
16.61	0.0204	0.0318	0.044	9.16E+08	9.81E+08	1.12E+09
19.61	0.0103	0.0215	0.0267	3.95E+08	5.48E+08	7.28E+08
22.61	0.0042	0.0134	0.0117	7.75E+07	7.50E+07	2.18E+08
25.61	0.0021	0.0113	0.0056	0.00E+00	0.00E+00	2.93E+07
28.61	0.0014	0.0122	0.0038	0.00E+00	0.00E+00	0.00E+00
31.61	0.0011	0.0148	0.0033	0.00E+00	0.00E+00	0.00E+00



# Thermal Flux at 1 kW with Tilt

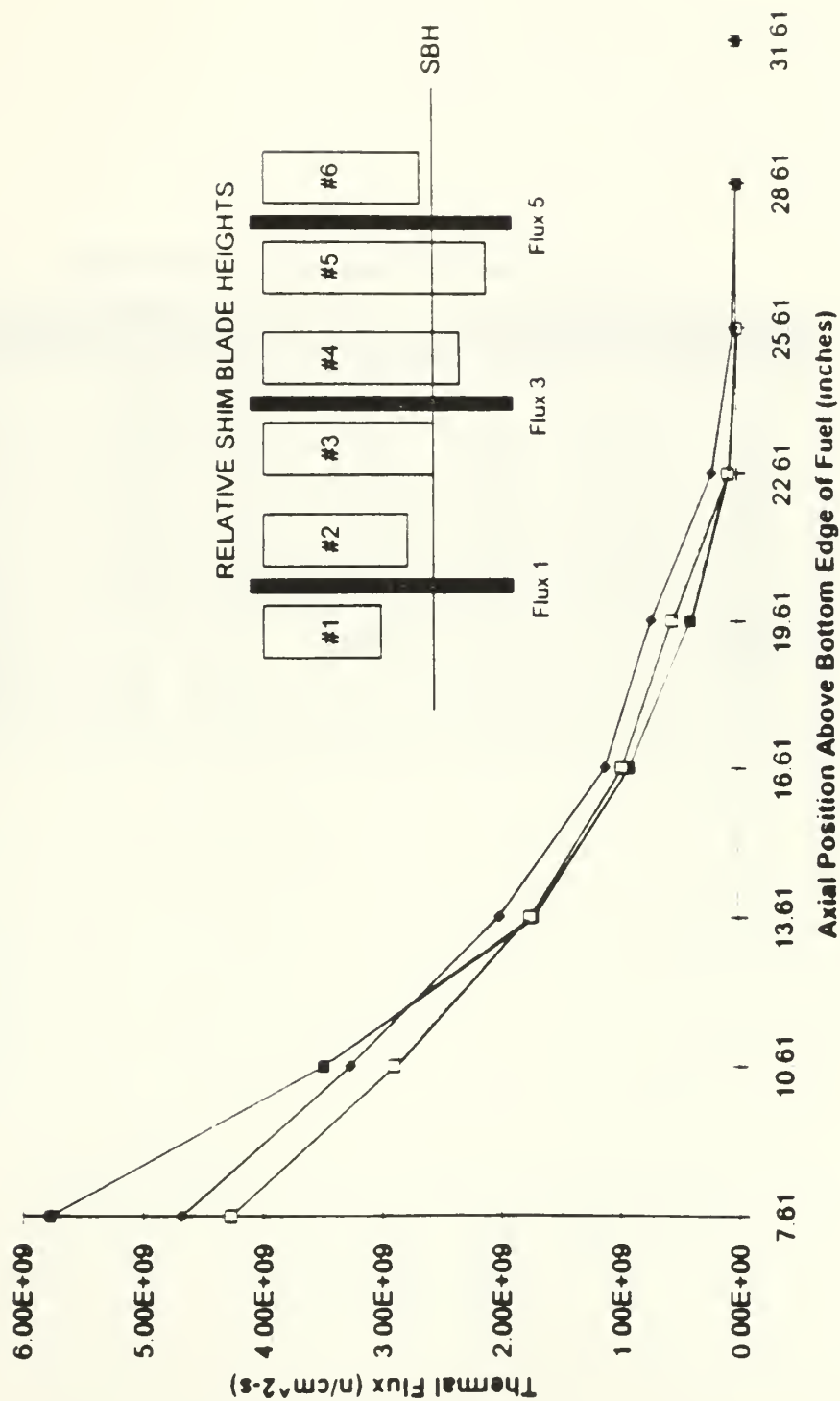


Figure 6 2 4-2 Neutron Flux at 1 kW with Tilt





Table 6.2.4-4: Normalized Flux Readings @ 1 kW

Axial Position	Tilt #1	Tilt #3	Tilt #5	No Tilt #1	No Tilt #3	No Tilt #5
7.61	1.1731	0.992	1.0027	1	1	1
10.61	0.7096	0.6734	0.701	0.6381	0.6667	0.6813
13.61	0.3519	0.4083	0.4324	0.3062	0.3949	0.4082
16.61	0.186	0.2272	0.2399	0.1702	0.2209	0.222
19.61	0.0801	0.1272	0.1558	0.0758	0.1218	0.145
22.61	0.0157	0.0174	0.0466	0.0157	0.0161	0.0412
25.61	0	0	0.0063	0	0	0.0027
28.61	0	0	0	0	0	0
31.61	0	0	0	0	0	0



# **Normalized Flux in Water Vent Hole #1 at 1 kW**

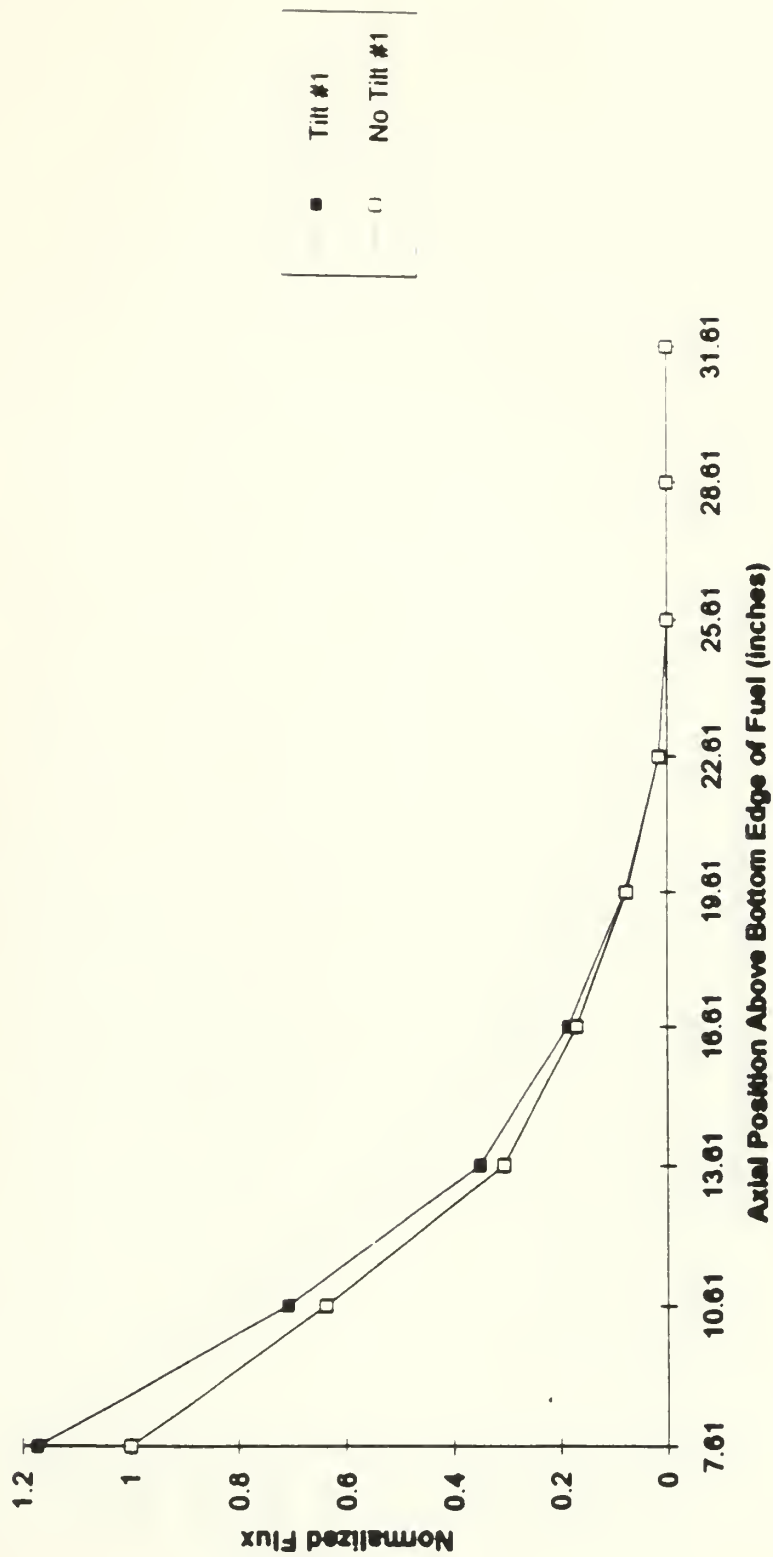


Figure 6.2.4-3: Normalized Tilt and No-Tilt Fluxes in Vent Hole #1 at 1 kW



# **Normalized Flux in Water Vent Hole #3 at 1 kW**

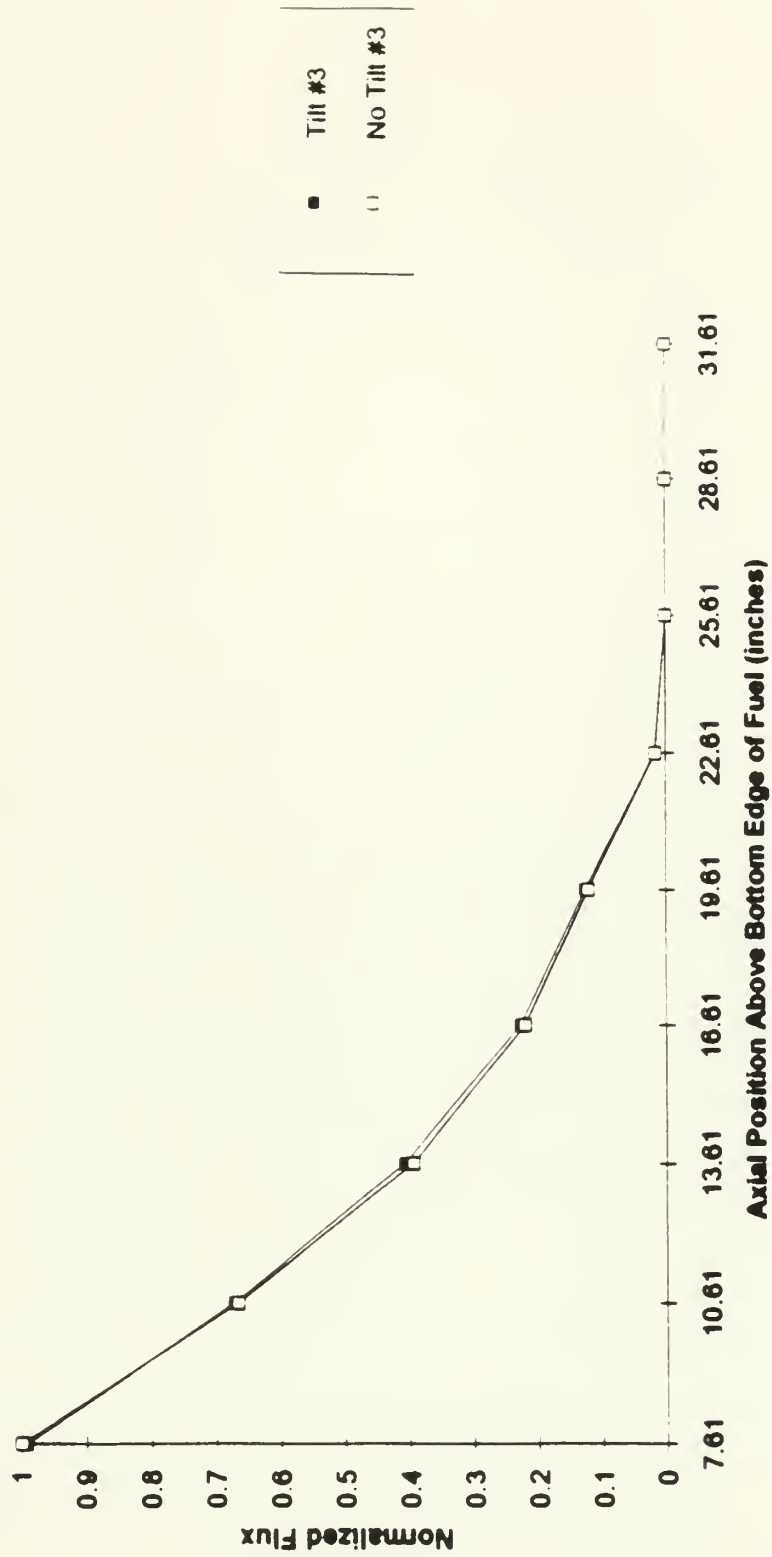


Figure 6.2.4-4: Normalized Tilt and No-Tilt Fluxes in Vent Hole #3 at 1 kW



# **Normalized Flux in Water Vent Hole #5 at 1 kW**

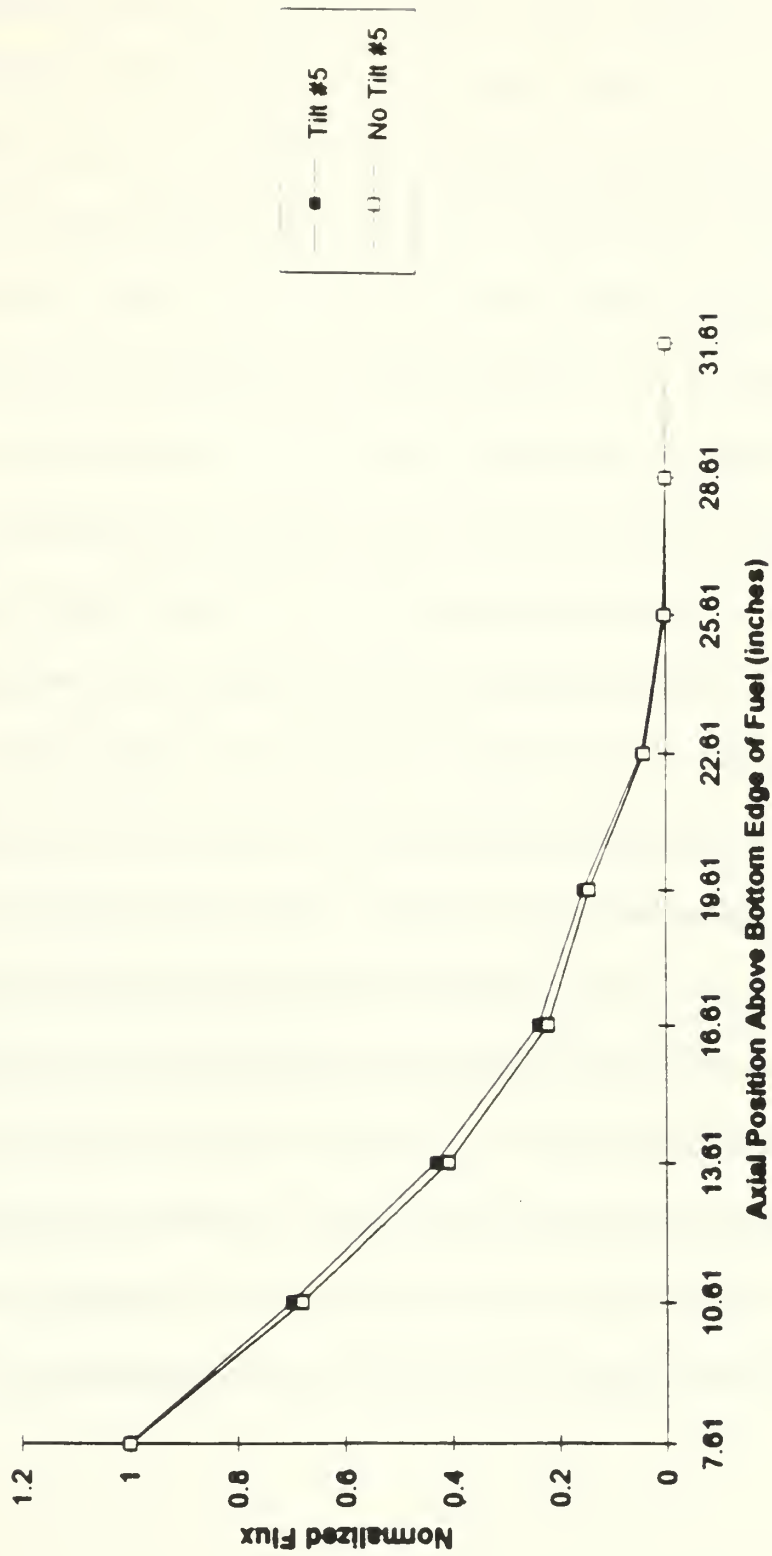


Figure 6.2.4-5: Normalized Tilt and No-Tilt Fluxes in Vent Hole #5 at 1 kW





Of the three previous figures, the one for water vent hole #1 shows the most significant change from the tilt to the no-tilt condition. And as would be expected from analyzing the locations of the shim blades and their adjusted heights, the flux in the tilted condition is higher for detector one than the no-tilt condition. This result is promising for the success of the instrumented synthesis method in being able to detect such a perturbation in the flux profile. An explanation for the flux profile variation results from observing the positions of the different shim blades in Table 6.2.4-2. The higher peak for the tilted flux in water vent hole #1 clearly results because it is surrounded by two shim blades which were moved above the bank height for the tilt. For the detector in water vent hole #3 however, shim blade #3 was not moved and shim blade #4 was moved in 2 inches. The results were just as expected; the flux for the tilted condition was only slightly lower than the no-tilt condition at the base of the water vent hole. For the most part however, the change in the flux in this vent hole was almost imperceptible. For water vent hole #5, however, the result is not as clear. This detector is surrounded by shim blade #5 which was pushed in four inches and shim blade #6 which was moved out one inch. Using the same rational as was used with the other two detectors, one would think that the tilted flux should be lower than the no-tilt case. Figure 6.2.4-5 shows that this is clearly not the case. In fact the flux for the tilted case is slightly higher than the no-tilt case throughout the core. Possibly the presence of the two dummy elements in cells A1 and A3 combined with the height of the shim blades around this detector act to retard the flux change.



## 6.2.5 FLUX TILTING AT 10 kW

With the data taken at 1 kW the decision was then made to raise power to 10 kW and repeat the tilt. At this higher power, however, the tilt could not be as extreme. As before the no-tilt condition was recorded first. For this case the shim bank height was 8.65 inches and the regulating rod position was 3.89 inches. The core tank temperature at the time this data was recorded was 35.4 °C. The net flux for the no-tilt condition is shown in Table 6.2.5-1.

The data from this table is plotted in Figure 6.2.5-1. As before this graph is provided for comparison to the flux tilt case. Once this data was taken the flux tilt was initiated. The positions of the shim blades and the regulating rod for this tilt are shown in Table 6.2.5-2. As before Figure 6.2.1-1 can be consulted to see the locations of the different control elements with respect to the different detectors. The core tank temperature for this flux tilt was 36.3 °C. It should be noted that the position of shim blade #6 for the tilt was supposed to be one inch below the bank height but because the reactor operator could not maintain the reactor critical with it in this position, it was left at 8.50 inches. The net flux for the tilt condition are shown in Table 6.2.5-3. This data is plotted in Figure 6.2.5-2.



Table 6 2 5-1 Net Flux at 10 kW with No Tilt

Axial Position	Water Hole #1 ( $\mu$ Amps)	Water Hole #3 ( $\mu$ Amps)	Water Hole #5 ( $\mu$ Amps)	Net Flux 1	Net Flux 3	Net Flux 5
7.61	0.8068	0.8742	1.2539	5.34E+10	4.86E+10	4.94E+10
10.61	0.5033	0.5734	0.8456	3.31E+10	3.04E+10	3.31E+10
13.61	0.2488	0.3411	0.5122	1.64E+10	1.81E+10	2.00E+10
16.61	0.1363	0.1916	0.2799	9.08E+09	1.02E+10	1.10E+10
19.61	0.0642	0.1171	0.1829	4.19E+09	6.06E+09	7.26E+09
22.61	0.018	0.0399	0.0635	1.05E+09	1.60E+09	2.38E+09
25.61	0.0058	0.0178	0.0182	2.61E+08	3.23E+08	5.58E+08
28.61	0.0029	0.014	0.0073	9.16E+07	5.19E+07	1.38E+08
31.61	0.0018	0.0154	0.0046	3.52E+07	5.77E+06	4.80E+07

Table 6.2.5-2: Shim Blade and Regulating Rod Heights for Tilt @ 10 kW

Control Component	Height with respect to Bank	Actual Height
Shim Blade #1	SBH + 2"	10.65"
Shim Blade #2	SBH + 1"	9.65"
Shim Blade #3	SBH + 0"	8.65"
Shim Blade #4	SBH - 1"	7.65"
Shim Blade #5	SBH - 2"	6.65"
Shim Blade #6	SBH - 0.15"	8.50"
Regulating Rod	N/A	7.90"

Note: SBH = Shim Bank Height



Table 6.2.5-3. Net Flux at 10 kW with Tilt

Axial Position	Water Hole #1 ( $\mu$ Amps)	Water Hole #3 ( $\mu$ Amps)	Water Hole #5 ( $\mu$ Amps)	Net Flux 1	Net Flux 3	Net Flux 5
7.61	0.845	0.8498	1.2204	5.61E+10	4.52E+10	4.80E+10
10.61	0.5312	0.5709	0.8536	3.51E+10	3.02E+10	3.34E+10
13.61	0.2632	0.3425	0.5193	1.74E+10	1.81E+10	2.03E+10
16.61	0.14	0.1905	0.2796	9.34E+09	1.01E+10	1.10E+10
19.61	0.0667	0.1161	0.1831	4.37E+09	6.01E+09	7.27E+09
22.61	0.0181	0.04	0.0648	1.06E+09	1.61E+09	2.44E+09
25.61	0.0058	0.018	0.019	2.61E+08	3.35E+08	5.90E+08
28.61	0.0027	0.0143	0.008	7.75E+07	6.92E+07	1.67E+08
31.61	0.0017	0.0154	0.0049	2.82E+07	5.77E+06	5.86E+07





# Baseline Readings at 10 kW

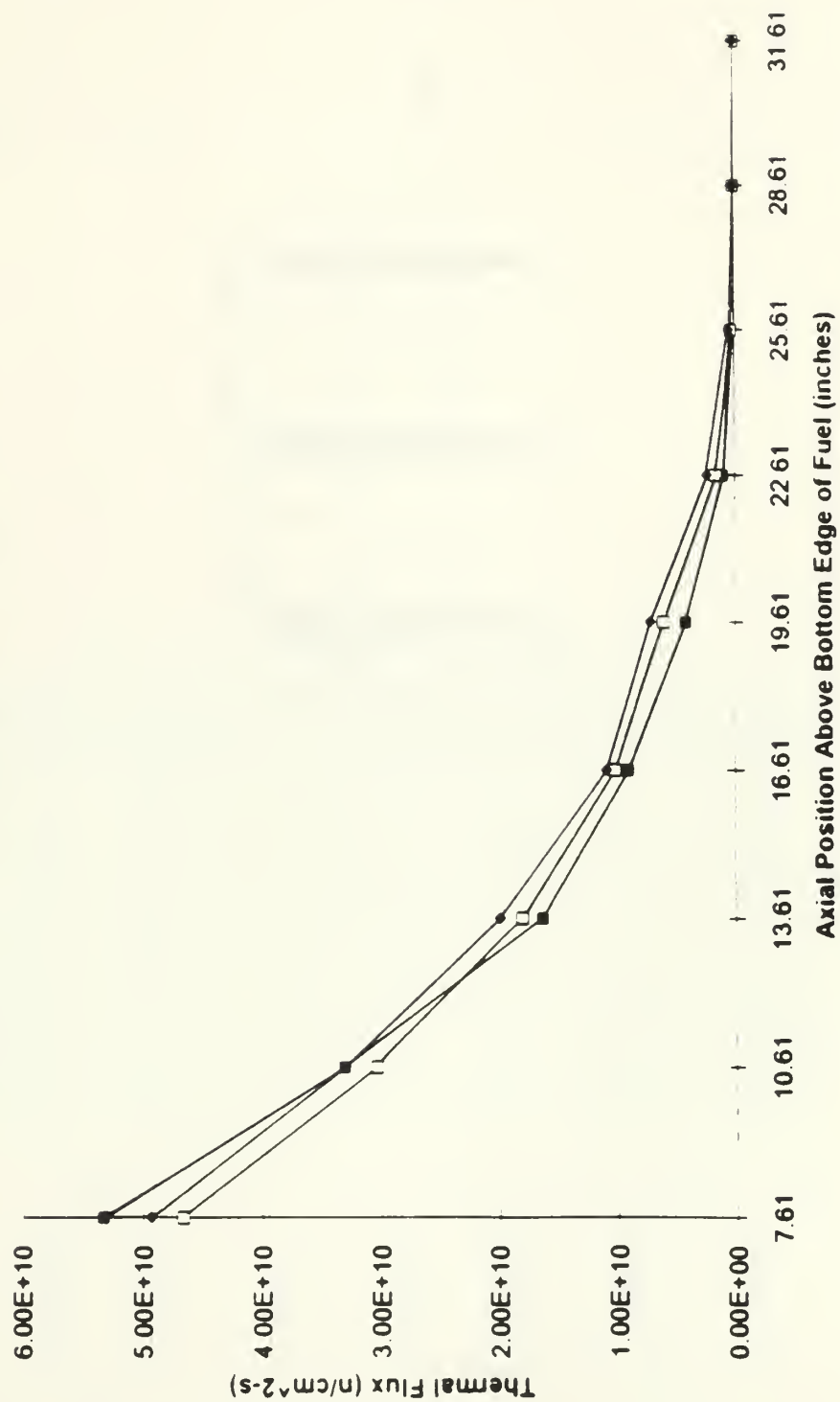


Figure 6.2.5-1: Neutron Flux at 10 kW with No Tilt



# **Thermal Flux at 10 kW with Tilt**

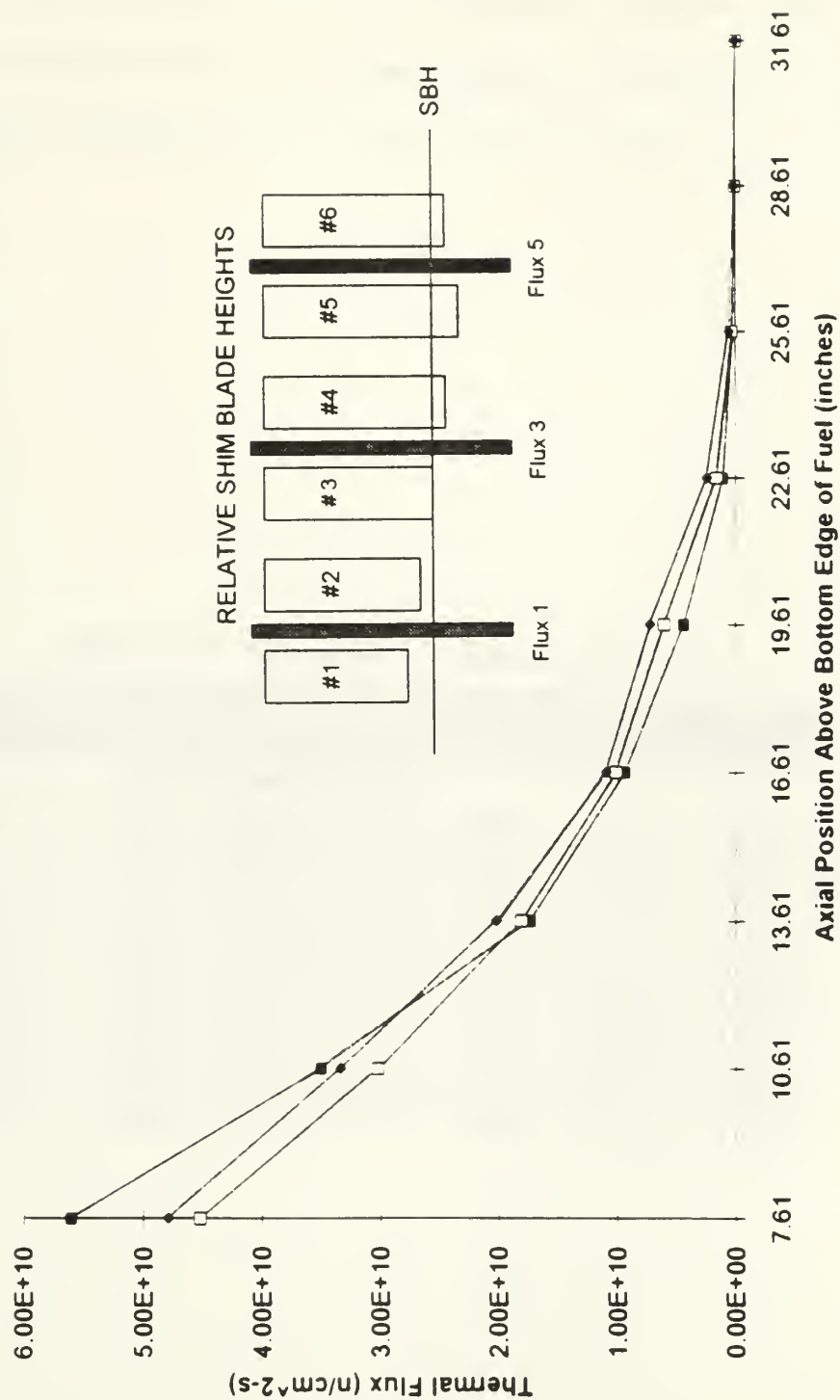


Figure 6.2.5-2: Neutron Flux at 10 kW with Tilt



From these two figures it is evident that the flux tilt had some effect, but it wasn't nearly as pronounced as the case at 1 kW. In order to discern the differences the normalized flux readings will be plotted. These normalized values are shown below in Table 6.2.5-4. These normalized values were calculated as in the previous case at 1 kW.

All of the data in this table is plotted in Figures 6.2.5-3 through 6.2.5-5 on the following pages. As before each curve contains only the data from a single water vent hole.

Table 6.2.5-4: Normalized Flux Readings @ 10 kW

Axial Position	Tilt #1	Tilt #3	Tilt #5	No Tilt #1	No Tilt #3	No Tilt #5
7.61	1.0507	0.9698	0.9716	1	1	1
10.61	0.6577	0.6483	0.677	0.6209	0.6514	0.6703
13.61	0.3259	0.3888	0.411	0.3069	0.3871	0.4049
16.61	0.1751	0.2174	0.2224	0.1702	0.2187	0.2227
19.61	0.0819	0.1288	0.1473	0.0786	0.13	0.1472
22.61	0.0198	0.0345	0.0494	0.0197	0.0344	0.0483
25.61	0.0049	0.0072	0.012	0.0049	0.0069	0.0113
28.61	0.0015	0.0015	0.0034	0.0017	0.0011	0.0028
31.61	0.0005	0.0001	0.0012	0.0007	0.0001	0.0009



# **Normalized Flux in Water Vent Hole #1 at 10 kW**

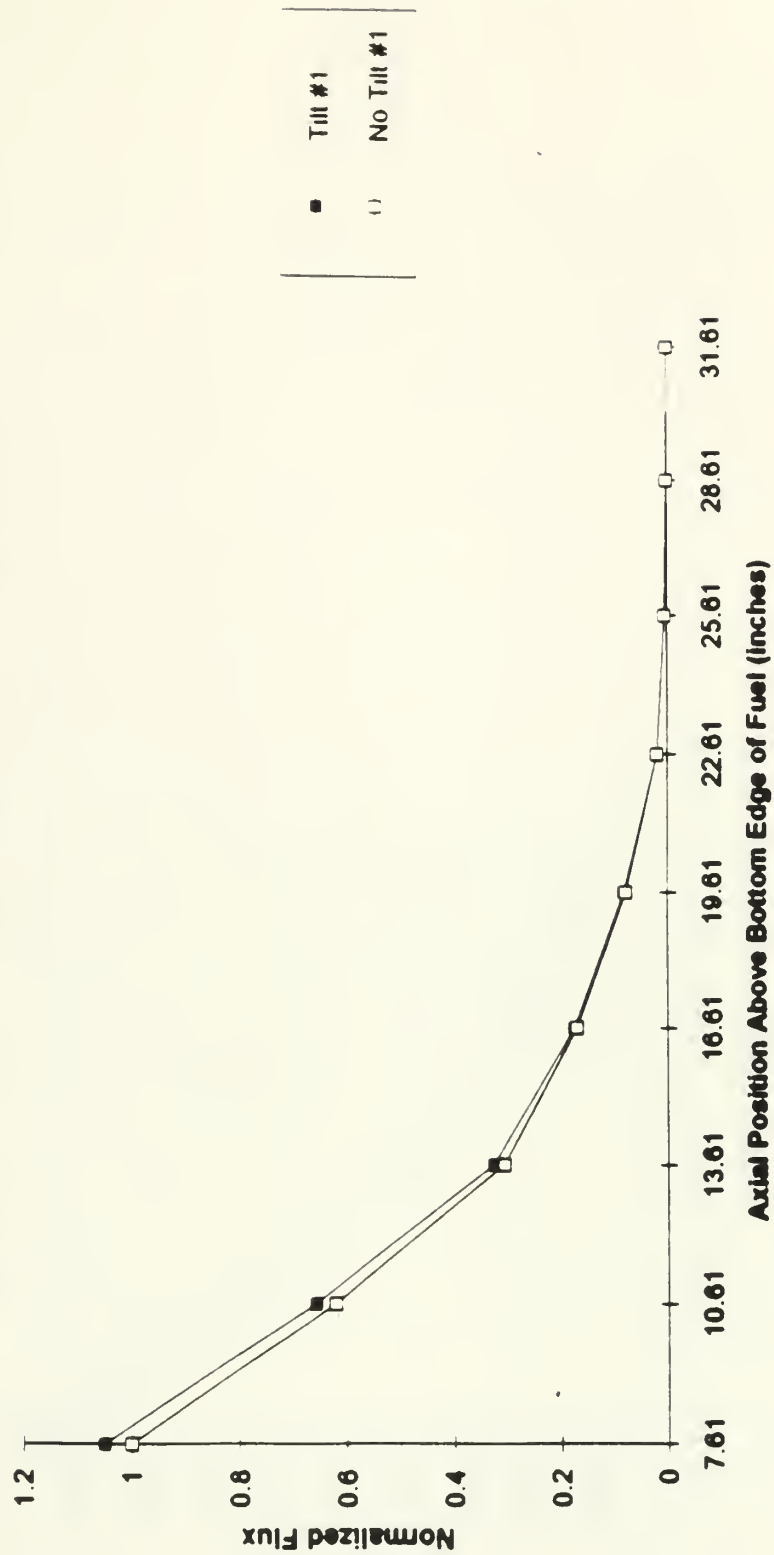


Figure 6.2.5-3: Normalized Tilt and No-Tilt Fluxes in Vent Hole #1 at 10 kW





# **Normalized Flux in Water Vent Hole #3 at 10 kW**

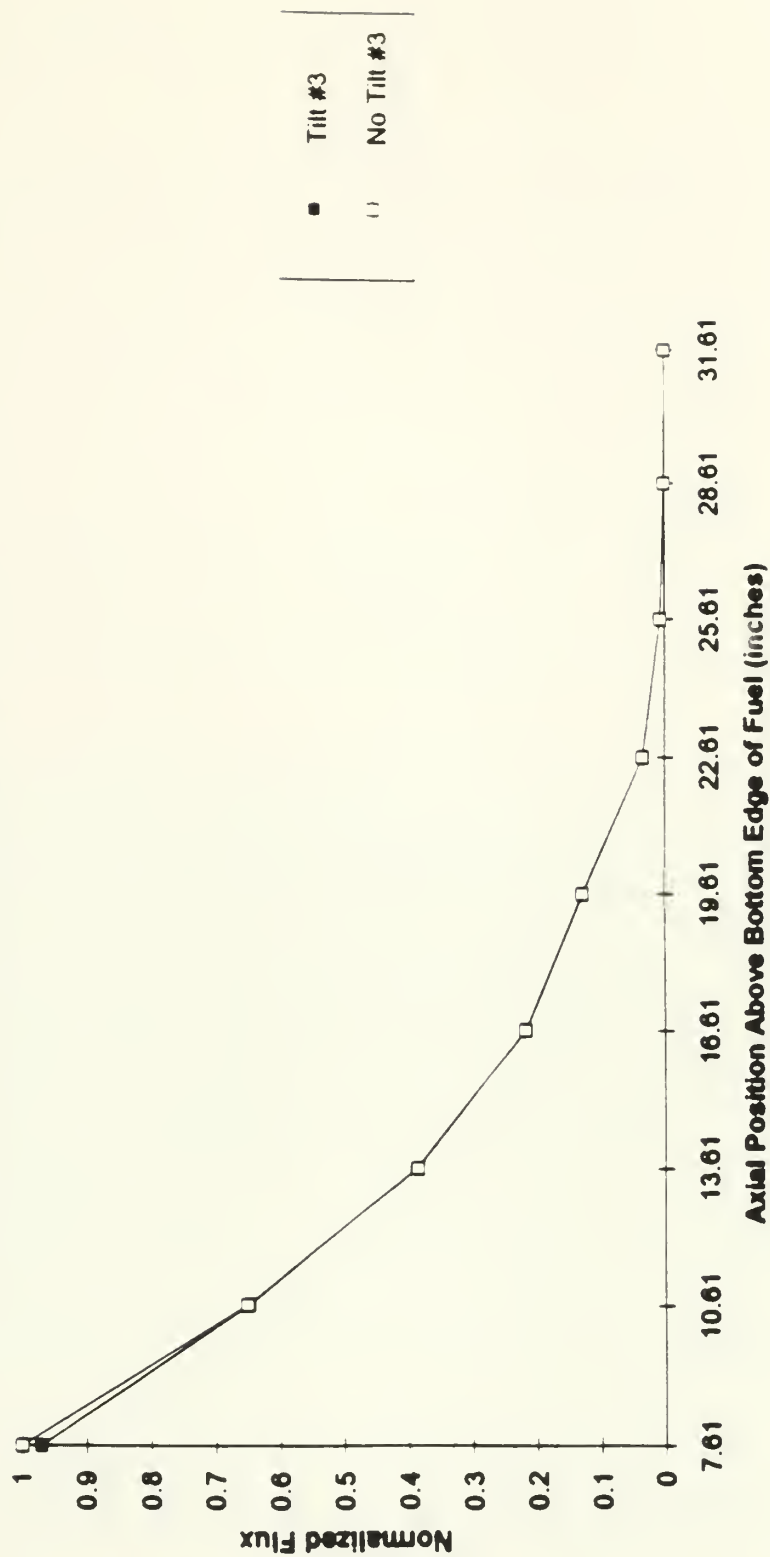


Figure 6.2.5-4: Normalized Tilt and No-Tilt Fluxes in Vent Hole #3 at 10 kW



# **Normalised Flux in Water Vent Hole #5 at 10 kW**

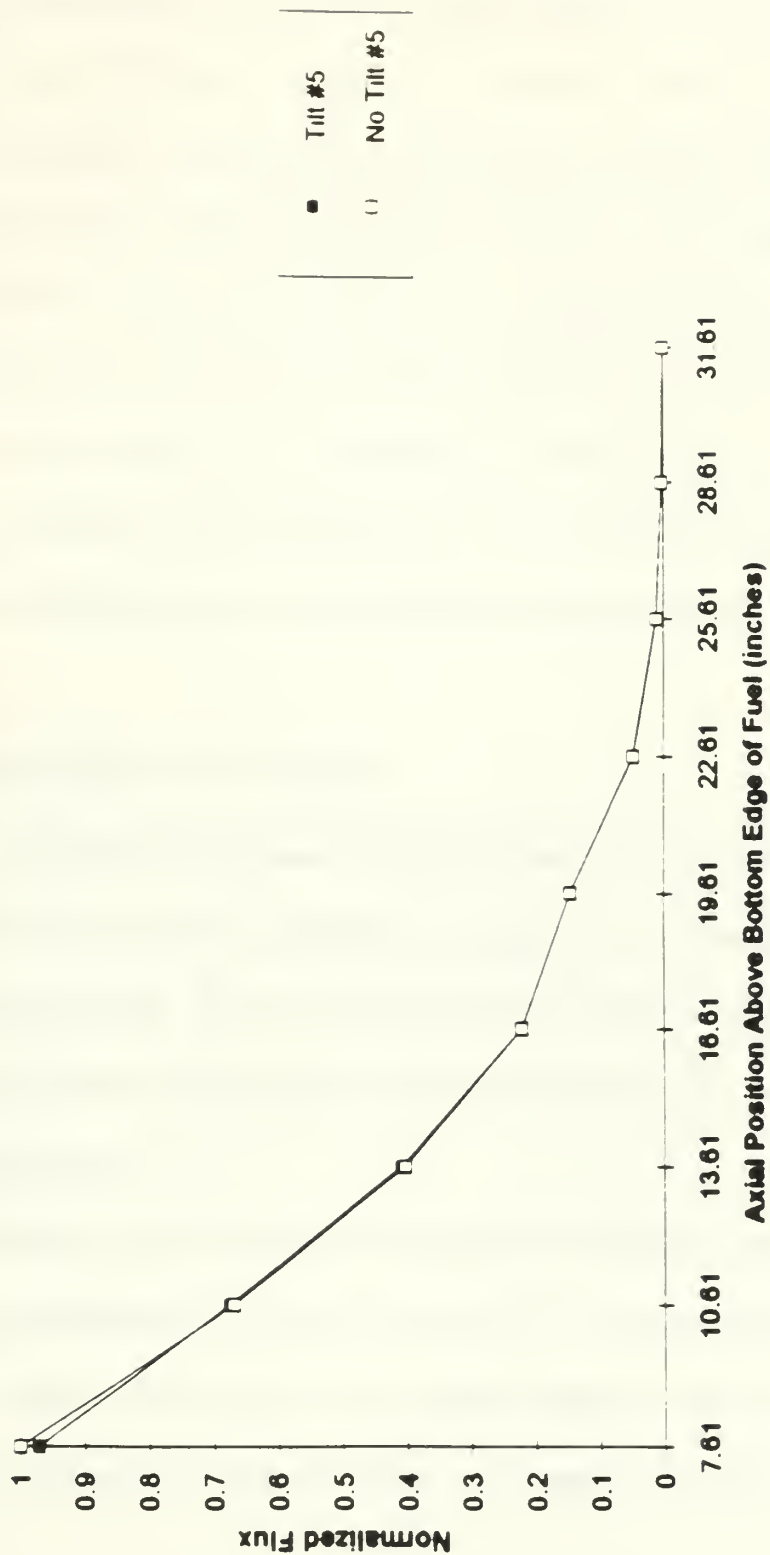


Figure 6.2.5-5: Normalized Tilt and No-Tilt Fluxes in Vent Hole #5 at 10 kW



As in the case at 1 kW the flux tilt was most pronounced in water vent hole #1. Again this is very encouraging for use with the synthesis method. By looking at the position of the various shim blades in Table 6.2.5-2 it should be noted that all of the normalized flux curves appear to make sense this time. Even the detector in water vent hole #5 responded as expected from the depression of the flux in that region. It is interesting to see that the change between the tilt and no-tilt condition for water vent hole #1 can be seen all the way up to 16.6 inches. For water vent holes 3 and 5 it is hard to see any change above about 10.6 inches. This is probably best explained from the position of the shim blades; the detector in water vent hole #1 is in the location of the greatest divergence from the bank height and as a result the flux there will be perturbed the most.

## 6.2.6 FLUX TILTING AT 50 kW

The final flux tilt performed in phase I of this experiment was at 50 kW. The shim bank height was 8.75 inches and the regulating rod height was 3.38 inches when the baseline "no-tilt" data was taken. The core tank temperature for this part of the test was 37.6 °C. The net flux for the no-tilt condition is compiled in Table 6.2.6-1 below. This data is plotted in Figure 6.2.6-1.

With the no-tilt data taken the flux tilt was initiated as shown in Table 6.2.6-2 below. The core tank temperature for the flux tilt was 41.2 °C. As in the previous case it was not possible to position shim blade #6 to the position called for in the test procedure because the reactor could not be maintained critical. As a result it was left at the shim



bank height for this portion of the test. The data resulting from the measurements with this flux tilt are provided in Table 6.2.6-3. This data is plotted in Figure 6.2.6-2.

Table 6.2.6-1. Net Flux at 50 kW with No Tilt

Axial Position	Water Hole #1 ( $\mu$ Amps)	Water Hole #3 ( $\mu$ Amps)	Water Hole #5 ( $\mu$ Amps)	Net Flux 1	Net Flux 3	Net Flux 5
7.61	3.859	4.073	5.908	2.68E+11	2.31E+11	2.44E+11
10.61	2.486	2.697	4.026	1.73E+11	1.53E+11	1.66E+11
13.61	1.24	1.603	2.449	8.62E+10	9.09E+10	1.01E+11
16.61	0.682	0.896	1.327	4.75E+10	5.08E+10	5.48E+10
19.61	0.32	0.535	0.874	2.22E+10	3.02E+10	3.62E+10
22.61	0.081	0.156	0.29	5.49E+09	8.30E+09	1.19E+10
25.61	0.023	0.048	0.076	1.47E+09	2.07E+09	2.97E+09
28.61	0.009	0.0237	0.0242	5.21E+08	6.12E+08	8.45E+08
31.61	0.0045	0.0191	0.0114	2.26E+08	2.19E+08	3.31E+08





Table 6.2.6-2: Shim Blade and Regulating Rod Heights for Tilt @ 50 kW

Control Component	Height with respect to Bank	Actual Height
Shim Blade #1	SBH + 2"	10.75"
Shim Blade #2	SBH + 1"	9.75"
Shim Blade #3	SBH + 0"	8.75"
Shim Blade #4	SBH - 1"	7.75"
Shim Blade #5	SBH - 2"	6.75"
Shim Blade #6	SBH + 0"	8.75"
Regulating Rod	N/A	6.65"

Note: SBH = Shim Bank Height

Table 6.2.6-3: Net Flux at 50 kW with Tilt

Axial Position	Water Hole #1 ( $\mu$ Amps)	Water Hole #3 ( $\mu$ Amps)	Water Hole #5 ( $\mu$ Amps)	Net Flux 1	Net Flux 3	Net Flux 5
7.61	4.114	4.017	5.792	2.86E+11	2.28E+11	2.39E+11
10.61	2.582	2.726	4.015	1.80E+11	1.55E+11	1.66E+11
13.61	1.3017	1.5958	2.431	9.06E+10	9.05E+10	1.00E+11
16.61	0.7067	0.8963	1.3231	4.93E+10	5.09E+10	5.46E+10
19.61	0.3232	0.5335	0.8773	2.24E+10	3.01E+10	3.63E+10
22.61	0.083	0.1581	0.2939	5.63E+09	8.42E+09	1.20E+10
25.61	0.0229	0.0482	0.0775	1.47E+09	2.08E+09	3.04E+09
28.61	0.0083	0.0243	0.0262	4.72E+08	6.46E+08	9.29E+08
31.61	0.042	0.0192	0.0118	2.87E+09	2.25E+08	3.47E+08



# Baseline Readings at 50 kW

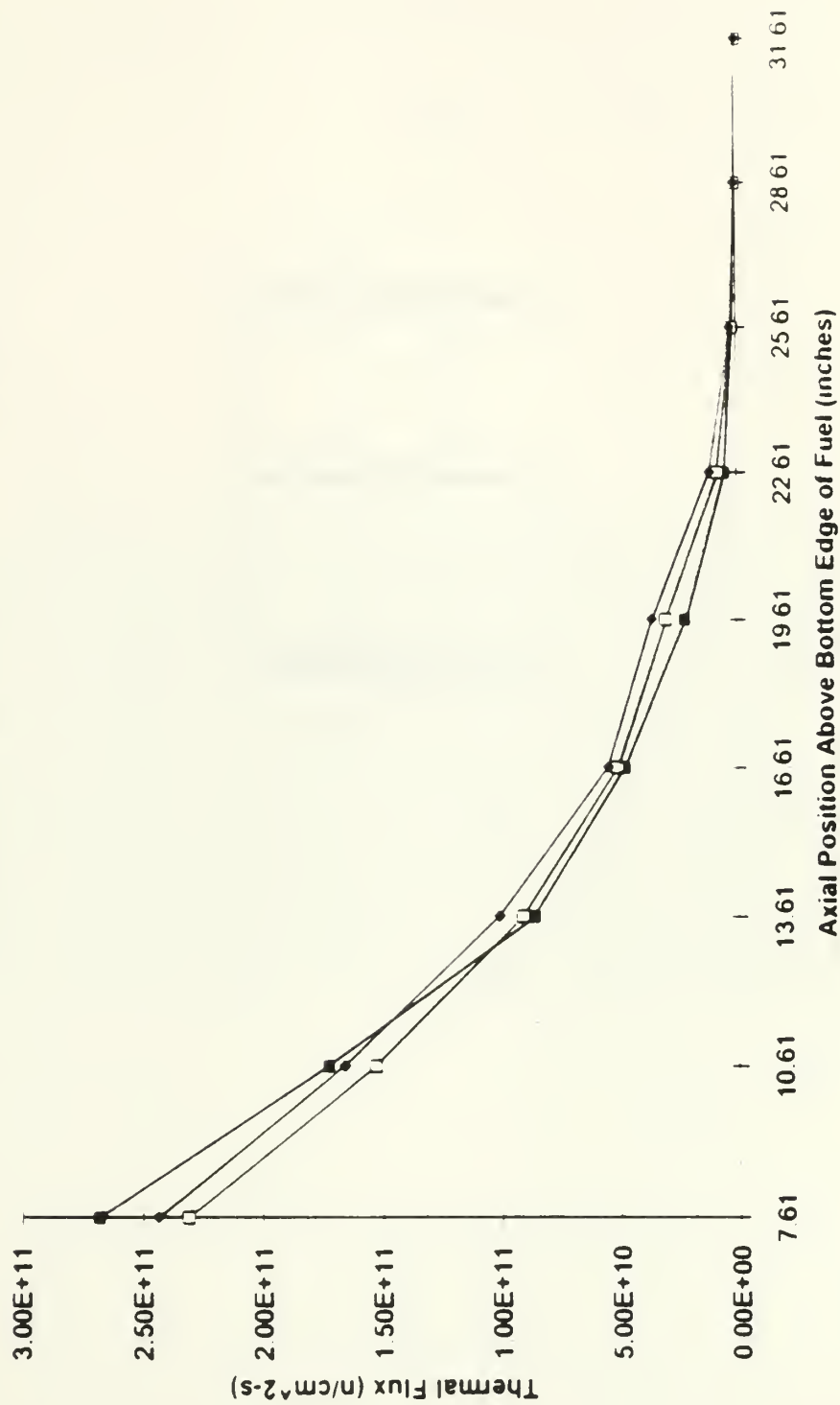


Figure 6 2 6-1: Neutron Flux at 50 kW with No Tilt



# Thermal Flux at 50 kW with Tilt

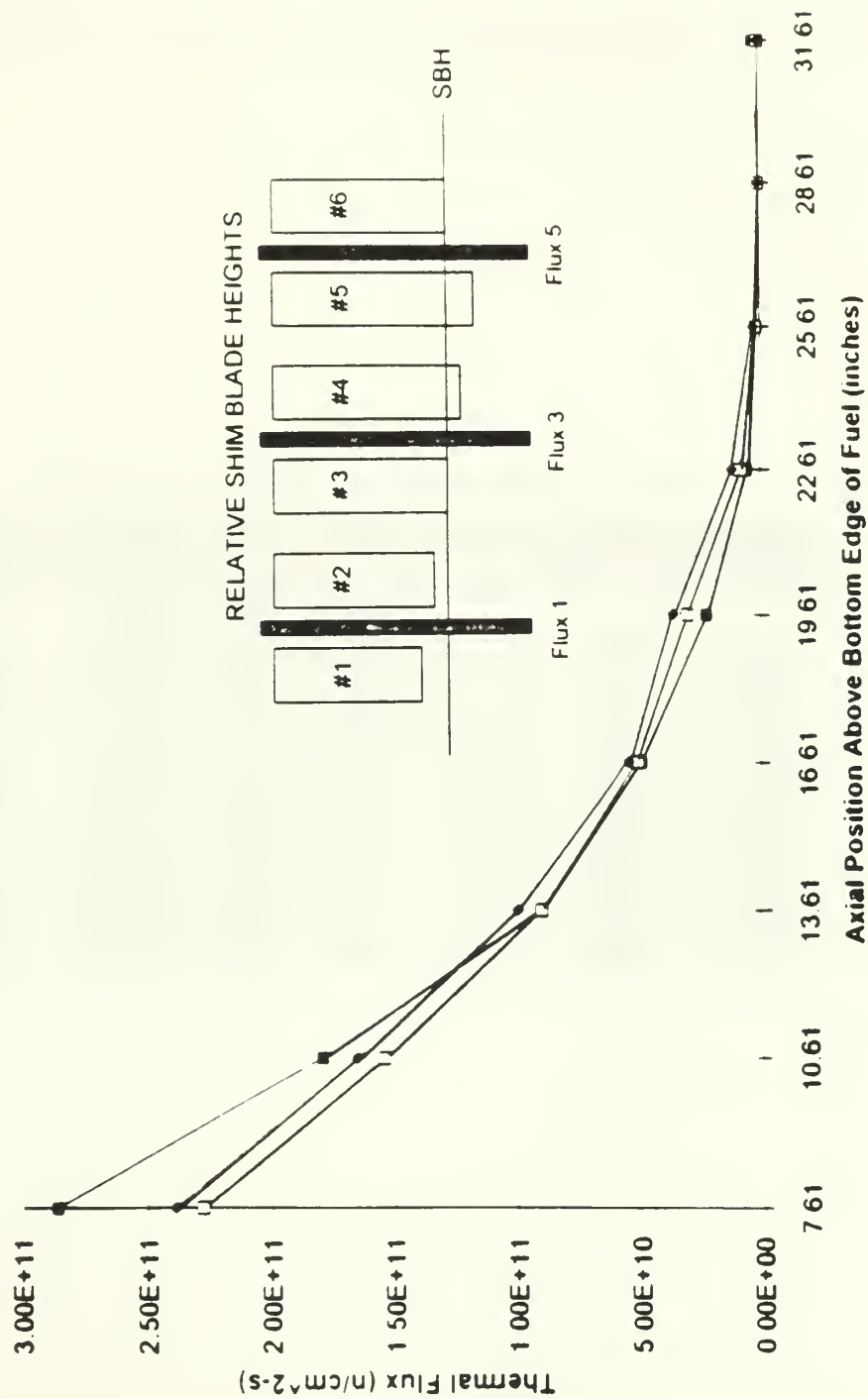


Figure 6 2 6-2 Neutron Flux at 50 kW with Tilt



As in the case at 10 kW it is evident from these two figures that the flux tilt had some effect. In order to discern the differences the normalized flux readings will be plotted. These normalized values are shown below in Table 6.2.6-4 below. All of the data in the this table is graphed in Figures 6.2.6-3 through 6.2.6-5. In each graph the tilt and no-tilt normalized fluxes for each individual water vent hole are plotted.

Table 6.2.6-4: Normalized Flux Readings @ 50 kW

<b>Axial Position</b>	<b>Tilt #1</b>	<b>Tilt #3</b>	<b>Tilt #5</b>	<b>No Tilt #1</b>	<b>No Tilt #3</b>	<b>No Tilt #5</b>
7.61	1.0669	0.986	0.9801	1	1	1
10.61	0.6691	0.6686	0.6788	0.6439	0.6614	0.6807
13.61	0.3374	0.3912	0.4108	0.3212	0.393	0.4139
16.61	0.1836	0.22	0.2239	0.1771	0.2199	0.2245
19.61	0.0836	0.1301	0.1488	0.0828	0.1305	0.1482
22.61	0.021	0.0364	0.0493	0.0204	0.0359	0.0486
25.61	0.0055	0.009	0.0124	0.0055	0.0089	0.0122
28.61	0.0018	0.0028	0.0038	0.0019	0.0026	0.0035
31.61	0.0107	0.001	0.0014	0.0008	0.0009	0.0014





# **Normalized Flux in Water Vent Hole #1 at 50 kW**

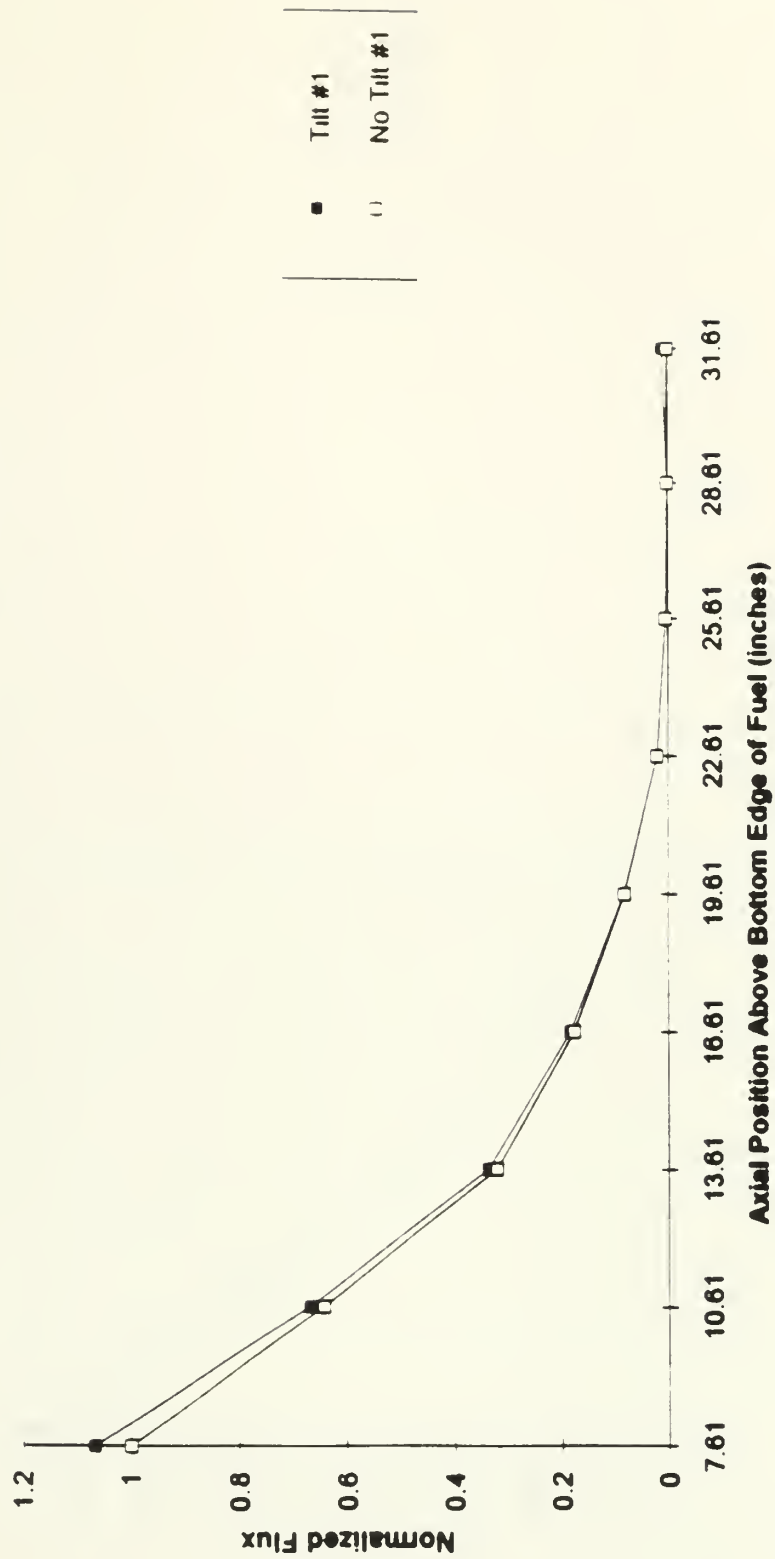


Figure 6.2.6-3: Normalized Tilt and No-Tilt Fluxes in Vent Hole #1 at 50 kW



# **Normalized Flux in Water Vent Hole #3 at 50 kW**

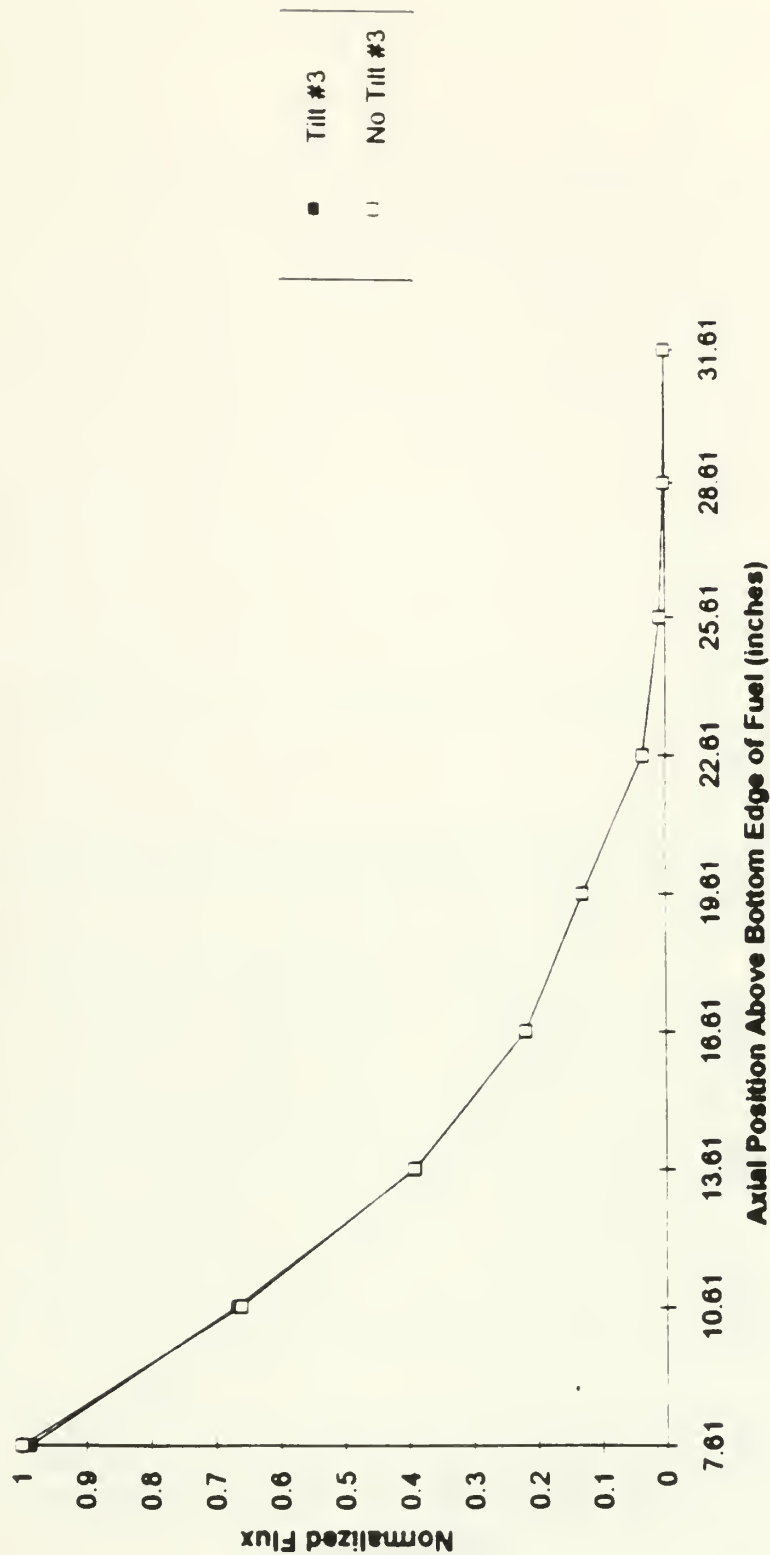
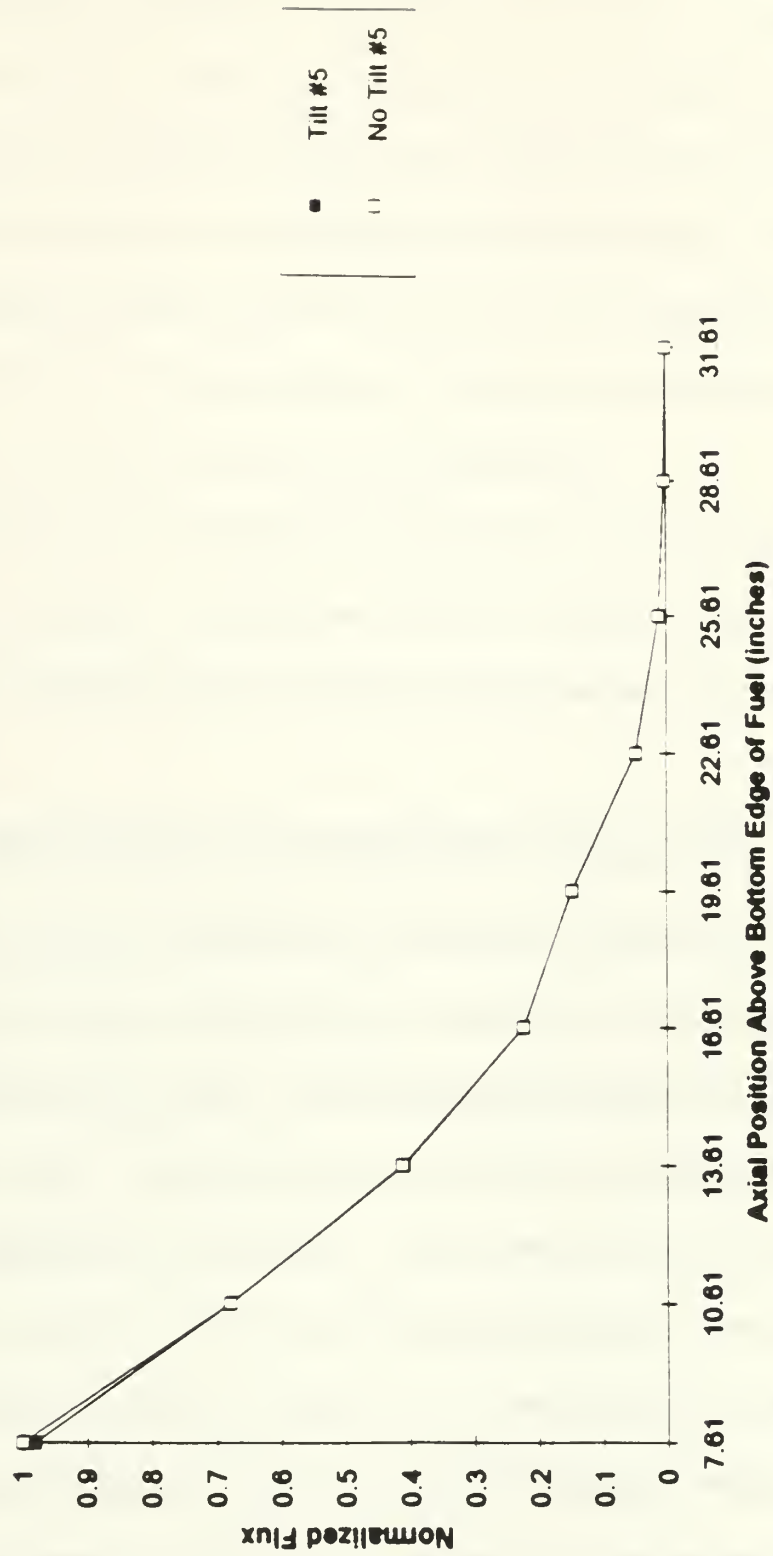


Figure 6.2.6-4: Normalized Tilt and No-Tilt Fluxes in Vent Hole #3 at 50 kW



# **Normalised Flux in Water Vent Hole #5 at 50 kW**



**Figure 6.2.6-5: Normalized Tilt and No-Tilt Fluxes in Vent Hole #5 at 50 kW**



From these figures it is once again apparent that the detector in water vent hole #1 is subject to the most extreme changes in the flux from the tilt. Again the readings are as would be expected from the positioning of the shim blades. The change in the flux in water vent hole #3 was very minimal, but again it was in the direction that was expected. In water vent hole #5 the change was only slightly more perceptible than in vent hole #3. As in the earlier cases, the changes in water vent holes #3 and #5 were only seen in the lower 10 inches of the core. For water vent hole #1 the change in flux between the tilt and no-tilt conditions was seen all the way up to the 16.6 inch position.

Once this final flux tilt was performed the reactor power was lowered to 500 watts and operated at this level until it was shutdown at 0300 on Tuesday, 30 March 1993. It was determined that the final background readings would be taken later that morning.

## **6.2.7 FINAL SHUTDOWN BACKGROUND READINGS**

Once all testing was completed and the reactor was shutdown, a final set of background readings was taken. This was done to ensure that no drastic changes had occurred in the background flux profile. The final background readings were performed at 0750 on Tuesday morning. These readings were performed in a similar manner to the ones taken at the beginning of the experiment. The temperature in the core tank during these measurements was 41.3 °C. The raw data from this portion can be seen in Appendix B.1. This data is shown graphically as Figure 6.2.7-1. From this figure it is evident that the flux shape did not change appreciably from the initial background readings shown in Figure 6.2.1-3. One interesting thing to note is that the initial flux readings are slightly





higher than the final measurements. One possible explanation for this is the difference in temperature between the two readings. The initial readings were taken with a core tank temperature of 32.5 °C and the final measurements were taken with the temperature at 41.3 °C. The higher temperature associated with the final measurement could have resulted in fewer thermal neutrons in the vicinity of the fission chamber detectors, and thus a lower current reading.



# Final Shutdown Background Data

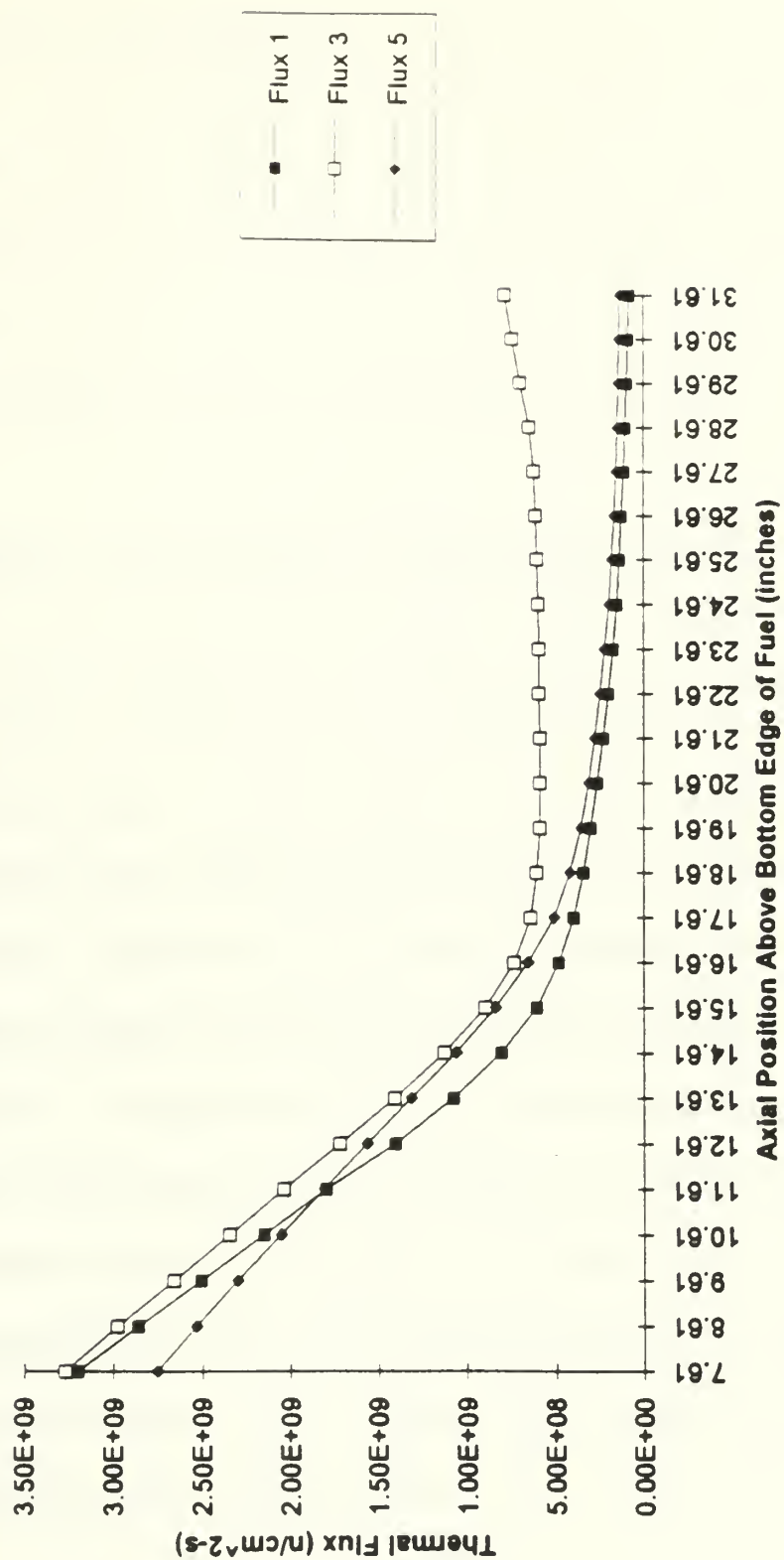


Figure 6 2.7-1: Final Shutdown Background Readings



## 6.3 PHASE II OF EXPERIMENT

This portion of the experiment was conducted on Tuesday, 20 April 1993. Unfortunately, problems continued to plague the A/D board and as a result the transient portions of the experiment were once again deleted. The core installed in the MITR-II was the same as the one used in Phase I of the experiment (described in Section 6.2.1). The raw data from this phase of the experiment can be found in Appendix B.2.

### 6.3.1 SHUTDOWN BACKGROUND MEASUREMENTS

The initial shutdown measurements were taken at 1608, 71.47 hours after the reactor had been shutdown. As before, the core was essentially Xenon free at the time these measurements were taken. The initial shutdown flux profile is shown in Figure 6.3.1-1. It is interesting to see the difference between the flux in water vent hole #1 and the other two vent holes. It is evident from this figure that something is happening with either the picoammeter's output or the power generation within the core has been skewed toward water vent hole #1. A check of the picoammeter's current output has revealed that it is tracking correctly with the other two meters. If the power is truly skewed, then it has occurred during operations since the last refueling on 29 March 1993. The initial background readings taken during Phase I of the experiment (see Figure 6.2.1-3) showed that all three fluxes were much closer than in this phase. These readings from Phase I were taken immediately after the core had been refueled.



# Initial Shutdown Background Readings

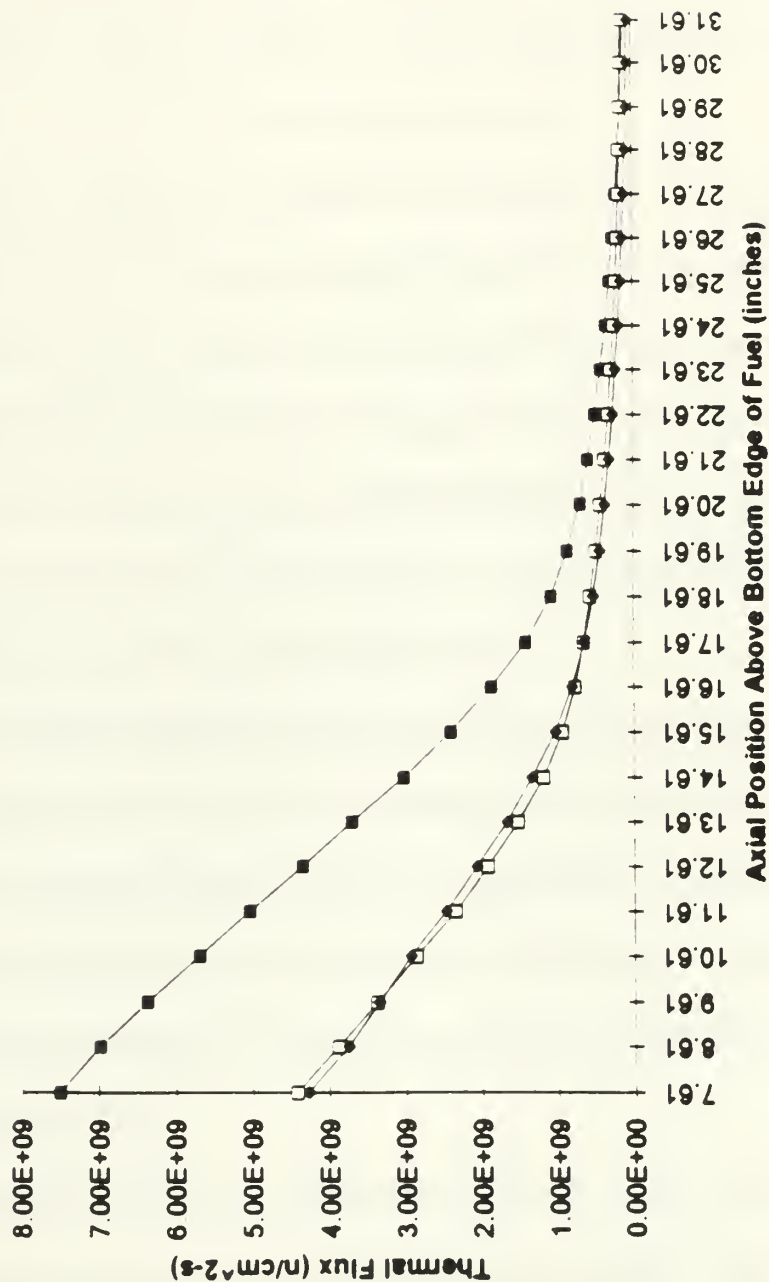


Figure 6.3.1-1: Initial Shutdown Background Readings - Phase II





### 6.3.2 FLUX TILTING AT 1 kW

After the reactor was started up, power was leveled at 1 kW. The shim bank height for this power was 10.30 inches and the regulating rod position was 2.64 inches. At this power level the no-tilt flux condition in the core was measured. The net flux measured at this power is shown in Table 6.3.2-1 and is plotted in Figure 6.3.2-1. The core tank temperature at the time this data was taken was 32.0 °C.

Once the no-tilt condition was measured, the first flux tilt was initiated. The positions of the shim blades and the regulating rod for this tilt are shown in Table 6.3.2-2. It should be noted that it wasn't possible to get shim blade #5 into the requested position because the Reactor Operator had trouble maintaining criticality. As a result it was moved only as far as he felt it could be positioned while still keeping the reactor at 1 kW. The core tank temperature for this portion of the test 38.1 °C. The net flux data from this first tilt is shown in Table 6.3.2-3 and is plotted in Figure 6.3.2-2.

When all of the flux measurements were taken with this tilt condition, the flux was shifted to the opposite side of the core by positioning shim blades as shown in Table 6.3.2-4. Again one of the shim blades could not be positioned as requested. This was done to **determine** if the fission chambers could detect the shift in the flux within the core. The **resulting measured net fluxes** in this condition are shown in Table 6.3.2-5. This data is then plotted in Figure 6.3.2-3.

While the flux tilt is very evident in Figures 6.3.2-2 and 6.3.2-3, it was decided that the **normalized values** would once again be plotted as done with Phase I data. Again the



normalized values were found by dividing all data in each water vent hole by the maximum no-tilt data in that vent hole. The normalized flux values are shown in Table 6.3.2-6. All of the normalized readings for each individual water vent hole are plotted in Figures 6.3.2-4 through 6.3.2-6.

The figures of the normalized flux readings clearly show the effect of the two tilts. In addition each fission chamber detected the shift in the tilt from one side of the core to the other. The tilt is most evident in water vent holes 1 and 3. This is as would be expected from the positioning of the shim blades as described in Tables 6.3.2-2 and 6.3.2-4. Because the change in the shim blades was the smallest in the vicinity of water vent hole #5, the flux tilt was not as evident there. This data is very encouraging for use with the instrumented synthesis method.



Table 6.3.2-1: Net Flux at 1 kW with No Tilt - Phase II

Axial Position	Water Hole #1 ( $\mu$ Amps)	Water Hole #3 ( $\mu$ Amps)	Water Hole #5 ( $\mu$ Amps)	Net Flux 1	Net Flux 3	Net Flux 5
7.61	0.215	0.157	0.209	7.65E+09	4.64E+09	4.47E+09
10.61	0.153	0.099	0.14	5.09E+09	2.85E+09	2.92E+09
13.61	0.096	0.05	0.083	3.06E+09	1.38E+09	1.80E+09
16.61	0.047	0.028	0.043	1.43E+09	8.42E+08	9.87E+08
19.61	0.024	0.014	0.024	8.17E+08	3.12E+08	5.56E+08
22.61	0.012	0.007	0.01	3.38E+08	7.50E+07	1.51E+08
25.61	0.0052	0.0037	0.0043	5.64E+07	0.00E+00	2.51E+07
28.61	0.0026	0.0028	0.0022	0.00E+00	0.00E+00	0.00E+00
31.61	0.0015	0.0024	0.0014	0.00E+00	0.00E+00	0.00E+00



# Baseline Readings at 1 kW

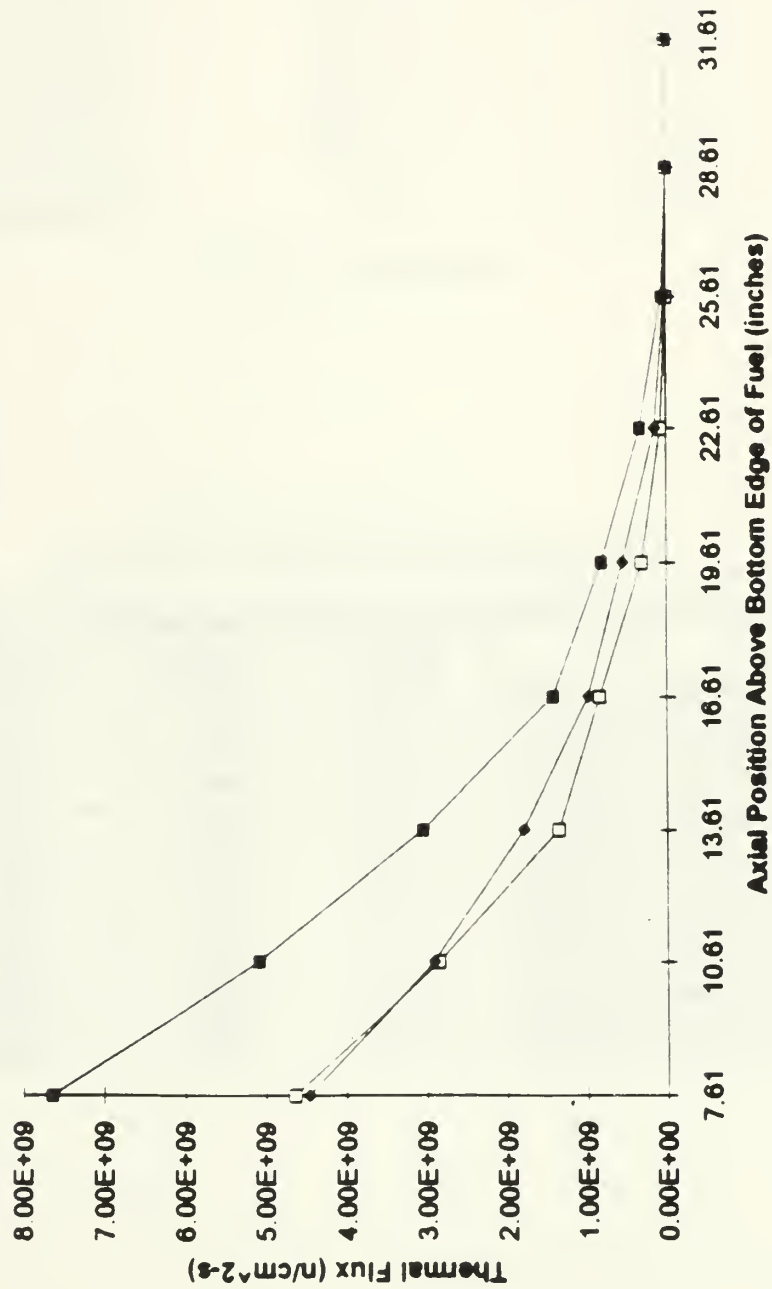


Figure 6.3.2-1: Neutron Flux at 1 kW with No Tilt - Phase II





Table 6.3.2-2: Shim Blade and Regulating Rod Heights for Tilt One @ 1kW

Control Component	Height with respect to Bank	Actual Height
Shim Blade #1	SBH + 6"	16.30"
Shim Blade #2	SBH + 2"	12.30"
Shim Blade #3	SBH - 2"	8.30"
Shim Blade #4	SBH - 6"	4.30"
Shim Blade #5	SBH - 2"	9.71"
Shim Blade #6	SBH + 2"	12.30"
Regulating Rod	N/A	16.81"

Note. SBH = Shim Bank Height

Table 6.3.2-3: Net Flux at 1 kW with Tilt One

Axial Position	Water Hole #1 ( $\mu$ Amps)	Water Hole #3 ( $\mu$ Amps)	Water Hole #5 ( $\mu$ Amps)	Net Flux 1	Net Flux 3	Net Flux 5
7.61	0.257	0.148	0.216	1.06E+10	4.12E+09	4.76E+09
10.61	0.183	0.095	0.145	7.20E+09	2.62E+09	3.13E+09
13.61	0.109	0.048	0.086	3.97E+09	1.24E+09	1.92E+09
16.61	0.052	0.027	0.044	1.78E+09	7.85E+08	1.03E+09
19.61	0.026	0.014	0.024	9.58E+08	3.12E+08	5.56E+08
22.61	0.013	0.007	0.01	4.09E+08	7.50E+07	1.51E+08
25.61	0.005	0.004	0.004	4.23E+07	1.15E+07	1.26E+07
28.61	0.0027	0.0029	0.0022	7.05E+06	0.00E+00	0.00E+00
31.61	0.0015	0.0024	0.0014	0.00E+00	0.00E+00	0.00E+00



# **Thermal Flux at 1 kW with Tilt One**

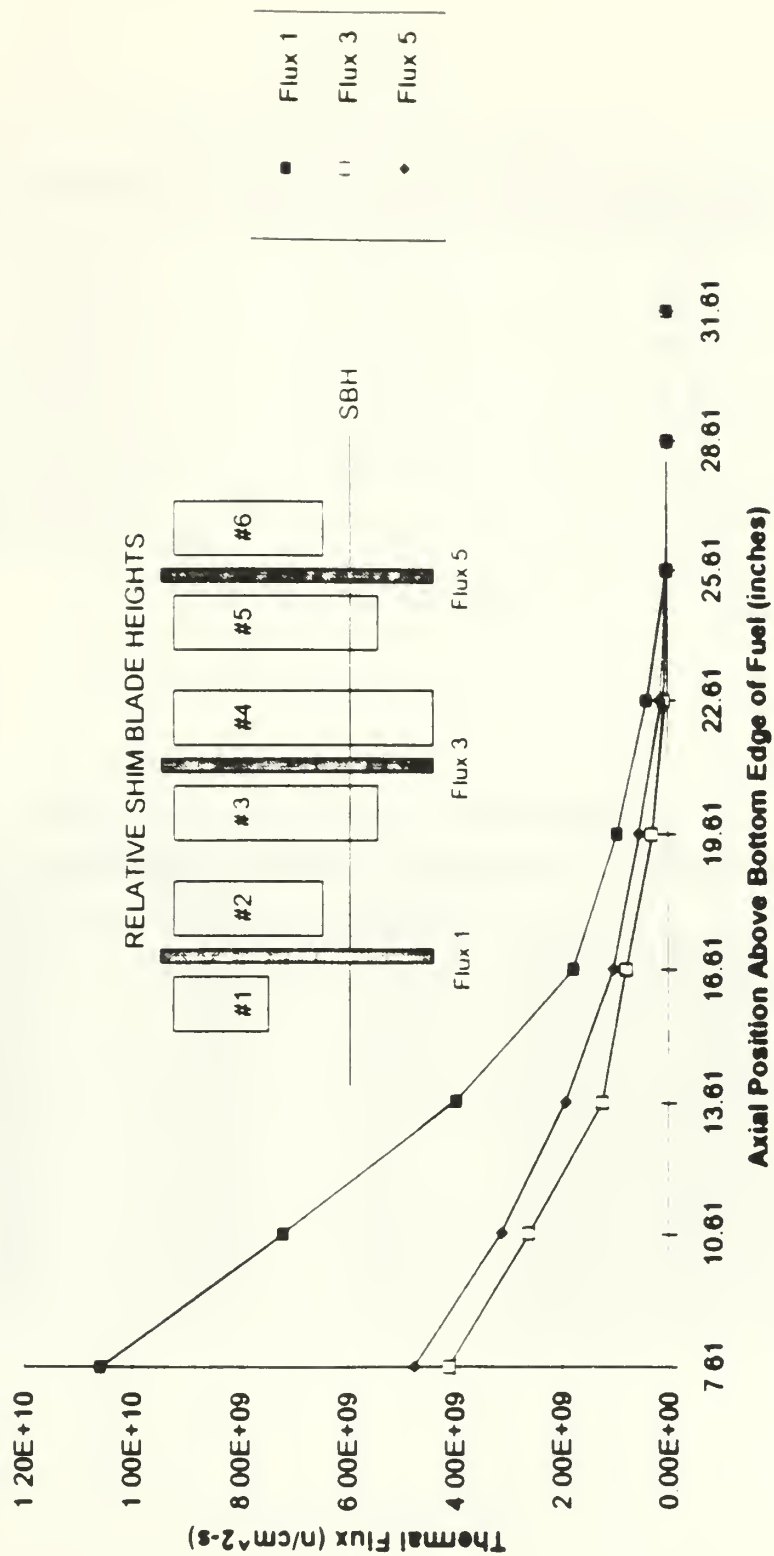


Figure 6.3 2-2: Neutron Flux at 1 kW with Tilt One



Table 6.3.2-4 Shim Blade and Regulating Rod Heights for Tilt Two @ 1kW

Control Component	Height with respect to Bank	Actual Height
Shim Blade #1	SBH - 6"	4.30"
Shim Blade #2	SBH - 2"	9.80"
Shim Blade #3	SBH + 2"	12.30"
Shim Blade #4	SBH + 6"	16.30"
Shim Blade #5	SBH + 2"	12.30"
Shim Blade #6	SBH - 2"	8.30"
Regulating Rod	N/A	7.85"

Note: SBH = Shim Bank Height

Table 6.3.2-5: Net Flux at 1 kW with Tilt Two

Axial Position	Water Hole #1 ( $\mu$ Amps)	Water Hole #3 ( $\mu$ Amps)	Water Hole #5 ( $\mu$ Amps)	Net Flux 1	Net Flux 3	Net Flux 5
7.61	0.1963	0.1801	0.2105	6.33E+09	5.97E+09	4.53E+09
10.61	0.1437	0.1085	0.1418	4.43E+09	3.40E+09	3.00E+09
13.61	0.0921	0.053	0.0838	2.78E+09	1.53E+09	1.83E+09
16.61	0.0456	0.0292	0.0436	1.33E+09	9.12E+08	1.01E+09
19.61	0.0235	0.0147	0.0241	7.82E+08	3.52E+08	5.61E+08
22.61	0.0118	0.0068	0.01	3.24E+08	6.35E+07	1.51E+08
25.61	0.0053	0.0038	0.0044	6.34E+07	0.00E+00	2.93E+07
28.61	0.0028	0.0027	0.0023	1.41E+07	0.00E+00	4.18E+06
31.61	0.0016	0.0023	0.0014	0.00E+00	0.00E+00	0.00E+00



# **Thermal Flux at 1 kW with Tilt Two**

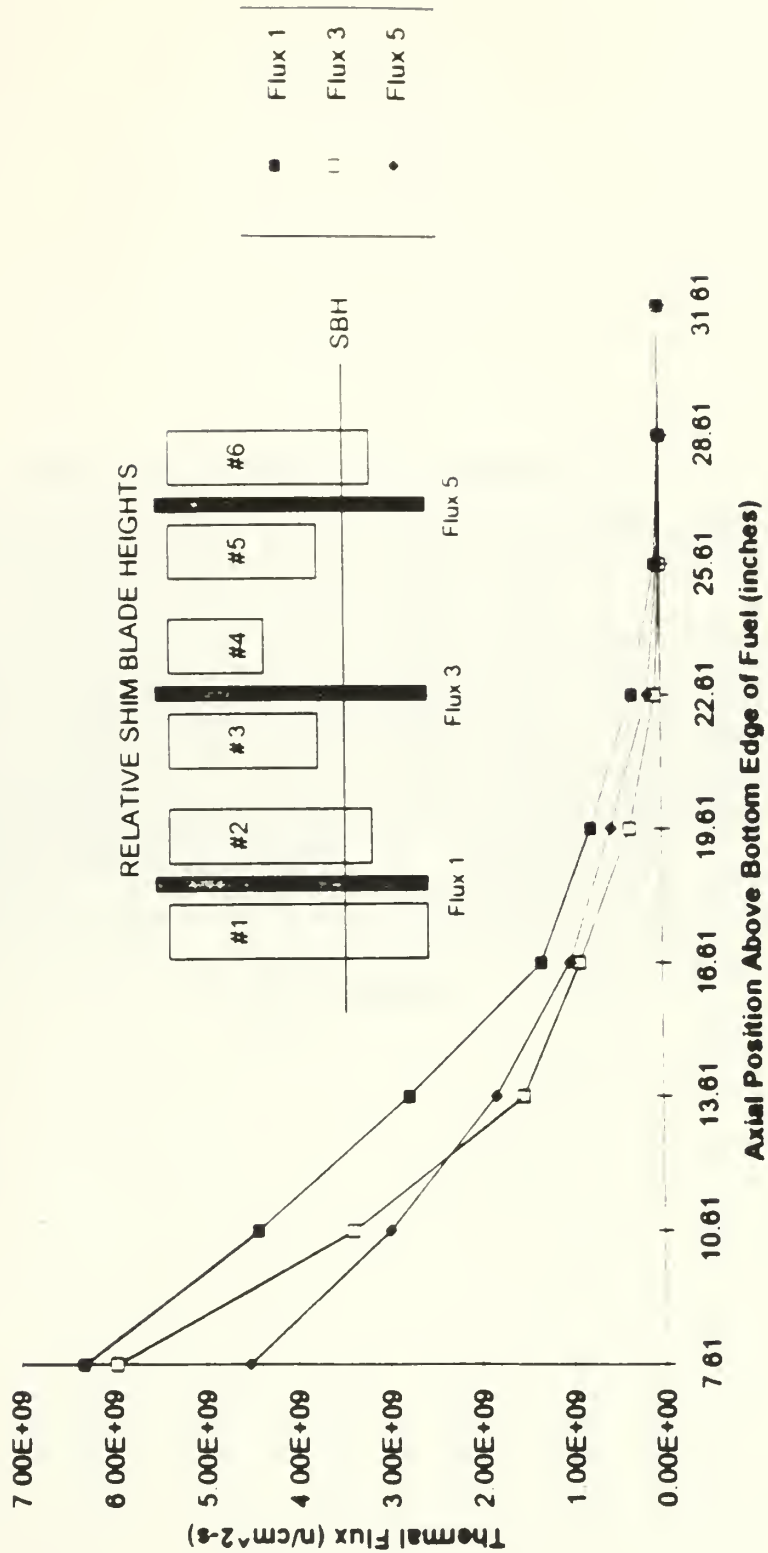


Figure 6.3.2-3 Neutron Flux at 1 kW with Tilt Two





Table 6.3 2-6: Normalized Flux Readings @ 1 kW

Axial Position	Tilt One VH #1	Tilt One VH #3	Tilt One VH #5	Tilt Two VH #1	Tilt Two VH #3	Tilt Two VH #5	No Tilt VH #1	No Tilt VH #3	No Tilt VH #5
7.61	1.3871	0.8881	1.0655	0.8276	1.2873	1.014	1	1	1
10.61	0.9419	0.5647	0.7004	0.5797	0.7326	0.6704	0.6654	0.6144	0.6536
13.61	0.5198	0.2674	0.4307	0.3641	0.3296	0.4101	0.4	0.2923	0.4026
16.61	0.2332	0.1692	0.2303	0.1742	0.1965	0.2266	0.1871	0.1816	0.221
19.61	0.1253	0.0672	0.1245	0.1023	0.0759	0.1255	0.1069	0.0672	0.1245
22.61	0.0535	0.0162	0.0337	0.0424	0.0137	0.0337	0.0442	0.0162	0.0337
25.61	0.0055	0.0025	0.0028	0.0083	0	0.0066	0.0074	0	0.0056
28.61	0.0009	0	0	0.0018	0	0.0009	0	0	0
31.61	0	0	0	0	0	0	0	0	0

Note: VH = Vent Hole



# **Normalized Flux in Water Vent Hole #1 at 1 kW - Phase II**

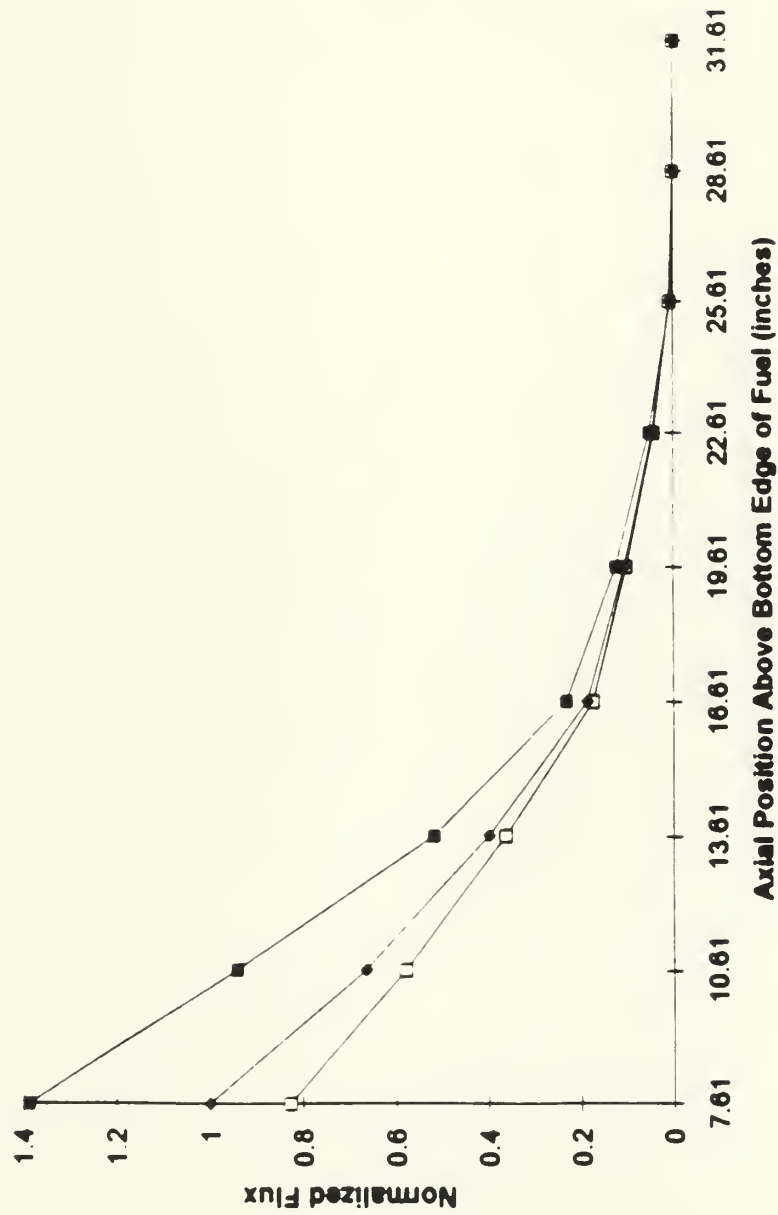
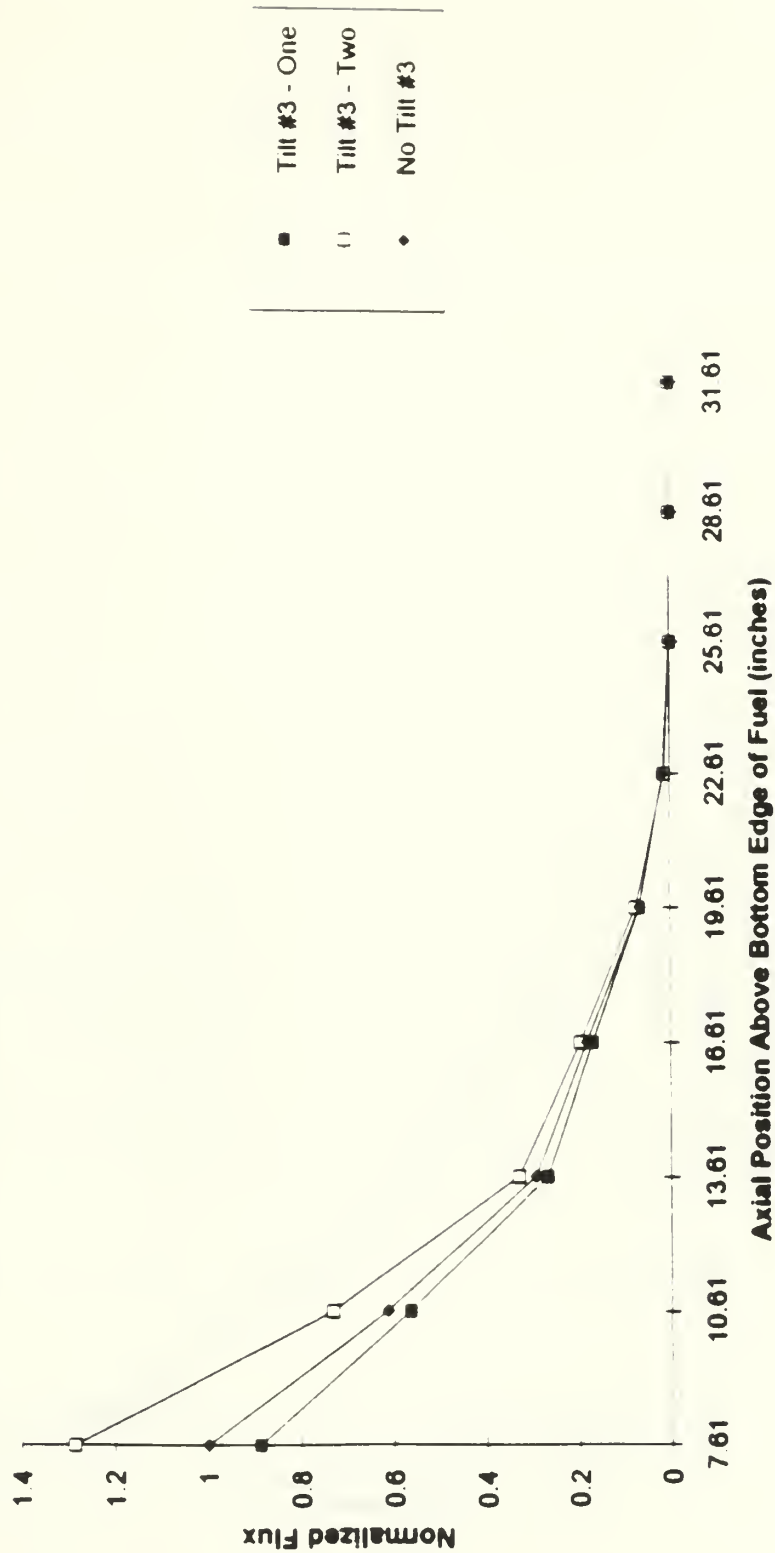


Figure 6.3.2-4: Normalized Tilt and No-Tilt Fluxes in Vent Hole #1 at 1 kW



# **Normalized Flux in Water Vent Hole #3 at 1 kw - Phase II**



**Figure 6.3.2-5: Normalized Tilt and No-Tilt Fluxes in Vent Hole #3 at 1 kW**



# **Normalized Flux in Water Vent Hole #5 at 1 kW - Phase II**

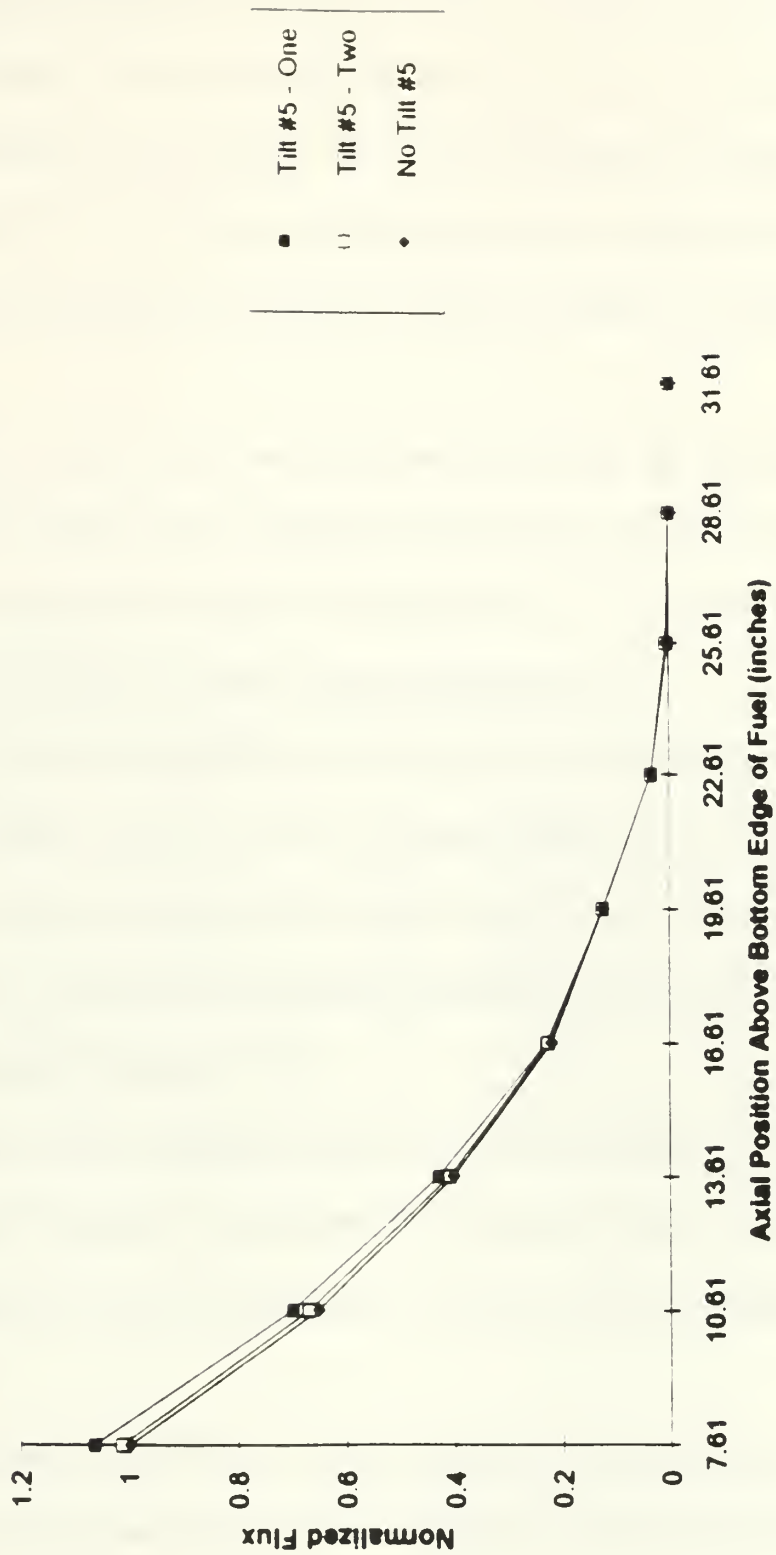


Figure 6.3.2-6: Normalized Tilt and No-Tilt Fluxes in Vent Hole #5 at 1 kW





### 6.3.3 FLUX TILTING AT 10 kW

After all data was taken at 1 kW reactor power was raised to 10 kW and the same procedure was repeated. The shim bank height for this power was 10.40 inches and the regulating rod position was 4.23 inches. The core tank temperature at the time this data was taken was 41.4 °C. At this power level the no-tilt flux condition in the core was measured. The net flux measured at this power is shown in Table 6.3.3-1 and is plotted in Figure 6.3.3-1.

As before, once the no-tilt data was taken, the first flux tilt was initiated. The positions of the shim blades and the regulating rod for this tilt are shown in Table 6.3.3-2. The core tank temperature for this portion of the test 43.0 °C. The net flux data from this first tilt is shown in Table 6.3.3-3 and is plotted in Figure 6.3.3-2.

When all of the flux measurements were taken with this tilt condition, the flux was shifted to the opposite side of the core by positioning shim blades as shown in Table 6.3.3-4. This was done to determine if the fission chambers could detect the shift in the flux within the core. The resulting net fluxes in this condition are shown in Table 6.3.3-5. This data is then plotted in Figure 6.3.3-3.

As in Phase I of this experiment, the flux tilt was not as evident at 10 kW as it was at 1 kW. Again all flux data was normalized and is shown in Table 6.3.3-6. All of the normalized readings for each individual water vent hole are plotted in Figures 6.3.3-4 through 6.3.3-6.

At this power level the flux tilt is most noticeable in water vent hole #1. While it can still be seen in water vent hole #3, the effect of the tilt is not as pronounced as it was



in the 1 kW case. Again the tilt is as would be expected from the positioning of the shim blades as described in Tables 6.3.3-2 and 6.3.3-4.

Table 6.3.3-1: Net Flux at 10 kW with No Tilt - Phase II

Axial Position	Water Hole #1 ( $\mu$ Amps)	Water Hole #3 ( $\mu$ Amps)	Water Hole #5 ( $\mu$ Amps)	Net Flux 1	Net Flux 3	Net Flux 5
7.61	1.21	0.87	1.16	7.75E+10	4.57E+10	4.42E+10
10.61	0.83	0.54	0.77	5.25E+10	2.81E+10	2.92E+10
13.61	0.51	0.26	0.44	3.19E+10	1.32E+10	1.69E+10
16.61	0.24	0.15	0.25	1.48E+10	8.11E+09	9.73E+09
19.61	0.14	0.06	0.14	8.85E+09	3.20E+09	5.54E+09
22.61	0.06	0.02	0.04	3.65E+09	7.67E+08	1.49E+09
25.61	0.02	0.01	0.01	8.88E+08	0.00E+00	3.89E+08
28.61	0.01	0	0	2.33E+08	0.00E+00	1.09E+08
31.61	0	0	0	0.00E+00	0.00E+00	4.60E+07



# Baseline Readings at 10 kW

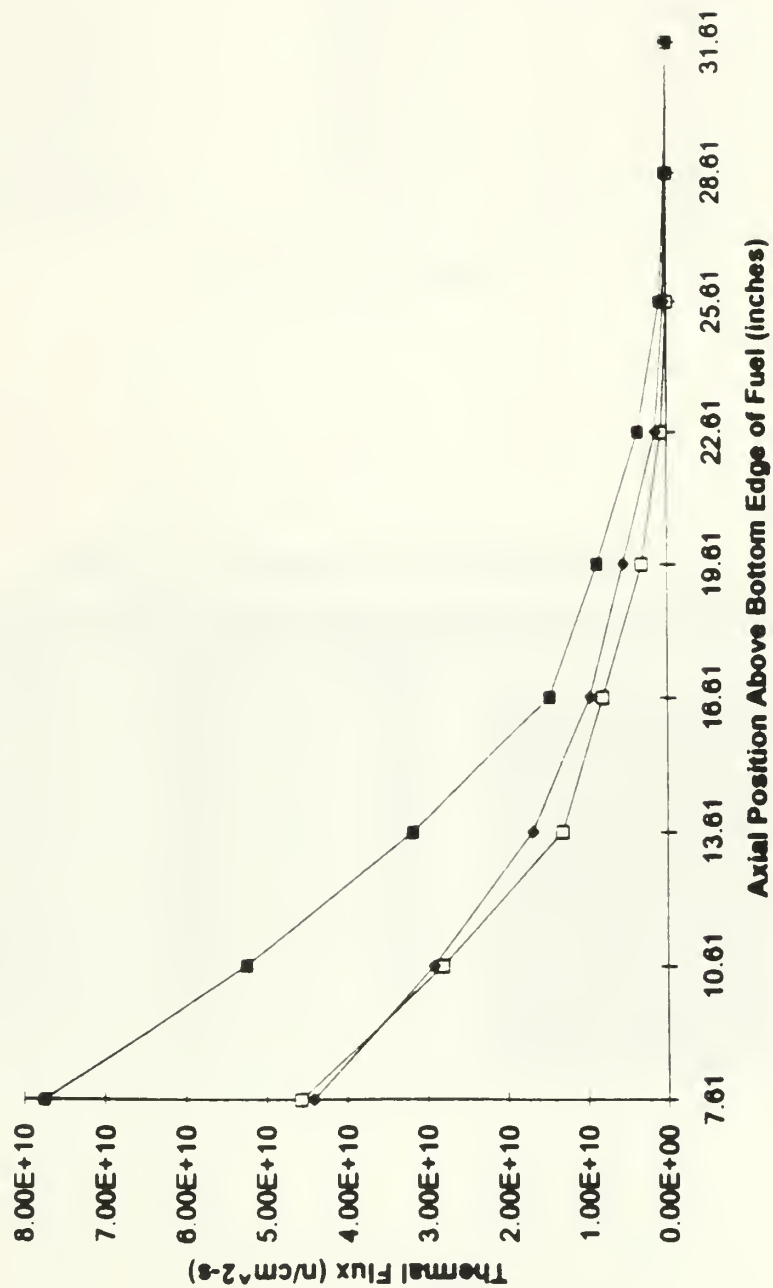


Figure 6.3.3-1: Neutron Flux at 10 kW with No Tilt - Phase II



Table 6.3.3-2: Shim Blade and Regulating Rod Heights for Tilt One @ 10kW

Control Component	Height with respect to Bank	Actual Height
Shim Blade #1	SBH + 2"	12.40"
Shim Blade #2	SBH + 1"	11.40"
Shim Blade #3	SBH - 1"	9.40"
Shim Blade #4	SBH - 2"	8.40"
Shim Blade #5	SBH - 1"	9.40"
Shim Blade #6	SBH + 1"	11.40"
Regulating Rod	N/A	5.72"

Note: SBH = Shim Bank Height

Table 6.3.3-3: Net Flux at 10 kW with Tilt One

Axial Position	Water Hole #1 ( $\mu$ Amps)	Water Hole #3 ( $\mu$ Amps)	Water Hole #5 ( $\mu$ Amps)	Net Flux 1	Net Flux 3	Net Flux 5
7.61	1.39	0.85	1.17	9.05E+10	4.44E+10	4.47E+10
10.61	0.88	0.52	0.76	5.66E+10	2.70E+10	2.87E+10
13.61	0.53	0.25	0.45	3.36E+10	1.27E+10	1.70E+10
16.61	0.25	0.15	0.26	1.57E+10	8.06E+09	9.86E+09
19.61	0.14	0.07	0.14	9.27E+09	3.31E+09	5.58E+09
22.61	0.06	0.02	0.04	3.76E+09	8.25E+08	1.52E+09
25.61	0.02	0.01	0.01	9.02E+08	2.19E+08	3.68E+08
28.61	0.01	0	0	2.26E+08	8.66E+07	1.05E+08
31.61	0	0	0	0.00E+00	0.00E+00	4.60E+07





# **Thermal Flux at 10 kW with Tilt One**

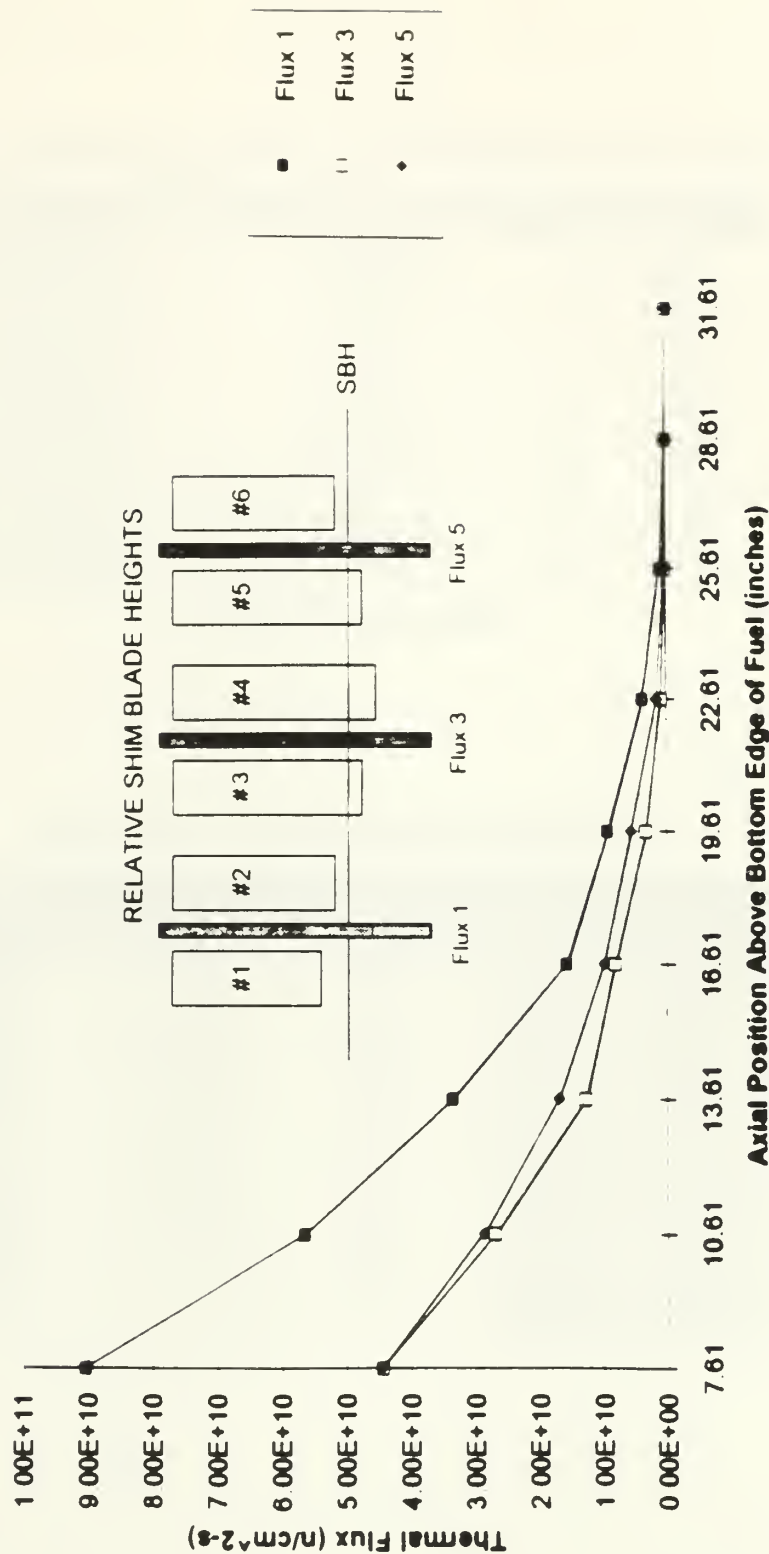


Figure 6.3.3-2: Neutron Flux at 10 kW with Tilt One



Table 6.3 3-4: Shim Blade and Regulating Rod Heights for Tilt Two @ 10 kW

Control Component	Height with respect to Bank	Actual Height
Shim Blade #1	SBH - 2"	8.40"
Shim Blade #2	SBH - 1"	9.40"
Shim Blade #3	SBH + 1"	11.40"
Shim Blade #4	SBH + 2"	12.40"
Shim Blade #5	SBH + 1"	11.40"
Shim Blade #6	SBH - 1"	9.40"
Regulating Rod	N/A	3.54"

Note: SBH = Shim Bank Height

Table 6.3.3-5: Net Flux at 10 kW with Tilt Two

Axial Position	Water Hole #1 ( $\mu$ Amps)	Water Hole #3 ( $\mu$ Amps)	Water Hole #5 ( $\mu$ Amps)	Net Flux 1	Net Flux 3	Net Flux 5
7.61	1.07	0.9	1.13	6.79E+10	4.75E+10	4.29E+10
10.61	0.76	0.55	0.75	4.77E+10	2.87E+10	2.84E+10
13.61	0.48	0.26	0.45	3.03E+10	1.35E+10	1.71E+10
16.61	0.23	0.16	0.25	1.40E+10	8.23E+09	9.65E+09
19.61	0.14	0.07	0.14	8.64E+09	3.25E+09	5.49E+09
22.61	0.06	0.02	0.04	3.58E+09	8.25E+08	1.53E+09
25.61	0.02	0.01	0.01	8.88E+08	2.02E+08	3.89E+08
28.61	0.01	0	0.01	2.40E+08	6.92E+07	1.17E+08
31.61	0	0	0	0.00E+00	0.00E+00	5.02E+07



Table 6.3.3-6: Normalized Flux Readings @ 10 kW

Axial Position	Tilt One VH #1	Tilt One VH #3	Tilt One VH #5	Tilt Two VH #1	Tilt Two VH #3	Tilt Two VH #5	No Tilt VH #1	No Tilt VH #3	No Tilt VH #5
7.61	1.17	0.97	1.01	0.88	1.04	0.97	1	1	1
10.61	0.73	0.59	0.65	0.62	0.63	0.64	0.68	0.62	0.66
13.61	0.43	0.28	0.38	0.39	0.3	0.39	0.41	0.29	0.38
16.61	0.2	0.18	0.22	0.18	0.18	0.22	0.19	0.18	0.22
19.61	0.12	0.07	0.13	0.11	0.07	0.12	0.11	0.07	0.13
22.61	0.05	0.02	0.03	0.05	0.02	0.03	0.05	0.02	0.03
25.61	0.01	0	0.01	0.01	0	0.01	0.01	0	0.01
28.61	0	0	0	0	0	0	0	0	0
31.61	0	0	0	0	0	0	0	0	0

Note: VH = Vent Hole



# **Normalized Flux in Water Vent Hole #1 at 10 kW - Phase II**

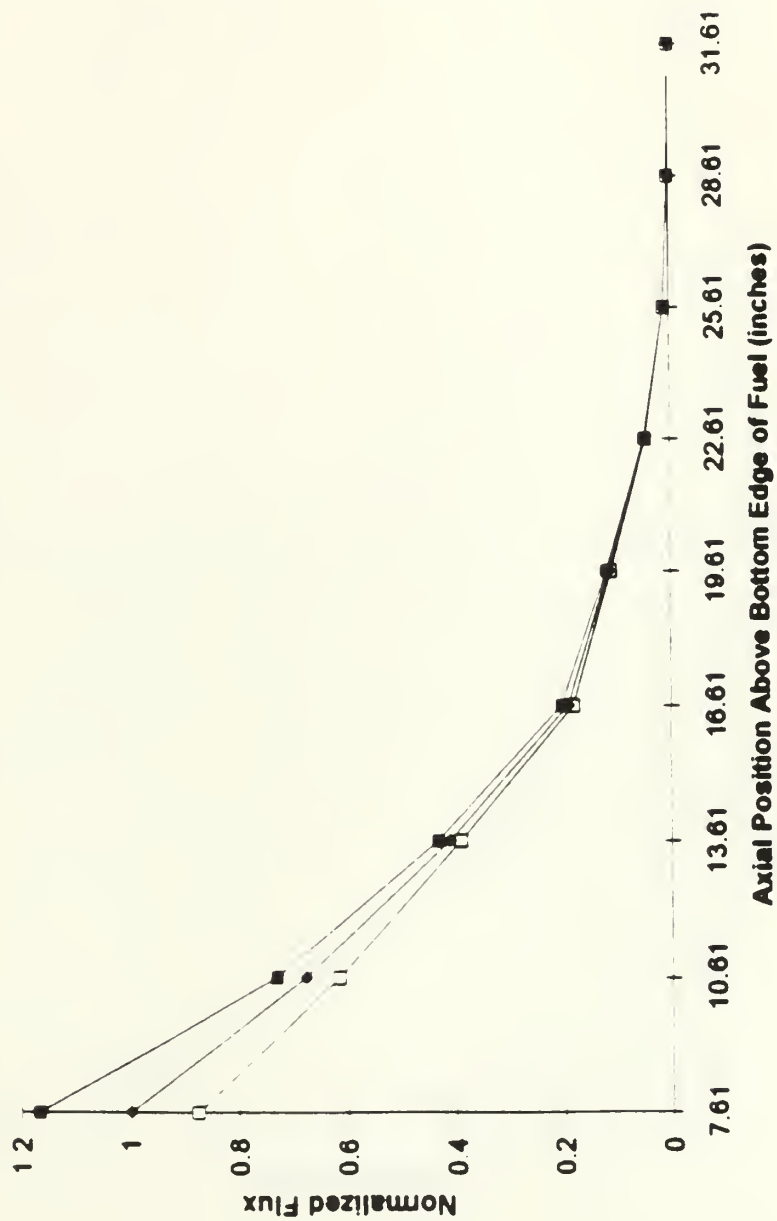
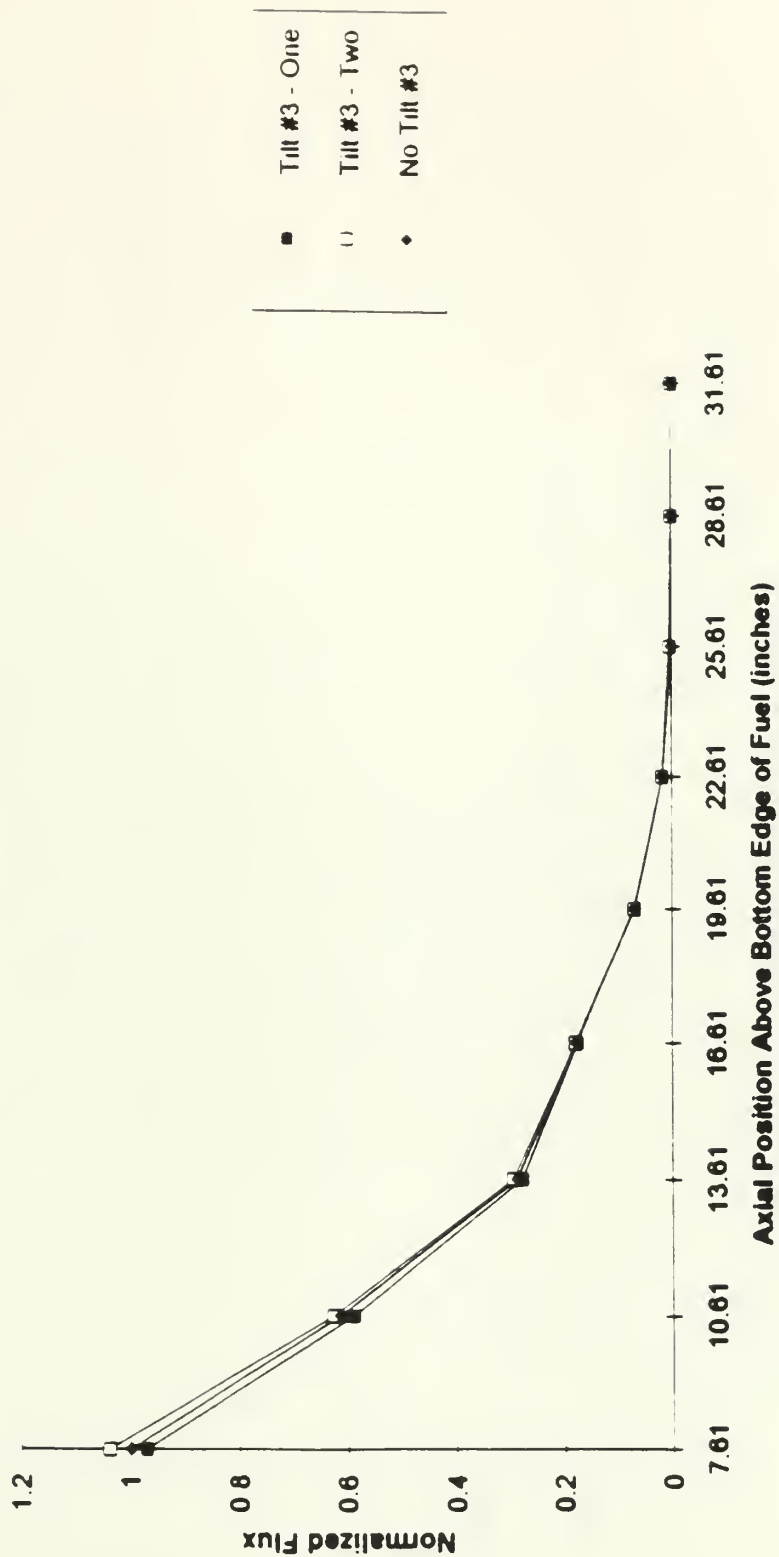


Figure 6.3.3-4: Normalized Tilt and No-Tilt Fluxes in Vent Hole #1 at 10 kW





# **Normalized Flux in Water Vent Hole #3 at 10 kW - Phase II**



**Figure 6.3.3-5: Normalized Tilt and No-Tilt Fluxes in Vent Hole #3 at 10 kW**



# **Normalized Flux in Water Vent Hole #5 at 10 kW - Phase II**

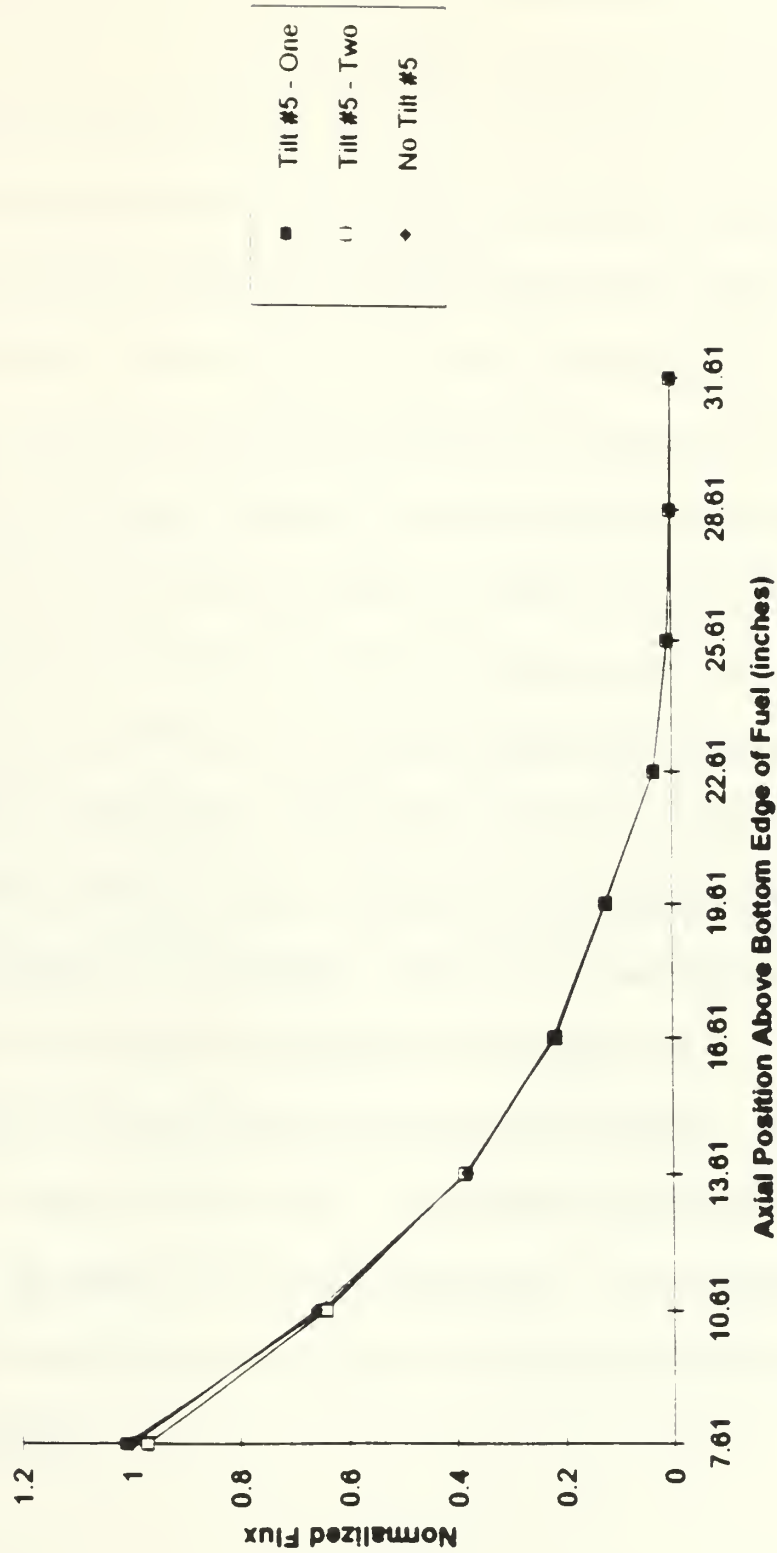


Figure 6.3.3-6: Normalized Tilt and No-Tilt Fluxes in Vent Hole #5 at 10 kW



### 6.3.4 FLUX TILTING AT 50 kW

Once all data was taken at 10 kW, reactor power was raised to 50 kW. The power was leveled there at 2218. The shim bank height for this power level was 10.50 inches and the regulating rod position was 3.70 inches. At this power level the no-tilt and tilt conditions were once again measured. As before the tilt was shifted to the opposite of the core to determine if the fission chambers could see the change in the flux shape.

The no-tilt data is shown in Table 6.3.4-1 and is graphed in Figure 6.3.4-1. The temperature in the core tank at the time these measurements were taken was 46.8 °C. The data for the first tilt is displayed in Table 6.3.4-3 and is graphed in Figure 6.3.4-2. The positions of the shim blades for this tilt are shown in Table 6.3.4-2. The temperature in the core tank for this first tilt was 47.9 °C. Once this data was taken, the flux tilt was shifted to the opposite side of the core. The corresponding shim blade and regulating rod positions are shown in Table 6.3.4-4. The net fluxes from this tilt are shown in Table 6.3.4-5 and graphed in Figure 6.3.4-3. As before the normalized flux readings were determined and graphed for each detector. Table 6.3.4-6 contains the normalized readings. These are shown graphically in Figures 6.3.4-4 through 6.3.4-6.

The data from this power level was once again very encouraging. The flux tilt is very well defined in water vent holes 1 and 3. And as before, the tilt is exactly as would be expected from the positions of the various shim blades. It is now evident that the fission chamber detectors can detect the changes in the flux shape within the core from control blade positioning.



Table 6.3.4-1: Net Flux at 50 kW with No Tilt - Phase II

Axial Position	Water Hole #1 ( $\mu$ Amps)	Water Hole #3 ( $\mu$ Amps)	Water Hole #5 ( $\mu$ Amps)	Net Flux 1	Net Flux 3	Net Flux 5
7.61	5.66	4.11	5.37	3.91E+11	2.33E+11	2.20E+11
10.61	3.82	2.46	3.52	2.63E+11	1.39E+11	1.45E+11
13.61	2.35	1.14	2.05	1.62E+11	6.43E+10	8.42E+10
16.61	1.14	0.71	1.18	7.86E+10	4.02E+10	4.86E+10
19.61	0.67	0.29	0.68	4.60E+10	1.63E+10	2.80E+10
22.61	0.28	0.08	0.17	1.92E+10	4.11E+09	7.01E+09
25.61	0.07	0.02	0.05	4.69E+09	0.00E+00	1.90E+09
28.61	0.02	0.01	0.02	1.26E+09	0.00E+00	5.61E+08
31.61	0.01	0.01	0.01	0.00E+00	0.00E+00	2.30E+08





# Baseline Readings at 50 kW

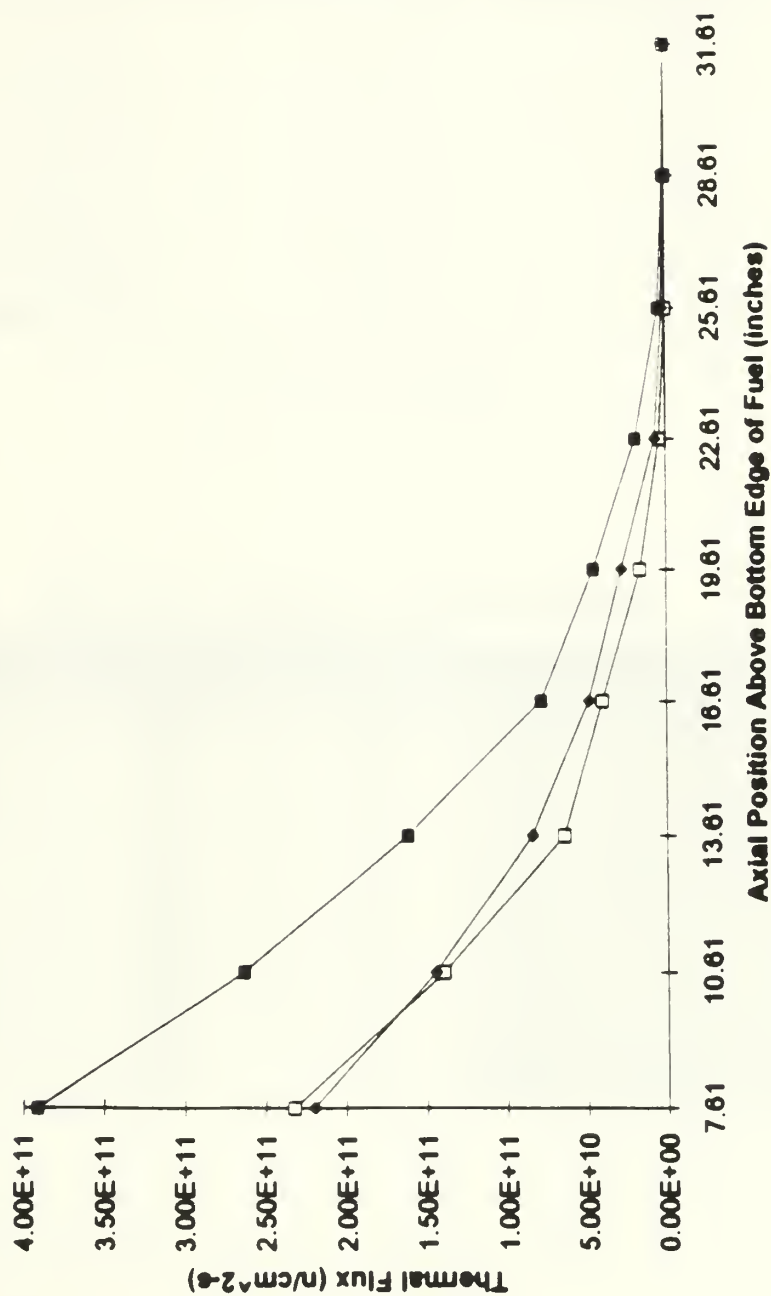


Figure 6.3.4-1: Neutron Flux at 50 kW with No Tilt - Phase II



Table 6.3 4-2: Shim Blade and Regulating Rod Heights for Tilt One @ 50 kW

Control Component	Height with respect to Bank	Actual Height
Shim Blade #1	SBH + 2"	12.50"
Shim Blade #2	SBH + 1"	11.50"
Shim Blade #3	SBH - 1"	9.50"
Shim Blade #4	SBH - 2"	8.50"
Shim Blade #5	SBH - 1"	9.50"
Shim Blade #6	SBH + 1"	11.50"
Regulating Rod	N/A	6.48"

Note. SBH = Shim Bank Height

Table 6.3.4-3: Net Flux at 50 kW with Tilt One

Axial Position	Water Hole #1 ( $\mu$ Amps)	Water Hole #3 ( $\mu$ Amps)	Water Hole #5 ( $\mu$ Amps)	Net Flux 1	Net Flux 3	Net Flux 5
7.61	6.49	3.88	5.44	4.50E+11	2.20E+11	2.23E+11
10.61	4.15	2.4	3.55	2.87E+11	1.35E+11	1.46E+11
13.61	2.52	1.12	2.11	1.74E+11	6.30E+10	8.64E+10
16.61	1.2	0.7	1.19	8.27E+10	3.97E+10	4.88E+10
19.61	0.7	0.29	0.67	4.82E+10	1.64E+10	2.74E+10
22.61	0.28	0.08	0.19	1.94E+10	4.00E+09	7.60E+09
25.61	0.08	0.02	0.05	4.98E+09	1.17E+09	1.90E+09
28.61	0.02	0.01	0.02	1.30E+09	4.67E+08	6.19E+08
31.61	0.01	0.01	0.01	0.00E+00	0.00E+00	2.76E+08



# **Thermal Flux at 50 kW with Tilt One**

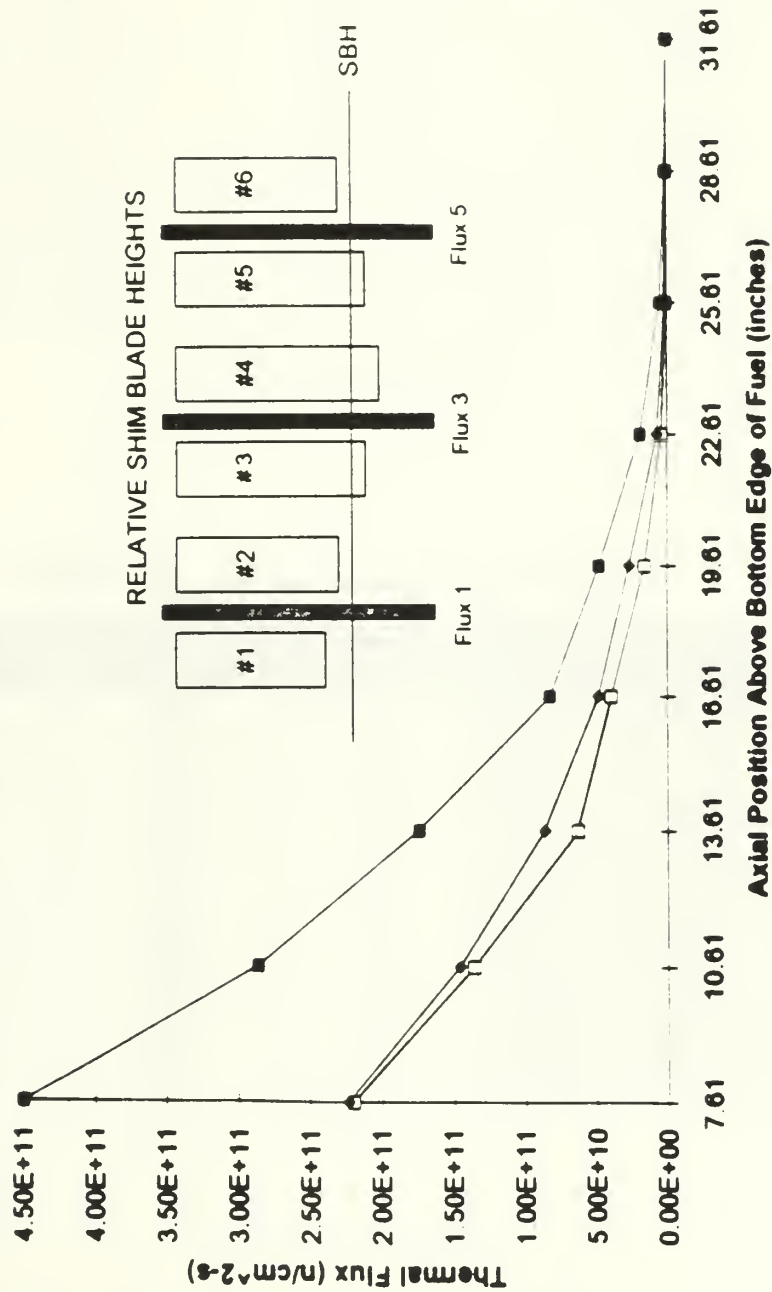


Figure 6.3 4-2. Neutron Flux at 50 kW with Tilt One



Table 6.3 4-4. Shim Blade and Regulating Rod Heights for Tilt Two @ 50 kW

Control Component	Height with respect to Bank	Actual Height
Shim Blade #1	SBH - 2"	8.50"
Shim Blade #2	SBH - 1"	9.50"
Shim Blade #3	SBH + 1"	11.50"
Shim Blade #4	SBH + 2"	12.50"
Shim Blade #5	SBH + 1"	11.50"
Shim Blade #6	SBH - 1"	9.50"
Regulating Rod	N/A	4.97"

Note: SBH = Shim Bank Height

Table 6.3.4-5: Net Flux at 50 kW with Tilt Two

Axial Position	Water Hole #1 ( $\mu$ Amps)	Water Hole #3 ( $\mu$ Amps)	Water Hole #5 ( $\mu$ Amps)	Net Flux 1	Net Flux 3	Net Flux 5
7.61	5.13	4.34	5.47	3.54E+11	2.46E+11	2.25E+11
10.61	3.61	2.58	3.52	2.49E+11	1.46E+11	1.44E+11
13.61	2.27	1.19	2.06	1.56E+11	6.73E+10	8.44E+10
16.61	1.1	0.73	1.17	7.56E+10	4.13E+10	4.83E+10
19.61	0.68	0.3	0.65	4.69E+10	1.66E+10	2.66E+10
22.61	0.28	0.08	0.19	1.89E+10	4.23E+09	7.56E+09
25.61	0.07	0.02	0.05	4.76E+09	1.17E+09	1.98E+09
28.61	0.02	0.01	0.02	1.30E+09	3.52E+08	6.19E+08
31.61	0.01	0.01	0.01	0.00E+00	0.00E+00	2.76E+08





# **Thermal Flux at 50 kW with Tilt Two**

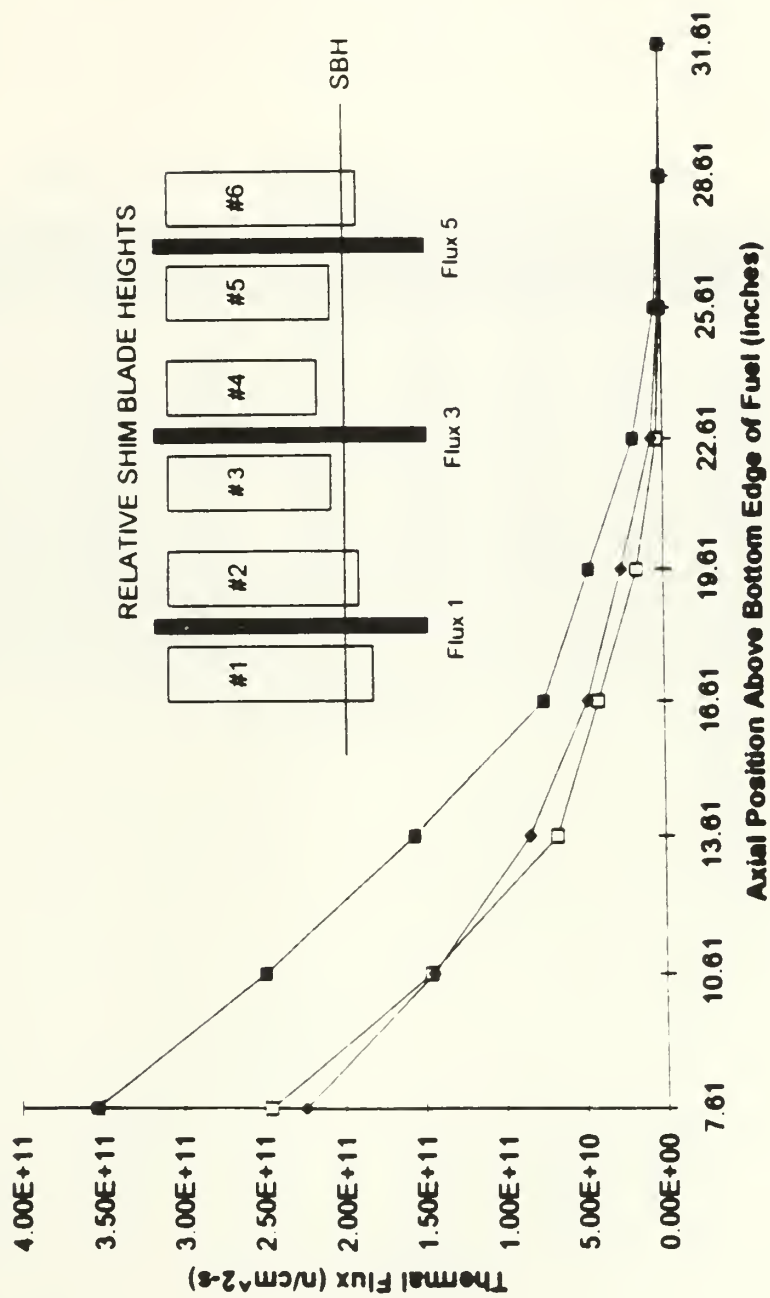


Figure 6.3.4-3: Neutron Flux at 50 kW with Tilt Two



Table 6.3.4-6: Normalized Flux Readings @ 50 kW

Axial Position	Tilt One VH #1	Tilt One VH #3	Tilt One VH #5	Tilt Two VH #1	Tilt Two VH #3	Tilt Two VH #5	No Tilt VH #1	No Tilt VH #3	No Tilt VH #5
7.61	1.15	0.94	1.01	0.91	1.06	1.02	1	1	1
10.61	0.73	0.58	0.66	0.64	0.63	0.66	0.67	0.6	0.66
13.61	0.44	0.27	0.39	0.4	0.29	0.38	0.41	0.28	0.38
16.61	0.21	0.17	0.22	0.19	0.18	0.22	0.2	0.17	0.22
19.61	0.12	0.07	0.12	0.12	0.07	0.12	0.12	0.07	0.13
22.61	0.05	0.02	0.03	0.05	0.02	0.03	0.05	0.02	0.03
25.61	0.01	0.01	0.01	0.01	0.01	0.01	0.01	0	0.01
28.61	0	0	0	0	0	0	0	0	0
31.61	0	0	0	0	0	0	0	0	0

Note: VH = Vent Hole



# **Normalized Flux in Water Vent Hole #1 at 50 kW - Phase II**

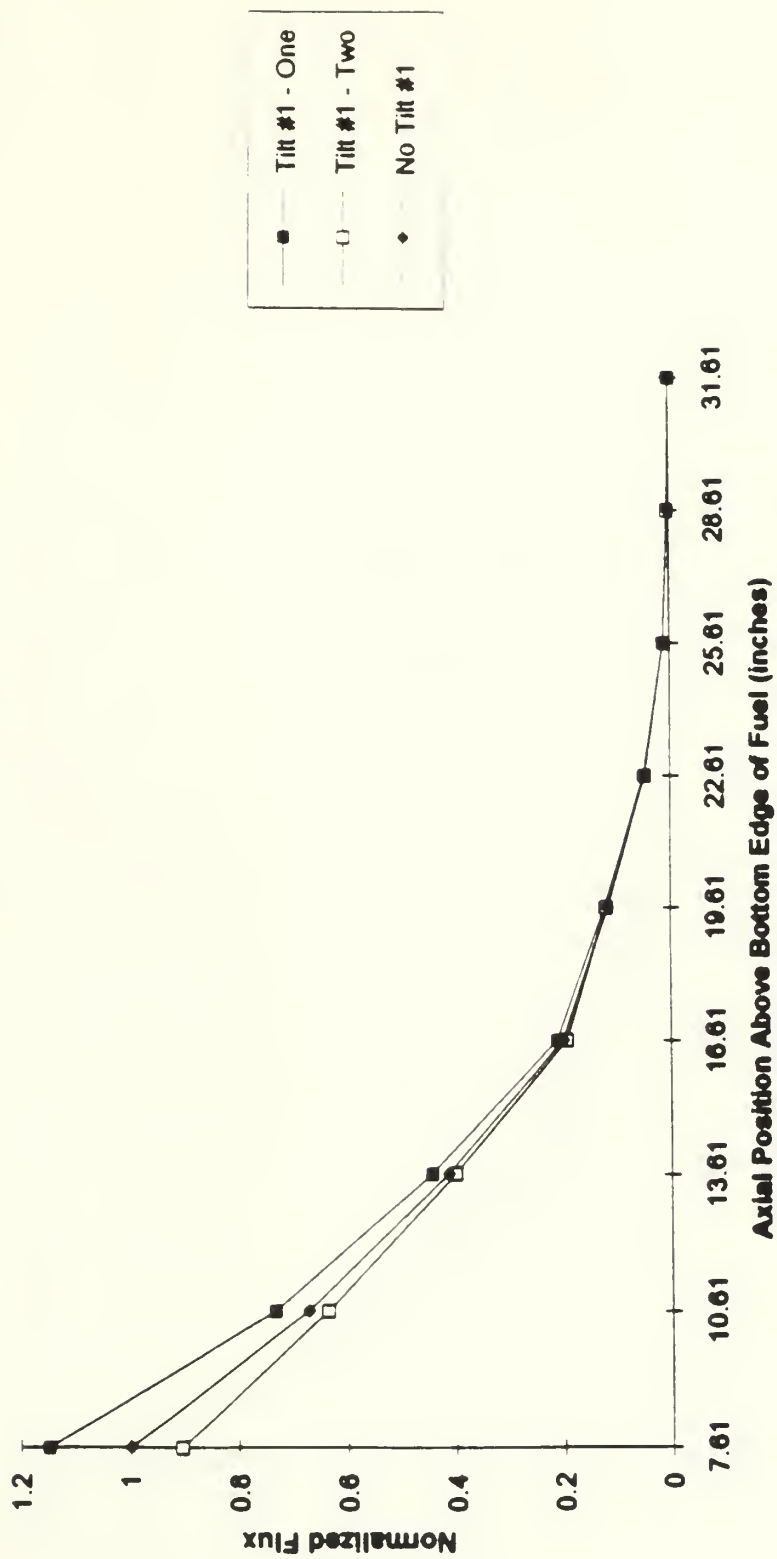


Figure 6.3.4-4: Normalized Tilt and No-Tilt Fluxes in Vent Hole #1 at 50 kW



# **Normalized Flux in Water Vent Hole #3 at 50 kW - Phase II**

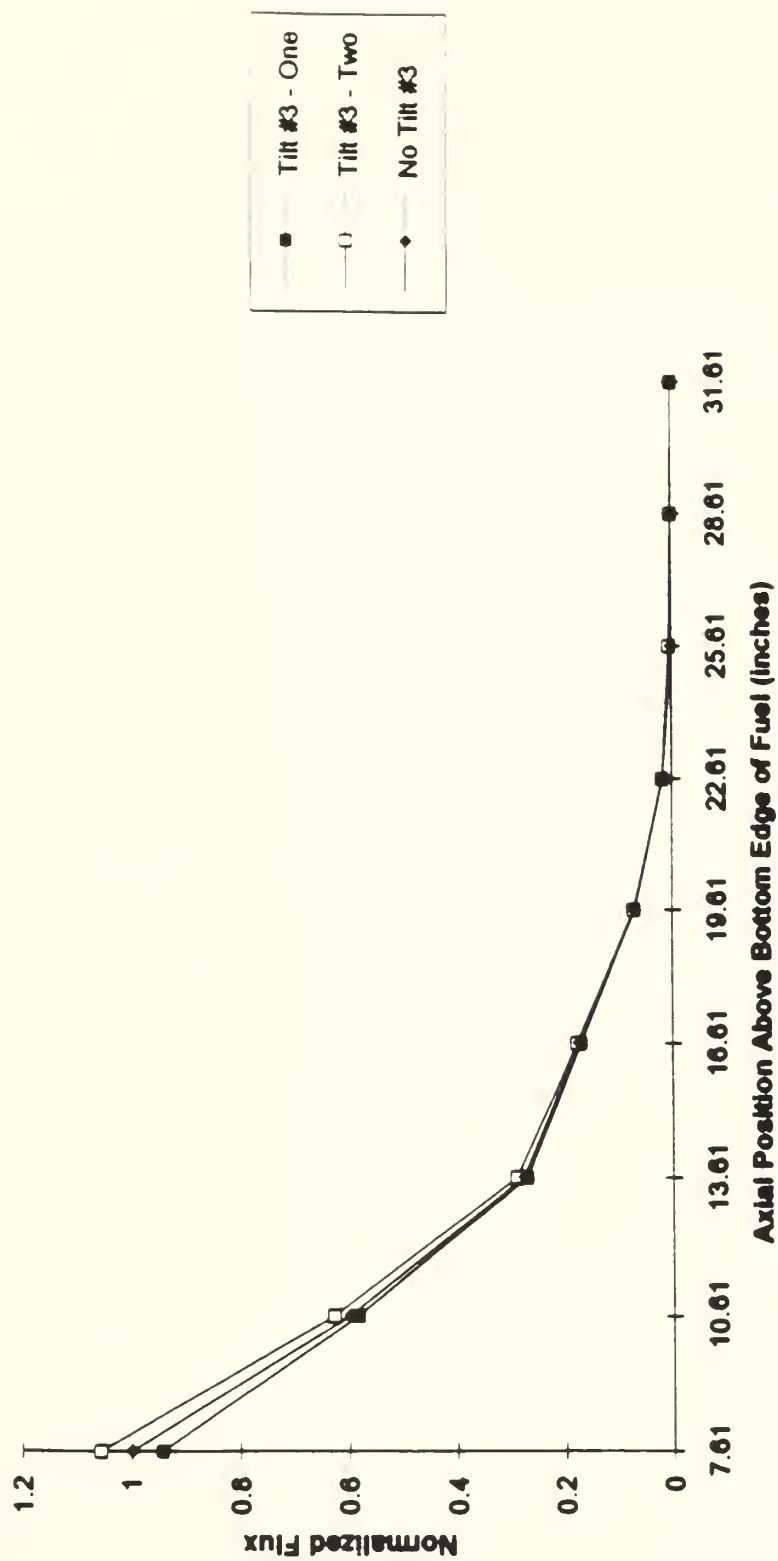


Figure 6.3.4-5: Normalized Tilt and No-Tilt Fluxes in Vent Hole #3 at 50 kW





# **Normalized Flux in Water Vent Hole #5 at 50 kW - Phase II**

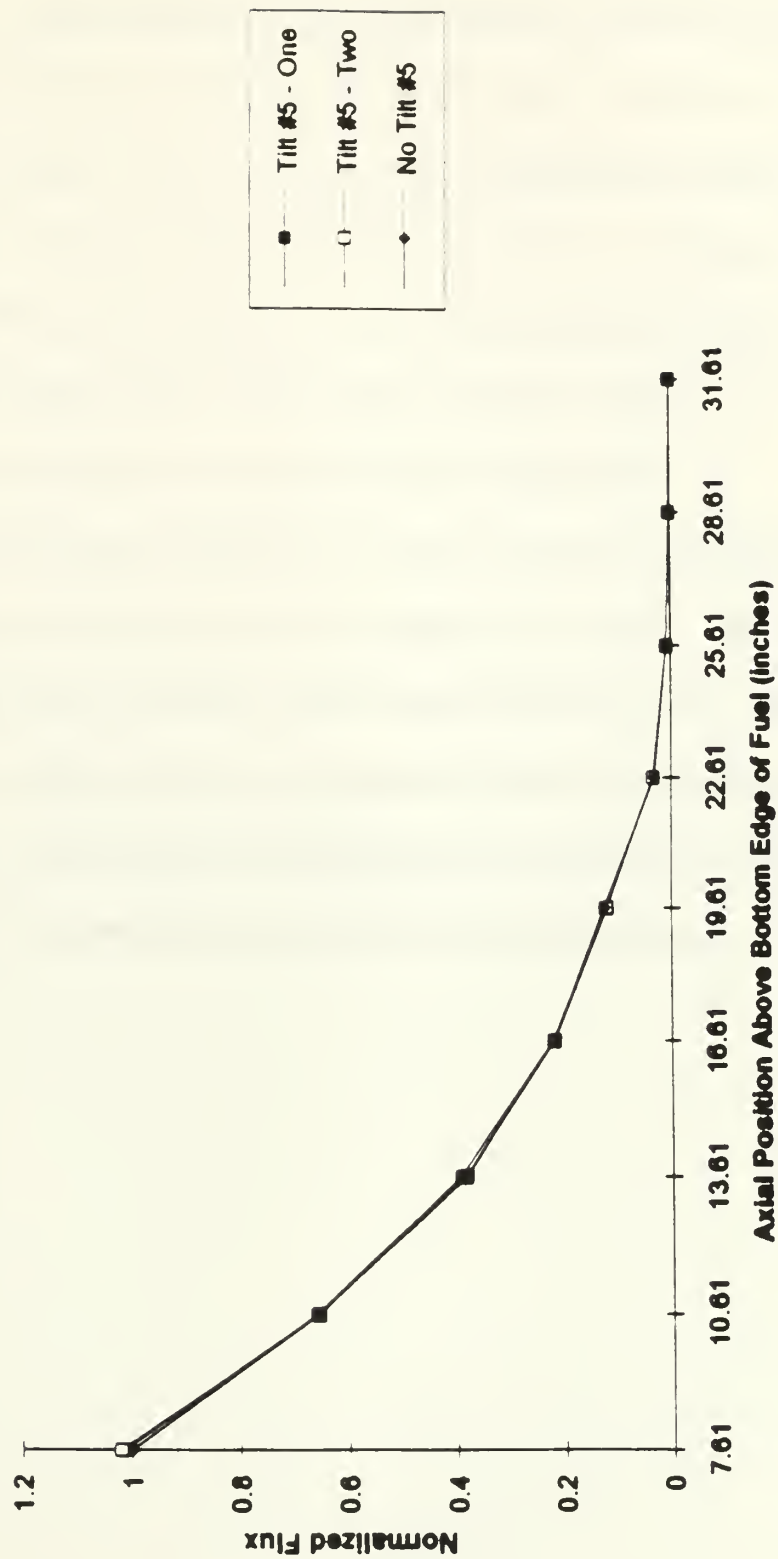


Figure 6.3.4-6: Normalized Tilt and No-Tilt Fluxes in Vent Hole #5 at 50 kW



### 6.3.7 FINAL SHUTDOWN BACKGROUND READINGS

Once all testing was completed at 50 kW, the reactor was shutdown. The time of this shutdown was 2240. At 2253 the final shutdown background readings were taken. The temperature in the core tank at this time was 49.1 °C. The data from these measurements can be seen in Appendix B.2 and is shown graphically in Figure 6.3.7-1. A comparison of this graph with the initial shutdown readings in Figure 6.3.1-1 reveals that the shutdown flux shapes did not change appreciably during the test.

After the background readings were taken, the detectors were raised above the active core region and placed into the fuel storage racks to decay. After one hour all detectors and aluminum guide tubes were removed from the reactor. Because these components were highly activated (see next section for details), the detectors were placed into the hot box to decay and the aluminum tubes were lowered into the hot cell. After decaying for about one week these components were placed into storage.



# **Final Shutdown Background Readings**

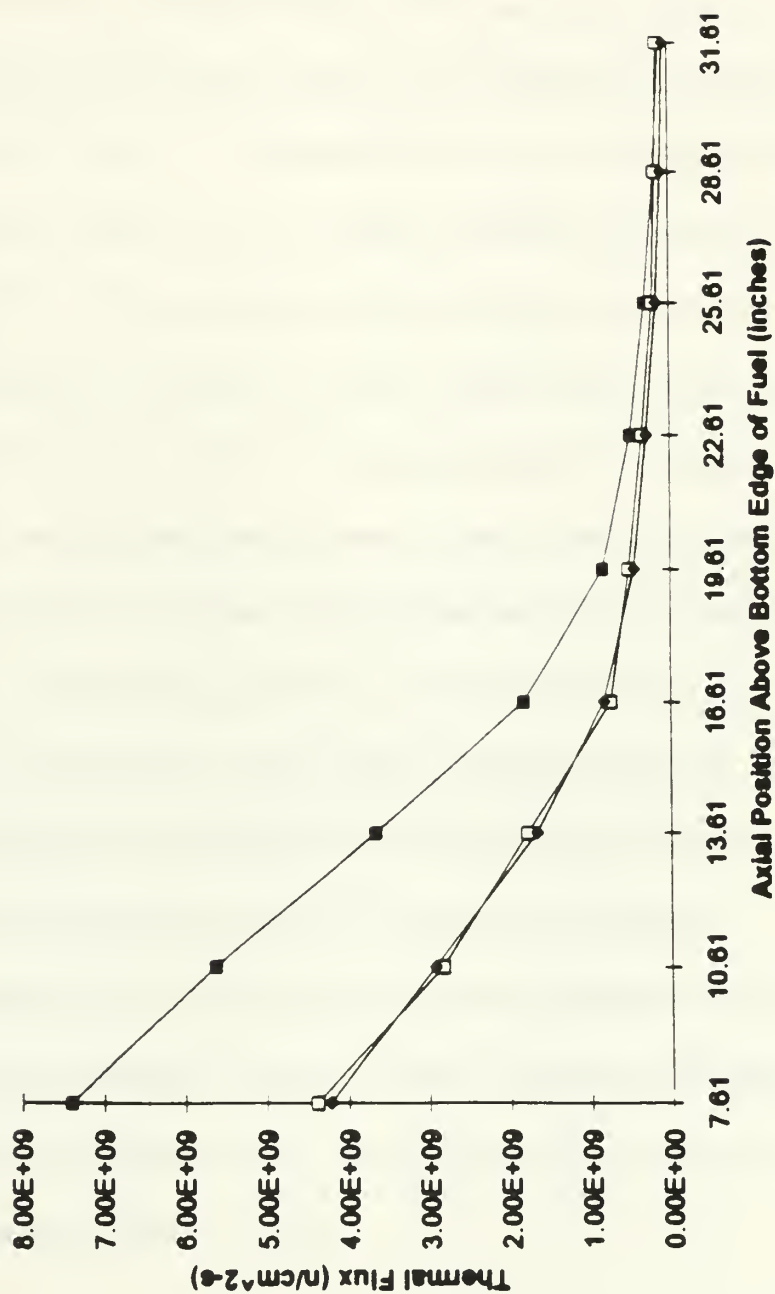


Figure 6.3.7-1: Final Shutdown Background Readings - Phase II



## 6.4 RESULTS FROM RADIATION SURVEYS

Throughout the course of the experiment, personnel from the Reactor Radiation Protection Office performed radiation surveys in the vicinity of the reactor top. These were conducted to ensure the radiation levels in the areas where personnel were working were within safe levels. The results of these surveys for each phase of the experiment are shown in Tables 6.4-1 and 6.4-3. The results of the on-contact survey measurements for the fission chamber detectors and the aluminum instrument guide tubes are shown in Tables 6.4-2 and 6.4-4. These readings were taken when these items were removed from the reactor. In Tables 6.4-1 and 6.4-3 the term "Edge" refers to survey readings taken above the edge of the reactor, just above the seating surface for the reactor top. The term "Center" refers to readings taken directly above the center of the open reactor top.

From these tables it is evident that the general area radiation levels remained well within safe levels. By maximizing the distance of personnel from the reactor top during idle moments in the procedure, it was possible to further reduce their exposure. The highest levels experienced were received from the fission chamber detectors during Phase II when they were removed from the reactor immediately after shutdown.

This information will be useful in planning future experiments for this research. It will allow the Reactor Radiation Protection Office to determine shielding requirements and storage needs for the detectors and instrument guide tubes once they are removed from the reactor at the completion of testing.





Table 6 4-1 Radiation Surveys for Phase I of Experiment

Power (kW)	Rx Top Gen. Area (mR/hr)	$\gamma$ Edge (mR/hr)	$\beta/\gamma$ Edge (mR/hr)	Fast Neut. Edge (mR/hr)	$\gamma$ Center (mR/hr)	$\beta/\gamma$ Center (mR/hr)	Fast Neut. Center (mR/hr)
0	0.6	3	8	0	24	30	0
0.5	0.6	4	8	50	26	45	8
5	0.8	8	18	16	70	90	44
10	0.9	18	25	20	120	150	80
50	1	45	60	80	600	600	560

Table 6 4-2: On-Contact Readings from Detectors and Aluminum Tubes

Component	Gamma (mR/hr)	Beta/Gamma (mR/hr)
Detector #1	260	1,400
Detector #2	390	1,200
Detector #3	310	1,000
Al Tube #1	38	360
Al Tube #2	32	380
Al Tube #3	35	310

Note: Readings taken five hours after reactor shutdown.



Table 6 4-3 Radiation Surveys for Phase II of Experiment

Power (kW)	Rx Top Gen. Area (mR/hr)	$\gamma$ Edge (mR/hr)	$\beta/\gamma$ Edge (mR/hr)	Fast Neut. Edge (mR/hr)	$\gamma$ Center (mR/hr)	$\beta/\gamma$ Center (mR/hr)	Fast Neut. Center (mR/hr)
0	0.5	2.5	7	0	22	48	0
1	0.5	6	15	12	24	60	20
10	1	22	34	30	120	180	100
50	1.7	60	80	40	600	600	520

Table 6 4-4 On-Contact Readings from Detectors and Aluminum Tubes

Component	Gamma (mR/hr)	Beta/Gamma (mR/hr)
Detector #1	3,200	20,000
Detector #2	1,500	19,000
Detector #3	800	12,000
Al Tube #1	400	2,100
Al Tube #2	150	1,400
Al Tube #3	320	1,600

Note: Readings taken 70 minutes after reactor shutdown.



## 6.5 DETECTOR AND GUIDE TUBE MATERIAL COMPOSITION

The material composition of the detectors and the instrument guide tubes is important for determining the neutron cross sections for all of the various components. This data will be used in Monte Carlo calculations for the MITR-II core. The cross sections must be known to determining the effect that these items have on the flux in the vicinity of the water vent holes. Figure 6.5-1 is a schematic showing the location of an aluminum instrument guide tube and a fission chamber detector in one of the water vent holes. The dimensions and material make-up of each item is also shown.

The instrument guide tube is made of 6061 Aluminum. Each tube has an outside diameter of one-half inch with a 0.065 inch wall thickness. The bottom end cap on each tube is made of solid 6061 Aluminum. The guide tubes are situated directly in the center of water vent holes 1, 3 and 5.

A typical fission chamber detector is also shown in Figure 6.5-1. The wire lead from each detector is 0.040 inches thick and is made of type 321 stainless steel. The detector has an outside diameter of 0.188 inches and is made out of 0.030 inch thick type 304 stainless steel. The one-quarter inch long "bullet nose" on each detector is made out of solid type 304 stainless steel. The inside of each detector is lined with 4.026 milligrams of U-235. The internal cavity of the detector is filled with argon gas. Each detector is identical and each was located at the center of the instrument guide tube.



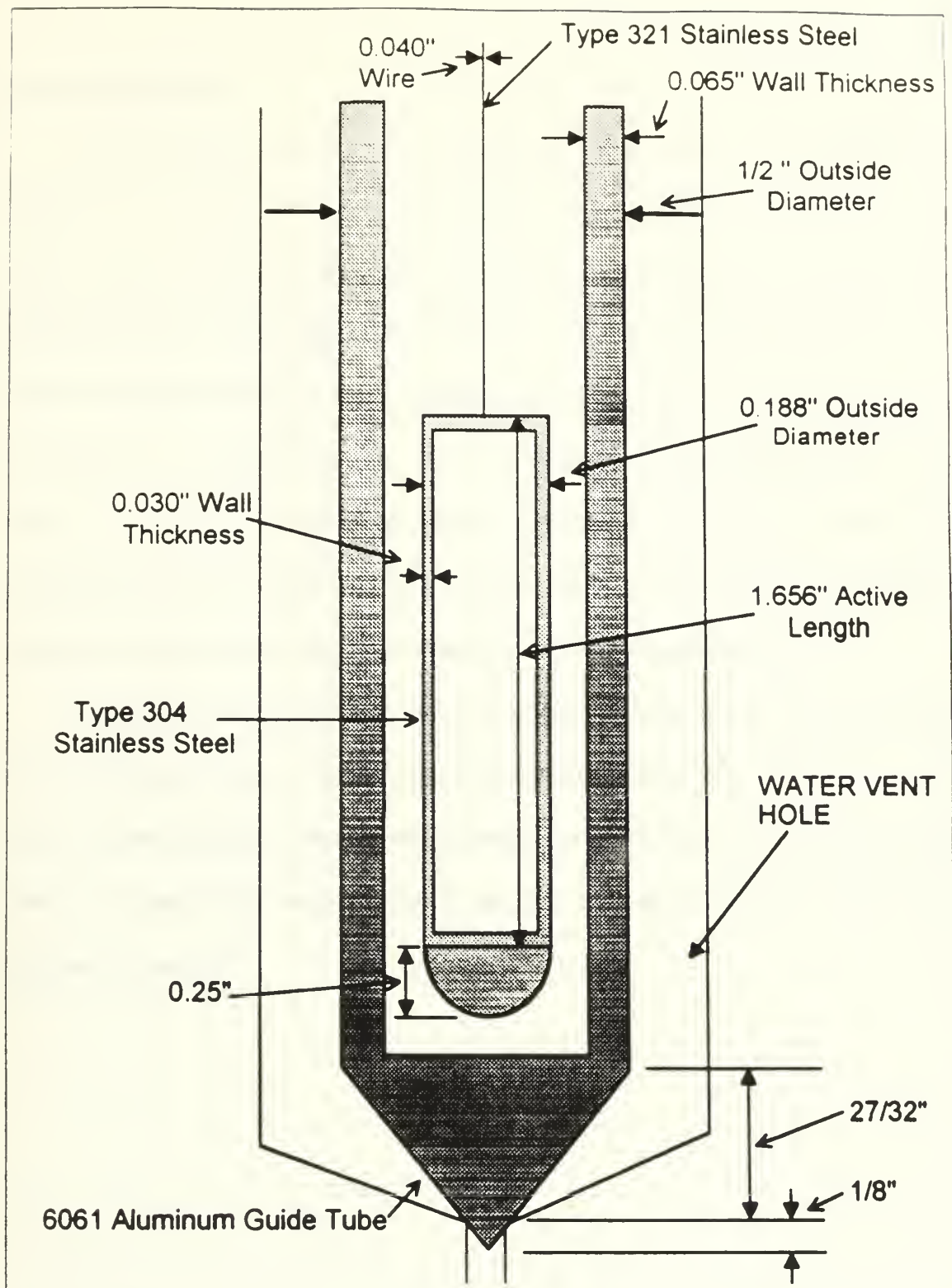


Figure 6.5-1: Detector and Instrument Guide Tube Material Compositions





## 6.6 SUMMARY

In this chapter all of the data received during the course of this research was displayed and analyzed. It is now apparent that the placement of the fission chamber detectors within the MITR-II core can detect changes in the neutron flux level and shape resulting from flux tilts and changes in power. It is unfortunate that the transient analysis could not be performed during the two phases of testing. Based on the results thus far in this research, it is apparent that the future of the instrumented synthesis is good. In addition, it is important to note that the signals received from the detectors was very stable and free from excessive noise. This bodes well for the incorporation of these signals with a computer based controller for implementation with the synthesis method.

Because the flux shapes were relatively unaffected above about ten inches from the bottom of the guide tubes, it is recommended that in the future the detectors be placed only in the lower regions of these tubes. If these experiments are ever conducted at higher powers it is possible that the flux shape in the upper regions of the core would be more important for analysis.



## **CHAPTER SEVEN: CONCLUSIONS AND RECOMMENDATIONS FOR FURTHER EXPERIMENTS**

### **7.1 SUMMARY OF EXPERIMENTAL RESULTS**

**This report has described the experimental evaluation of the instrumented synthesis method. Although there is still much work to be done, this effort has the program off to a good start. The work performed to date involved the steady-state analysis of the flux levels and shapes within the MITR-II core with and without shim blade initiated tilts. No**



transient data was obtained due to problems experienced with the electronics during testing. The results of this work are summarized below:

1.     **Instrumentation System:**

- Designed and built an instrumentation system capable of obtaining thermal flux data from the MITR-II core. Unfortunately, encountered problems with the interface between the picoammeters and the A/D board, and as a result only steady-state data could be obtained during each phase of the experiment. Problems resolved by tying ground level of picoammeter and A/D board together.

2.     **Instrument Guide Tubes:**

- Designed and built a support system for the three fission chamber detectors to be used during the experiment. This structure is easily transportable and quickly installed and removed from the core. Each detector cable was affixed with a position keeping system to keep track of the axial location of the fission chambers within each guide tube.

3.     **Flux Mapping:**

- The instrumentation system designed for this research was used to determine the flux levels within the core at various power levels. This provided researchers with the necessary baseline data required for comparison to various conditions imposed on the core with the control elements. This data will be



needed for comparison with the flux tilt conditions and the shim blade initiated transients to be conducted in the future.

#### 4 Flux Tilting:

- Flux tilts of varying degrees were implemented by positioning the shim blades at different heights. The flux within the core was then mapped and compared to the no-tilt conditions mapped earlier.
- Instrumentation system detected flux tilt conditions in all cases. In some instances the flux tilts were more evident than others; especially for the extreme tilts conducted at 1 kW.

## 7.2 CONCLUSIONS

From the data contained in Chapter Six, it is evident that the instrumentation system is sensitive enough to detect changes in the shape and intensity of the thermal flux within the core at varying power levels and flux tilt conditions. In most cases two of the three detectors saw a significant change in the flux shape, while the third was located in a position where the flux level didn't change appreciably. For the extreme flux tilts conducted at 1 kW, the instrumentation system detected the flux changes in all three instrument guide tubes. The results of this experiment show that an instrumentation system can be used to detect changes in the flux within the MITR-II core resulting from known perturbations. This data is very encouraging for the success of the instrumented





synthesis method. Once the full system is implemented, the instrumentation system designed here can be incorporated to provide the flux data needed for the method.

### 7.3 RECOMMENDATIONS FOR FURTHER EXPERIMENTS

The following areas are suggested for further research:

1. Transient Analysis:

- Because of problems encountered with the A/D board, this portion of the experiment could not be conducted. It is suggested that the transient analysis be performed at the earliest available opportunity. The procedure contained in Appendix C.2 should be consulted for the recommended transients.

2. Incorporation of additional detectors into instrumentation system:

- The purchase of six additional fission chamber detectors for incorporation into the detection system should be accomplished as soon as possible. This will allow the monitoring of the flux at three separate axial positions simultaneously. Because it is now known that the flux in the upper regions of the core will not change appreciably at low powers, it is recommended that the fission chambers be placed in the lower ten inches of the guide tube. One scheme might be to place one at zero, five and ten inches above the bottom of the guide tube.

3. Investigate possibility of conducting testing at higher powers:



- It would be useful to conduct this same testing at powers closer to the normal operating power levels for the core. In order to accomplish this, a new method would have to be developed for supporting the detectors and positioning them within the guide tubes while the reactor top is on. In addition, the guide tubes would have to be supported to prevent movement with full coolant flow.



## **APPENDIX A: INITIAL TESTING**



## **A.1: PROCEDURE FOR DIMENSIONAL MEASUREMENT AND SHIM BLADE DROP TIME TESTING OF WATER VENT HOLES**





1990 Procedure for Dimensional Measurement of Water Vent Holes in the Fuel  
Core and Measurement of Shim Blade Drop Time

Submitted by E. Lau Date 8 June, 1990

File number if required N/A

Does the item change or contradict the

Technical Specifications? Yes X No  
SAR? Yes X No

\* Attach explanation

Description of Change (Attach extra pages if necessary):

See attached sheet.

Safety Evaluation (Attach extra pages if necessary):

See attached sheet.

#### Summary of Review:

a) Does the proposal:	<u>Yes</u>	<u>No</u>
i) involve an unreviewed safety question (10CFR50.59(a)(2))	<u>      </u>	<u>X</u>
ii) decrease scope of requalification program (10CFR50.54(i-1))	<u>      </u>	<u>X</u>
iii) decrease effectiveness of security plan (10CFR50.54(p))	<u>      </u>	<u>X</u>
iv) decrease effectiveness of emergency plan (10CFR50.54(q))	<u>      </u>	<u>X</u>

b) Reviewer's Comments:

Recommend Approval ✓✓ Yes        No

Reviewer Ann Samant Date 06/09/92

Reviewer Chris Schick Date 6/9/92

Approved John A. Smith Date 6-9-92  
(Director of Reactor Operations)

10CFR50.59 & 50.54(p and q) changes logged for reporting to NRC, Date       

Copy to Director for Operations

Copies circulated to and initialled by all Licensed Personnel

Original to Safety Review File



Unreviewed Safety Question (URSQ) Determination for SR#-0-92-6

This safety review does NOT involve an URSQ. The basis for that conclusion is documented below as required by 10 CFR 50.59(b).

- (a) The change does not meet any of the three criteria that define an URSQ. This is shown below:
- No increase in probability of occurrence or consequences of any accident or malfunction of equipment important to safety previously evaluated in the safety analysis report (SAR) will occur because this change does not increase the severity of any accident analyzed in the SAR. The change involves only the creation of a special procedure for measuring the dimensions of water vent holes in the fuel core and for measuring the shim blade drop times when such a vent hole is blocked with the measuring tube. The measuring tube and all related tools will be removed from the core immediately upon completion of the measurement. The normal reactor core operation configuration will not be affected.
  - No new type of accident is created.
  - No margin of safety is reduced because the proposed change does not alter or contradict any of the bases for the technical specifications.



Procedure for Dimensional Measurement of Water Vent Holes in the Fuel  
Core and Measurement of Shim Blade Drop Time

A. Prerequisites:

1. Reactor shutdown greater than 48 hours.
2. Core outlet temperature (MTS-1 and 1A) less than 50 °C.
3. Circuit breakers for primary pumps MM-1 and 1A tagged off at MCC-2.

B. Procedure:

- E Verify prerequisites are met.
- E Verify experiment is ready and all necessary materials are on hand in the vicinity of the reactor top.
- E Verify proper operation of reactor top hand-held spotlight.
- E Prepare and clean all tools and the aluminum blank with acetone.
- E Establish communications between the reactor top and control room.
- E A licensed Senior Reactor Operator and an experimenter present on the reactor top. One licensed Reactor Operator present in the control room. Supervisor notified of start of the experiment.
- E Remove the reactor top shield lid.
- E Align the grid latch with water vent holes if necessary.
- E Attach the aluminum blank to extension arm in preparation for lowering it into the core tank. Carefully lower the aluminum blank into core tank from a position directly above water vent hole #1 (refer to the attached figure).

**CAUTION:** Care must be taken to keep the aluminum blank close to the outer walls of the core tank to prevent the rod from being held above the fuel elements. For this reason it is important to stand directly above the targeted water vent hole.

- E Carefully insert the aluminum rod fully into water vent hole #1. Be careful to note any resistance encountered. **DO NOT FORCE THE ALUMINUM ROD INTO THE WATER VENT HOLE.** Once the rod is fully inserted note the depth to which the rod has been inserted, for comparison with each of the five separate water vent holes.
- E With the aluminum blank in water vent hole #1, perform Shim Blade Drop Time Test for Shim Blades #1 and #2 and record the data on the attached data sheet.
- E Carefully raise the aluminum blank from water vent hole #1 and move it slowly to water vent hole #2. Follow the caution outlined above. Again



note the depth to which the rod is inserted. Any differences between the different water vent holes must be noted.

E With the aluminum blank in water vent hole #2, perform the Shim Blade Drop Time Test for Shim Blades #2 and #3 and record the data on the attached data sheet.

E Carefully raise the aluminum blank from water vent hole #2 and move it slowly to water vent hole #3. Follow the caution outlined above. Again note the depth to which the rod is inserted. Any differences between the different water vent holes must be noted.

E With the aluminum blank in water vent hole #3, perform the Shim Blade Drop Time Test for Shim Blades #3 and #4 and record the data on the attached data sheet.

E Carefully raise the aluminum blank from water vent hole #3 and move it slowly to water vent hole #4. Follow the caution outlined above. Again note the depth to which the rod is inserted. Any differences between the different water vent holes must be noted.

E With the aluminum blank in water vent hole #4, perform the Shim Blade Drop Time Test for Shim Blades #4 and #5 and record the data on the attached data sheet.

E Carefully raise the aluminum blank from water vent hole #4 and move it slowly to water vent hole #5. Follow the caution outlined above. Again note the depth to which the rod is inserted. Any differences between the different water vent holes must be noted.

E With the aluminum blank in water vent hole #5, perform the Shim Blade Drop Time Test for Shim Blades #5 and #6 and record the data on the attached data sheet.

E Carefully remove the aluminum blank from the core tank. Dry the aluminum blank with absorbent paper. Carefully wrap and seal the aluminum blank in a plastic bag.

**Note:** The aluminum blank will be activated slightly by the shutdown neutron flux in the core. Care must be taken to avoid possible high Al-28  $\beta$  exposure on contact.

E A licensed Senior Reactor Operator inspect the core tank for any foreign objects left behind from the experiment.

E If no additional experiments are to be performed within the core tank, replace the reactor top shield lid.

E Remove and store all tools used in this procedure. Notify the control room and the Reactor Supervisor that the experiment has been completed. If not required for other procedures, remove the primary pump circuit breaker tags.





Data Sheet for Shim Blade Drop Time Tests

1. Aluminum blank in water vent hole #1.

Shim blade #1 drop time 602

Shim blade #2 drop time 519

2. Aluminum blank in water vent hole #2.

Shim blade #2 drop time \_\_\_\_\_

Shim blade #3 drop time \_\_\_\_\_

3. Aluminum blank in water vent hole #3.

Shim blade #3 drop time 481

Shim blade #4 drop time 469

4. Aluminum blank in water vent hole #4.

Shim blade #4 drop time \_\_\_\_\_

Shim blade #5 drop time \_\_\_\_\_

5. Aluminum blank in water vent hole #5.

Shim blade #5 drop time \_\_\_\_\_

Shim blade #6 drop time \_\_\_\_\_

Test performed  
on 6/13/92

Water hole numbers used  
... Test on - unnumbered.

Blade drop timer failed  
to function



Data Sheet for Shim Blade Drop Time Tests

7/10/92

Measurements made  
with low range scope  
installed and 44-24  
S. Tucker

1. Aluminum blank in water vent hole #1.

Shim blade #1 drop time .589.

Shim blade #2 drop time —.

2. Aluminum blank in water vent hole #2.

Shim blade #2 drop time —.

Shim blade #3 drop time —.

3. Aluminum blank in water vent hole #3.

Shim blade #3 drop time —.

Shim blade #4 drop time —.

4. Aluminum blank in water vent hole #4.

Shim blade #4 drop time .468.

Shim blade #5 drop time .486.

5. Aluminum blank in water vent hole #5.

Shim blade #5 drop time .479.

Shim blade #6 drop time .504.

6. Aluminum blanks in holes #1, 3, and 5.

Shim blade #1 drop time .568.

Shim blade #2 drop time .554.

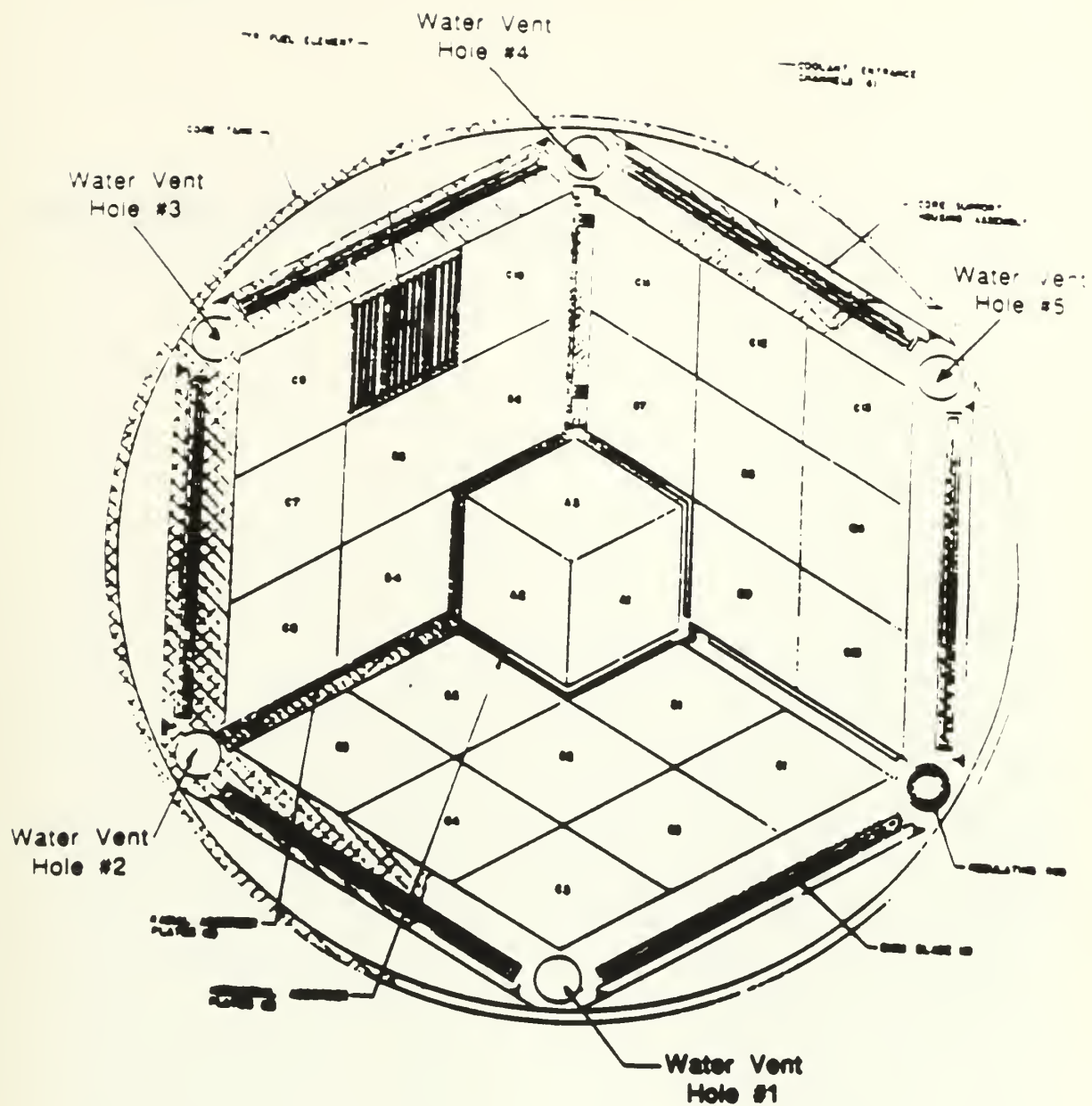
Shim blade #3 drop time .480.

Shim blade #4 drop time .474.

Shim blade #5 drop time .494.

Shim blade #6 drop time .503.





Top View of M.I.T.R. II Reactor Core Tank and Water Vent Hole Arrangement

SR#-0-92-6

JUN 09 1992



## APPENDIX B: RAW DATA





## B.1: EXPERIMENT PHASE I DATA

Table B.1-1: Initial Shutdown Background Readings

Axial Position	Water Hole #1 ( $\mu$ Amps)	Water Hole #3 ( $\mu$ Amps)	Water Hole #5 ( $\mu$ Amps)	Flux 1	Flux 3	Flux 5
0	0.0493	0.0659	0.0742	3.47E+09	3.80E+09	3.10E+09
1	0.044	0.0598	0.0681	3.10E+09	3.45E+09	2.85E+09
2	0.0385	0.0534	0.0615	2.71E+09	3.08E+09	2.57E+09
3	0.0331	0.0469	0.0549	2.33E+09	2.71E+09	2.30E+09
4	0.0275	0.0408	0.048	1.94E+09	2.35E+09	2.01E+09
5	0.0215	0.0343	0.0413	1.52E+09	1.98E+09	1.73E+09
6	0.0164	0.0282	0.0345	1.16E+09	1.63E+09	1.44E+09
7	0.0122	0.0225	0.0278	8.60E+08	1.30E+09	1.16E+09
8	0.0093	0.0181	0.0219	6.55E+08	1.04E+09	9.16E+08
9	0.0074	0.0148	0.0172	5.21E+08	8.54E+08	7.20E+08
10	0.0062	0.0131	0.0132	4.37E+08	7.56E+08	5.52E+08
11	0.0053	0.0124	0.0108	3.74E+08	7.16E+08	4.52E+08
12	0.0047	0.012	0.0093	3.31E+08	6.92E+08	3.89E+08
13	0.0041	0.012	0.0081	2.89E+08	6.92E+08	3.39E+08
14	0.0035	0.012	0.0071	2.47E+08	6.92E+08	2.97E+08
15	0.0031	0.0121	0.0065	2.18E+08	6.98E+08	2.72E+08
16	0.0027	0.0121	0.0059	1.90E+08	6.98E+08	2.47E+08
17	0.0024	0.0122	0.0054	1.69E+08	7.04E+08	2.26E+08
18	0.0021	0.0122	0.0049	1.48E+08	7.04E+08	2.05E+08
19	0.0019	0.0123	0.0045	1.34E+08	7.10E+08	1.88E+08
20	0.0017	0.0125	0.0042	1.20E+08	7.21E+08	1.76E+08
21	0.0016	0.0131	0.004	1.13E+08	7.56E+08	1.67E+08
22	0.0015	0.014	0.0038	1.06E+08	8.08E+08	1.59E+08
23	0.0013	0.0148	0.0036	9.16E+07	8.54E+08	1.51E+08
24	0.0013	0.0153	0.0035	9.16E+07	8.83E+08	1.46E+08



Table B.1-2: Steady State Readings at 500 Watts

Axial Position	Water Hole #1 ( $\mu$ Amps)	Water Hole #3 ( $\mu$ Amps)	Water Hole #5 ( $\mu$ Amps)	Flux 1	Flux 3	Flux 5
0	0.0839	0.1032	0.1303	5.91E+09	5.95E+09	5.45E+09
3	0.0545	0.0718	0.0931	3.84E+09	4.14E+09	3.90E+09
6	0.027	0.0428	0.0575	1.90E+09	2.47E+09	2.41E+09
9	0.0132	0.0229	0.0292	9.30E+08	1.32E+09	1.22E+09
12	0.0071	0.0162	0.0171	5.00E+08	9.35E+08	7.15E+08
15	0.0034	0.0121	0.0083	2.40E+08	6.98E+08	3.47E+08
18	0.002	0.0109	0.0045	1.41E+08	6.29E+08	1.88E+08
21	0.0014	0.0121	0.0032	9.87E+07	6.98E+08	1.34E+08
24	0.0012	0.0149	0.003	8.46E+07	8.60E+08	1.26E+08

Table B.1-3: Steady State Readings at 5 kW

Axial Position	Water Hole #1 ( $\mu$ Amps)	Water Hole #3 ( $\mu$ Amps)	Water Hole #5 ( $\mu$ Amps)	Flux 1	Flux 3	Flux 5
0	0.416	0.465	0.6616	2.93E+10	2.68E+10	2.77E+10
3	0.2661	0.3126	0.459	1.88E+10	1.80E+10	1.92E+10
6	0.1318	0.1856	0.2783	9.29E+09	1.07E+10	1.16E+10
9	0.0702	0.1024	0.1486	4.95E+09	5.91E+09	6.22E+09
12	0.0336	0.0636	0.0965	2.37E+09	3.67E+09	4.04E+09
15	0.01	0.0255	0.0347	7.05E+08	1.47E+09	1.45E+09
18	0.0038	0.0143	0.0113	2.68E+08	8.25E+08	4.73E+08
21	0.002	0.0131	0.0053	1.41E+08	7.56E+08	2.22E+08
24	0.0014	0.0152	0.0038	9.87E+07	8.77E+08	1.59E+08



Table B.1-4: Baseline Readings at 1 kW

Axial Position	Water Hole #1 ( $\mu$ Amps)	Water Hole #3 ( $\mu$ Amps)	Water Hole #5 ( $\mu$ Amps)	Flux 1	Flux 3	Flux 5
0	0.1192	0.1406	0.1859	8.40E+09	8.11E+09	7.78E+09
3	0.0777	0.0967	0.131	5.48E+09	5.58E+09	5.48E+09
6	0.0378	0.0577	0.0801	2.66E+09	3.33E+09	3.35E+09
9	0.0193	0.0313	0.042	1.36E+09	1.81E+09	1.76E+09
12	0.01	0.0211	0.0255	7.05E+08	1.22E+09	1.07E+09
15	0.0042	0.0133	0.0111	2.96E+08	7.67E+08	4.64E+08
18	0.0021	0.0111	0.0052	1.48E+08	6.41E+08	2.18E+08
21	0.0015	0.012	0.0034	1.06E+08	6.92E+08	1.42E+08
24	0.0012	0.0146	0.003	8.46E+07	8.42E+08	1.26E+08

Table B.1-5: Readings at 1 kW with Flux Tilt

Axial Position	Water Hole #1 ( $\mu$ Amps)	Water Hole #3 ( $\mu$ Amps)	Water Hole #5 ( $\mu$ Amps)	Flux 1	Flux 3	Flux 5
0	0.1313	0.14	0.1862	9.25E+09	8.08E+09	7.79E+09
3	0.0827	0.0972	0.1332	5.83E+09	5.61E+09	5.57E+09
6	0.041	0.0587	0.0828	2.89E+09	3.39E+09	3.46E+09
9	0.0204	0.0318	0.044	1.44E+09	1.83E+09	1.84E+09
12	0.0103	0.0215	0.0267	7.26E+08	1.24E+09	1.12E+09
15	0.0042	0.0134	0.0117	2.96E+08	7.73E+08	4.90E+08
18	0.0021	0.0113	0.0056	1.48E+08	6.52E+08	2.34E+08
21	0.0014	0.0122	0.0038	9.87E+07	7.04E+08	1.59E+08
24	0.0011	0.0146	0.0033	7.75E+07	8.42E+08	1.38E+08



Table B 1-6. Baseline Readings at 10 kW

Axial Position	Water Hole #1 ( $\mu$ Amps)	Water Hole #3 ( $\mu$ Amps)	Water Hole #5 ( $\mu$ Amps)	Flux 1	Flux 3	Flux 5
0	0.8066	0.8742	1.2539	5.68E+10	5.04E+10	5.25E+10
3	0.5033	0.5734	0.8456	3.55E+10	3.31E+10	3.54E+10
6	0.2488	0.3411	0.5122	1.75E+10	1.97E+10	2.14E+10
9	0.1363	0.1916	0.2799	9.61E+09	1.11E+10	1.17E+10
12	0.0642	0.1171	0.1829	4.52E+09	6.76E+09	7.65E+09
15	0.018	0.0399	0.0635	1.27E+09	2.30E+09	2.66E+09
18	0.0058	0.0178	0.0182	4.09E+08	1.03E+09	7.62E+08
21	0.0029	0.014	0.0073	2.04E+08	8.08E+08	3.05E+08
24	0.0018	0.0154	0.0046	1.27E+08	8.89E+08	1.92E+08

Table B.1-7: Readings at 10 kW with Flux Tilt

Axial Position	Water Hole #1 ( $\mu$ Amps)	Water Hole #3 ( $\mu$ Amps)	Water Hole #5 ( $\mu$ Amps)	Flux 1	Flux 3	Flux 5
0	0.845	0.8498	1.2204	5.95E+10	4.90E+10	5.11E+10
3	0.5312	0.5709	0.8536	3.74E+10	3.29E+10	3.57E+10
6	0.2632	0.3425	0.5193	1.85E+10	1.98E+10	2.17E+10
9	0.14	0.1905	0.2796	9.87E+09	1.10E+10	1.17E+10
12	0.0667	0.1161	0.1831	4.70E+09	6.70E+09	7.66E+09
15	0.0181	0.04	0.0648	1.28E+09	2.31E+09	2.71E+09
18	0.0058	0.018	0.019	4.09E+08	1.04E+09	7.95E+08
21	0.0027	0.0143	0.008	1.90E+08	8.25E+08	3.35E+08
24	0.0017	0.0154	0.0049	1.20E+08	8.89E+08	2.05E+08







Table B.1-8: Baseline Readings at 50 kW

Axial Position	Water Hole #1 ( $\mu$ Amps)	Water Hole #3 ( $\mu$ Amps)	Water Hole #5 ( $\mu$ Amps)	Flux 1	Flux 3	Flux 5
0	3.859	4.073	5.908	2.72E+11	2.35E+11	2.47E+11
3	2.486	2.697	4.026	1.75E+11	1.56E+11	1.68E+11
6	1.24	1.603	2.449	8.74E+10	9.25E+10	1.02E+11
9	0.682	0.896	1.327	4.81E+10	5.17E+10	5.55E+10
12	0.32	0.535	0.874	2.26E+10	3.09E+10	3.66E+10
15	0.081	0.156	0.29	5.71E+09	9.00E+09	1.21E+10
18	0.023	0.048	0.076	1.62E+09	2.77E+09	3.18E+09
21	0.009	0.0237	0.0242	6.34E+08	1.37E+09	1.01E+09
24	0.0045	0.0191	0.0114	3.17E+08	1.10E+09	4.77E+08

Table B.1-9: Readings at 50 kW with Flux Tilt

Axial Position	Water Hole #1 ( $\mu$ Amps)	Water Hole #3 ( $\mu$ Amps)	Water Hole #5 ( $\mu$ Amps)	Flux 1	Flux 3	Flux 5
0	4.114	4.017	5.792	2.90E+11	2.32E+11	2.42E+11
3	2.582	2.726	4.015	1.82E+11	1.57E+11	1.68E+11
6	1.3017	1.5958	2.431	9.17E+10	9.21E+10	1.02E+11
9	0.7067	0.8963	1.3231	4.98E+10	5.17E+10	5.54E+10
12	0.3232	0.5335	0.8773	2.28E+10	3.08E+10	3.67E+10
15	0.083	0.1581	0.2939	5.85E+09	9.12E+09	1.23E+10
18	0.0229	0.0482	0.0775	1.61E+09	2.78E+09	3.24E+09
21	0.0083	0.0243	0.0262	5.85E+08	1.40E+09	1.10E+09
24	0.042	0.0192	0.0118	2.96E+09	1.11E+09	4.94E+08



Table B.1-10: Final Shutdown Background Readings

Axial Position	Water Hole #1 ( $\mu$ Amps)	Water Hole #3 ( $\mu$ Amps)	Water Hole #5 ( $\mu$ Amps)	Flux 1	Flux 3	Flux 5
0	0.0454	0.0567	0.0659	3.20E+09	3.27E+09	2.76E+09
1	0.0406	0.0516	0.0606	2.86E+09	2.98E+09	2.54E+09
2	0.0356	0.0462	0.0551	2.51E+09	2.67E+09	2.31E+09
3	0.0306	0.0407	0.0492	2.16E+09	2.35E+09	2.06E+09
4	0.0256	0.0354	0.0433	1.80E+09	2.04E+09	1.81E+09
5	0.02	0.0299	0.0375	1.41E+09	1.73E+09	1.57E+09
6	0.0153	0.0245	0.0315	1.08E+09	1.41E+09	1.32E+09
7	0.0115	0.0196	0.0254	8.10E+08	1.13E+09	1.06E+09
8	0.0087	0.0156	0.0202	6.13E+08	9.00E+08	8.45E+08
9	0.0069	0.0128	0.0158	4.86E+08	7.39E+08	6.61E+08
10	0.0057	0.0112	0.0123	4.02E+08	6.46E+08	5.15E+08
11	0.0049	0.0106	0.0101	3.45E+08	6.12E+08	4.23E+08
12	0.0043	0.0103	0.0086	3.03E+08	5.94E+08	3.60E+08
13	0.0038	0.0103	0.0075	2.68E+08	5.94E+08	3.14E+08
14	0.0033	0.0103	0.0067	2.33E+08	5.94E+08	2.80E+08
15	0.0029	0.0104	0.006	2.04E+08	6.00E+08	2.51E+08
16	0.0025	0.0104	0.0054	1.76E+08	6.00E+08	2.26E+08
17	0.0022	0.0105	0.0048	1.55E+08	6.06E+08	2.01E+08
18	0.002	0.0106	0.0044	1.41E+08	6.12E+08	1.84E+08
19	0.0018	0.0107	0.0041	1.27E+08	6.17E+08	1.72E+08
20	0.0016	0.0109	0.0038	1.13E+08	6.29E+08	1.59E+08
21	0.0015	0.0114	0.0036	1.06E+08	6.58E+08	1.51E+08
22	0.0014	0.0123	0.0035	9.87E+07	7.10E+08	1.46E+08
23	0.0013	0.0131	0.0034	9.16E+07	7.56E+08	1.42E+08
24	0.0012	0.0138	0.0033	8.46E+07	7.96E+08	1.38E+08



## B.2: EXPERIMENT PHASE II DATA

Table B 2-1: Initial Shutdown Background Readings

Axial Position	Water Hole #1 ( $\mu$ Amps)	Water Hole #3 ( $\mu$ Amps)	Water Hole #5 ( $\mu$ Amps)	Flux 1	Flux 3	Flux 5
7.61	0.1065	0.0766	0.1022	7.51E+09	4.42E+09	4.28E+09
8.61	0.0992	0.0673	0.0898	6.99E+09	3.88E+09	3.76E+09
9.61	0.0904	0.0585	0.08	6.37E+09	3.38E+09	3.35E+09
10.61	0.0808	0.0496	0.0702	5.69E+09	2.86E+09	2.94E+09
11.61	0.0716	0.0407	0.0591	5.05E+09	2.35E+09	2.47E+09
12.61	0.0618	0.0334	0.0494	4.36E+09	1.93E+09	2.07E+09
13.61	0.0526	0.0265	0.04	3.71E+09	1.53E+09	1.67E+09
14.61	0.043	0.0207	0.0322	3.03E+09	1.19E+09	1.35E+09
15.61	0.0342	0.0163	0.0249	2.41E+09	9.41E+08	1.04E+09
16.61	0.0267	0.0134	0.0194	1.88E+09	7.73E+08	8.12E+08
17.61	0.0202	0.0114	0.0155	1.42E+09	6.58E+08	6.49E+08
18.61	0.0155	0.0099	0.0127	1.09E+09	5.71E+08	5.31E+08
19.61	0.0124	0.0086	0.0107	8.74E+08	4.96E+08	4.48E+08
20.61	0.01	0.0075	0.0091	7.05E+08	4.33E+08	3.81E+08
21.61	0.0085	0.0066	0.0076	5.99E+08	3.81E+08	3.18E+08
22.61	0.0072	0.0057	0.0064	5.07E+08	3.29E+08	2.68E+08
23.61	0.0061	0.005	0.0054	4.30E+08	2.89E+08	2.26E+08
24.61	0.0051	0.0043	0.0045	3.59E+08	2.48E+08	1.88E+08
25.61	0.0044	0.0038	0.0037	3.10E+08	2.19E+08	1.55E+08
26.61	0.0037	0.0034	0.0032	2.61E+08	1.96E+08	1.34E+08
27.61	0.0031	0.0031	0.0026	2.18E+08	1.79E+08	1.09E+08
28.61	0.0026	0.0029	0.0022	1.83E+08	1.67E+08	9.21E+07
29.61	0.0022	0.0028	0.0019	1.55E+08	1.62E+08	7.95E+07
30.61	0.0019	0.0026	0.0016	1.34E+08	1.50E+08	6.69E+07
31.61	0.0016	0.0025	0.0014	1.13E+08	1.44E+08	5.66E+07



Table B 2-2 Baseline Readings at 1 kW

Axial Position	Water Hole #1 (μAmps)	Water Hole #3 (μAmps)	Water Hole #5 (μAmps)	Flux 1	Flux 3	Flux 5
7.61	0.215	0.157	0.209	7.65E+09	4.64E+09	4.47E+09
10.61	0.153	0.099	0.14	5.09E+09	2.85E+09	2.92E+09
13.61	0.096	0.05	0.083	3.08E+09	1.36E+09	1.80E+09
16.61	0.047	0.028	0.043	1.43E+09	8.42E+08	9.87E+08
19.61	0.024	0.014	0.024	8.17E+08	3.12E+08	5.56E+08
22.61	0.012	0.007	0.01	3.38E+08	7.50E+07	1.51E+08
25.61	0.0052	0.0037	0.0043	5.64E+07	0.00E+00	2.51E+07
28.61	0.0026	0.0028	0.0022	0.00E+00	0.00E+00	0.00E+00
31.61	0.0015	0.0024	0.0014	0.00E+00	0.00E+00	0.00E+00

Table B.2-3: Readings at 1 kW with First Flux Tilt

Axial Position	Water Hole #1 (μAmps)	Water Hole #3 (μAmps)	Water Hole #5 (μAmps)	Flux 1	Flux 3	Flux 5
7.61	0.257	0.148	0.216	1.06E+10	4.12E+09	4.76E+09
10.61	0.183	0.095	0.145	7.20E+09	2.62E+09	3.13E+09
13.61	0.109	0.048	0.086	3.97E+09	1.24E+09	1.92E+09
16.61	0.052	0.027	0.044	1.78E+09	7.85E+08	1.03E+09
19.61	0.026	0.014	0.024	9.58E+08	3.12E+08	5.56E+08
22.61	0.013	0.007	0.01	4.09E+08	7.50E+07	1.51E+08
25.61	0.005	0.004	0.004	4.23E+07	1.15E+07	1.26E+07
28.61	0.0027	0.0029	0.0022	7.05E+06	0.00E+00	0.00E+00
31.61	0.0015	0.0024	0.0014	0.00E+00	0.00E+00	0.00E+00





Table B.2-4. Readings at 1 kW with Second Flux Tilt

Axial Position	Water Hole #1 ( $\mu$ Amps)	Water Hole #3 ( $\mu$ Amps)	Water Hole #5 ( $\mu$ Amps)	Flux 1	Flux 3	Flux 5
7.61	0.1963	0.1801	0.2105	6.33E+09	5.97E+09	4.53E+09
10.61	0.1437	0.1085	0.1418	4.43E+09	3.40E+09	3.00E+09
13.61	0.0921	0.053	0.0838	2.78E+09	1.53E+09	1.83E+09
16.61	0.0456	0.0292	0.0436	1.33E+09	9.12E+08	1.01E+09
19.61	0.0235	0.0147	0.0241	7.82E+08	3.52E+08	5.61E+08
22.61	0.0118	0.0068	0.01	3.24E+08	6.35E+07	1.51E+08
25.61	0.0053	0.0038	0.0044	6.34E+07	0.00E+00	2.93E+07
28.61	0.0028	0.0027	0.0023	1.41E+07	0.00E+00	4.18E+06
31.61	0.0016	0.0023	0.0014	0.00E+00	0.00E+00	0.00E+00

Table B.2-5: Baseline Readings at 10 kW

Axial Position	Water Hole #1 ( $\mu$ Amps)	Water Hole #3 ( $\mu$ Amps)	Water Hole #5 ( $\mu$ Amps)	Flux 1	Flux 3	Flux 5
7.61	1.206	0.869	1.158	7.75E+10	4.57E+10	4.42E+10
10.61	0.826	0.537	0.769	5.25E+10	2.81E+10	2.92E+10
13.61	0.505	0.255	0.444	3.19E+10	1.32E+10	1.69E+10
16.61	0.237	0.154	0.252	1.48E+10	8.11E+09	9.73E+09
19.61	0.138	0.064	0.143	8.85E+09	3.20E+09	5.54E+09
22.61	0.059	0.019	0.042	3.65E+09	7.67E+08	1.49E+09
25.61	0.017	0.007	0.013	8.88E+08	0.00E+00	3.89E+08
28.61	0.0059	0.0041	0.0048	2.33E+08	0.00E+00	1.09E+08
31.61	0.0025	0.003	0.0025	0.00E+00	0.00E+00	4.60E+07



Table B.2-6: Readings at 10 kW with First Flux Tilt

Axial Position	Water Hole #1 ( $\mu$ Amps)	Water Hole #3 ( $\mu$ Amps)	Water Hole #5 ( $\mu$ Amps)	Flux 1	Flux 3	Flux 5
7.61	1.39	0.846	1.17	9.05E+10	4.44E+10	4.47E+10
10.61	0.884	0.517	0.757	5.66E+10	2.70E+10	2.87E+10
13.61	0.529	0.247	0.446	3.36E+10	1.27E+10	1.70E+10
16.61	0.25	0.153	0.255	1.57E+10	8.06E+09	9.86E+09
19.61	0.144	0.066	0.144	9.27E+09	3.31E+09	5.58E+09
22.61	0.0606	0.02	0.0428	3.76E+09	8.25E+08	1.52E+09
25.61	0.0172	0.0076	0.0125	9.02E+08	2.19E+08	3.68E+08
28.61	0.0058	0.0044	0.0047	2.26E+08	8.66E+07	1.05E+08
31.61	0.0025	0.0032	0.0025	0.00E+00	0.00E+00	4.60E+07

Table B.2-7: Readings at 10 kW with Second Flux Tilt

Axial Position	Water Hole #1 ( $\mu$ Amps)	Water Hole #3 ( $\mu$ Amps)	Water Hole #5 ( $\mu$ Amps)	Flux 1	Flux 3	Flux 5
7.61	1.07	0.9	1.128	6.79E+10	4.75E+10	4.29E+10
10.61	0.757	0.547	0.748	4.77E+10	2.87E+10	2.84E+10
13.61	0.482	0.261	0.448	3.03E+10	1.35E+10	1.71E+10
16.61	0.226	0.156	0.25	1.40E+10	8.23E+09	9.65E+09
19.61	0.135	0.065	0.142	8.64E+09	3.25E+09	5.49E+09
22.61	0.058	0.02	0.043	3.58E+09	8.25E+08	1.53E+09
25.61	0.017	0.0073	0.013	8.88E+08	2.02E+08	3.89E+08
28.61	0.006	0.0041	0.005	2.40E+08	6.92E+07	1.17E+08
31.61	0.0028	0.003	0.0026	0.00E+00	0.00E+00	5.02E+07



Table B 2-8: Baseline Readings at 50 kW

Axial Position	Water Hole #1 ( $\mu$ Amps)	Water Hole #3 ( $\mu$ Amps)	Water Hole #5 ( $\mu$ Amps)	Flux 1	Flux 3	Flux 5
7.61	5.658	4.107	5.365	3.91E+11	2.33E+11	2.20E+11
10.61	3.817	2.462	3.524	2.63E+11	1.39E+11	1.45E+11
13.61	2.346	1.14	2.052	1.62E+11	6.43E+10	8.42E+10
16.61	1.142	0.71	1.18	7.86E+10	4.02E+10	4.86E+10
19.61	0.665	0.291	0.681	4.60E+10	1.63E+10	2.80E+10
22.61	0.28	0.077	0.174	1.92E+10	4.11E+09	7.01E+09
25.61	0.071	0.023	0.049	4.69E+09	0.00E+00	1.90E+09
28.61	0.0205	0.0097	0.0156	1.26E+09	0.00E+00	5.61E+08
31.61	0.0074	0.0055	0.0069	0.00E+00	0.00E+00	2.30E+08

Table B.2-9: Readings at 50 kW with First Flux Tilt

Axial Position	Water Hole #1 ( $\mu$ Amps)	Water Hole #3 ( $\mu$ Amps)	Water Hole #5 ( $\mu$ Amps)	Flux 1	Flux 3	Flux 5
7.61	6.488	3.883	5.442	4.50E+11	2.20E+11	2.23E+11
10.61	4.15	2.396	3.549	2.87E+11	1.35E+11	1.46E+11
13.61	2.521	1.119	2.105	1.74E+11	6.30E+10	8.64E+10
16.61	1.2	0.701	1.185	8.27E+10	3.97E+10	4.88E+10
19.61	0.697	0.292	0.665	4.82E+10	1.64E+10	2.74E+10
22.61	0.283	0.075	0.188	1.94E+10	4.00E+09	7.60E+09
25.61	0.075	0.024	0.049	4.98E+09	1.17E+09	1.90E+09
28.61	0.021	0.011	0.017	1.30E+09	4.67E+08	6.19E+08
31.61	0.009	0.006	0.008	0.00E+00	0.00E+00	2.76E+08



Table B 2-10: Readings at 50 kW with Second Flux Tilt

Axial Position	Water Hole #1 ( $\mu$ Amps)	Water Hole #3 ( $\mu$ Amps)	Water Hole #5 ( $\mu$ Amps)	Flux 1	Flux 3	Flux 5
7.61	5.132	4.338	5.472	3.54E+11	2.48E+11	2.25E+11
10.61	3.614	2.582	3.523	2.49E+11	1.46E+11	1.44E+11
13.61	2.272	1.192	2.058	1.56E+11	6.73E+10	8.44E+10
16.61	1.099	0.729	1.174	7.58E+10	4.13E+10	4.83E+10
19.61	0.678	0.297	0.647	4.69E+10	1.66E+10	2.66E+10
22.61	0.275	0.079	0.187	1.89E+10	4.23E+09	7.56E+09
25.61	0.072	0.024	0.051	4.76E+09	1.17E+09	1.98E+09
28.61	0.021	0.009	0.017	1.30E+09	3.52E+08	6.19E+08
31.61	0.008	0.006	0.008	0.00E+00	0.00E+00	2.76E+08

Table B.2-11: Final Shutdown Background Readings

Axial Position	Water Hole #1 ( $\mu$ Amps)	Water Hole #3 ( $\mu$ Amps)	Water Hole #5 ( $\mu$ Amps)	Flux 1	Flux 3	Flux 5
7.61	0.105	0.076	0.101	7.40E+09	4.39E+09	4.23E+09
10.61	0.08	0.049	0.07	5.64E+09	2.83E+09	2.93E+09
13.61	0.052	0.031	0.04	3.66E+09	1.79E+09	1.67E+09
16.61	0.026	0.013	0.02	1.83E+09	7.50E+08	8.37E+08
19.61	0.012	0.009	0.011	8.46E+08	5.19E+08	4.60E+08
22.61	0.007	0.006	0.007	4.93E+08	3.46E+08	2.93E+08
25.61	0.0044	0.0037	0.0039	3.10E+08	2.14E+08	1.63E+08
28.61	0.0027	0.003	0.0024	1.90E+08	1.73E+08	1.00E+08
31.61	0.0017	0.0025	0.0016	1.20E+08	1.44E+08	6.69E+07





## APPENDIX C: EXPERIMENTAL PROCEDURES



## APPENDIX C: EXPERIMENTAL PROCEDURES



## C.1: EXPERIMENT PHASE I PROCEDURE

### Procedure for Experimental Evaluation of an Instrumented Synthesis Method for the Real-Time Estimation of Reactivity.

#### A. Prerequisites:

1. Reactor shutdown and reactor coolant temperature less than 25 °C.
2. Reactor top shield lid is off.
3. Reactor is ready for startup or startup checklist is near completion.
4. When the reactor is critical during the experiment, the reactor coolant temperature must be maintained below 50 °C. Since coolant flow degrades the accuracy of the results, the reactor coolant pumps will be secured for the experiment. If at any time during the experiment the coolant temperature reaches 50 °C, testing will be halted and primary coolant flow will be established to reduce coolant temperature. **CAUTION:** The reactor must be subcritical prior to restoring flow.
5. Calculate the reactivity worth of the fission chambers prior to inserting them in the core.

#### B. Procedure:

- \_\_\_\_\_ Verify prerequisites are met.
- \_\_\_\_\_ Verify Experiment is ready and all necessary materials are on hand in the vicinity of the reactor top.
- \_\_\_\_\_ Verify proper operation of the reactor top hand-held spotlight.
- \_\_\_\_\_ Prepare and clean all three aluminum instrument guide tubes to be inserted into the reactor.
- \_\_\_\_\_ Establish communications between the reactor top and the control room.
- \_\_\_\_\_ A licensed Senior Reactor Operator (SRO) and an experimenter present on the reactor top. One licensed Reactor Operator (RO) present in the control room. Supervisor and RRPO notified of start of the experiment.



- \_\_\_\_\_ Align the grid latch with water vent holes if necessary.
- \_\_\_\_\_ Insert the three fission chamber detectors into each of the aluminum instrument guide tubes. Push each of the detectors all the way to the bottom of the guide tubes.
- \_\_\_\_\_ Notify the control room that the fission chamber detectors and the aluminum guide tubes are to be inserted into the core.

**CAUTION** When lowering the aluminum guide tubes into the core, care must be taken to keep the tubes close to the outer walls of the core tank to prevent the rod from being held above the fuel elements. For this reason it is important to stand directly above the targeted water vent hole.

- \_\_\_\_\_ SRO carefully insert the aluminum tubes fully into each of the three designated water vent holes. **DO NOT FORCE THE ALUMINUM TUBES INTO THE WATER VENT HOLES.**
- \_\_\_\_\_ Notify the control room when the above step has been completed.
- \_\_\_\_\_ Experimenter perform preliminary check of electronics and complete final setup of equipment on reactor top front platform. Once this has been completed, experimenter perform a full set of background readings. Be sure to return all three fission chamber detectors to the 0" position prior to conducting the reactor startup. Record the coolant outlet temperature at the time these readings are taken:

Coolant outlet temperature: \_\_\_\_\_°C

- \_\_\_\_\_ Notify control room that experimenter is ready to commence and request the control room to conduct a reactor startup. Raise reactor power to 75 kW. (**CAUTION**: The reactor critical position may be different than the ECP because of the presence of the aluminum tubes and detectors in the core.) Note the total time that the reactor was shutdown prior to this startup.

Shutdown time prior to startup: \_\_\_\_\_ hrs.

- \_\_\_\_\_ With reactor power at 75 kW experimenter will conduct flux mapping with the three fission chamber neutron detectors at the 0" position. Note the position of all control blades and the regulating rod below. Also note the coolant outlet temperature.

Control Blade #1 Position: \_\_\_\_\_





Control Blade #2 Position \_\_\_\_\_  
Control Blade #3 Position \_\_\_\_\_  
Control Blade #4 Position: \_\_\_\_\_  
Control Blade #5 Position: \_\_\_\_\_  
Control Blade #6 Position: \_\_\_\_\_  
Regulating Rod Height: \_\_\_\_\_  
Coolant outlet temperature: \_\_\_\_\_°C

- \_\_\_\_\_ Upon completion of the above step, the SRO will notify the control room and move each detector out one inch. The RO should watch channel 7 readout carefully while detectors are moved. If fluctuations on this detector exceed  $\pm 10\%$  of the steady state value, stop the procedure and notify the superintendent. With each of the three fission chamber detectors repositioned, the experimenter will take data.
- \_\_\_\_\_ The SRO and the experimenter will repeat the above step until all three fission chamber detectors are at the 24 inch position.
- \_\_\_\_\_ Note the shim bank and regulating rod position, and the coolant outlet temperature below before starting the next step.

SBH: \_\_\_\_\_  
RRH: \_\_\_\_\_  
Temp: \_\_\_\_\_°C

- \_\_\_\_\_ If conditions permit, the experimenter will request the control room to lower the shim bank via ARI for two seconds in order to initiate a step power decrease. Note the new shim bank and regulating rod position at the completion of this two second shim (hold the shim bank position at the end of the two seconds). At sixty seconds following the initiation of the step power decrease, restore power to 75 kW. Note the new shim bank and regulating rod position, and coolant outlet temperature once power is restored.

**Fission Chamber Detectors at 24 inches:**

SBH (after 2 second shim): \_\_\_\_\_  
RRH (after 2 second shim): \_\_\_\_\_  
New SBH (power restored to 75 kW): \_\_\_\_\_  
New RRH (power restored to 75 kW): \_\_\_\_\_  
Coolant outlet temperature: \_\_\_\_\_°C

- \_\_\_\_\_ When ready, experimenter request the control room to restore the control bank to the original position (as it was before the two second shim). Use



the regulating rod to compensate and keep power at 75 kW. Note the shim bank height and regulating rod position below.

SBH \_\_\_\_\_  
RRH \_\_\_\_\_

\_\_\_\_\_ With reactor power restored to 75 kW the SRO will notify the control room and reinsert each of the three fission chamber detectors 3 inches and then repeat the above step power decrease step. This will be repeated until all three fission detectors reach the 0 inch position. Each time the fission chamber detectors are moved, the RO should watch channel 7 readout carefully and if fluctuations on this detector exceed  $\pm 10\%$  of the steady state value, stop the procedure and notify the superintendent.

Fission Chamber Detectors at 21 inches:

SBH (before ARI): \_\_\_\_\_  
RRH (before ARI): \_\_\_\_\_  
SBH (after 2 second shim): \_\_\_\_\_  
RRH (after 2 second shim): \_\_\_\_\_  
New SBH (power restored to 75 kW): \_\_\_\_\_  
New RRH (power restored to 75 kW): \_\_\_\_\_  
Coolant outlet temperature: \_\_\_\_\_°C

Fission Chamber Detectors at 18 inches:

SBH (before ARI): \_\_\_\_\_  
RRH (before ARI): \_\_\_\_\_  
SBH (after 2 second shim): \_\_\_\_\_  
RRH (after 2 second shim): \_\_\_\_\_  
New SBH (power restored to 75 kW): \_\_\_\_\_  
New RRH (power restored to 75 kW): \_\_\_\_\_  
Coolant outlet temperature: \_\_\_\_\_°C

Fission Chamber Detectors at 15 inches:

SBH (before ARI): \_\_\_\_\_  
RRH (before ARI): \_\_\_\_\_  
SBH (after 2 second shim): \_\_\_\_\_  
RRH (after 2 second shim): \_\_\_\_\_  
New SBH (power restored to 75 kW): \_\_\_\_\_  
New RRH (power restored to 75 kW): \_\_\_\_\_  
Coolant outlet temperature: \_\_\_\_\_°C

Fission Chamber Detectors at 12 inches:



SBH (before ARI): \_\_\_\_\_  
RRH (before ARI): \_\_\_\_\_  
SBH (after 2 second shim): \_\_\_\_\_  
RRH (after 2 second shim): \_\_\_\_\_  
New SBH (power restored to 75 kW): \_\_\_\_\_  
New RRH (power restored to 75 kW): \_\_\_\_\_  
Coolant outlet temperature: \_\_\_\_\_°C

Fission Chamber Detectors at 9 inches:

SBH (before ARI): \_\_\_\_\_  
RRH (before ARI): \_\_\_\_\_  
SBH (after 2 second shim): \_\_\_\_\_  
RRH (after 2 second shim): \_\_\_\_\_  
New SBH (power restored to 75 kW): \_\_\_\_\_  
New RRH (power restored to 75 kW): \_\_\_\_\_  
Coolant outlet temperature: \_\_\_\_\_°C

Fission Chamber Detectors at 6 inches:

SBH (before ARI): \_\_\_\_\_  
RRH (before ARI): \_\_\_\_\_  
SBH (after 2 second shim): \_\_\_\_\_  
RRH (after 2 second shim): \_\_\_\_\_  
New SBH (power restored to 75 kW): \_\_\_\_\_  
New RRH (power restored to 75 kW): \_\_\_\_\_  
Coolant outlet temperature: \_\_\_\_\_°C

Fission Chamber Detectors at 3 inches:

SBH (before ARI): \_\_\_\_\_  
RRH (before ARI): \_\_\_\_\_  
SBH (after 2 second shim): \_\_\_\_\_  
RRH (after 2 second shim): \_\_\_\_\_  
New SBH (power restored to 75 kW): \_\_\_\_\_  
New RRH (power restored to 75 kW): \_\_\_\_\_  
Coolant outlet temperature: \_\_\_\_\_°C

Fission Chamber Detectors at 0 inches:

SBH (before ARI): \_\_\_\_\_  
RRH (before ARI): \_\_\_\_\_  
SBH (after 2 second shim): \_\_\_\_\_  
RRH (after 2 second shim): \_\_\_\_\_



New SBH (power restored to 75 kW) \_\_\_\_\_  
New RRH (power restored to 75 kW) \_\_\_\_\_  
Coolant outlet temperature \_\_\_\_\_°C

\_\_\_\_\_ After completing the above step, lower power to 25 kW. Note the position of the shim bank and the regulating rod below.

SBH: \_\_\_\_\_  
RRH: \_\_\_\_\_

\_\_\_\_\_ When ready, the experimenter should request the RO to move control blade #6 out to establish a 50 second steady period. Once 50 second period is attained, note control blade #6 position below. When reactor power reaches 60 kW, reinsert shim blade #6 and level power at 75 kW. Again note control blade #6 position when power is leveled at 75 kW. Also note the coolant outlet temperature.

Fission Chamber Detectors at 0 inches:

Control Blade #6 Position with 50 second period: \_\_\_\_\_  
Control Blade #6 Position with power restored to 75 kW: \_\_\_\_\_  
Coolant outlet temperature: \_\_\_\_\_°C

\_\_\_\_\_ When experimenter is ready, lower power to 25 kW and restore shim blade #6 to the bank height.

\_\_\_\_\_ With power leveled at 25 kW the SRO will notify the control room and reposition the three fission chamber detectors to the 6 inch position. Repeat the above reactor power increase transient at successive six inch detector positions until the detectors reach the 24 inch position. Each time the fission chamber detectors are moved, the RO should watch channel 7 readout carefully and if fluctuations on this detector exceed  $\pm 10\%$  of the steady state value, stop the procedure and notify the superintendent. Be sure to note the control bank and regulating rod position before the transient and note control blade #6 position during and after the transient as above. Also note the coolant outlet temperature.

Fission Chamber Detectors at 6 inches:

SBH before transient: \_\_\_\_\_  
RRH before transient: \_\_\_\_\_

Control Blade #6 Position with 50 second period: \_\_\_\_\_  
Control Blade #6 Position with power restored to 75 kW: \_\_\_\_\_  
Coolant outlet temperature: \_\_\_\_\_°C





Fission Chamber Detectors at 12 inches

SBH before transient: \_\_\_\_\_

RRH before transient: \_\_\_\_\_

Control Blade #6 Position with 50 second period: \_\_\_\_\_

Control Blade #6 Position with power restored to 75 kW: \_\_\_\_\_

Coolant outlet temperature: \_\_\_\_\_°C

Fission Chamber Detectors at 18 inches:

SBH before transient: \_\_\_\_\_

RRH before transient: \_\_\_\_\_

Control Blade #6 Position with 50 second period: \_\_\_\_\_

Control Blade #6 Position with power restored to 75 kW: \_\_\_\_\_

Coolant outlet temperature: \_\_\_\_\_°C

Fission Chamber Detectors at 24 inches:

SBH before transient: \_\_\_\_\_

RRH before transient: \_\_\_\_\_

Control Blade #6 Position with 50 second period: \_\_\_\_\_

Control Blade #6 Position with power restored to 75 kW: \_\_\_\_\_

Coolant outlet temperature: \_\_\_\_\_°C

\_\_\_\_\_ After completing the last transient above and when the experimenter is ready lower reactor power to 50 kW and restore all control blades to the same height.

\_\_\_\_\_ Note the control bank and regulating rod positions and coolant outlet temperature below.

SBH: \_\_\_\_\_

RRH: \_\_\_\_\_

Temp: \_\_\_\_\_°C

\_\_\_\_\_ With reactor power at 50 kW experimenter will conduct flux mapping with the three fission chamber neutron detectors at the 24" position for baseline data.

\_\_\_\_\_ Upon completion of the above step, the SRO will notify the control room and move each detector in six inches. The RO should watch channel 7



readout carefully while detectors are moved. If fluctuations on this detector exceed  $\pm 10\%$  of the steady state value, stop the procedure and notify the superintendent. With each of the three fission chamber detectors repositioned, the experimenter will take data.

- \_\_\_\_\_ The SRO and the experimenter will repeat the above step until all three fission chamber detectors are at the 0 inch position. Note the coolant outlet temperature at the completion of this step:

Coolant outlet temperature: \_\_\_\_\_°C

- \_\_\_\_\_ After the above baseline data is taken establish a flux tilt by moving the control blades in the following manner (maintain reactor power at 50 kW by compensating with the regulating rod):

Control Blade #1: SBH + 2"  
Control Blade #2: SBH + 1"  
Control Blade #3: SBH  
Control Blade #4: SBH - 1"  
Control Blade #5: SBH - 2"  
Control Blade #6: SBH - 1"

- \_\_\_\_\_ Note the positions of all control blades and the regulating rod below:

Control Blade #1 Position: \_\_\_\_\_  
Control Blade #2 Position: \_\_\_\_\_  
Control Blade #3 Position: \_\_\_\_\_  
Control Blade #4 Position: \_\_\_\_\_  
Control Blade #5 Position: \_\_\_\_\_  
Control Blade #6 Position: \_\_\_\_\_  
Regulating Rod Position: \_\_\_\_\_

- \_\_\_\_\_ The control room will notify the experimenter once this flux tilt is achieved.

- \_\_\_\_\_ When the experimenter has recorded data with fission chamber detectors at 0 inches, the SRO will notify the control room and move each detector out six inches. Each time the fission chamber detectors are moved, the RO should watch channel 7 readout carefully and if fluctuations on this detector exceed  $\pm 10\%$  of the steady state value, stop the procedure and notify the superintendent. With each of the three fission chamber detectors repositioned, the experimenter will take data.

- \_\_\_\_\_ The SRO and the experimenter will repeat the above step until all three fission chamber detectors are at the 24 inch position.



\_\_\_\_\_ When ready, experimenter request the control room to restore all control blades to the bank height. Compensate with the regulating rod to maintain power at 50 kW

\_\_\_\_\_ Note the new shim bank and regulating rod positions below. Also note the coolant outlet temperature.

SBH: \_\_\_\_\_  
RRH: \_\_\_\_\_  
Temp: \_\_\_\_\_°C

\_\_\_\_\_ When ready, experimenter request the control room to reshim control blade #4 out 1/2 inch while driving in the regulating rod to compensate. Note the new regulating rod position at the completion of the shim.

Fission Chamber Detectors at 24 inches:

RRH with blade #4 1/2 inch above bank: \_\_\_\_\_

\_\_\_\_\_ When ready, experimenter request the control room to reshim control blade #4 to the bank height. Maintain power at 50 kW by compensating with the regulating rod. Note the new regulating rod position below. Also note the coolant outlet temperature.

RRH with blade #4 restored to bank height: \_\_\_\_\_  
Coolant outlet temperature: \_\_\_\_\_°C

\_\_\_\_\_ When ready, SRO notify the control room and insert each fission chamber detector six inches and repeat the above steps until the detectors are at the 0 inch position. Each time the fission chamber detectors are moved, the RO should watch channel 7 readout carefully and if fluctuations on this detector exceed  $\pm 10\%$  of the steady state value, stop the procedure and notify the superintendent.

Fission Chamber Detectors at 18 inches:

RRH with blade #4 1/2 inch above bank: \_\_\_\_\_  
RRH with blade #4 restored to bank height: \_\_\_\_\_  
Coolant outlet temperature: \_\_\_\_\_°C

Fission Chamber Detectors at 12 inches:

RRH with blade #4 1/2 inch above bank: \_\_\_\_\_  
RRH with blade #4 restored to bank height: \_\_\_\_\_  
Coolant outlet temperature: \_\_\_\_\_°C



Fission Chamber Detectors at 6 inches:

RRH with blade #4 1/2 inch above bank: \_\_\_\_\_  
RRH with blade #4 restored to bank height: \_\_\_\_\_  
Coolant outlet temperature: \_\_\_\_\_°C

Fission Chamber Detectors at 0 inches:

RRH with blade #4 1/2 inch above bank: \_\_\_\_\_  
RRH with blade #4 restored to bank height: \_\_\_\_\_  
Coolant outlet temperature: \_\_\_\_\_°C

\_\_\_\_\_ At the completion of the above step, raise reactor power to 75 kW and reshim to even the control blades. Note the control bank and regulating rod position below. Also note the coolant outlet temperature.

SBH: \_\_\_\_\_  
RRH: \_\_\_\_\_  
Temp: \_\_\_\_\_°C

\_\_\_\_\_ When ready, SRO notify control room and reposition all three fission chamber detectors to the 9 inch position. Console Operator should watch channel 7 readout carefully while detectors are moved. If fluctuations on this detector exceed  $\pm 10\%$  of the steady state value, stop the procedure and notify the superintendent.

\_\_\_\_\_ When ready, experimenter request the control room to drop control blade #6.

\_\_\_\_\_ When ready, experimenter request the control room to restore reactor power to 75 kW. Note the new shim bank and regulating rod positions below. Also note the coolant outlet temperature.

SBH: \_\_\_\_\_  
RRH: \_\_\_\_\_  
Temp: \_\_\_\_\_°C

\_\_\_\_\_ When ready, experimenter request the control room to drop control blade #6 again.

\_\_\_\_\_ When ready, experimenter request the control room to conduct a reactor shutdown.





- \_\_\_\_\_ Once reactor shutdown has been completed, experimenter conduct a full set of background readings
- \_\_\_\_\_ Once all testing is completed carefully, remove the three fission chamber detectors from the aluminum instrument guide tubes. Care must be taken in handling the detectors since they will be slightly activated from the neutron flux.
- \_\_\_\_\_ Carefully remove the three aluminum instrument guide tubes from the reactor core tank. Dry the aluminum tubes with absorbent rags (**CAUTION**: High beta exposure on contact with aluminum tubes.)
- \_\_\_\_\_ A licensed SRO inspect the core tank for any foreign objects left behind from the experiment.
- \_\_\_\_\_ If no additional experiments are to be performed within the core tank, replace the reactor top shield lid.
- \_\_\_\_\_ Remove and store all tools used in this procedure. Notify the control room, the Reactor Supervisor, and RRPO that the experiment has been completed.



## C.2: EXPERIMENT PHASE II PROCEDURE

### Procedure for Experimental Evaluation of an Instrumented Synthesis Method for the Real-Time Estimation of Reactivity (Part II).

#### A. Prerequisites

1. Reactor shutdown and reactor coolant temperature less than 25 °C.
2. Reactor top shield lid is off.
3. Reactor is ready for startup or startup checklist is near completion.
4. When the reactor is critical during the experiment, the reactor coolant temperature must be maintained below 50 °C. Since coolant flow degrades the accuracy of the results, the reactor coolant pumps will be secured for the experiment. If at any time during the experiment the coolant temperature reaches 50 °C, testing will be halted and primary coolant flow will be established to reduce coolant temperature. **CAUTION:** The reactor must be shutdown prior to restoring flow.
5. Calculate the reactivity worth of the fission chambers prior to inserting them in the core.

#### B. Procedure:

- \_\_\_\_\_ Verify prerequisites are met.
- \_\_\_\_\_ Verify Experiment is ready and all necessary materials are on hand in the vicinity of the reactor top.
- \_\_\_\_\_ Verify proper operation of the reactor top hand-held spotlight.
- \_\_\_\_\_ Prepare and clean all three aluminum instrument guide tubes to be inserted into the reactor.
- \_\_\_\_\_ Establish communications between the reactor top and the control room.
- \_\_\_\_\_ A licensed Senior Reactor Operator (SRO) and an experimenter present on the reactor top. One licensed Reactor Operator (RO) present in the control room. Supervisor and RRPO notified of start of the experiment.



- \_\_\_\_\_ Align the grid latch with water vent holes if necessary.
- \_\_\_\_\_ Notify the control room that the aluminum guide tubes are to be inserted into the core.

**CAUTION:** When lowering the aluminum guide tubes into the core, care must be taken to keep the tubes close to the outer walls of the core tank to prevent the rod from being held above the fuel elements. For this reason it is important to stand directly above the targeted water vent hole.

- \_\_\_\_\_ SRO carefully insert the aluminum tubes fully into each of the three designated water vent holes. **DO NOT FORCE THE ALUMINUM TUBES INTO THE WATER VENT HOLES.**
- \_\_\_\_\_ Notify the control room when the above step has been completed.
- \_\_\_\_\_ Insert the three fission chamber detectors into each of the aluminum instrument guide tubes. Push each of the detectors all the way to the bottom of the guide tubes.
- \_\_\_\_\_ Experimenter perform preliminary check of electronics and complete final setup of equipment on reactor top front platform. Once this has been completed, experimenter perform a full set of background readings. Be sure to return all three fission chamber detectors to the 0" position prior to conducting the reactor startup. Record the core tank temperature at the time these readings are taken:

Core tank temperature: \_\_\_\_\_°C

- \_\_\_\_\_ Notify control room that experimenter is ready to commence and request the control room to conduct a reactor startup. Raise reactor power to 1 kW.

Note Startup Time: \_\_\_\_\_

Shutdown time prior to startup: \_\_\_\_\_ hrs.

- \_\_\_\_\_ With reactor power at 1 kW experimenter will conduct flux mapping with the three fission chamber neutron detectors at the 0" position. Note the position of all control blades and the regulating rod below. Also note the core tank temperature.

Shim Bank Height (SBH): \_\_\_\_\_

Regulating Rod Height (RRH): \_\_\_\_\_

Core tank temperature: \_\_\_\_\_°C



- \_\_\_\_\_ Upon completion of the above step, the SRO will notify the control room and move each detector out three inches. With each of the three fission chamber detectors repositioned, the experimenter will take data.
- \_\_\_\_\_ The SRO and the experimenter will repeat the above step until all three fission chamber detectors are at the 24 inch position.
- \_\_\_\_\_ After the above baseline data is taken establish a flux tilt by moving the control blades in the following manner (RO maintain the reactor critical at 1 kW by compensating with the regulating rod):

Control Blade #1: SBH + 6"  
Control Blade #2: SBH + 2"  
Control Blade #3: SBH - 2"  
Control Blade #4: SBH - 6"  
Control Blade #5: SBH - 2"  
Control Blade #6: SBH + 2"

- \_\_\_\_\_ Note the positions of all control blades and the regulating rod below:

Control Blade #1 Position: \_\_\_\_\_  
Control Blade #2 Position: \_\_\_\_\_  
Control Blade #3 Position: \_\_\_\_\_  
Control Blade #4 Position: \_\_\_\_\_  
Control Blade #5 Position: \_\_\_\_\_  
Control Blade #6 Position: \_\_\_\_\_  
RRH: \_\_\_\_\_

- \_\_\_\_\_ The control room will notify the experimenter once this flux tilt is achieved.
- \_\_\_\_\_ When the experimenter has recorded data with fission chamber detectors at 24 inches, the SRO will notify the control room and move each detector in three inches. With each of the three fission chamber detectors repositioned, the experimenter will take data.
- \_\_\_\_\_ The SRO and the experimenter will repeat the above step until all three fission chamber detectors are at the 0 inch position.
- \_\_\_\_\_ When ready, experimenter request the control room to shift the flux tilt to the other side of the core as follows (RO maintain the reactor critical at 1 kW by compensating with the regulating rod):

Control Blade #1: SBH - 6"  
Control Blade #2: SBH - 2"  
Control Blade #3: SBH + 2"





Control Blade #4 SBH + 6"

Control Blade #5: SBH + 2"

Control Blade #6: SBH - 2"

\_\_\_\_ Note the positions of all control blades and the regulating rod below:

Control Blade #1 Position: \_\_\_\_\_

Control Blade #2 Position: \_\_\_\_\_

Control Blade #3 Position: \_\_\_\_\_

Control Blade #4 Position: \_\_\_\_\_

Control Blade #5 Position: \_\_\_\_\_

Control Blade #6 Position: \_\_\_\_\_

RRH: \_\_\_\_\_

\_\_\_\_ The control room will notify the experimenter once this flux tilt is achieved.

\_\_\_\_ When the experimenter has recorded data with fission chamber detectors at 0 inches, the SRO will notify the control room and move each detector out three inches. With each of the three fission chamber detectors repositioned, the experimenter will take data.

\_\_\_\_ The SRO and the experimenter will repeat the above step until all three fission chamber detectors are at the 24 inch position.

\_\_\_\_ When ready, experimenter request the control room to raise reactor power to 10 kW and reshim.

\_\_\_\_ Note the new shim bank and regulating rod positions below once power is leveled at 10 kW. Also note the core tank temperature.

SBH: \_\_\_\_\_

RRH: \_\_\_\_\_

Temp: \_\_\_\_\_°C

\_\_\_\_ With reactor power at 10 kW experimenter will conduct flux mapping with the three fission chamber neutron detectors at the 24" position.

\_\_\_\_ Upon completion of the above step, the SRO will notify the control room and move each detector in three inches. With each of the three fission chamber detectors repositioned, the experimenter will take data.

\_\_\_\_ The SRO and the experimenter will repeat the above step until all three fission chamber detectors are at the 0 inch position.



\_\_\_\_\_ After the above baseline data is taken establish a flux tilt by moving the control blades in the following manner (RO maintain the reactor critical at 10 kW by compensating with the regulating rod):

Control Blade #1: SBH + 2"  
Control Blade #2: SBH + 1"  
Control Blade #3: SBH - 1"  
Control Blade #4: SBH - 2"  
Control Blade #5: SBH - 1"  
Control Blade #6: SBH + 1"

\_\_\_\_\_ Note the positions of all control blades and the regulating rod below. Also note the core tank temperature.

Control Blade #1 Position: \_\_\_\_\_  
Control Blade #2 Position: \_\_\_\_\_  
Control Blade #3 Position: \_\_\_\_\_  
Control Blade #4 Position: \_\_\_\_\_  
Control Blade #5 Position: \_\_\_\_\_  
Control Blade #6 Position: \_\_\_\_\_  
RRH: \_\_\_\_\_  
Core Tank Temp: \_\_\_\_\_

\_\_\_\_\_ The control room will notify the experimenter once this flux tilt is achieved.

\_\_\_\_\_ When the experimenter has recorded data with fission chamber detectors at 0 inches, the SRO will notify the control room and move each detector out three inches. With each of the three fission chamber detectors repositioned, the experimenter will take data.

\_\_\_\_\_ The SRO and the experimenter will repeat the above step until all three fission chamber detectors are at the 24 inch position.

\_\_\_\_\_ When ready, experimenter request the control room to shift the flux tilt to the other side of the core as follows (RO maintain the reactor critical at 10 kW by compensating with the regulating rod):

Control Blade #1: SBH - 2"  
Control Blade #2: SBH - 1"  
Control Blade #3: SBH + 1"  
Control Blade #4: SBH + 2"  
Control Blade #5: SBH + 1"  
Control Blade #6: SBH - 1"



\_\_\_\_\_ Note the positions of all control blades and the regulating rod below. Also note the core tank temperature.

Control Blade #1 Position: \_\_\_\_\_

Control Blade #2 Position: \_\_\_\_\_

Control Blade #3 Position: \_\_\_\_\_

Control Blade #4 Position: \_\_\_\_\_

Control Blade #5 Position: \_\_\_\_\_

Control Blade #6 Position: \_\_\_\_\_

RRH: \_\_\_\_\_

Core Tank Temp: \_\_\_\_\_

\_\_\_\_\_ The control room will notify the experimenter once this flux tilt is achieved.

\_\_\_\_\_ When the experimenter has recorded data with fission chamber detectors at 24 inches, the SRO will notify the control room and move each detector in three inches. With each of the three fission chamber detectors repositioned, the experimenter will take data.

\_\_\_\_\_ The SRO and the experimenter will repeat the above step until all three fission chamber detectors are at the 0 inch position.

\_\_\_\_\_ When ready, experimenter request the control room to raise reactor power to 50 kW and reshim.

\_\_\_\_\_ Note the new shim bank and regulating rod positions below once power is leveled at 50 kW. Also note the core tank temperature.

SBH: \_\_\_\_\_

RRH: \_\_\_\_\_

Temp: \_\_\_\_\_°C

\_\_\_\_\_ With reactor power at 50 kW experimenter will conduct flux mapping with the three fission chamber neutron detectors at the 0" position

\_\_\_\_\_ Upon completion of the above step, the SRO will notify the control room and move each detector out three inches. With each of the three fission chamber detectors repositioned, the experimenter will take data.

\_\_\_\_\_ The SRO and the experimenter will repeat the above step until all three fission chamber detectors are at the 24 inch position.

\_\_\_\_\_ After the above baseline data is taken establish a flux tilt by moving the control blades in the following manner (RO maintain the reactor critical at 50 kW by compensating with the regulating rod):



Control Blade #1: SBH + 2"  
Control Blade #2: SBH + 1"  
Control Blade #3: SBH - 1"  
Control Blade #4: SBH - 2"  
Control Blade #5: SBH - 1"  
Control Blade #6: SBH + 1"

\_\_\_\_\_ Note the positions of all control blades and the regulating rod below:

Control Blade #1 Position: \_\_\_\_\_  
Control Blade #2 Position: \_\_\_\_\_  
Control Blade #3 Position: \_\_\_\_\_  
Control Blade #4 Position: \_\_\_\_\_  
Control Blade #5 Position: \_\_\_\_\_  
Control Blade #6 Position: \_\_\_\_\_  
RRH: \_\_\_\_\_

\_\_\_\_\_ The control room will notify the experimenter once this flux tilt is achieved.

\_\_\_\_\_ When the experimenter has recorded data with fission chamber detectors at 24 inches, the SRO will notify the control room and move each detector in three inches. With each of the three fission chamber detectors repositioned, the experimenter will take data.

\_\_\_\_\_ The SRO and the experimenter will repeat the above step until all three fission chamber detectors are at the 0 inch position.

\_\_\_\_\_ When ready, experimenter request the control room to shift the flux tilt to the other side of the core as follows (RO maintain the reactor critical at 50 kW by compensating with the regulating rod):

Control Blade #1: SBH - 2"  
Control Blade #2: SBH - 1"  
Control Blade #3: SBH + 1"  
Control Blade #4: SBH + 2"  
Control Blade #5: SBH + 1"  
Control Blade #6: SBH - 1"

\_\_\_\_\_ Note the positions of all control blades and the regulating rod below:

Control Blade #1 Position: \_\_\_\_\_  
Control Blade #2 Position: \_\_\_\_\_  
Control Blade #3 Position: \_\_\_\_\_  
Control Blade #4 Position: \_\_\_\_\_





Control Blade #5 Position. \_\_\_\_\_  
Control Blade #6 Position. \_\_\_\_\_  
RRH: \_\_\_\_\_

\_\_\_\_\_ The control room will notify the experimenter once this flux tilt is achieved.

\_\_\_\_\_ When the experimenter has recorded data with fission chamber detectors at 0 inches, the SRO will notify the control room and move each detector out three inches. With each of the three fission chamber detectors repositioned, the experimenter will take data.

\_\_\_\_\_ The SRO and the experimenter will repeat the above step until all three fission chamber detectors are at the 24 inch position.

\_\_\_\_\_ When ready, experimenter request the control room to reshim with power at 50 kW.

\_\_\_\_\_ Note the new shim bank and regulating rod positions below after the reshim. Also note the core tank temperature.

SBH: \_\_\_\_\_  
RRH: \_\_\_\_\_  
Temp: \_\_\_\_\_°C

\_\_\_\_\_ With power steady at 50 kW, drive in with shim blade #6 for ten seconds. Note the position of shim blade #6 after this shim (hold the remainder of the shim bank and regulating rod positions constant during this ten second shim). At sixty seconds following the initiation of the step power decrease, restore power to 50 kW using shim blade #6 and the regulating rod. Note shim blade #6 position, the regulating rod position, and the core tank temperature once power is restored to 50 kW.

**Fission Chamber Detectors at 24 inches:**

**Shim Blade #6 Position (after 10 second shim):** \_\_\_\_\_  
**Shim Blade #6 Position (power restored to 50 kW):** \_\_\_\_\_  
**New RRH (power restored to 50 kW):** \_\_\_\_\_  
**Core tank temperature:** \_\_\_\_\_°C

\_\_\_\_\_ When ready, experimenter request the control room to restore the control bank to the original position (as it was before the ten second shim). Use the regulating rod to compensate and keep power at 50 kW. Note the shim bank height and regulating rod position below.

SBH. \_\_\_\_\_



RRH: \_\_\_\_\_

- \_\_\_\_\_ With reactor power restored to 50 kW the SRO will notify the control room and reinsert each of the three fission chamber detectors 6 inches and then repeat the above step power decrease. This will be repeated until all three fission detectors reach the 0 inch position.

Fission Chamber Detectors at 18 inches:

SBH (before shim): \_\_\_\_\_  
RRH (before shim): \_\_\_\_\_  
Shim Blade #6 Position (after 10 second shim): \_\_\_\_\_  
Shim Blade #6 Position (power restored to 50 kW): \_\_\_\_\_  
New RRH (power restored to 50 kW): \_\_\_\_\_  
Core tank temperature: \_\_\_\_\_°C

Fission Chamber Detectors at 12 inches:

SBH (before shim): \_\_\_\_\_  
RRH (before shim): \_\_\_\_\_  
Shim Blade #6 Position (after 10 second shim): \_\_\_\_\_  
Shim Blade #6 Position (power restored to 50 kW): \_\_\_\_\_  
New RRH (power restored to 50 kW): \_\_\_\_\_  
Core tank temperature: \_\_\_\_\_°C

Fission Chamber Detectors at 6 inches:

SBH (before shim): \_\_\_\_\_  
RRH (before shim): \_\_\_\_\_  
Shim Blade #6 Position (after 10 second shim): \_\_\_\_\_  
Shim Blade #6 Position (power restored to 50 kW): \_\_\_\_\_  
New RRH (power restored to 50 kW): \_\_\_\_\_  
Core tank temperature: \_\_\_\_\_°C

Fission Chamber Detectors at 0 inches:

SBH (before shim): \_\_\_\_\_  
RRH (before shim): \_\_\_\_\_  
Shim Blade #6 Position (after 10 second shim): \_\_\_\_\_  
Shim Blade #6 Position (power restored to 50 kW): \_\_\_\_\_  
New RRH (power restored to 50 kW): \_\_\_\_\_  
Core tank temperature: \_\_\_\_\_°C



- \_\_\_\_\_ After completing the above step, maintain power at 50 kW and reshim. Note the position of the shim bank and the regulating rod below. Also note the core tank temperature.

SBH: \_\_\_\_\_

RRH: \_\_\_\_\_

Temp: \_\_\_\_\_

- \_\_\_\_\_ When ready, repeat the above steps with shim blade #3.

- \_\_\_\_\_ With power steady at 50 kW, drive in with shim blade #3 for ten seconds. Note the position of shim blade #3 after this shim (hold the remainder of the shim bank and regulating rod positions constant during this ten second shim). At sixty seconds following the initiation of the step power decrease, restore power to 50 kW using shim blade #3 and the regulating rod. Note shim blade #3 position, the regulating rod position, and the core tank temperature once power is restored to 50 kW.

Fission Chamber Detectors at 0 inches:

Shim Blade #3 Position (after 10 second shim): \_\_\_\_\_

Shim Blade #3 Position (power restored to 50 kW): \_\_\_\_\_

New RRH (power restored to 50 kW): \_\_\_\_\_

Core tank temperature: \_\_\_\_\_°C

- \_\_\_\_\_ When ready, experimenter request the control room to restore the control bank to the original position (as it was before the ten second shim). Use the regulating rod to compensate and keep power at 50 kW. Note the shim bank height and regulating rod position below.

SBH: \_\_\_\_\_

RRH: \_\_\_\_\_

- \_\_\_\_\_ With reactor power restored to 50 kW the SRO will notify the control room and move each of the three fission chamber detectors out 6 inches and then repeat the above step power decrease. This will be repeated until all three fission detectors reach the 24 inch position.

Fission Chamber Detectors at 6 inches:

SBH (before shim): \_\_\_\_\_

RRH (before shim): \_\_\_\_\_

Shim Blade #3 Position (after 10 second shim): \_\_\_\_\_

Shim Blade #3 Position (power restored to 50 kW): \_\_\_\_\_

New RRH (power restored to 50 kW): \_\_\_\_\_



Core tank temperature \_\_\_\_\_°C

Fission Chamber Detectors at 12 inches:

SBH (before shim): \_\_\_\_\_

RRH (before shim): \_\_\_\_\_

Shim Blade #3 Position (after 10 second shim): \_\_\_\_\_

Shim Blade #3 Position (power restored to 50 kW): \_\_\_\_\_

New RRH (power restored to 50 kW): \_\_\_\_\_

Core tank temperature: \_\_\_\_\_°C

Fission Chamber Detectors at 18 inches:

SBH (before shim): \_\_\_\_\_

RRH (before shim): \_\_\_\_\_

Shim Blade #3 Position (after 10 second shim): \_\_\_\_\_

Shim Blade #3 Position (power restored to 50 kW): \_\_\_\_\_

New RRH (power restored to 50 kW): \_\_\_\_\_

Core tank temperature: \_\_\_\_\_°C

Fission Chamber Detectors at 24 inches:

SBH (before shim): \_\_\_\_\_

RRH (before shim): \_\_\_\_\_

Shim Blade #3 Position (after 10 second shim): \_\_\_\_\_

Shim Blade #3 Position (power restored to 50 kW): \_\_\_\_\_

New RRH (power restored to 50 kW): \_\_\_\_\_

Core tank temperature: \_\_\_\_\_°C

- \_\_\_\_\_ After completing the above step, lower power to 5 kW and reshim. Note the position of the shim bank and regulating rod below. Also note the core tank temperature.

SBH: \_\_\_\_\_

RRH: \_\_\_\_\_

Temp: \_\_\_\_\_

- \_\_\_\_\_ When ready, the experimenter should request the RO to move control blade #6 out to establish a 50 second steady period. Once the 50 second period is attained, note control blade #6 position below. When reactor power reaches 50 kW, reinsert shim blade #6 and level power at 60 kW. Again note control blade #6 position when power is leveled at 60 kW. Also note the core tank temperature.

Fission Chamber Detectors at 24 inches:





Control Blade #6 Position with 50 second period: \_\_\_\_\_  
Control Blade #6 Position with power leveled at 60 kW: \_\_\_\_\_  
Core tank temperature: \_\_\_\_\_°C

\_\_\_\_\_ When experimenter is ready, lower power to 5 kW and restore shim blade #6 to the bank height.

\_\_\_\_\_ With power leveled at 5 kW the SRO will notify the control room and reposition the three fission chamber detectors to the 18 inch position. Repeat the above reactor power increase transient at successive six inch detector positions until the detectors reach the 0 inch position. Be sure to note the control bank and regulating rod position before the transient and note control blade #6 position during and after the transient as above. Also note the core tank temperature.

**Fission Chamber Detectors at 18 inches:**

SBH before transient: \_\_\_\_\_  
RRH before transient: \_\_\_\_\_

Control Blade #6 Position with 50 second period: \_\_\_\_\_  
Control Blade #6 Position with power leveled at 60 kW: \_\_\_\_\_  
Core tank temperature: \_\_\_\_\_°C

**Fission Chamber Detectors at 12 inches:**

SBH before transient: \_\_\_\_\_  
RRH before transient: \_\_\_\_\_

Control Blade #6 Position with 50 second period: \_\_\_\_\_  
Control Blade #6 Position with power leveled at 60 kW: \_\_\_\_\_  
Core tank temperature: \_\_\_\_\_°C

**Fission Chamber Detectors at 6 inches:**

SBH before transient: \_\_\_\_\_  
RRH before transient: \_\_\_\_\_

Control Blade #6 Position with 50 second period: \_\_\_\_\_  
Control Blade #6 Position with power leveled at 75 kW: \_\_\_\_\_  
Core tank temperature: \_\_\_\_\_°C

**Fission Chamber Detectors at 0 inches:**



SBH before transient: \_\_\_\_\_

RRH before transient: \_\_\_\_\_

Control Blade #6 Position with 50 second period: \_\_\_\_\_

Control Blade #6 Position with power leveled at 75 kW: \_\_\_\_\_

Core tank temperature: \_\_\_\_\_°C

\_\_\_\_\_ After completing the last transient above and when the experimenter is ready lower reactor power to 50 kW and reshim.

\_\_\_\_\_ Note the control bank and regulating rod positions and core tank temperature below.

SBH: \_\_\_\_\_

RRH: \_\_\_\_\_

Temp: \_\_\_\_\_°C

\_\_\_\_\_ When ready, SRO notify control room and reposition all three fission chamber detectors to the 9 inch position.

\_\_\_\_\_ When ready, experimenter request the control room to drop control blade #1.

\_\_\_\_\_ When ready, experimenter request the control room to restore reactor power to 50 kW. Note the new shim bank and regulating rod positions below. Also note the core tank temperature.

SBH: \_\_\_\_\_

RRH: \_\_\_\_\_

Temp: \_\_\_\_\_°C

\_\_\_\_\_ When ready, experimenter request the control room to conduct a reactor shutdown.

\_\_\_\_\_ Once reactor shutdown has been completed, experimenter conduct a full set of background readings. This will include readings with each detector moved to each of the other two instrument guide tubes for normalization of all readings.

\_\_\_\_\_ Once all testing is completed, carefully remove the three fission chamber detectors from the aluminum instrument guide tubes. Care must be taken in handling the detectors since they will be slightly activated from the neutron flux.



- \_\_\_\_\_ Carefully remove the three aluminum instrument guide tubes from the reactor core tank. Dry the aluminum tubes with absorbent rags (**CAUTION:** High beta exposure on contact with aluminum tubes.)
- \_\_\_\_\_ A licensed SRO inspect the core tank for any foreign objects left behind from the experiment.
- \_\_\_\_\_ If no additional experiments are to be performed within the core tank, replace the reactor top shield lid.
- \_\_\_\_\_ Remove and store all tools used in this procedure. Notify the control room, the Reactor Supervisor, and RRPO that the experiment has been completed.

Supervisor: \_\_\_\_\_ Date: \_\_\_\_\_



## REFERENCES

1. Aviles, B., "Digital Control Strategies for Spatially-Dependent Reactor Cores with Thermal-Hydraulic Feedback", Ph.D. Thesis, Nuclear Engineering Department, Massachusetts Institute of Technology, Cambridge, MA (Feb. 1990).
2. Kaplan, S., "Some New Methods of Flux Synthesis", Nuclear Science and Engineering, 13, pp. 13-25 (1962).
3. Kaplan, S., O.J. Marlowe, J. Bewick, "Application of Synthesis Techniques to Problems Involving Time-Dependence", Nuclear Science and Engineering, 18, p. 163 (1964).
4. Bernard, J.A., D.D. Lanning, A.F. Henry, "Experimental Evaluation of an Instrumented Synthesis Method for the Real-Time Estimation of Reactivity", a proposal submitted to the U.S. Department of Energy for Nuclear Engineering Research, (1992).
5. Stacey, W.M., Variational Methods in Nuclear Reactor Physics, Academic Press, New York, NY (1974).
6. Bernard, J.A., Startup and Control of Nuclear Reactors Characterized by Space-Independent Kinetics, Report No. MITNRL-039, Massachusetts Institute of Technology, Cambridge, MA, May 1990.
7. Bernard, J.A. and D.D. Lanning, Fault-Tolerant Systems Approach Toward Closed-Loop Digital Control of Nuclear Power Reactors, CPE-8317878, National Science Foundation, Washington, D.C., Jan. 1988.
8. Bernard, J.A., Ray, A., and D.D. Lanning, "Digital Control of Power Transients in a Nuclear Reactor", IEEE Transactions on Nuclear Science, Vol. NS-31, No. 1, Feb. 1984, pp. 701-705.
9. Bernard, J.A., Lanning, D.D., and A. Ray, "Experimental Evaluation of Reactivity Constraints for the Closed-Loop Control of Reactor Power", Proceedings of the NRC-EPRI Symposium on New Technologies in Nuclear Power Plant Instrumentation and Control, Washington, D.C., Nov. 1984, pp. 99-111.
10. Bernard, J.A., Lanning, D.D., and A. Ray, "Use of Reactivity Constraints for the Automatic Control of Reactor Power", IEEE Transactions on Nuclear Science, Vol. NS-32, No. 1, Feb. 1985, pp. 1036-1040.





11. Bernard, J. A. and D. D. Lanning, "Consideration in the Design and Implementation of Control Laws for the Digital Operation of Research Reactors", Nuclear Science and Engineering, Vol. 110, No. 4, Apr. 1992, pp. 425-444.
12. Bernard, J.A., "MITR-II Fuel Management, Core Depletion, and Analysis: Codes Developed for the Diffusion Theory Program Citation", Masters and Engineers Thesis, Nuclear Engineering Department, Massachusetts Institute of Technology, Cambridge, MA (June 1979).
13. Jacqmin, R., "A Semi-Experimental Nodal Synthesis Method for the On-Line Reconstruction of Three-Dimensional Neutron Flux-Shapes and Reactivity", Ph.D. Thesis, Nuclear Engineering Department, Massachusetts Institute of Technology, Cambridge, MA (Feb. 1991).
14. Yasinski, J.B. and A.F. Henry, "Some Numerical Experiments Concerning Space-Time Reactor Kinetics Behavior", Nuclear Science and Engineering, 22, p. 171 (1965).
15. Henry, A.F., Nuclear-Reactor Analysis, MIT Press, Cambridge, MA (1975).
16. Stacey, W.M., Space-Time Nuclear Reactor Analysis, Academic Press, New York, NY (1969).
17. Knoll, G.F., Radiation Detection and Measurement, John Wiley & Sons, New York, NY (1979).
18. Keithley Model 485 Autoranging Picoammeter Instruction Manual, Jan. 1990.
19. Data Translation's "Book of Data Acquisition and Image Processing", Vol. 3, No. 1, 1993.













GAYLORD S







3 2768 00036274 3